



AFRL-VA-WP-TR-2006-3078

HIGH OPERATIONS TEMPO ENERGETIC ACCESS TO GLOBE AND LAUNCH EXPERIMENT (HOT EAGLE)

Phase 1

Daniel P. Raymer

Conceptual Research Corporation

JANUARY 2006

Final Report

Approved for public release; distribution unlimited.

See additional restrictions described on inside pages

STINFO COPY

**AIR FORCE RESEARCH LABORATORY
AEROSPACE SYSTEMS DIRECTORATE
WRIGHT-PATTERSON AIR FORCE BASE, OH 45433-7541
AIR FORCE MATERIEL COMMAND
UNITED STATES AIR FORCE**

NOTICE AND SIGNATURE PAGE

Using Government drawings, specifications, or other data included in this document for any purpose other than Government procurement does not in any way obligate the U.S. Government. The fact that the Government formulated or supplied the drawings, specifications, or other data does not license the holder or any other person or corporation; or convey any rights or permission to manufacture, use, or sell any patented invention that may relate to them.

This report was cleared for public release by the USAF 88th Air Base Wing (88 ABW) Public Affairs Office (PAO) and is available to the general public, including foreign nationals.

Copies may be obtained from the Defense Technical Information Center (DTIC)
(<http://www.dtic.mil>).

AFRL-VA-WP-TR-2006-3078 HAS BEEN REVIEWED AND IS APPROVED FOR
PUBLICATION IN ACCORDANCE WITH ASSIGNED DISTRIBUTION STATEMENT.

*//Signature//

COLE DOUPE
Project Engineer
Aerodynamic Configuration Branch

//Signature//

CHRISTOPER R. REMILLARD, Chief
Aerodynamic Configuration Branch
Aeronautical Sciences Division

//Signature//

MICHAEL J. STANEK, Technical Advisor
Principal Scientist
Aeronautical Sciences Division
Air Vehicles Directorate

This report is published in the interest of scientific and technical information exchange, and its publication does not constitute the Government's approval or disapproval of its ideas or findings.

*Disseminated copies will show “//Signature//” stamped or typed above the signature blocks.

REPORT DOCUMENTATION PAGE				Form Approved OMB No. 0704-0188	
<p>The public reporting burden for this collection of information is estimated to average 1 hour per response, including the time for reviewing instructions, searching existing data sources, gathering and maintaining the data needed, and completing and reviewing the collection of information. Send comments regarding this burden estimate or any other aspect of this collection of information, including suggestions for reducing this burden, to Department of Defense, Washington Headquarters Services, Directorate for Information Operations and Reports (0704-0188), 1215 Jefferson Davis Highway, Suite 1204, Arlington, VA 22202-4302. Respondents should be aware that notwithstanding any other provision of law, no person shall be subject to any penalty for failing to comply with a collection of information if it does not display a currently valid OMB control number. PLEASE DO NOT RETURN YOUR FORM TO THE ABOVE ADDRESS.</p>					
1. REPORT DATE (DD-MM-YY) January 2006		2. REPORT TYPE Final		3. DATES COVERED (From - To) 01 October 2002 – 31 May 2005	
4. TITLE AND SUBTITLE HIGH OPERATIONS TEMPO ENERGETIC ACCESS TO GLOBE AND LAUNCH EXPERIMENT (HOT EAGLE)				5a. CONTRACT NUMBER F42620-00-D-0039-RZ05	
				5b. GRANT NUMBER	
				5c. PROGRAM ELEMENT NUMBER 62201F	
6. AUTHOR(S) Daniel P. Raymer				5d. PROJECT NUMBER A072	
				5e. TASK NUMBER N/A	
				5f. WORK UNIT NUMBER 0E	
7. PERFORMING ORGANIZATION NAME(S) AND ADDRESS(ES) By: Conceptual Research Corporation P.O. Box 5429 Playa del Rey, CA 90296-5429				For: University of Dayton Research Institute 300 College Park Drive Dayton, OH 45469-0104	
9. SPONSORING/MONITORING AGENCY NAME(S) AND ADDRESS(ES) Air Force Research Laboratory Aerospace Systems Directorate Wright-Patterson Air Force Base, OH 45433-7541 Air Force Materiel Command United States Air Force				8. PERFORMING ORGANIZATION REPORT NUMBER	
				10. SPONSORING/MONITORING AGENCY ACRONYM(S) AFRL/RQH V	
				11. SPONSORING/MONITORING AGENCY REPORT NUMBER(S) AFRL-RQ-WP-TR-2006-3078	
12. DISTRIBUTION/AVAILABILITY STATEMENT Approved for public release; distribution unlimited.					
13. SUPPLEMENTARY NOTES PA Case Number: 88ABW-2016-0689; Clearance Date: 18 Feb 2016. The distribution of this report has widened to be approved for public release. Downloads of all previous versions should be replaced with this version. The original branch and directorate symbol for this report was AFRL/VAAA.					
14. ABSTRACT In this report, the researchers defined and assessed a reusable launch vehicle upper stage that is suitable for use with a reusable first stage. A subscale demonstrator that is intended for the flight test validation of key HOT EAGLE technologies and system concepts has been defined and sized to allow flight on an existing first-stage booster. This report also includes studies on propulsion, structure, and systems and avionics.					
15. SUBJECT TERMS reusable, launch vehicle, upper stage, first stage, booster, hybrid launch vehicle, HLV					
16. SECURITY CLASSIFICATION OF:			17. LIMITATION OF ABSTRACT: SAR	18. NUMBER OF PAGES 217	19a. NAME OF RESPONSIBLE PERSON (Monitor) Cole Doupe 19b. TELEPHONE NUMBER (Include Area Code) N/A
a. REPORT Unclassified	b. ABSTRACT Unclassified	c. THIS PAGE Unclassified			

TABLE OF CONTENTS

Section	Page
LIST OF FIGURES	iv
NOMENCLATURE	x
1. INTRODUCTION AND SUMMARY	1
2. APPROACH	3
2.1. Propulsion Options and Analysis (XCOR Aerospace)	3
2.2. Structure Concepts and Analysis (Convergence Engineering with support from Composite Engineering Inc.)	4
2.3. Avionics and Subsystems (Universal Space Lines)	4
3. BACKGROUND: SYSTEM APPLICATIONS	5
3.1 RUS	5
3.2 Global Troop Transport.....	6
4. BACKGROUND: VEHICLE CONFIGURATION	7
5. THOUGHT EXPERIMENT – IMPACT OF REUSABILITY	9
5.1 Thought Experiment Overview	9
5.2 Calculations.....	9
5.3 Reusability Thought Experiment Conclusions.....	14
6. RUS.....	15
6.1 Design Requirements	15
6.2 RUS Configuration Concepts.....	20
6.3 Vehicle Analysis – Propulsion	24
6.4 Vehicle Analysis – Aerodynamics	25
6.5 Vehicle Analysis – Weights	27
6.6 Mission Timeline and Trajectory Analysis	30
6.7 Reusable Upper Stage Summary and Conclusions	33
7. GLOBAL TROOP TRANSPORT	35
7.1 Design Requirements and Compartment Dimensions	35
7.2 Global Troop Transport Vehicle Analysis	36
7.3 Global Troop Transport – Near-Term Concept.....	36
7.4 Global Troop Transport – Rocket Lander	41
7.5 Super Global Troop Transport	42
7.6 Global Range Troop Transport Summary and Conclusions	49
8. HOT EAGLE DEMONSTRATOR	50
8.1 Design Requirements	50
8.2 HOT EAGLE Demonstrator Analysis.....	52
8.3 HOT EAGLE Demonstrator Configuration Concepts	52
8.4 HOT EAGLE Demonstrator Cost and Schedule Estimate.....	59
9. SUMMARY AND CONCLUSIONS	63
10. REFERENCES	64
11. APPENDICES	65
APPENDIX A: XCOR – HOT EAGLE Report	66
A1. EXECUTIVE SUMMARY	66
A2. OVERVIEW	67
A3. PROPULSION SYSTEMS.....	68
A3.1 Propellant.....	68

A3.2	Nozzles	69
A3.3	Demonstrator Vehicles	70
A3.4	Operational HL Vehicle.....	73
A4.	APPLICABLE PROPULSION TECHNOLOGIES AND CONCEPTS	74
A5.	PROPULSION PENALTIES OF VERTICAL LANDING	77
A6.	DEVELOPMENT COST AND SCHEDULE	78
	APPENDIX B: Preliminary Structural Analysis	79
B1	INTRODUCTION	85
B2.	FINITE ELEMENT MODEL	87
B2.1	Model, Design, and Analysis Assumptions.....	87
B2.2	Model Geometry and Configuration.....	87
B2.3	Material Properties	88
B2.4	Primary Structures	90
B2.4.1	Nosecone	90
B2.4.2	Fuselage.....	91
B2.4.3	Wing and Wing Carry-Through	91
B2.4.4	Payload Cone.....	95
B2.4.5	Engine Bulkhead and Cone Assembly	97
B2.4.6	Rear Aero Flap	98
B2.4.7	Propellant Tanks.....	98
B2.5.	Mass Properties	100
B3.	TRADE STUDIES.....	101
B3.1	Propellant Tank Material Selection	101
B4.	ANALYSIS.....	104
B4.1	Analysis Load Cases.....	104
B4.2	Local Analysis	105
B4.2.1.	Propellant Tank	105
B4.3	Vehicle Analysis.....	109
B4.3.1	Ground Handling Horizontal Lift Load Case.....	109
B4.3.2	Ground Handling Vertical Lift Load Case.....	110
B4.3.3	Launch Load Case.....	112
B4.3.4	Powered Flight: Exo-Atmospheric.....	121
B4.3.5	Re-Entry Load Case	125
B4.3.6	Chute Deployment Load Case.....	132
B4.3.7	Vehicle Landing Load Case	136
B4.3.8	Demonstration Vehicle Launch Load Case.....	140
B5.	TPS TRADE STUDY AND ANALYSIS.....	148
B6.	SUMMARY AND CONCLUSIONS	151
B7.	REFERENCES	152
	APPENDIX BA: Tsai-Wu Failure Criteria.....	153
	APPENDIX BB: Loads Document.....	155
BB.1	Other important notes:	157
	APPENDIX C: HOT EAGLE Subsystems.....	158
C1.	Introduction.....	162
C2.	Top Level Requirements.....	163
C2.1	Environments.....	163

C2.1.1	Radiation	163
C2.1.2	Vibration.....	163
C2.1.3	Shock.....	164
C2.1.4	Acceleration	165
C2.1.5	Temperature	165
C2.2	Control System Implementation.....	165
C2.2.1	Control system latency	165
C2.2.2	Redundancy.....	165
C2.3	Program Requirements	165
C2.3.1	Development and acceptance test requirements.....	165
C2.3.2	Programmatic requirements	166
C3.	System Requirements / Implementations.....	167
C3.1	Air Data Sensor (ADS).....	167
C3.2	Vertical Position Accuracy Requirements.....	167
C3.3	Navigation / Vehicle State Sensing	169
C3.3.1	Navigation Baseline Configuration.....	169
C3.4	Aero Surface Actuator Loading.....	171
C3.4.1	Body Flaps.....	171
C3.4.2	Elevon.....	171
C3.4.3	Rudder	172
C3.4.4	Candidate Actuators	172
C3.4.5	Actuation Options (Aerosurface and TVC)	174
C3.5	Vehicle Management System	177
C3.5.1	Vehicle interfaces.....	177
C3.5.2	Memory and throughput.....	180
C3.5.3	Obsolescence	180
C3.5.4	VMS Baseline Configuration.....	180
C3.6	Instrumentation and Communications.....	181
C3.7	Flight Safety Systems	182
C3.8	Power	183
C3.9	Reaction Control System	184
C4.	Systems Weight Estimate	186
C4.1	Battery Sizing	186
C4.2	Weight Estimates	189
C4.2.1	Electronics.....	189
C4.2.2	Power and Wiring.....	189
C4.2.3	Actuation – Electrical.....	192
C4.2.4	Actuation – Hydraulic	192
C4.2.5	Actuation System Selection	194
C4.2.6	Landing Gear – Horizontal Landing	194
C4.2.7	RCS	196
C4.2.8	Miscellaneous.....	199
C4.3	System Weight Comparisons	202

LIST OF FIGURES

Figure	Page
Figure 1. Preferred Aerodynamic Concept – Swept Tails with Outboard Elevons	8
Figure 2. Thought Experiment Approach	9
Figure 3. Contributors to Weight Change	12
Figure 4. Orbit Weights vs. Inclination	17
Figure 5. RUS Configuration - HL	20
Figure 6. RUS Configuration - VL	21
Figure 7. Alternate RUS Configuration – VL	23
Figure 8. XCOR RUS Engine	24
Figure 9. RUS Lift Curve	26
Figure 10. RUS L/D Ratio	27
Figure 11. Upper Stage Trajectory Analysis	32
Figure 12. Reentry Trajectory Analysis	34
Figure 13. Troop Transport Compartment	35
Figure 14. Global Troop Transport (HotGlobe) Configuration	37
Figure 15. Fulton Recovery Analysis Geometry	38
Figure 16. Near-Term Global Transport Weights	39
Figure 17. Global Troop Transport – Rocket Lander	41
Figure 18. Super Global Troop Transport – Rocket Land and Egress	43
Figure 19. HotGlobe2 Reentry Trajectory Analysis	46
Figure 20. Towed Recovery Scheme	47
Figure 21. Global Troop Transport Vertical Attitude Lander – External Troop Compartment	48
Figure 22. Vertical Attitude Lander Troop Compartment Deployment	49
Figure 23. HOT EAGLE Demonstrator External Three-View (HL)	53
Figure 24. HOT EAGLE Demonstrator External Three-View (VL)	53
Figure 25. Impact of Sea Level Bias on Isp (XCOR)	55
Figure 26. HOT EAGLE Demonstrator Self-Launch Trajectory Analysis	58
Figure 27. HOT EAGLE Demonstrator Trajectory Analysis – FalconV Launch	59
Figure 28. Tentative Program Schedule	60
Figure 29. Near-term Structures Demonstrator	61
Figure A-1. Extendible Nozzle for Altitude Compensation	70
Figure A-2. Diagram of an Aerospike Nozzle	70
Figure A-3. Dual Bell Nozzle Test	70
Figure A-4. Concept Drawing of the Demonstrator VL Engine	71
Figure A-5. Concept Drawing of the Demonstrator HL Engine	72
Figure A-6. Concept Drawing of Operational HL Engine Based on XCOR’s Analyses	73
Figure B-1. FEM with Top Level Dimensions	88
Figure B-2. Primary Structures and Components Included in the Model	88
Figure B-3. Nosecone with Parachute Door Opening (0° Ply Direction Shown)	93
Figure B-4. Design Concept for Steel Ring around the Chute Door Opening	93
Figure B-5. Fuselage Section (0° Ply Direction Shown)	94
Figure B-6. Modeling of the Wing Skin and Wing Carry-through (0° Ply Direction Shown)	95
Figure B-7. Payload Cone with Forward Bi-mese Attach Lug (0° Ply Direction Shown)	96
Figure B-8. Nosecone/Payload Cone/Fuselage Interface Joint	97
Figure B-9. Engine Support Structure (0° Ply Direction Shown)	97

Figure B-10. Model Details of the Rear Flap	98
Figure B-11. Model Details of the Propellant Tanks	100
Figure B-12. Model Details for Propellant Tank Analysis	106
Figure B-13. Tsai-Wu Survey Plot of the Liner and External Shell for the Thermal and Pressure Load	107
Figure B-14. von Mises Stress in the Foam Core for the Thermal and Pressure Load Case	107
Figure B-15. Tsai-Wu Stress Survey Plot of Composite Structure for the Thermal-only Load Case	108
Figure B-16. von Mises Stress in the Foam Core for the Thermal-only Load Case	108
Figure B-17. Deflection of the Vehicle with a 4 g Horizontal Lift	109
Figure B-18. Resultant Displacement of Structure during Horizontal Lift	110
Figure B-19. Tsai-Wu Stress Survey Plot of the Composite Structures during Horizontal Lift ..	110
Figure B-20. Deformed Geometry Plot of the Vehicle for a Vertical Lift	111
Figure B-21. Resultant Displacement Contour Plot of the Vehicle for a Vertical Lift	111
Figure B-22. Tsai-Wu Stress Survey Plot of the Composite Structures during Vertical Lift	112
Figure B-23. Vehicle Cp Plot from CFD Analysis for $M = 2.0$ and $AOA = 2.0$	113
Figure B-24. Vehicle Aero Load Pressure Profile for $q=1200$ psf, $M=2.0$ and $AOA=2.0$	113
Figure B-25. Aero Load Pressure Profile on Vehicle's Wing for $q=1200$ psf, $M=2.0$ and $AOA=2.0$	114
Figure B-26. Boundary Conditions and Loads on Model for Launch Loads Analysis	115
Figure B-27. Pressure Profile in Propellant Tanks	115
Figure B-28. Deformed Geometry Plot of the Vehicle for the Launch Load Case	116
Figure B-29. Resultant Displacement Contour Plot for the Launch Load Case	117
Figure B-30. Tsai-Wu Stress Survey of the Vehicle Composite Structures for the Launch Load	118
Figure B-31. Tsai-Wu Stress Survey of the Vehicle's Propellant Tanks for the Launch Load Case	118
Figure B-32. Tsai-Wu Stress Survey of Vehicle Composite Structures without the Propellant Tanks	119
Figure B-33. Tsai-Wu Stress Survey of Vehicle Composite Structures without Propellant Tanks	119
Figure B-34. Tsai-Wu Stress Survey of Wing Waffle and Wing Carry-through Composite Structures	120
Figure B-35. Tsai-Wu Stress Survey of Vehicle Engine Support and Payload Cone Structures	120
Figure B-36. Boundary Conditions on Model for Powered Flight Analysis	121
Figure B-37. Pressure Profile in Propellant Tanks	122
Figure B-38. Deformed Geometry Plot of the Vehicle for Powered Flight	122
Figure B-39. Resultant Displacement Contour Plot of the Vehicle for Powered Flight	123
Figure B-40. Resultant Displacement Contour Plot of Engine Support Structure for Powered Flight	123
Figure B-41. Tsai-Wu Stress Survey of the Vehicle's Composite Structures for Powered Flight	124
Figure B-42. Tsai-Wu Stress Survey of the Engine Support Structure for Powered Flight	124
Figure B-43. Vehicle Cp Plot from CFD Analysis for $M = 25.0$ and $AOA = 70.0$	125
Figure B-44. Vehicle Aero Load Pressure Profile for $q=190$ psf, $M=25.0$ and $AOA=70.0$	126
Figure B-45. Vehicle Aero Load Pressure Profile for $q=190$ psf, $M=25.0$ and $AOA=70.0$	126
Figure B-46. Boundary Conditions on Model for Re-entry Loads Analysis	127

Figure B-47. Pressure Profile in Propellant Tanks	127
Figure B-48. Deformed Geometry Plot of the Vehicle for Re-entry Loads	128
Figure B-49. Deformed Geometry Plot of the Vehicle's Wing for Re-entry Loads.....	128
Figure B-50. Resultant Displacement Contour Plot for Re-entry Loads	129
Figure B-51. Tsai-Wu Stress Survey of the Vehicle's Composite Structures for Re-entry	129
Figure B-52. Tsai-Wu Stress Survey of the Vehicle's Composite Structures for Re-entry Loads.....	130
Figure B-53. Tsai-Wu Stress Survey of the Vehicle's Composite Structures for Re-entry Loads.....	130
Figure B-54. Tsai-Wu Stress Survey of the Vehicle's Wing Waffle and Wing Carry-through Section.....	131
Figure B-55. Tsai-Wu Stress Survey of the Vehicle's Wing Waffle and Wing Carry-through Section.....	132
Figure B-56. Chute Deployment Force Applied to the FEM.....	133
Figure B-57. Pressure Profile in Propellant Tanks	133
Figure B-58. Deformed Geometry Plot of the Vehicle during Chute Deployment.....	134
Figure B-59. Resultant Displacement Contour Plot of the Vehicle during Chute Deployment ..	134
Figure B-60. Tsai-Wu Stress Survey of Vehicle's Composite Structures during Chute Deployment.....	135
Figure B-61. Tsai-Wu Stress Survey Plot of the Nosecone during Chute Deployment	135
Figure B-62. Landing Gear Geometry during Landing	136
Figure B-63. Vehicle Velocity and Acceleration Profiles during Landing	137
Figure B-64. Reaction Force on Landing Gear during Landing.....	137
Figure B-65. Resultant Displacement Plot of the Vehicle's Aft Skirt Region for Landing Loads.....	138
Figure B-66. Tsai-Wu Stress Survey of the Vehicle's Composite Structures during Landing ...	139
Figure B-67. Tsai-Wu Stress Survey Plot of the Vehicle's Aft Skirt Region during Landing....	140
Figure B-68. Vehicle Cp Plot from CFD Analysis for $M = 2.0$ and $AOA = 2.0$	141
Figure B-69. Vehicle Aero Load Pressure Profile for $q=1200$ psf, $M=2.0$ and $AOA=2.0$	141
Figure B-70. Aero Load Pressure Profile on Vehicle's Wing for $q=1200$ psf, $M=2.0$ and $AOA=2.0$	142
Figure B-71. Boundary Conditions and Loads on Model for Demonstrator Launch Loads Analysis.....	142
Figure B-72. Pressure Profile in Propellant Tanks	143
Figure B-73. Deformed Geometry Plot of the Vehicle for Demonstrator Launch	143
Figure B-74. Resultant Displacement Contour Plot of the Vehicle for Demonstrator Launch ...	144
Figure B-75. Deflection Contour Plot of Engine Support Structure for the Demonstrator Launch.....	144
Figure B-76. Tsai-Wu Stress Survey of Vehicle's Composite Structures for the Demonstrator Launch.....	145
Figure B-77. Tsai-Wu Stress Survey of Vehicle's Composite Structures for the Demonstrator Launch.....	145
Figure B-78. Tsai-Wu Stress Survey of Vehicle's Composite Structures for the Demonstrator Launch.....	146
Figure B-79. Tsai-Wu Stress Survey of Vehicle's Composite Structures for the Demonstrator Launch.....	146

Figure B-80. Tsai-Wu Stress Survey of Vehicle's Composite Structures for the Demonstrator Launch.....	147
Figure B-81. Tsai-Wu Stress Survey of Vehicle's Composite Structures for the Demonstrator Launch.....	147
Figure B-82. Mechanical TPS Attach Concept.....	150
Figure BA-1. Tsai-Wu Failure Envelope Compared with Three Other Failure Criteria	154
Figure C-1 – LEO Radiation Environment.....	163
Figure C-2 – Launch Vehicle Vibration Environments - Qualification	164
Figure C-3 – Left Wing Elevon with Actuator Rod	172
Figure C-4 – Actuation Comparison.....	174
Figure C-5 – Hydraulic Actuator	175
Figure C-6 – Baseline Avionics Configuration	181
Figure C-7 – Traditional Flight Termination System	182
Figure C-8 – Autonomous Flight Safety System.....	183
Figure C-9 – Pneumatic TVC Implementation.....	187
Figure C-10 – RCS System Configuration	196
Figure C-11 – Quad Valve Configuration	197
Figure C-12 – ATCS Block Diagram	199

LIST OF TABLES

Table	Page
Table 1. Delta II Weight Progression – Expendable to RUS.....	11
Table 2. Falcon I Weight Progression – Expendable to RUS.....	13
Table 3. Existing Launcher Payload to 100 nmi Orbit	16
Table 4. Approximate USAF Payload Characteristics	17
Table 5. Design-To Requirements – HOT EAGLE RUS	19
Table 6. Payload Bay Geometry	19
Table 7. Reusable Upper Stage Design Data	21
Table 8. Reusable Upper Stage Tail and Reference Geometries	22
Table 9. HL RUS Weights	28
Table 10. HL Reusable Upper Stage Weights - Conservative.....	29
Table 11. Effect of Bay Location on RUS c.g. and Stability.....	29
Table 12. VL RUS Weights	30
Table 13. Trajectory Analysis- Boost End Conditions and Orbit.....	33
Table 14. Weight Estimates for 13-Soldier Squad.....	36
Table 15. Near-Term Global Transport Weights.....	40
Table 16. Global Transport Rocket Lander Weights.....	42
Table 17. Super Global Transport Weights	44
Table 18. Global Troop Transport Comparative Design Data.....	45
Table 19. Candidate Demo Booster Weight and Performance Data	51
Table 20. HOT EAGLE Demonstrator Design Data	54
Table 21. HOT EAGLE Demonstrator Tail and Reference Geometries	54
Table 22. HOT EAGLE Demonstrator Weights (HL).....	56
Table 23. HOT EAGLE Demonstrator Weights (VL).....	57
Table 24. Cost ROM.....	62
Table 25. Structural Test Article Cost ROM	62
Table 26. Summary and Comparison of HOT EAGLE Concept Design Data.....	65
Table B-1 Analysis Assumptions and Rationale	87
Table B-2. Mechanical Material Properties Used in the Analysis.....	90
Table B-3. Ply Schedule for All Primary Structures.....	91
Table B-4. Vehicle Mass Properties	101
Table B-5. Results of Material Trade Study for the Propellant Tanks	103
Table B-6. Vehicle Analysis Matrix	104
Table BB-1. Vehicle Load Cases.....	155
Table C-1 – Astech DG18 GPS Real Time Position Accuracy	168
Table C-2 – Navigation Sensor Physical Attributes	170
Table C-3 – Navigation Sensor Environmental Attributes	170
Table C-4 – Actuator Hinge Moment & Force Requirements.....	172
Table C-5 – EMA Attributes.....	173
Table C-6 – Hydraulic Actuators	173
Table C-7. VMS Interfaces	178
Table C-8 – Battery Sizing, Baseline Mission, Power Control	186
Table C-9 – Battery Sizing, Baseline Mission, Pneumatic TVC.....	186
Table C-10 – HOT EAGLE Power Analysis.....	188

Table C-11 – Avionics / Electronics Weight Estimate	190
Table C-12 – Power and Wiring Weight Estimate	191
Table C-13 – Electrical Actuation Weight.....	193
Table C-14 – Hydraulic Actuation Weight Estimate.....	193
Table C-15 – Landing Gear Actuation Weight Estimate – Horizontal Landing	195
Table C-16 – RCS Weight Estimate	198
Table C-17 – Miscellaneous Systems Weight Estimates.....	201
Table C-18 – CERV Mass Summary.....	202
Table C-19 – X-33 Mass Summary	203

NOMENCLATURE

<i>A</i>	= Aspect Ratio (span ² /reference area, applied to wings and tails)
<i>C_L</i>	= Wing Lift Coefficient
<i>CAD</i>	= Computer-Aided Design
<i>CFD</i>	= Computational Fluid Dynamics
<i>cg</i>	= Center of Gravity (mass)
<i>DATCOM</i>	= Data Compendium (USAF aerodynamics methodology report)
<i>GLOW</i>	= Gross Liftoff Weight
<i>HL</i>	= Horizontal Landing
<i>HotEagle</i>	= High Operations Tempo Energetic Access to Globe and Launch Experiment
<i>ISR</i>	= Intelligence-Surveillance-Reconnaissance
<i>L/D</i>	= Lift-to-Drag Ratio
<i>M</i>	= Mach Number
<i>NS</i>	= Navier-Stokes (high-end CFD)
<i>psf</i>	= pounds per square foot
<i>RCS</i>	= Reaction Control System
<i>RDS</i>	= Aerospace vehicle design software (product of Conceptual Research Corp.)
<i>ROAST</i>	= RDS Optimal AeroSpace Trajectories (launch analysis module)
<i>RUS</i>	= Reusable Upper Stage
<i>t/c</i>	= Airfoil thickness/chord length
<i>TOGW</i>	= Aircraft Takeoff Gross Weight
<i>TPS</i>	= Thermal Protection System
<i>T/W</i>	= Thrust-to-weight ratio
<i>TPS</i>	= thermal protection system
<i>W/S</i>	= Wing loading (weight/area)
<i>W_e</i>	= Empty Weight
<i>VL</i>	= Vertical Landing
<i>VTHL</i>	= Vertical Takeoff and Horizontal Landing
<i>VTVL</i>	= Vertical Takeoff and Vertical Landing

1. INTRODUCTION AND SUMMARY

Conceptual Research Corporation (CRC) has completed its contracted effort for Phase 1 of the High Operations Tempo Energetic Access to Globe and Launch Experiment (HOT EAGLE) project. Under this contract, CRC and its subcontractor team defined and assessed a reusable upper stage suitable for use with a reusable first stage[†]. A subscale demonstrator intended for flight test validation of key HOT EAGLE technologies and system concepts has been defined and has been sized to allow flight on an existing first-stage booster. A manned global transport system was also defined based on the HOT EAGLE vehicle concept to perform certain high-value objectives in time-critical operational scenarios.

This effort was funded and managed by the United States Air Force Research Laboratory Air Vehicles (AFRL/VA) Directorate and was structured as a subcontract from the University of Dayton Research Institute. UDRI also played a managerial and technical role in the test planning, structure, and thermal protection areas.

The CRC HOT EAGLE team included the following organizations performing the tasks indicated:

Conceptual Research Corporation - CRC (Playa del Rey, CA): Project and Engineering Management, Vehicle Concept Design, Configuration Control, Performance Analysis, Strategic Planning

Universal Space Lines - USL (Newport Beach, CA): Vehicle Subsystems Definition and Design including Avionics, Electrical, Actuation, Environmental Control, and Power.

XCOR Aerospace (Mojave, CA): Propulsion design, integration, analysis, and technology studies.

Convergent Engineering – (Reno, NV): Structural Design, finite element analysis (FEA), and structural weight estimation. Previous CRC structures team member Composite Engineering Inc. has participated in an unfunded consulting role, and remains interested in fabricating the structure for the HOT EAGLE demonstrator. Convergence Engineering supported CEi in the previous study phases.

Two other firms participated extensively in the related Micro-X studies thereby making important indirect contributions to the HOT EAGLE effort and are deserving of recognition:

Analytical Methods Inc. - AMI (Redmond, WA): CFD aerodynamics analysis from subsonic to M25, including controls effects and aeroheating.

Computer Aided Engineering Design Support Services Inc. - CAEDSS (Rocklin, CA): CAD solid modeling and design support.

[†] For example, that being defined for the proposed Hybrid Launch Vehicle (HLV, formerly known as ARES).

This project was fortunate to leverage a substantial technical base from previous design studies conducted by CRC. These previous Micro-X studies were focused on system concepts and a technology demonstrator for reusable *first* stage systems. This effort extended over several years and five major study phases, culminating in a viable configuration concept with a reusable first stage and an expendable upper stage. This system design anticipated and in many ways was similar to the USAF-SMC HLV/ARES project.

This prior database of design concepts, technologies, and performance analysis was available for the HOT EAGLE effort and proved to be invaluable. To make this report more of an integrated overview of the HOT EAGLE concept, appropriate material from the previous efforts has been seamlessly integrated into this write-up.

The Phase 1¹ and Phase 2² Micro-X studies produced a concept baseline for a reusable rocket powered technology demonstrator vehicle with outstanding performance and affordable cost. The Phase 3³ study subjected the overall design concept to an initial review by structures and fabrication experts at Composite Engineering Inc. The Phase 4⁴ study explored a larger and more-capable Micro-X demonstrator vehicle and included design and analysis of potential operation USAF reusable boosters based on the Micro-X design approach.

The recent Phase 5 Micro-X effort⁵ included an aerodynamic design study for a vehicle configuration with acceptable augmented stability despite the extreme-aft center of gravity typical of a high propellant mass fraction vehicle during a propellant-out glide. Phase 5 also included a preliminary design study of a reusable upper stage vehicle suitable for use with an HLV/ARES-class vehicle. This proved to be especially useful for the HOT EAGLE effort.

2. APPROACH

This HOT EAGLE study was actually three studies in one – the HOT EAGLE demonstrator, the operational Reusable Upper Stage, and the Global Transport Stage. All are geometrically based on the aerodynamic configuration optimized in the previous Micro-X design study.

The project began with a study of requirements and technologies. System design requirements for a fully reusable military upper stage were defined and prioritized. Capabilities of current and projected upper and lower stages were tabulated and assessed to determine desired upper stage orbit insertion abilities and available lower stage lift capabilities. Operational reusable upper stage requirements were then defined.

A thought experiment was conducted to identify and assess the sources of the increased empty weight of a reusable vs. expendable upper stage. Several existing upper stages were incrementally changed to a reusable configuration, analytically tracking the impact of those changes. This included the incorporation of reentry capability, recovery apparatus, and return-to-launch site capability. This pointed towards the strategy of maximum leverage for a reusable upper stage design.

A survey of available and emerging technologies was then conducted to establish applicability to the HOT EAGLE program. This included a qualitative risk assessment and was largely conducted by the CRC subcontractor team. Results can be seen in the subcontractor reports, attached to this overview report.

Next, system design concepts for a reusable upper stage (RUS) were created including both horizontal and vertical landing concepts. These were analyzed as to weights, drag, installed propulsion, and performance. A number of trade studies were conducted, described below.

The next activity in the CRC HOT EAGLE study was the design of a global transport stage. This is an urgent insertion system capable of transporting a USMC squad of 13 across global range via suborbital launch, ingress into a hostile area, landing on an unprepared site, and egress with a substantial outbound range. This is an ambitious mission objective, yet analysis described below offers both near-term and future systems that could attain this capability.

The final effort was the definition of a subscale technology demonstrator that would permit technology and system concept validation in an affordable, incremental flight test program. This was sized to maximize demonstrator scalability to an operational system while minimizing demonstrator cost. The demonstrator vehicle was designed both for self-launch and for launch from existing booster stages.

The CRC subcontractor team members played a critical role in this effort. Their efforts especially addressed the structure, subsystems, and propulsion required for a successful HOT EAGLE system. Study efforts in these areas are summarized below and are detailed in the separate subcontractor final reports that are included as an appendix to this report.

2.1. Propulsion Options and Analysis (XCOR Aerospace)

Propulsion options for the HOT EAGLE operational and demonstrator designs were defined

and analyzed, including engine, nozzle, propellant feed, and thrust vector actuation. Propulsion system data sufficient for vehicle design purposes was provided for alternative HOT EAGLE systems including vertical land, horizontal land, and upper stage applications. Technologies offering near and far-term improvements in propulsions system weight and performance were described and assessed.

2.2. Structure Concepts and Analysis (Convergence Engineering with support from Composite Engineering Inc.)

This task included structural design, FEA, and weight and cost estimation for the HOT EAGLE vehicles. A major new element of the HOT EAGLE design was the incorporation of structurally integral propellant tanks, versus the separate tanks of the prior designs. Another new and important activity was the structural design and assessment of alternative means to attach the thermal protection system (TPS), including both bonded and mechanically attached thermal TPS.

2.3. Avionics and Subsystems (Universal Space Lines)

Avionics, electrical, actuation, and other subsystems were defined for the HOT EAGLE demonstrator design with variations suitable for both RUS and global troop transport systems. This definition was based on a detailed listing of mission and system requirements, and included preliminary selection of off-the-shelf components where suitable. The avionics effort defined the avionics system top-level requirements and functions including data buses and computers. The flight control effort defined the flight control system top level requirements and functions including flight control interfaces, redundancy management and control effector mechanization, actuators, reaction controls, and sensors. Weights were detailed and used in the vehicle design analysis.

3. BACKGROUND: SYSTEM APPLICATIONS

3.1 RUS

The USAF has a significant need for space launch capability that is affordable, flexible, and responsive. While the total number of flights per year is small compared to, say, aircraft flights, the military value of those flights is almost immeasurably high. Space assets provide essential capabilities including intelligence, surveillance, and reconnaissance (ISR), signals intelligence (SIGINT), communications, navigation, remote sensing, weather prediction, and event detection, and are an integral force multiplier for almost every military operation today.

The desirability of a reusable launch vehicle is self-evident. With the exception of portions of the Space Shuttle, the launch vehicles used for USAF space launches are destroyed during each flight. Purchase of vehicle hardware is a substantial portion of the launch cost, unlike aircraft where the air vehicle itself is an amortized and reusable asset.

Disposable launch hardware also has an impact on responsiveness and surge capability. It is unaffordable to keep a number of expendable launch vehicles at the ready to respond to an emerging need such as for a reconnaissance asset over a new world trouble spot. Instead, an emerging need must be met by accelerating and rescheduling a launch already in the queue. Surge capability is limited by production capacity and the availability of long-lead manufacturing items. This contrasts to aircraft, where an emerging need can be met by using an aircraft in the hanger, and an immediate surge requirement can be met by putting on additional ground crew shifts to turn the aircraft more quickly. Such a capability for the USAF launch vehicle fleet would be highly desirable.

Greater responsiveness and lower price per flight would quite likely further increase the role of space assets in USAF operations, much as the lowered price of global satellite positioning (GPS) receivers has produced an explosion of applications, many not anticipated.

The obvious advantages of reusability must be measured against the negatives. A reusable launch vehicle must be designed to reenter, return to base, and land in some fashion. The thermal protection system, aerodynamic surfaces, control actuation, long-duration subsystems, and landing gear all add weight to the vehicle. Due to the large growth factor inherent in launch vehicle design, the weight penalty is multiplied many times over when applied to a system requirement.

The decision – reusable vs. expendable – depends ultimately upon the available level of technology. Previously, the provision of reusability increased the weight and cost so much that the cost benefits of reusability were swamped by the added costs of the heavier, more-complicated booster. Recent studies by the USAF and Aerospace Corp. indicate that the tide may have turned, and that a fully reusable first stage now offers a net benefit for USAF applications. This is the basis for the hybrid launch vehicle contracts recently announced* (HLV, formerly known as ARES).

*In the interest of full disclosure, CRC is a major subcontractor on the Science and Technology Applications Inc. winning team for HLV/ARES, and will perform the design studies.

HLV is based on a reusable first stage with an expendable upper stage, which the Aerospace Corp. study results indicate is optimal with today's level of technology. CRC agrees with this conclusion, but also thinks that in the foreseeable future the level of technology may permit a reusable upper stage as well. This would further reduce launch costs and improve launch responsiveness. Thus, a major objective for the HOT EAGLE study was the design and analysis of such a reusable upper stage ("RUS") and the determination of the required level of technology to make it feasible.

3.2 Global Troop Transport

The other operational system being considered by the HOT EAGLE project is an out of the box idea for providing a highly desirable national military capability – the insertion of ground troops to anywhere in the world in an extremely short amount of time. Recent events have offered several cases where such a capability could have accomplished major military objectives such as the capture of terrorist leaders whose location was momentarily known, or the securing of suspected weapons of mass destruction as they were being transported away from a known location.

Today, such troop insertion would be accomplished by helicopter or parachute from a cargo airplane, but the flight time alone would often exceed the time window of opportunity. Obtaining diplomatic permission for over flight by weapons-carrying troops is problematic and certainly not rapid. Helicopters are vulnerable, and parachutes do not provide a means of egress.

The notional HOT EAGLE solution is a rocket-boosted global range troop transport. This vehicle would carry a standard 13-man USMC squad and would be launched using either an expendable first stage booster or a reusable HLV-type booster. The vehicle would follow a suborbital or part-orbit trajectory and reenter over the target area, gliding downward and making a vertical or short landing in an unprepared location. Egress would be provided either by flying the vehicle out under power or by getting it towed out by a recovery aircraft such as a C-17.

This is, obviously, quite challenging. It may be impossible or at least impractical and unaffordable. However, the HOT EAGLE study results below show several possible approaches including at least one near-term option that would be feasible with current technologies. Given the high value of such a capability, it is worth continuing the study of such a system despite the DARPA-hard nature of its development.

Such a system could even be used for cargo delivery. While most cargo would not be worth the expense, one can imagine missions for which it would such as the resupply of already-inserted special troops, or the delivery of an antidote for a biological warfare pathogen.

4. BACKGROUND: VEHICLE CONFIGURATION

The HOT EAGLE project was able to leverage from the previous Micro-X design studies conducted by CRC for the USAF (AFRL/VA). Under Micro-X, various design concepts for a reusable first stage were defined, analyzed, and optimized. A subscale demonstrator vehicle was also designed and assessed, and numerous design and technology trade studies were conducted.

As the Micro-X studies progressed, a problem was uncovered which, perhaps, has not received sufficient attention in previous studies of reusable launch vehicles that are to glide back in a horizontal attitude. Such vehicles must have a propellant mass fraction (PMF) of over 80% to attain the desired performance at an affordable gross weight. While innovative vehicle arrangements are conceivable, most design concepts have the rocket engines and other heavy masses in the rear. When the propellant tanks are empty such vehicles have an extremely rearward center-of-gravity (c.g.). This makes it difficult to provide an aerodynamically stable configuration during the horizontal gliding phase.

CFD analysis of the baseline Micro-X concept uncovered such instability, and in a follow-on study a number of design layout alternatives were studied to find an optimal solution. These are detailed in the final report for that project phases. The best configuration, and the basis for the HOT EAGLE designs, resembles the X-20 Dynasoar design with the addition of all-moving outboard triangular elevons. X-20 was to have been the follow-on to the X-15 program and would have paved the way for a Space Shuttle-like design, but was cancelled in favor of the capsule re-entry approach used for Apollo.

The X-20 configuration attained acceptable stability by using large tail surfaces that extended behind the aft end of the fuselage, and furthermore the reentry vehicle did not have large propellant tanks (it was to be boosted by expendable lower stages). To make such a design stable with large empty propellant tanks, and without extending the tails behind the plane of the rocket exhausts, appears quite impossible. Instead the HOT EAGLE design was configured to be moderately unstable, with artificial stability provided by all-moving triangular elevons as shown below.

This design proved to have an acceptable level of instability with reasonable control surface gains* at all Mach numbers. CRC subcontractor Analytical Methods Inc. modeled and analyzed this concept using their vortex lattice code VLAERO, then modeled it for high-end CFD analysis using their Navier-Stokes solver, NSAERO. Results are detailed in the AMI project final report⁶. Note that this design is not naturally stable, but it is not too unstable and has sufficient control authority to allow the flight control computer to provide the desired level of artificial stability during gliding flight, much like a modern fighter aircraft.

* This refers to the ratio of control deflection to vehicle angle excursion. For example, in pitch it would be the required elevon deflection to recover divided by the upset angle of attack. A gain of one implies that 1 degree of downward elevon deflection is required to recover from a 1 degree nose-up pitch excursion. This is considered to be the reasonable upper limit by stability and control engineers and was used in the HOT EAGLE design effort.

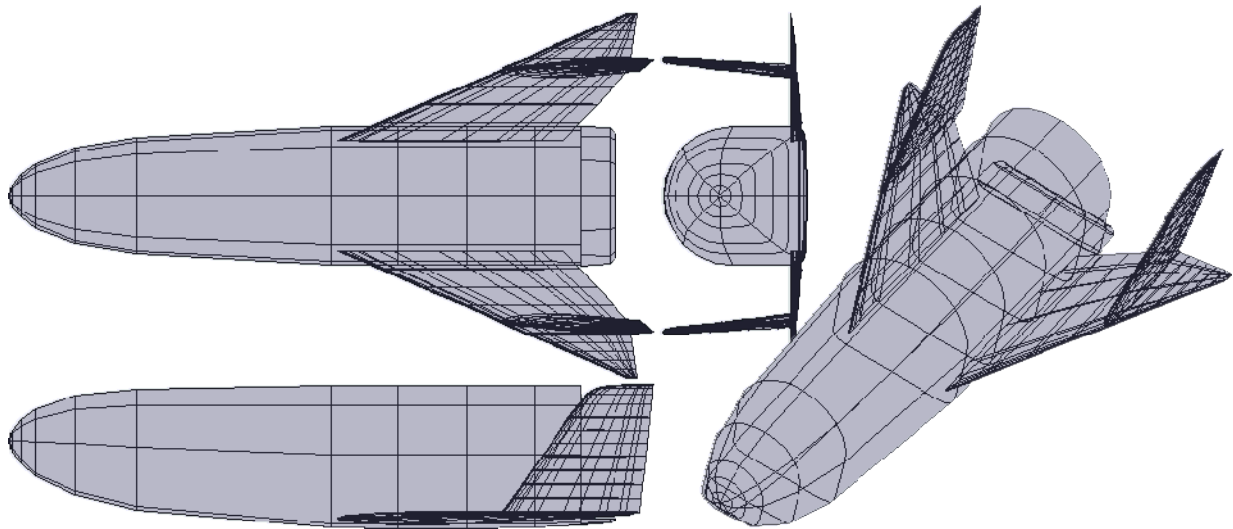


Figure 1. Preferred Aerodynamic Concept – Swept Tails with Outboard Elevons

The outboard elevons would not be used during reentry. They would be locked in an undeflected position to avoid local heating effects. As with the Space Shuttle, the reaction control system (RCS) would be used for control during reentry. The elevons would become active once the vehicle reached a low enough altitude that the dynamic pressure built up to a level where the RCS becomes inadequate. The body flaps could be used during reentry if needed for trim and roll control.

These tail surfaces are quite large. As the HOT EAGLE project evolves it will be a design goal to reduce their size to the minimum consistent with providing adequate artificial stability while maintaining acceptable control gains and margins of safety. This will be done by an improved knowledge of the vehicle aerodynamics gained from future CFD and wind tunnel tests, by 6-DOF dynamic simulation with actuation response modeling, and by positioning of the vehicle center of gravity as far forward as possible through judicious component relocation.

This last strategy involves a tradeoff – many components could be moved forward but will result in an increase in vehicle empty weight. For example, if the propellant pumps are located in the nose it would help the center of gravity problem but would add long propellant lines carrying cryogenic fluids at high pressure - slightly over engine chamber pressure. These lines would be heavy and dangerous as well. Similarly, batteries could be moved to the nose but would require long heavy power cables and would reduce the delivered amperage, requiring even larger batteries.

5. THOUGHT EXPERIMENT – IMPACT OF REUSABILITY

5.1 Thought Experiment Overview

As the planning for the HOT EAGLE project was initiated, a simple question often arose: “why do reusable launch vehicle designs have such poor propellant mass fractions compared to expendable boosters?” This is a crucial question considering the impact of propellant mass fraction on performance. It was therefore decided to devote a small portion of the project effort to investigate this question via a thought experiment, so-called because it relies more on relative measures and traceable changes than rigorous technical analysis.

Basically, existing expendable upper stages were incrementally modified to obtain recovery and reusability, and the attendant weights changes were traced step-by-step, as depicted below. The results are interesting, although perhaps not conclusive.

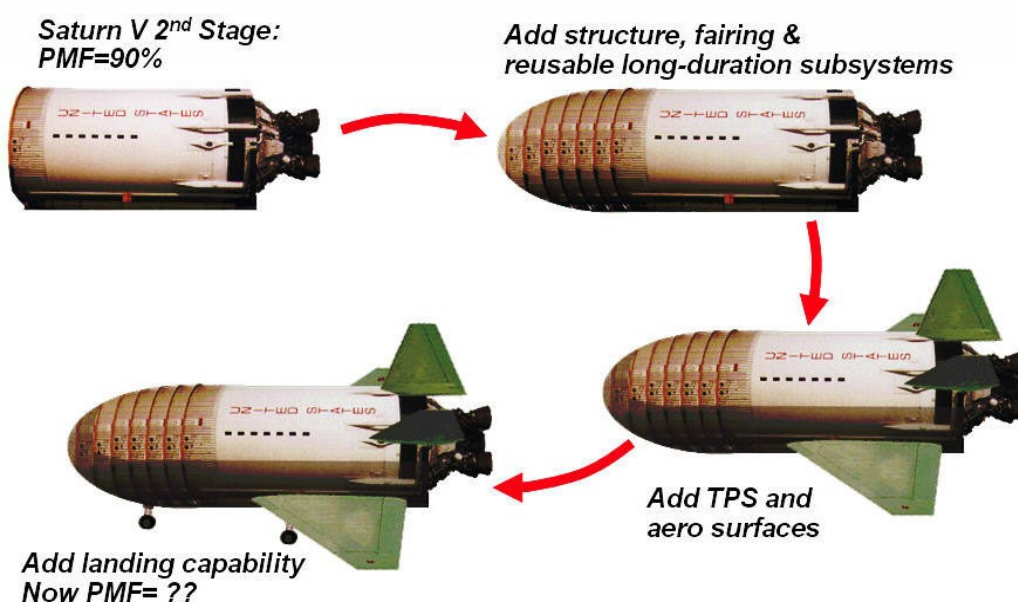


Figure 2. Thought Experiment Approach

5.2 Calculations

Conceptual Research Corporation began this effort with the selection of an existing upper stage to use as the starting point. Initially it was thought that the Saturn V second stage would be a good candidate due to its excellent PMF. This was used in the task approach illustration presented at the kickoff briefing (above). However, the Saturn V second stage was deselected due to poor traceability to the likely reusable upper stage designs. The Saturn stage is far larger than any likely new stage. Using it for the thought experiment would draw the argument, of course you can build something with a high propellant mass fraction if it's that enormous.

The Delta II upper stage was ultimately selected for the initial thought experiment. This decision was made because the Delta upper stage is the smallest of the readily available upper stages with significant capability, and because there is the possibility of traceably removing a great deal of weight from the secondary structure in the area of the payload fairing support structure. The tanks are constructed from stainless steel, the rocket engine is a pressure fed AJ-

10 storable propellant engine. The stage already includes avionics. Currently in production, the Delta II upper stage is one of the most reliable stages in existence, and has a propellant mass fraction of over 87%.

To make the stage reusable, a series of modifications were notionally defined*. A permanent aerodynamic nose cone and payload fairing would be required to support reentry, atmospheric gliding flight, and mission abort with payload retained. On the actual Delta II the payload fairing is discarded as soon as the vehicle leaves the atmosphere, to improve performance.

A thermal protection system is also necessary to protect the vehicle during reentry. For the Delta II upper stage, the higher allowable temperatures of the stainless steel structure suggest that TPS thickness and weight can be reduced from the values required for an all-aluminum or all-composite design. Should aluminum or composite structure be selected for an actual reusable upper stage, the structure weight would decrease while the TPS weight would increase, with a relatively minor net change in system weight.

A landing system is required – it was decided to assume a winged horizontal landing to avoid the need to traceably add the extra propellant volume for landing fuel, and the complexities of traceably modifying upper stage engines for efficient operation at sea level, throttled conditions.

The design of the landing system is made more complex by the fact that the system must land with the payload either present or absent. Most current designs for reusable launch vehicles show the payload carried externally in a piggyback location, although this has an unfavorable drag effect on ascent. This was assumed here, but a detailed layout was not prepared for this thought experiment nor was the drag impact accounted for in the delta-V calculations below.

The vehicle structure of a Delta upper stage is not designed to take horizontal loads during gliding flight, which are primarily applied at the wing root, nor is it designed for landing impact loads. These are the primary drivers of structural weight in aircraft, and must be accounted for in any credible assessment of the impact of reusability on stage design. Use of vertical landing** will reduce the additional loadings but not eliminate them entirely – the vehicle must still reenter and glide horizontally through the often-turbulent atmosphere, and a vertical launch vehicle is not stressed for such loads.

An RCS system is required to control attitude during coast and reentry. Actuation power for the aerodynamics surfaces during gliding flight and landing is also required.

* There is no intention of proposing nor building a reusable upper stage which is actually based on an existing expendable stage. The design, engineering, and test effort this would entail is at least equal to that of an all-new reusable upper stage, and performance would suffer from the older technology and scar weights of the old components.

** A vertical landing stage must carry additional propellant and equipment for that landing, which should be charged against the usable PMF.

The resulting weight changes to a Delta II upper stage are summarized below, assuming a 4,000-lb payload requirement. Beginning with the existing stage, a new fairing is added which is assumed to weigh 2/3 less than the original because of its smaller size, the use of advanced technology, and the elimination of vertical carry-through loads. A TPS is assumed to be externally applied, at about 2/3 the overall areal weight of the shuttle's TPS (which weighs 1.54 psf) due to the higher temperature substructure and the use of advanced technology over the shuttle baseline.

Wing and stabilizer weights were estimated by comparison with the detailed weight estimates done by Composite Engineering Inc.³ for the Micro-X study. These weights were found to be similar to those of the aero-surfaces of the Learjet 24, a business jet with similar landing weight and gross weight, which provides an independent corroboration.

The structural weight penalty of the addition of horizontal lift and landing loads was estimated as a 30% penalty. This is just a guess, and would be a good subject for detailed analysis but that level of detail is beyond the scope of this task.

Table 1. Delta II Weight Progression – Expendable to RUS

Item	Weight (lbm)	Comments
Upper Stage Empty Mass	1,931	From Delta II Weight Statement
Delete Excess Structure	-400	Payload fairing adapter
Add Nosecone & Fairing	600	~1/3 current fairing wt - smaller, adv tech, no carry-through load
Add horizontal loads penalty	639	WAG - 30% penalty
Add Wings/Stabilizers	1,000	Micro-X VTHL, Lear 24 wing+tails stabilizers (~same W-landing)
Add RCS & propellant	450	Micro-X analysis
Add actuation power supply	515	Micro-X analysis
Add TPS	700	Assumed 1.0 lb/ft ² (over hot structure)
Add Undercarriage	500	5% of landed weight
Total Empty Weight	5,935	
Payload	4,000	Assumed requirement
Total Landed Weight	9,935	
Propellant Weight	13,400	From Delta II Weight Statement
Gross Weight	23,335	
Propellant Mass Fraction	69.3%	Gross weight excludes payload
Propellant Mass Fraction	57.4%	Gross weight includes payload
Ideal Delta-V	12,131	fps - no payload
Ideal Delta-V	8,771	fps - with payload
Ideal PMF, original stage	87.4%	Gross weight excludes payload
Delta-V, original stage	21,282	fps - no payload

For the landing gear, five percent of landing weight was assumed. This is assumed to be 3% for the gear itself, and 2% more for installation and the thermally sealed doors required for hot-side landing gear, taking into account the fact that this landing gear is only for landing so a weight savings should be expected vs. aircraft landing gear.

The weight of the power supply for the aerodynamic surface actuators, which must operate continuously during glide and landing, was estimated from Micro-X analysis, as was additional RCS system weight required for attitude control during coast and reentry.

This Delta II stage already has substantial flight control avionics, the Redundant Inertial Flight Control Assembly (RIFCA, built by L3 Communications). It was assumed that the increased capabilities required for autonomous reentry and landing would be met by new avionics of the same installed weight.

The results are interesting. Excluding the payload, the propellant mass fraction goes from 87% for the original expendable stage, to 69% for the notional reusable stage. The contributors to this can be seen below (note that the “Delete Excess Structure” item is actually a reduction in weight). The original weight, the large blue sector behind the legend box, is the largest item. Addition of the aerodynamic surfaces is the largest change but not by an overt amount. Other items are all about the same, indicating that no single item drives the weight increase. Instead it results from a number of similar contributors, indicating that no one fix will greatly impact this result.

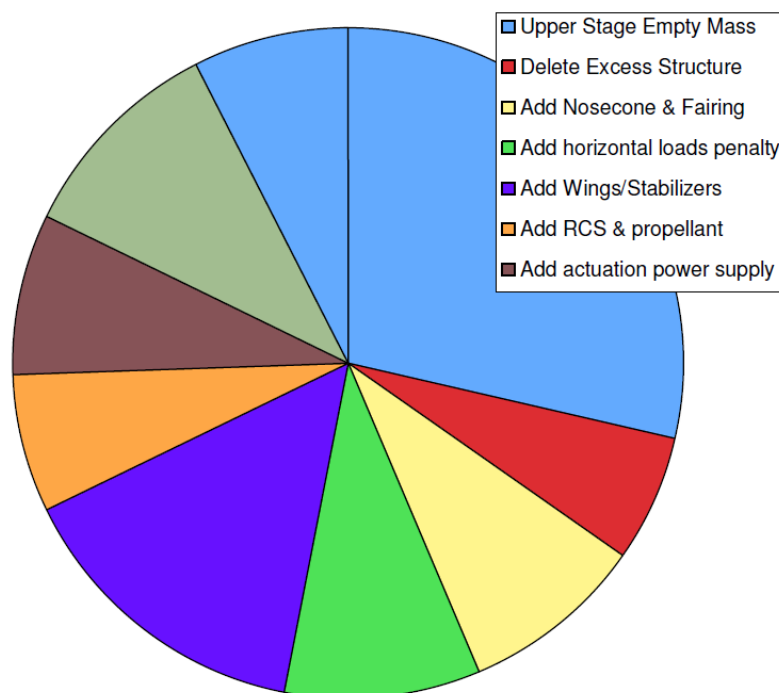


Figure 3. Contributors to Weight Change

Following this analysis, a second thought experiment was made starting with the Space-X Falcon I first stage. Unlike the Delta II second stage, the Falcon I first stage uses dense RP propellant. This reduces stage size and structural weight providing a better PMF, but at the cost of a poorer Isp.

The weight impacts of adding recovery and reusability to the Falcon I were estimated similarly to the previous thought experiment based on stage geometry and landed weight. Results are

shown in Table 2*. The actual Falcon I first stage enjoys a PMF of almost 94%. Adding aircraft-like reusability drops that to about 83% – better than either the modified Delta II or the Micro-X design, but still a 12% reduction.

Table 2. Falcon I Weight Progression – Expendable to RUS

Item	Weight (lbm)	Comments
Upper Stage Empty Mass	3032	From Falcon Data
Delete Excess Structure	-250	Fairing
Add Nosecone & Fairing	600	~1/3 of current Delta fairing
Add horizontal loads penalty	1,015	WAG - 30% penalty
Add Wings/Stabilizers	1,320	10% landed wt from Micro-X VTHL, Lear 24
Add RCS & propellant	600	Micro-X analysis ratioed up 33% for change in wt
Add actuation power supply	686	Micro-X analysis ratioed up 33% for change in wt
Add TPS	1500	Assumed 1.5 lb/ft ² (over cold structure)
Add Undercarriage	660	5% of landed weight
Total Empty Weight	9,163	
Payload	4,000	Assumed requirement
Total Landed Weight	13,163	
Propellant Weight	42341	From Falcon data
Gross Weight	55,504	
Propellant Mass Fraction	82.2%	Gross weight excludes payload
Propellant Mass Fraction	76.3%	Gross weight includes payload
Ideal Delta-V	17,734	fps - no payload
Ideal Delta-V	14,782	fps - with payload
PMF, original stage	93.3%	Gross weight excludes payload
Ideal Delta-V, original stage	27,792	fps - no payload

In comparing these propellant mass fractions with those of proposed designs, the effects of scale must be considered. Larger aerospace vehicles tend to have a lower fraction of weight taken up with empty weight items such as structure, propulsion, and equipment, when compared with smaller vehicles. This leaves more weight available for propellant for the larger vehicles. Based on a CRC regression analysis of historical data, going from the 50,000 lb gross weight of the Falcon I first stage to the likely 500,000 lb of a USAF operational stage would improve the propellant mass fraction by about 2.5%, or from 82.2% to 84.2% for the modified stage. This should be considered in comparing proposed designs to these thought experiments.

* Note that the Falcon I is considered by Space-X to be reusable in that it is designed to deploy a parachute and be recovered from a water splashdown and be refurbished. This level of reusability, while beneficial, is unlike the land it and fly it reusability that the USAF desires. Also, being a first stage this vehicle does not already have near-orbital reentry capabilities so it must be added for our thought experiment.

5.3 Reusability Thought Experiment Conclusions

Two existing expendable stages, the upper stage of the Delta II and the first stage of the Falcon I, were notionally modified to reusable upper stage designs in an attempt to answer the question, "Why do proposed reusable launch vehicle designs have poor propellant mass fractions compared to existing expendable boosters?"

Based on this analysis the simple conclusion would be "because recovery and reusability add a lot of weight."

This unsurprising conclusion is supported by an item-by-item weight buildup of the required changes to obtain reentry, recovery, and reuse. The weight impacts detailed above are debatable, and any of them could be argued down. However, it is doubtful that all of the weight increases described above can be greatly reduced, and the total system weight gain comes not from one or two "big ones", but from a number of roughly-equivalent penalties.

Thus, the key lesson from this thought experiment is that we should not be looking for a single "breakthrough" to obtain high PMF in a reusable launch vehicle. The problem is the summation of a number of penalties rather than one single big penalty. Obtaining reusability in a launch vehicle with desirable performance will require improvements in a number of areas - structure, TPS, RCS, subsystems power supply, landing gear, etc.

6. RUS

6.1 Design Requirements

The RUS design effort began with the definition of design requirements. When setting requirements it is always crucial to strike a balance between meeting all legitimate customer needs, and promising too much to gain the widest support – the everything for everybody trap. This drives up weight, cost, and risk, and ultimately reduces the likelihood of eventual program success. CRC addressed requirements definition by starting with a historical survey of boosters and payloads. Ideal delta-V calculations and a spreadsheet-based trajectory code were used to assess and normalize capabilities, with graphs prepared of the results. Design-to requirements were then defined.

Current and recent domestic and foreign stages were identified and tabulated based largely on data from Isakowitz's *International Guide to Space Launch Systems*⁷, plus information from the online Encyclopedia Astronautica⁸ (www.astronautix.com) and several manufacturers' websites. In some cases educated guesses were used to fill out missing information. Available performance figures for launch of payloads to 100 nmi circular orbits were also collected. The full data tabulation is available in a previous CRC report⁵.

Where 100 nmi orbit data was not available, a spreadsheet-based trajectory code* was employed to estimate the payload to 100 nmi. This was done by taking the closest available performance point and using the trajectory code to back out what the stage performance and staging conditions were that resulted in that payload value. Then the staging conditions were adjusted for inclination using trigonometry and the trajectory code was rerun for a 100 nmi orbital altitude. Launch was run for three combinations of launch latitude and inclination – 28.5 degrees representing Canaveral/KSC launch, and 52 and 90 degrees for Vandenberg AFB launch. Non-U.S. vehicles were also analyzed as if they were being launched from U.S. ranges. Results are tabulated and graphed in the figures and tables that follow.

The data shows a wide range of capabilities, ranging from 732 lb to polar orbit (Pegasus), to 21,000 lb to a 29 degree LEO (Ariane 4). There are a number of launchers in roughly the 5,000-lb payload category, including the Delta and Titan which have been extensively used by the USAF and are shown by heavy lines on the graph.

*Excel-based fourth order Runge-Kutta numerical integration of the equations of motion, with mathematical adjustment for Earth rotation. Written by M. Burnside Clapp (not at government expense).

Table 3. Existing Launcher Payload to 100 nmi Orbit

	Orbit Inclination (deg)		
	29	52	90
Angara	5,394	4,316	3,790
Ariane 4	21,400	18,659	18,300
Athena	4,520	3,755	3,470
Atlas II	16,130	13,997	13,650
Delta 7320	6,320	5,142	4,620
Kosmos	3,225	2,692	2,502
Long	8,610	6,352	4,905
Minotaur	1,408	1,146	1,030
M-V	4,100	3,309	2,940
Pegasus	977	803	732
PSLV	6,120	5,029	4,580
Rockot	4,805	3,903	3,500
Shavit LK2	3,645	2,959	2,650
Taurus	2,910	2,416	2,230
Titan 23G	5,414	4,518	4,200
Tsiklon	7,290	5,847	5,150
Falcon 1	1,525	1,200	1,080
Falcon 5	13,310	11,300	9,859

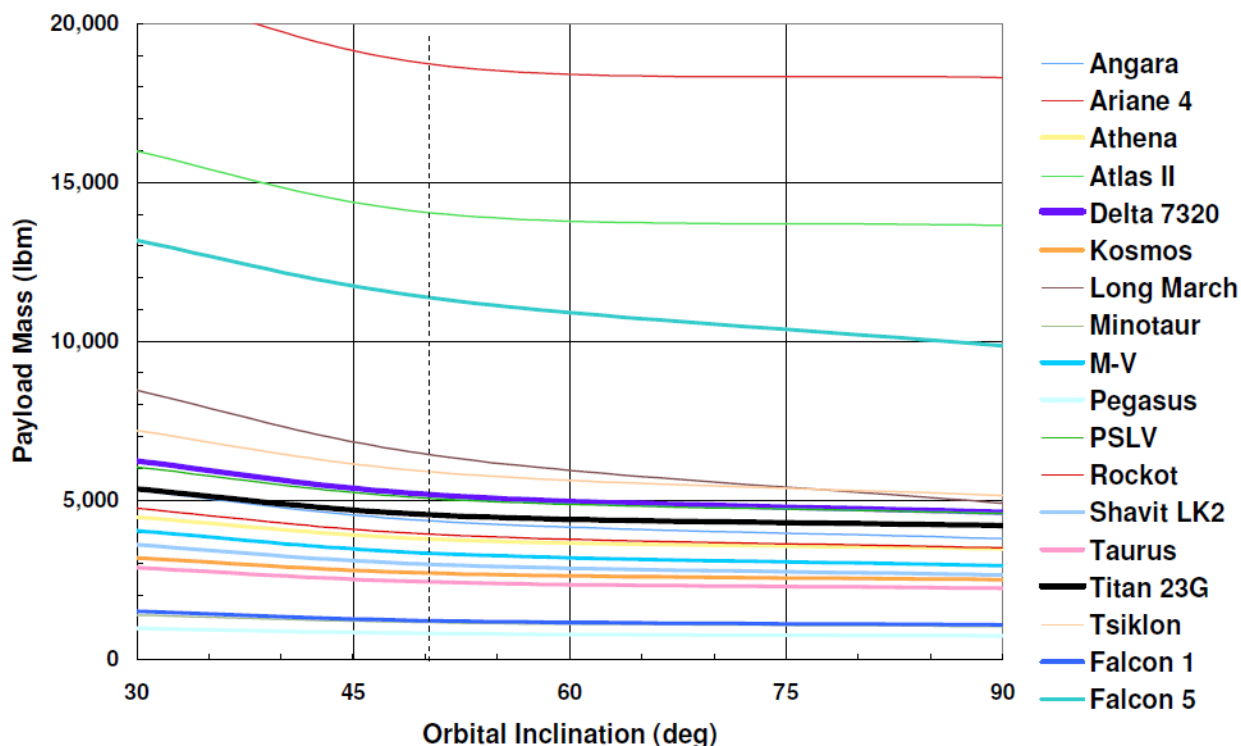


Figure 4. Orbit Weights vs. Inclination

To assist in the definition of system requirements, an attempt was also made to obtain mass and orbit data on a number of existing USAF payloads. This proved to be difficult in an unclassified environment. Relevant information was found in the online Encyclopedia Astronautica⁸ but its accuracy is uncertain. Also, this public source information undoubtedly does not represent the most current, let alone future payloads. However, Table 4 is presented as a rough guide to USAF expectations in launcher capabilities.

Table 4. Approximate USAF Payload Characteristics

Name	Category	Orbit	Weight kg	Weight lb	Typical Launch Vehicle
Milstar	Communications	GEO	4,500	9,900	Titan IV
DSP block 14	Early Warning	GEO	2,358	5,188	Shuttle, Titan 4
Singleton	Signals intelligence	430 nmi	1,700	3,740	Titan II
KH-9 Big Bird	Film-return reconnaissance	140 nmi	11,400	25,080	Titan 3D, 34D

Obviously, the full range of USAF booster requirements encompasses both large and small payloads. Attempting to meet all USAF needs with a single next-generation launch system will drive the cost skyward (pun intended).

Other considerations in defining requirements for the HOT EAGLE reusable upper stage are the stated desires of the USAF/SMC, as expressed in the HLV/ARES solicitation. ARES was the original acronym, later changed to HLV (Hybrid Launch Vehicle), and is to consist of a reusable first stage with an expendable second stage. Tables in the solicitation indicate a desire

for at least 10,000-lb payload to a 100 nmi LEO at the Canaveral/KSC inclination (15,000 lb is preferred).

Based on the information and analysis above, HOT EAGLE reusable upper stage design requirements were defined under the following three fundamental strategies and assumptions:

- Equivalent capabilities as Delta (~5,000 lbs)
- Compatibility with expected HLV/ARES reusable first stage
- Recovery of payload in abort scenarios

A greater payload than the Delta's would be desirable to increase the number of payloads that could be launched by this reusable system. A lesser payload capability would reduce the reusable upper stage cost, but would tend to exclude many payloads that the USAF commonly launches. A 5,000-lb capability seems just right and would place this system about in the middle of the current and recent boosters shown above. This payload capability ensures that many USAF payloads could be launched from this system, and of course other launch systems will exist which could handle heavier payloads.

Compatibility with HLV is based on the presumption that the HLV program will continue, succeed, and eventually place an operational system into the inventory. Such a system will have an expendable upper stage which could potentially be replaced by the HOT EAGLE Reusable Upper Stage for some missions.

HLV is to have a payload weight of 10,000 to 15,000 lb to LEO using an expendable upper stage. A reusable upper stage with a payload weight of around 5,000 lbs is likely to weigh about the same as an expendable stage of 10,000 to 15,000 lb, namely about 75,000 lb*. One can postulate a flexible system with a reusable first stage, where the few larger payloads use (and discard) an expendable upper stage, while the bulk of launches use the available reusable upper stage. This offers a spiral development approach as well – the initial HLV/ARES would be developed with near-term technologies then a later reusable upper stage would be developed with a later technology level.

The final strategy assumed for RUS requirements definition is the ability to recover the payload in an abort scenario. This stresses the system design requirements, but offers such cost savings for the few times it will be used that it will likely pay for itself in the long run. It also expands future applications of the reusable upper stage including the possibility of a man-rated version at some future date.

Based on the above data and considerations, the HOT EAGLE reusable upper stage system design requirements were therefore established and are tabulated in Table 5.

* Based on a spreadsheet delta-V calculation incorporating publicly-stated HLV/ARES staging conditions

Table 5. Design-To Requirements – HOT EAGLE RUS

Kinematic Performance
5,000 pounds to LEO - Canaveral/KSC launch 3,000 pounds to LEO - Polar orbit Launch from expendable or HLV/ARES-derived 1st stage All-altitude abort and engine-out capability with payload
Operational Attributes
Aircraft-like turnaround operations, robust subsystems, BIT Propulsion minimizes or eliminates catastrophic failure modes Affordable, reusable, & low maintenance TPS Adverse weather capability
System Goals
Ground crew and operations personnel less than ten people Landing-to-launch turnaround time of 4 to 24 hours Overall system reliability of 99.9%.

Launch from HLV requires keeping the RUS weight below that which the HLV can boost – whatever HLV design is ultimately selected. While the selected contractors will define their own system concepts, previous analysis indicates that an HLV-class booster should be able to place a 75,000 lb upper stage at a velocity of over 7,000 fps and an altitude of about 200,000 ft. It was further assumed that about 2,000 lb of additional weight would be required for attachments and equipment associated with carrying and releasing an upper stage, leaving 73,000 lb for the upper stage GLOW.

The dimensions of the RUS payload were inferred by historical comparison. A survey of existing USAF stages (below) indicates an average payload density of 5.5 lb per cubic foot. Rounding this down to 5 lb per cubic foot yields a required volume of 1,000 cubic feet, and assuming an 8-foot payload diameter yields a payload length of 20 feet.

Table 6. Payload Bay Geometry

	Weight	Length	Diameter	Width	Height	Approx Vol	Density
DSP	5250	28	13.7			4125.4262	1.27
DSCS	2716	6		6	7	252	10.78
MilStar	10000	51	8			2562.24	3.90
GPS	1860	17.5	5			343.4375	5.42
KH-7	4400	35	5			686.875	6.41
Average:							5.55
HOT EAGLE RUS	5000	20	8		1004.8		4.98

6.2 RUS Configuration Concepts

The configuration concept for the HOT EAGLE RUS was based on the aerodynamic configuration developed during the Micro-X Phase Five study⁵, as described above. This features a highly swept wing with vertical tails near the tips. Outboard of the vertical tails are all-moving elevons, configured to provide maximum pitch authority.

Two baseline versions were defined for study – HL (horizontal lander*) and VL (vertical lander[†]), shown in Figure 5.

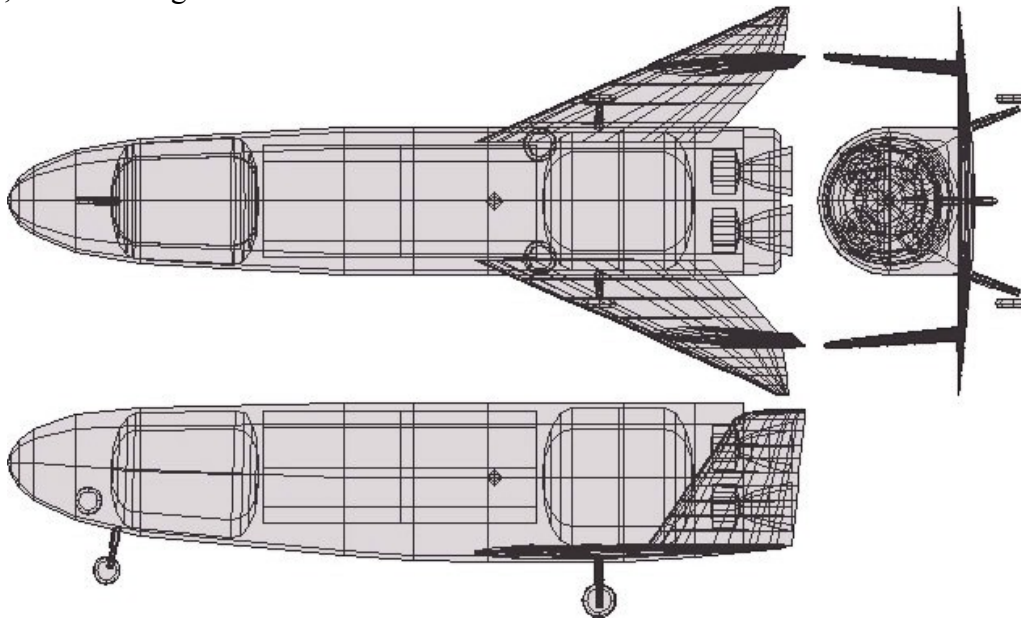


Figure 5. RUS Configuration - HL

* Referred to as “HE-RUS” in data file naming

[†] Referred to as “HE-RUSVL” in data file naming

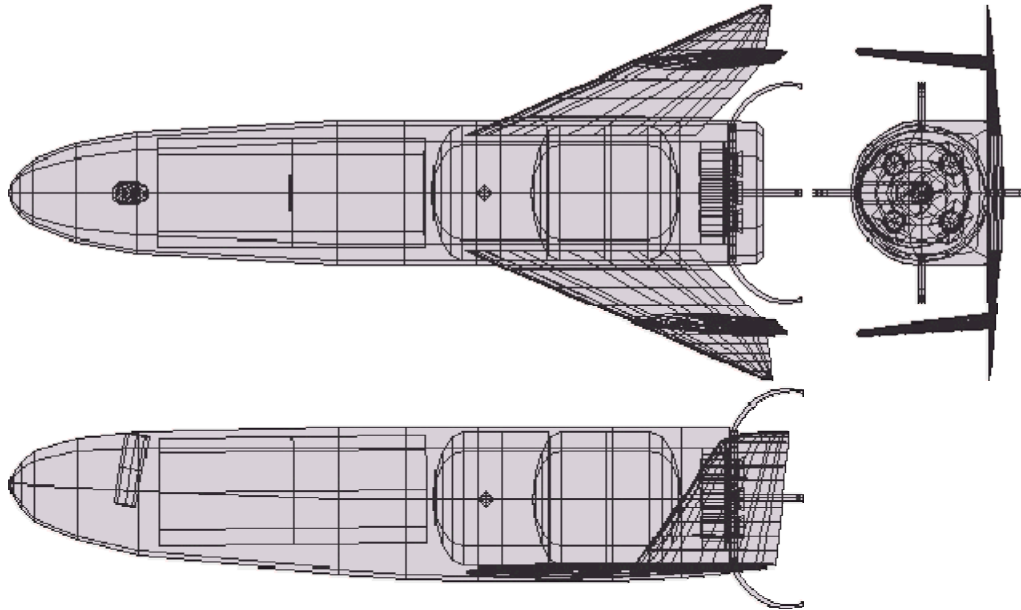


Figure 6. RUS Configuration - VL

These have the same external configuration since it was found that the horizontal tails required for stability are actually large enough to act as wings and provide a reasonable stall speed. Both Reusable Upper Stage concepts were sized to the maximum allowable GLOW of 73,000 lb to allow carriage and launch on an HLV/ARES-class reusable first stage. This gives a length of 57.3 ft., with a span of 27.9 ft and body diameter of 10.8 ft.

Space Shuttle-like landing gear is incorporated on the HL version, whereas the VL version has curved gear legs extending from the base that wrap around the engines when retracted.

Table 7. Reusable Upper Stage Design Data

	HE-RUS	HE-RUSVL
W-gross	73000	73000
W-empty	10353	10314
W-payload	5000	5000
W-misc UL	1201	2503
W-propellant	56446	55183
PMF	77.3%	75.6%
# engines	4	5
T per engine	20000	16000
T/W	1.1	1.1
Length	57.3	57.3
Diameter	10.8	10.8

One of the design requirements is for abort recovery with the payload. Thus, the vehicle must be capable of controlled flight and landing with payload in or out. The payload is a substantial fraction of the vehicle empty weight, so its location has a huge effect on center of gravity. This is especially a problem for the horizontal landing version, which must slow nearly to stall speed

for landing. At low speed, a vehicle with c.g. far enough forward with payload out has a c.g. too far forward with payload in, and possibly could not be trimmed for landing. For this reason, the baseline HL version above has its payload placed between the LOX and CH4 tanks whereas the vertical lander can have the payload in front of both tanks. The latter approach permits integrated common-bulkhead tanks which results in a weight savings both in tank and in insulation. An alternate horizontal lander with the payload in front was defined as well*, attaining a slight weight savings, but detailed analysis will be required to prove that it is possible to trim it for landing.

The RUS external vehicle aerodynamic geometry is tabulated below, and is identical for HL and VL versions. The TrapWing column is the equivalent trapezoidal wing used for analysis reference, and is found by extending the inner wing leading edge out to the tip of the outer elevon surface, then adjusting the trailing edge to obtain an area equal to the total of these surfaces.

Table 8. Reusable Upper Stage Tail and Reference Geometries

	Wing-Inner	Wing-out2	Tails	TrapWing
Area Sref	320	43	75	363
Aspect Ratio	1.2	1.59	1.3	2.14
Taper Ratio	0.42	0.08	0.44	0.13
Sweep (LE)	66.3	66.3	35	66.3
Sweep (c/4)	62.703	60.146	28.839	62.467
Airfoil	NACA 64A-010	NACA 64A-010	NACA 64A-010	NACA 64A-010
Thickness t/c	0.06	0.06	0.099	0.06
Dihedral	3	3	85	3
Twist	0	0	0	0
Span	19.596	8.269	9.874	27.871
Root Chord	23	9.63	10.549	23.051
Tip Chord	9.66	0.77	4.642	2.997
Mean Chord	17.221	6.452	7.97	15.582
Y-bar	4.232	1.48	4.297	5.18
X loc (apex)	24.44	46.77	46.63	24.44
X loc (c/4)	38.386	51.755	51.631	40.135

Composite primary structure is assumed, with a tile or blanket thermal protection system plus carbon-carbon nose cap and leading edges. Tanks are load bearing and are of composite integral construction, actually forming the primary loadbearing structure of the fuselage in that area. This design approach is detailed in the companion HOT EAGLE structural design report by Convergence Engineering.

* Referred to as "HE-RUS2" in data file naming

On these baseline designs, the payload is carried internally. This reduces drag on ascent and, when the payload is being recovered, improves cross range and glide ratio on reentry and landing. Potential problems with vertical center of gravity on launch and vertical landing are minimized with this approach. Internal carriage also simplifies the flight acceptance of other payloads because there are no airloads on the payload, and the vehicle external configuration doesn't change with a change in payload.

An alternate design concept based on a semi-permanent external payload shroud is shown below for the vertical landing RUS* (the HL version would be similar except for landing gear). Note that the vehicle's fuselage is smaller than those of the designs above since the payload is not contained in the fuselage, but of course the huge external pod adds its own weight and drag. In the absence of detailed aerodynamic analysis it was assumed that tail sizes would be unchanged. Probably, the horizontal tails could be slightly reduced in size but the vertical tails would have to be increased in size. Also, the vertical c.g. location may make it difficult to land vertically with the landing gear shown. All in all, such a design would probably have similar system capabilities to the baseline with internal carriage, but was not studied in detail in this contract.

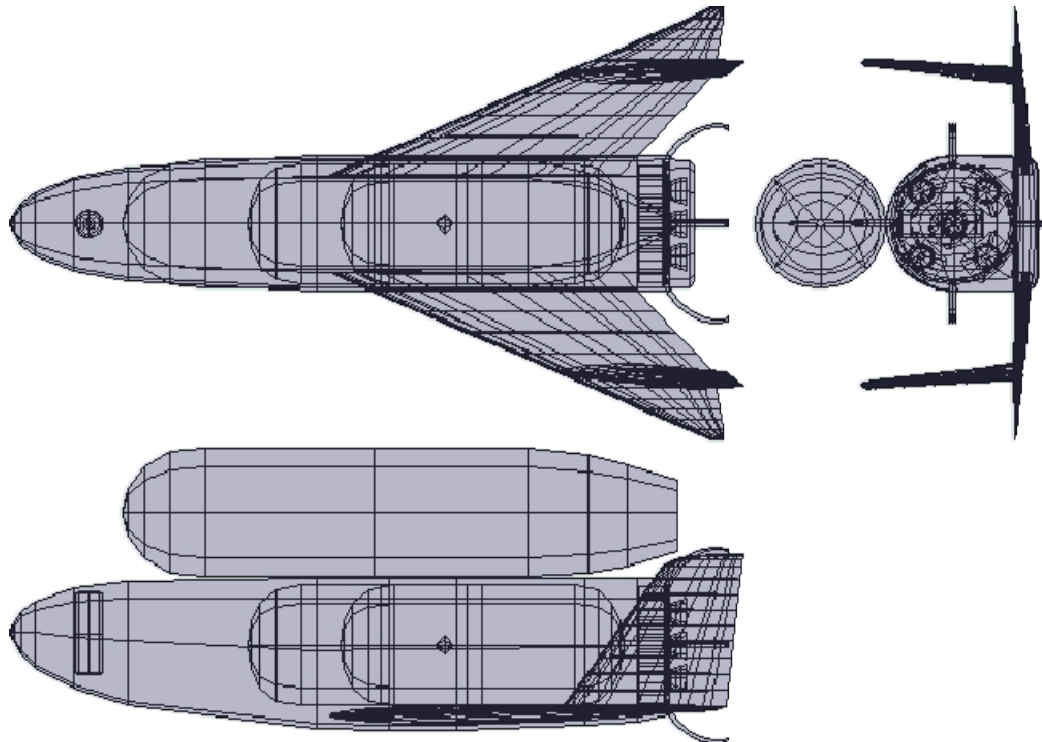


Figure 7. Alternate RUS Configuration – VL

* Referred to as “HERUS-EX” in data file naming

6.3 Vehicle Analysis – Propulsion

Propulsion for the HOT EAGLE design studies was defined and analyzed by XCOR Aerospace Inc. based on CRC-provided thrust needs and operation scenarios. In their final report, attached as an appendix to this report, the details of their assumptions and analysis can be found. The XCOR engine designs incorporate their piston-pump technology integrated into the engine head. Piston-pump technology potentially offers lower development cost and good throttleability, but the resulting engine design parameters are not atypical for turbopump designs and the use of the piston-pump design for this study should not be taken to restrict the HOT EAGLE project to such engine designs.

It was decided based on prior study and consultation with XCOR and others to use LOX-methane rocket engines for the RUS. Methane provides an improved Isp and promises maintenance benefits, and it facilitates a common bulkhead integral tank since the temperatures are similar to those of LOX. XCOR also defined LOX-RP engines for comparison study.

The engines designed by XCOR for the Reusable Upper Stage operational system are optimized for upper stage use and hence have large bell nozzles which would restrict operation much below 100,000 ft. altitude (see below). This is not a problem for a RUS which glides to a horizontal landing, but is problematic for a vertical landing design. A VL-RUS would need one or more engines compromised for sea level operation which would somewhat impact total Isp.

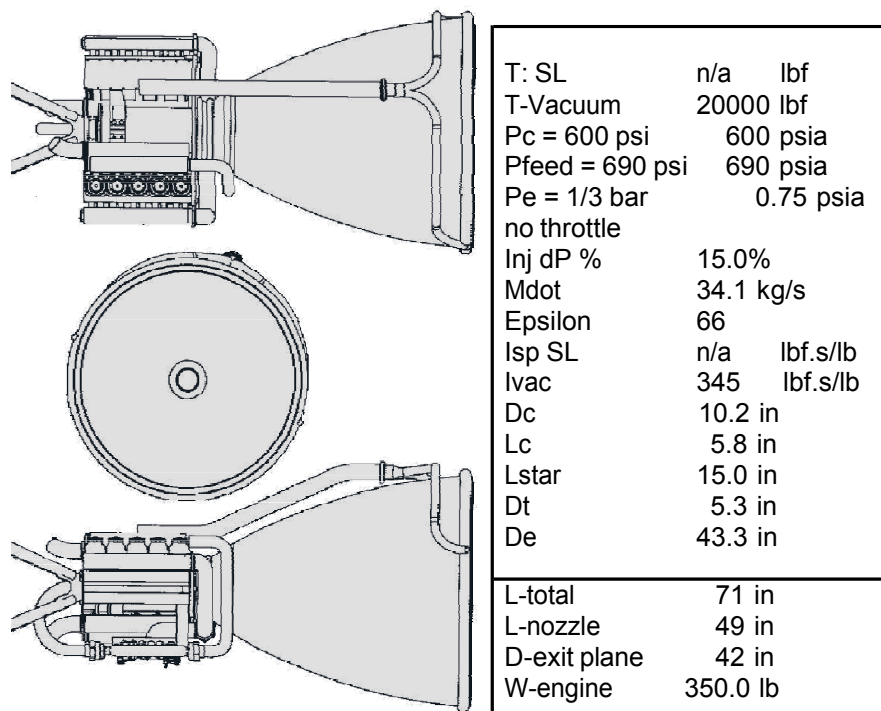


Figure 8. XCOR RUS Engine

XCOR performed a study of advanced technologies that could be used to improve the performance and weight of 2015 time-frame operational engines. Results indicate that a modest Isp benefit may be obtained, on the order of 7% better than the baseline technology Isp of 345.

This improved Isp value of 370 seconds was used for the RUS studies below. A bigger savings is found in the propulsion weights, estimated at 30% and used in the weight calculations below.

Parametric analysis reported in the Micro-X study⁵ indicates that four engines should be used for a horizontal landing vehicle. This is driven by the desire to shorten the nozzles and to provide an engine-out capability for abort scenarios, allowing the vehicle to reposition itself for a safe recovery if an engine failure prevents attainment of orbit. According to XCOR weight analysis this only imposes a weight penalty of about 100 lb total versus a single, longer engine. Multiple engines also avoid the need for throttling since one can shut off engines as propellant burns off and acceleration becomes excessive. This in turn provides an Isp, weight, and engine complexity benefit, although the greater number of engines adds its own complexity.

For a vertical landing vehicle, the required number of engines is driven by the throttling capability for landing. It is necessary to reduce total thrust to slightly less than the landing weight. For the demonstrator design (see below), an expected landing weight of 20% GLOW and a comfortable throttling capability of 68% indicates that five engines are required. This was used for all VL designs in this study.

6.4 Vehicle Analysis – Aerodynamics

For performance purposes the aerodynamic analysis was performed using the classical methods of the RDS-Professional program (as described in Raymer⁹), calibrated and adjusted using results from the Micro-X computational aero studies⁶. Aerodynamic analysis results are summarized in the following graphs. The first shows the calculated slope of the lift curve, including comparisons with the computational results from AMI's VLAERO and NSAERO codes. These show reasonable agreement, with the RDS results being generally more conservative (the vehicles are not exactly identical, but close enough for comparison purposes). Next is the calculated lift-to-drag ratio (L/D) in reentry and gliding flight. At hypersonic speeds, where the vehicle flies at high angles of attack, the lift is about equal to the drag. During subsonic gliding flight the L/D indicates that the vehicle goes almost four feet forward for every foot of altitude lost.

Maximum lift coefficients were estimated using RDS empirical methods (mostly DATCOM adjusted for Newtonian lift at high Mach number). These indicate a subsonic maximum lift coefficient of almost 1.5, but CRC subcontractor AMI determined that the usable lift at low speeds would likely be much lower due to trim effects and the extreme angle at which maximum lift would be obtained. Thus, the available subsonic maximum lift was estimated at 0.75, reducing to the Newtonian value of 0.3 at high Mach number. This provides enough lift for a reasonable horizontal flight stall speed so the horizontal landing version does not need additional wing area to land. The tail size required for stability provides enough lifting area for landing.

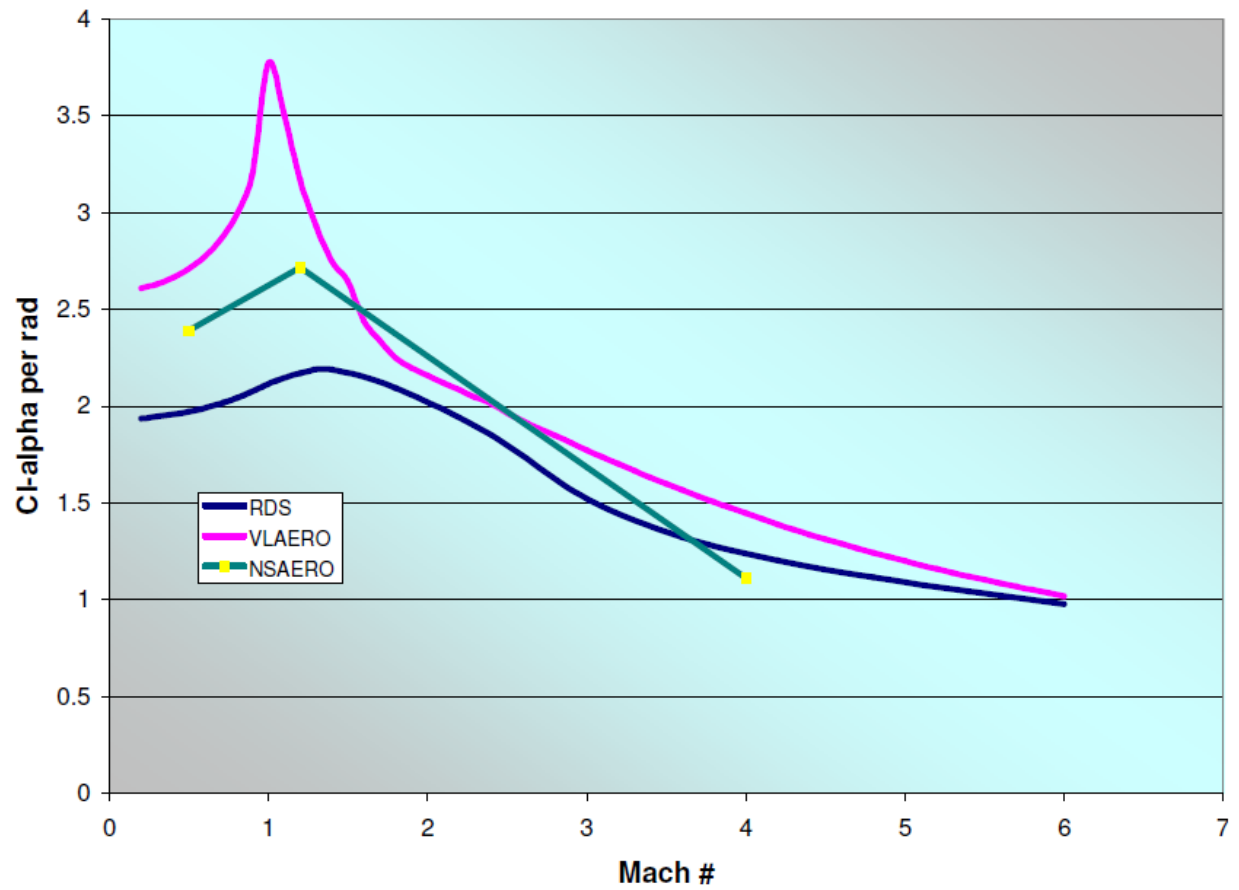


Figure 9. RUS Lift Curve

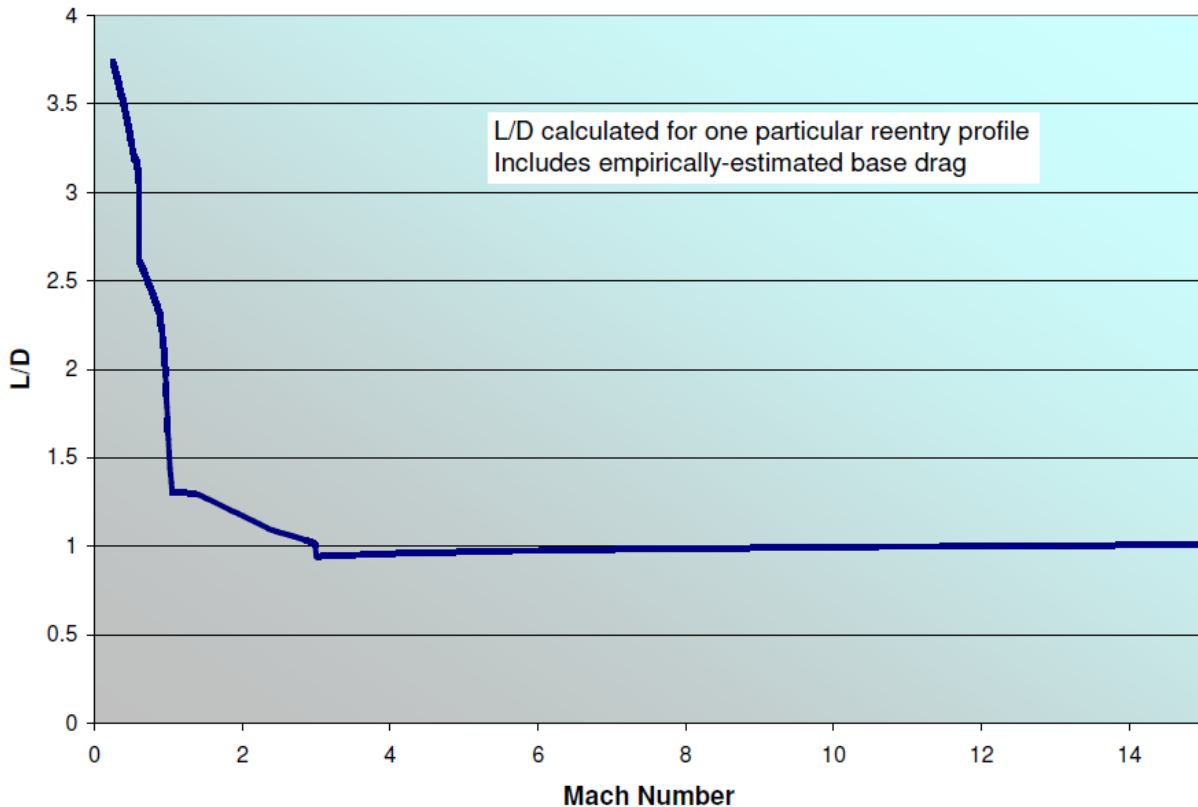


Figure 10. RUS L/D Ratio

6.5 Vehicle Analysis – Weights

Vehicle weights were calculated by a detailed build-up method. The structural weights were based upon structural design and FEM analysis performed under subcontract by Convergence Engineering, Inc., with unfunded assistance from previous CRC subcontractor Composites Engineering Inc. To save time and permit a greater fidelity Convergence actually designed and analyzed the major structural components for the already-available Micro-X demonstrator configuration including body, tails, tanks, tank supports, thrust support, and landing gear, then performed FEM stress analysis to determine required skin and substructure thicknesses. The resulting weights estimates were ratioed and adjusted to represent the HOT EAGLE Reusable Upper Stage geometry and loading conditions. The work done by Convergence Engineering is described in detail in their companion report.

Subsystem and avionics weights were estimated by CRC subcontractor Universal Space Lines, based on architecture definition and component selection as described above. See their companion report for full details; also see the comparison table in the Appendices to this report. The USL subsystems and avionics weights results were adjusted to represent the RUS operations and conditions.

TPS weights are based on work done by the University of Dayton Research Institute under separate funding. UDRI provided TPS weights for different regions of the vehicle based upon thermal analysis and TPS system optimization. Installation and attachment weights were estimated by Convergence Engineering and added to the UDRI TPS weights.

Other weights are based upon off-the-shelf equipment, statistical analysis, and expert opinion.

The resulting weights estimates are shown below for the horizontal landing RUS. These weights have been adjusted to represent likely 2015 technology levels and should be considered attainable but “DARPA-hard”. The estimated empty weight includes a 2% margin and totals 10,353 lbs. Following that is a conservative re-estimation of weight representing current technology, and including a 5% empty weight margin. This yields an empty weight totaling 15,015 lbs, which essentially uses up the desired payload weight. Thus, a clear conclusion at this point is the urgent need for technologies producing substantial weight reductions.

This analysis is based on the configuration where the payload is placed between the LOX and CH₄ tanks. As described above, it would be desirable from a weight point of view to place the tanks together sharing a common bulkhead. This places the payload at the front of the vehicle which is problematic from a balance point of view, but reduces the empty weight to 10,115 lbs, a savings of 238 lbs. This seems insufficient of a savings to incur the balance problems. Results are summarized below.

Table 9. HL RUS Weights

	Weight lbs	Loc ft	Moment ft-lbs		Weight lbs	Loc ft	Moment ft-lbs
STRUCTURES	5747		195253	EQUIPMENT	2469		81253
Wing (inner panel)	205	47.0	9655	Flight Controls (EMA)	877	42.0	36835
Wing (outer panel)	85	52.4	4451	Instrumentation	14	5.0	69
Wing (carry-through)	90	44	3967	Wiring	476	34.0	16174
Tails	237	52.4	12420	Electrical (Power)	46	34.0	1564
Fuselage	1380	30.0	41390	Avionics - Fwd Bay	85	4.0	340
Door & Bay Cutout	227	28.6	6489	Avionics - Engine Bay	263	51.0	13404
Body Flaps	71	54.9	3908	Avionics - Thermal Mgmt	330	30.0	9888
Integral Tanks	777	31.3	24335	Battery	162	5.0	808
			0		0	5.5	0
Gear Doors&Wells	221	33.6	7409	Misc Equipment	0	4	0
Landing Gear	441	33.6	14818	RCS System	217	10	2171.157
TPS	2012	33.0	66411	(% We Allowance)	2		
			0	Empty Weight Allowance	203	35.9	7288
PROPULSION	1935		87909	TOTAL WEIGHT EMPTY	10353	35.9	371704
Engines (4)	978	52.9	51740				
Mount & Misc Install	321	50.7	16285	USEFUL LOAD	62647		
			0	Start & Residual Prop	805	31.3	25205
			0	Boost Propellant	56446	31.3	1766752
			0	RCS Propellant	396	17.8	7048
			0	Land Propellant			0
Prop Pressurization	360	31.3	11272	Payload	5000	28.6	143000
Propellant Insulation	275	31.3	8612				
			0	TAKEOFF GROSS WEIGHT	73000	31.7	2313708

Table 10. HL Reusable Upper Stage Weights - Conservative

	Weight lbs	Loc ft	Moment ft-lbs		Weight lbs	Loc ft	Moment ft-lbs
STRUCTURES	8557		289164	EQUIPMENT	3122		104207
Wing (inner panel)	289	47.0	13577	Flight Controls (EMA)	1169	42.0	49113
Wing (outer panel)	119	52.4	6259	Instrumentation	14	5.0	69
Wing (carry-through)	127	44	5579	Wiring	595	34.0	20218
Tails	333	52.4	17466	Electrical (Power)	46	34.0	1564
Fuselage	2217	30.0	66520	Avionics - Fwd Bay	106	4.0	426
Door & Bay Cutout	274	28.0	7659	Avionics - Engine Bay	329	51.0	16755
Body Flaps	100	54.9	5495	Avionics - Thermal Mgmt	412	30.0	12360
Integral Tanks	1250	31.3	39109	Battery	162	5.0	808
			0			5.5	0
Gear Doors&Wells	276	33.6	9261	Misc Equipment	0	4	0
Landing Gear	551	33.6	18522	RCS System	289	10	2894.876
TPS	3022	33.0	99716	(% We Allowance)	5		
			0	Empty Weight Allowance	715	35.9	25668
PROPULSION	2621		119998	TOTAL WEIGHT EMPTY	15015	35.9	539038
Engines (4)	1397	52.9	73915				
Mount & Misc Install	402	50.7	20356	USEFUL LOAD	57985		
			0	Start & Residual Prop	759	31.3	23746
			0	Boost Propellant	51830	31.3	1622292
			0	RCS Propellant	396	17.8	7048
			0	Land Propellant			0
Prop Pressurization	450	31.3	14090	Payload	5000	15.3	76500
Propellant Insulation	372	31.3	11638				
			0	TAKEOFF GROSS WEIGHT	73000	31.1	2268624

Table 11. Effect of Bay Location on RUS c.g. and Stability

	Mid Bay	Forward
Xcg-empty	35.9	36.8
Xcg-with	33.0	32.5
Δ Xcg	2.9	4.3
Δ - % Stability	18.4%	27.6%
Empty Weight	10353	10115

Weights are estimated below for the vertical landing (VL) design. This concept has its tanks together, sharing a common bulkhead. The payload is therefore at the front of the vehicle which should not be a problem for a vertical landing vehicle. The VL landing propellant weight includes an estimated boiloff of 1% per hour for a 12-hour maximum mission length.

Table 12. VL RUS Weights

	Weight lbs	Loc ft	Moment ft-lbs		Weight lbs	Loc ft	Moment ft-lbs
STRUCTURES	5457		191662	EQUIPMENT	2654		82271
Wing (inner panel)	205	47.0	9655	Flight Controls (EMA)	877	42.0	36835
Wing (outer panel)	85	52.4	4451	Instrumentation	14	5.0	69
Wing (carry-through)	90	44	3967	Wiring	476	34.0	16174
Tails	237	52.4	12420	Electrical (Power)	46	34.0	1564
Fuselage	1311	30.0	39321	Avionics - Fwd Bay	85	4.0	340
Door & Bay Cutout	182	21.1	3843	Avionics - Engine Bay	263	51.0	13404
Body Flaps	71	54.9	3908	Avionics - Thermal Mgmt	330	30.0	9888
Integral Tanks	689	41.2	28397	Battery	162	5.0	808
			0	Pitchover Chute	185	5.5	1018
			0	Misc Equipment	0	4	0
Landing Gear	574	33.6	19289	RCS System	217	10	2171.157
TPS	2012	33.0	66411	(% We Allowance)	2		
			0	Empty Weight Allowance	202	36.8	7440
PROPULSION	2001		98086	TOTAL WEIGHT EMPTY	10314	36.8	379459
Engines (5)	1076	52.9	56914				
Mount & Misc Install	321	50.7	16285	USEFUL LOAD	62686		
			0	Start & Residual Prop	793	41.2	32651
			0	Boost Propellant	55183	41.2	2273523
			0	RCS Propellant	396	17.8	7048
			0	Land Propellant	1314	41.2	54156
Prop Pressurization	360	41.2	14837	Payload	5000	21.1	105500
Propellant Insulation	244	41.2	10050				
			0	TAKEOFF GROSS WEIGHT	73000	39.1	2852338

Empty weight for the VL version totals 10,314 lb, slightly down from the 10,353 lb of the horizontal landing design. The difference is minor because the designs are essentially the same other than the landing gear and tank geometry. This differs from prior studies where the vertical lander had much smaller aerodynamic surfaces and therefore benefited from a substantial structural weight savings. As described above, the tails found to be required for stability turn out to be large enough for landing, and don't need to be increased in size. However, the vertical lander still requires an additional amount of propellant for landing estimated as 1314 lb, so the vertical landing design suffers a nontrivial disadvantage in available propellant for boost.

6.6 Mission Timeline and Trajectory Analysis

HOT EAGLE RUS missions will begin with launch from a first-stage booster which may be an HLV/ARES-derived or similar reusable stage, or from an expendable first stage booster. Separation would occur at about 2 to 3 minutes at approximately 200,000 ft. The upper stage burn would take about 4 minutes at which point orbit would be obtained.

Alternatively, and with somewhat better performance, the upper stage burn could be cut short and restarted after a coasting period to circularize the orbit. Payload would then be released.

Reentry could occur at the end of a 90-minute once-around orbit, but a substantial cross range capability would be required to return to base (~1,500 nmi). This was a significant cost driver for the Space Shuttle and should be avoided for HOT EAGLE. Instead, a de-orbit burn at 7 ½ orbits will result in a landing at the launch site, half an orbit later. This results in a total mission time of just under 12 hours. Recovery could occur at a West coast location only two orbits after an East coast launch, but that is operationally less desirable.

Trajectory analysis of the Reusable Upper Stage was done using a module of the RDS design program called "ROAST" ("RDS Optimal AeroSpace Trajectories"). This is based on the equations and methods in Sutton¹⁰, Bate¹¹, Griffin¹², and Koelle¹³ and follows the vehicle through time step integration of $F=ma$. ROAST has been verified with comparisons to the industry-standard POST program, and seems to give credible results for preliminary studies. The ROAST runs used in this study are available in EXCEL format from CRC.

The trajectory analysis assumed first stage separation conditions of an HLV/ARES-class launcher, namely 7,000 fps at 200,000 ft altitude. The target orbit for the 5,000-lb payload is a 100 nmi circular orbit from a due-East Canaveral launch. Trajectory results indicate that the baseline RUS misses its target orbit by 613 fps, which is equivalent to 850 lb of empty weight turning magically into propellant. Parametric trajectory runs indicated several ways to attain orbit, the first being to reduce the payload to 4,150 lb (shown in the figures below). Or, the full 5000 lb payload could be orbited provided that the first stage can provide separation at 250,000 ft and 7,500 fps. The full payload could also be orbited if the RUS GLOW were increased to 78,000 lb without increasing the empty weight.

This analysis is based on the need to obtain full orbital speed in the HE-RUS so that it can make enough orbits to return to its original launch point. Other options are possible, including fly-back using turbojets or tow-back using a catcher aircraft (see Figure 11), or simply recovery at a different location. These would permit a once-around trajectory which reduces the delta-V requirement by about 1,300 fps, according to analysis by Schafer & Associates. Parametrically rerunning the HE-RUS trajectory with this assumption finds an increase in payload to orbit to 6,800 lb from the 250,000 ft, 7,500 fps staging point, assuming no change in vehicle weight. This is a 60% increase in payload, so this option deserves serious consideration.

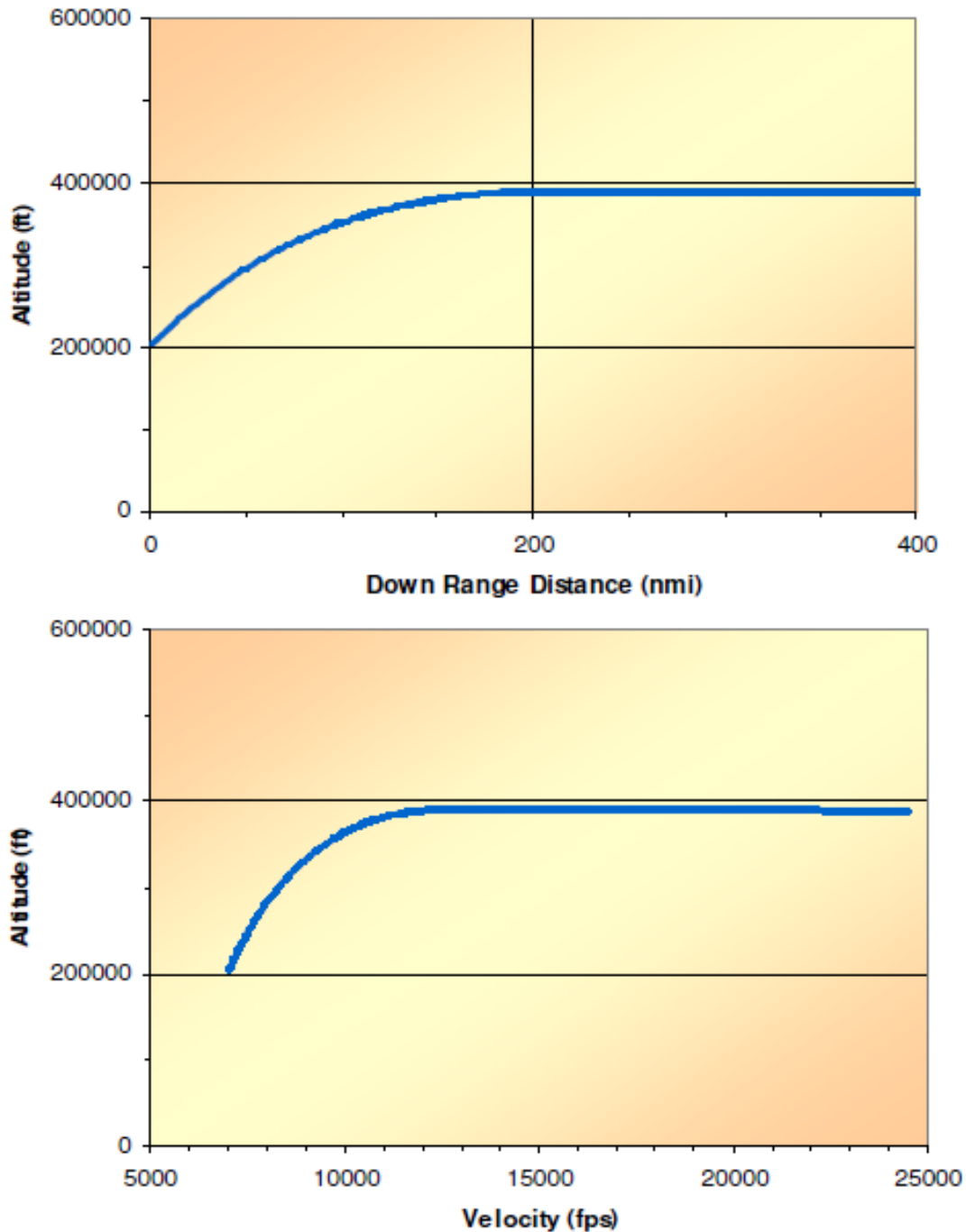


Figure 11. Upper Stage Trajectory Analysis

Even more, if a once-around orbit is always used then the subsystems requirements are relaxed compared to a long duration orbit requirement. This reduces electrical power, RCS, and internal thermal control requirements saving an estimated 532 lb in system weight and 310 lb in RCS propellant weight. This increases the payload weight to 7600 lb for a once-around orbit.

The upper stage boost end conditions and the calculation of the propellant required to circularize its orbit are tabulated below. This propellant weight is included in the total boost propellant, and is set aside in the ROAST boost calculations. Propellant for the de-orbit burn is estimated and included separately (see weight estimates above).

Table 13. Trajectory Analysis- Boost End Conditions & Orbit

1st Burn Cutoff Altitude 1st	389106	ft fps
Burn Cutoff Velocity V-cutoff+	24488	fps ft
V-Earth	25788	fps
Target Orbit: Altitude	607600	fps
Vorbit Transfer Orbit: Vperigee	25578	fps
Vapogee	25774	lbs
Circ. Burn Propellant Weight	25513	

Next is the reentry trajectory analysis. This assumes an initial condition of 100 nmi and 24,000 fps. Skip and no-skip trajectories are shown. The skip trajectory maintains the initial reentry angle of attack until the Mach number falls below 3.0, which occurs at about 135,000 ft. The no-skip trajectory reduces angle of attack such that lift equals weight as soon as the velocity vector points horizontally, and therefore takes a greater distance to slow down.

6.7 Reusable Upper Stage Summary and Conclusions

The Phase One study results for the HOT EAGLE Reusable Upper Stage indicate that such a system is possible, offering substantial payload to orbit from an HLV/ARES-class reusable first stage booster. As would be expected, this payload is less than that obtained from an expendable upper stage. Detailed cost tradeoff studies including the operational benefits of reusability need to be conducted to ultimately validate the utility and desirability of reusability for an upper stage. It is important to realize that these favorable benefits depend upon the aggressive use of advanced technologies, some of which have yet to be realized.

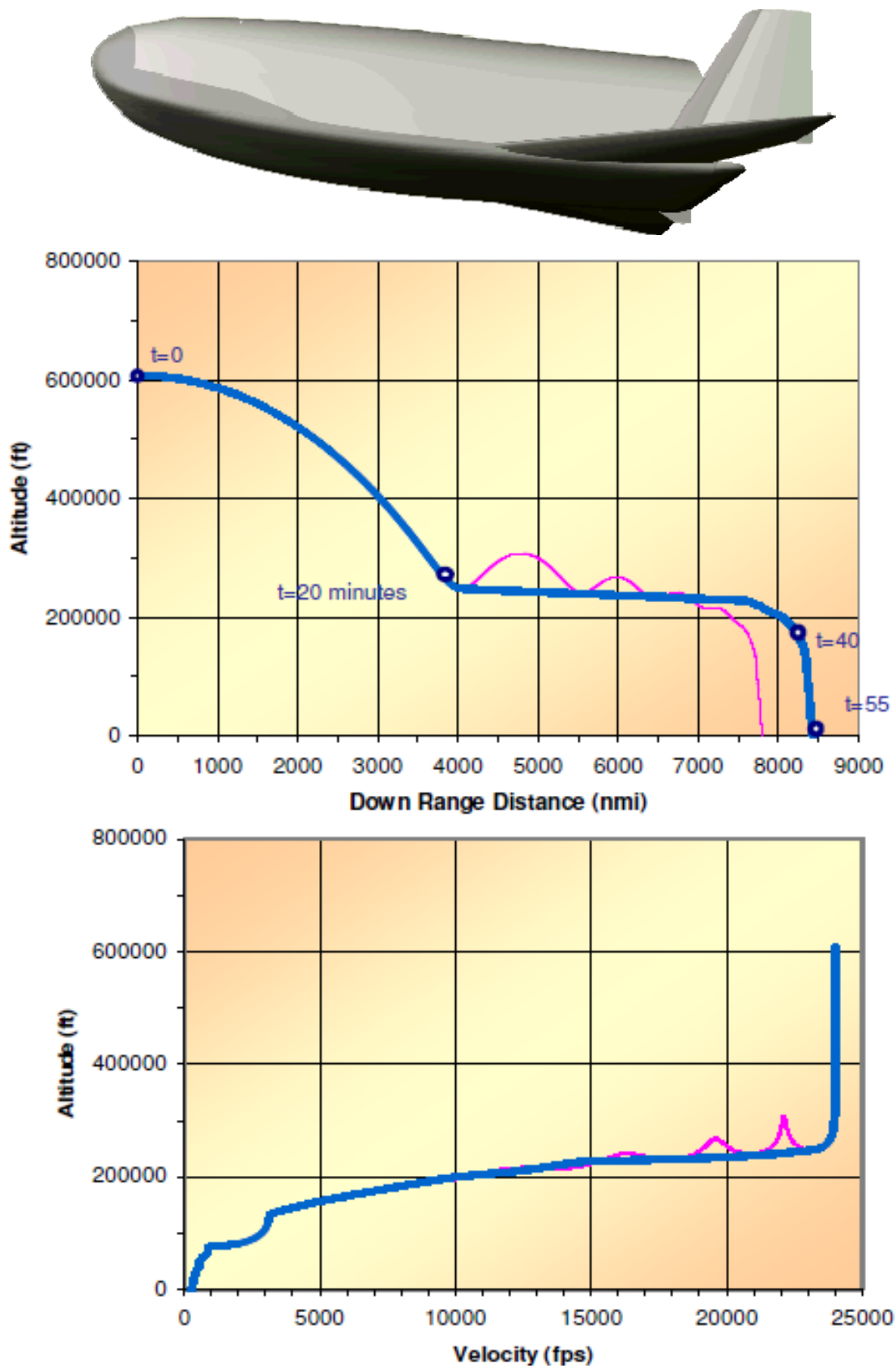


Figure 12. Reentry Trajectory Analysis

7. GLOBAL TROOP TRANSPORT

7.1 Design Requirements and Compartment Dimensions

The HOT EAGLE Global Troop Transport, briefly described in the Background section above, is an “out of the box” idea for providing the capability to insert ground troops to anywhere in the world in an extremely short amount of time. This could be used to quickly seize strategic locations, capture terrorist leaders, secure suspected weapons of mass destruction, or transport super-high-value assets such as antidotes to biological weapons. Fundamentally it consists of a reusable reentry and landing vehicle which is boosted using either an expendable first stage booster or a reusable HLV-type booster. The vehicle would follow a suborbital or part-orbit trajectory and would reenter over the target area, gliding downward and making a vertical or short landing in an unprepared location. After completion of the ground mission the vehicle would egress and recovery in some fashion (options are investigated below).

The troop/cargo compartment requirement is based on carrying a standard 13-man USMC Rifle Squad. The Rifle Squad can be considered to be the “elementary molecule” of US ground power projection and was standardized in its current form on May 1944 under Table of Organization F-1. It consists of a Squad leader (Sergeant) and three fire teams, each consisting of a Corporal commanding three Privates.

For the Global Transport design work, a minimal-size troop compartment was sized based on standard dimensions for military personnel as used when designing military troop-carrying aircraft such as the C-17. These dimensions are shown below. After studies of different arrangements it was decided that the optimum arrangement is simply side-by-side seating in seven rows. An extra space is provided in the first row for an additional seat or for bulky equipment. This arrangement generates a cylindrical compartment which is 24 ft in length and 6 feet in diameter, with 36-inch seat pitch. There is no aisle for entrance or egress. Instead, three staggered gull-wing doors are provided, two on one side and one on the other, such that when these doors are open a nearly 360-degree field-of-fire is afforded.

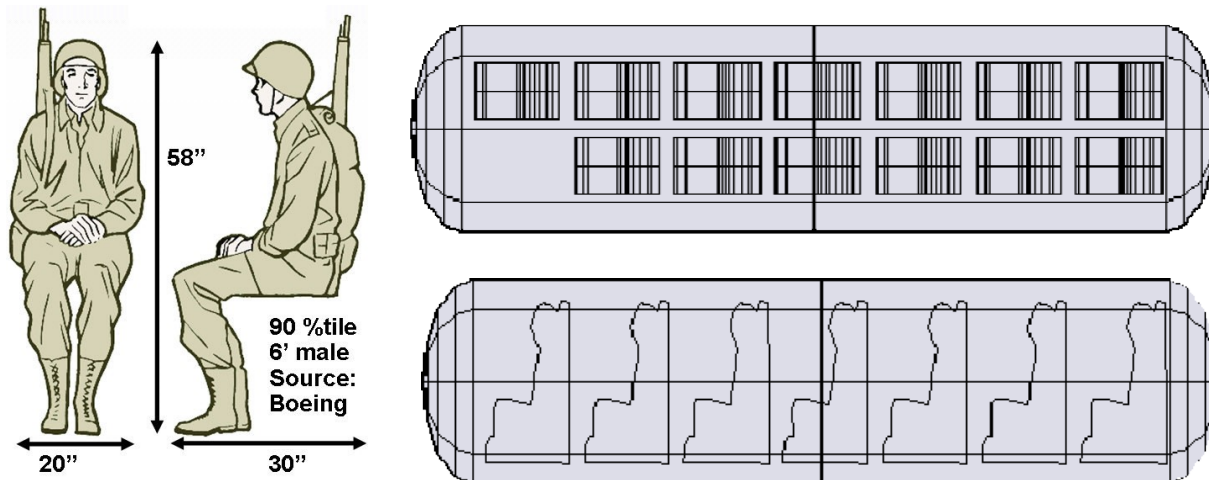


Figure 13. Troop Transport Compartment

Weights estimates for this 13-Man USMC Rifle Squad and associated equipment are shown in Table 14.

Table 14. Weight Estimates for 13-Soldier Squad

Weight with equipment	~ 13 x (180+100)	=	3640 lb
Seat weight	~ 13 x (14 x 1.5*)	=	273 lb
TBD equipment and misc (7% margin on above)			287 lb
ECS equipment and consumables (based on CERV)			2256 lb
Total weight allowance			6456 lb
(*extra allowance for high-g and restraints)			

7.2 Global Troop Transport Vehicle Analysis

The Global Troop Transport designs described below were analyzed using the same methods and data as the Reusable Upper Stage concept analysis. Propulsion for the Global Troop Transport design studies was based on the engine designs done by XCOR Aerospace Inc., as described in their separate report. Aerodynamics is virtually identical to that of the RUS because the geometries are similar, although scaled and slightly reshaped.

Vehicle weights were again calculated by a detailed build-up method, leveraged from the work done by Convergence Engineering, USL, UDRI, and XCOR, and adjusted for the design peculiarities of the Global Troop Transport concepts. As for the RUS, weights were adjusted to represent likely 2015 technology levels and should be considered attainable but “DARPA-hard”. Results were shown below for each concept.

Trajectory simulations where appropriate were analyzed using the ROAST module of RDS-Professional, as described above. For the around-the-world boost, trajectory analyses were not conducted - it was assumed that a large enough first-stage booster would be employed, allowing the study to focus on the landing and recovery aspects of these designs.

7.3 Global Troop Transport – Near-Term Concept

The HOT EAGLE Global Transport Stage configuration geometry, like the Reusable Upper Stage, is based on the aerodynamic configuration developed during the Micro-X Phase Five study as described above. Two different designs were developed, a smaller one with near-term technologies and limited capabilities, and the other larger and more capable. The smaller version is geometrically similar to the HOT EAGLE Demonstrator as described below, whereas the other has substantial design commonality with the RUS.

The smaller, simpler version is a serious attempt to provide the essential HOT EAGLE Global Troop Transport capability in a near-term system using only existing or near-term technologies, and in a design which minimizes development cost, time, and risk. This was done by off-loading much of the required capability. HotGlobe has no rocket engines of its own other than small RCS and de-orbit engines. HotGlobe cannot fly itself away for egress, relying upon the assistance of a recovery aircraft. Finally, HotGlobe is relatively small, at 35 feet being shorter than a typical school bus.

This design is shown below* – note that the troop compartment as defined above comprises most of the vehicle length.

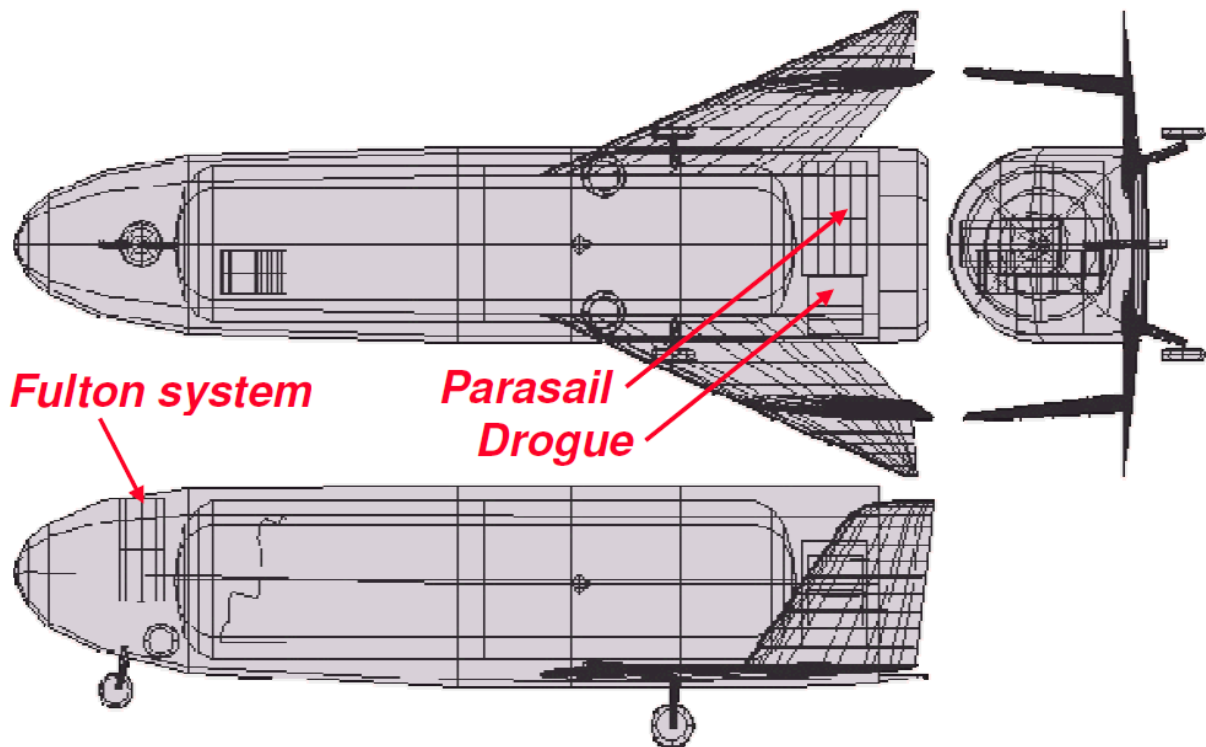


Figure 14. Global Troop Transport (HotGlobe) Configuration

With neither landing rockets nor fly-away egress capability, how does it operate? For landing, it relies upon the proven parasail technology as developed and tested by Zodiac/Pioneer Aerospace. This parasail design completed 13 successful flight and landing tests and was intended to be man-rated for the NASA X-38 Crew Return Vehicle. It is capable of landing a 25,000 lb payload with an onboard GPS guidance system which can automatically maneuver to an into-the-wind spot landing, performing an auto flare maneuver at the appropriate time just before touchdown. Technical characteristics include:

- 7,500 ft² Wing
- 150 ft span, 50 ft chord
- 1,165 lb total parafoil pack weight
- Glide ratio ~3
- Sink rate 20 fps, flare to 8 fps landing sink, ~100 ft stop

This existing parasail system including drogue chute is shown at the back of the HotGlobe vehicle. Suspension lines would extend forward to the vehicle center of gravity.

*Referred to as HOTGLOBE in data file naming

For post-mission egress, an old system dating back to the Vietnam War is postulated for use, namely, the Fulton Recovery System. This was used to extract one or two troops from the ground. A helium-filled balloon would be released from the ground and used to raise a 450-ft lift line. A recovery aircraft such as the modified MC-130P would engage the line with a V-shaped yoke in its nose, pulling the individual almost straight up out of the recovery zone. The individual would then be reeled on board. The success rate was very high, with apparently only one fatality in 17 years of operation due to the system itself (the line broke). The individual reportedly experienced about a 3-g load factor, and the wind buffeting while being reeled into the aircraft was apparently more troubling than the extraction itself.

While it seems quite a stretch to use this method to extract an entire vehicle, simulation analysis indicates that it should work. The ROAST trajectory program was modified to incorporate a stretching tow line with geometry as indicated below, and the pulling force was found as the line stretch times an assumed spring constant. To simplify the analysis it was assumed that the HotGlobe nose and the line pulling force would always point directly at the recovery aircraft, and the rope drag and inertia were ignored. This is probably conservative.

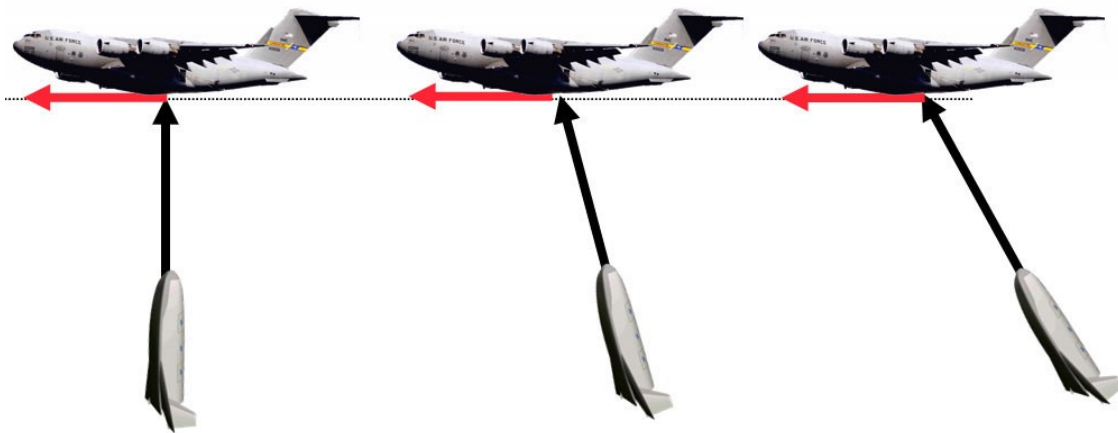


Figure 15. Fulton Recovery Analysis Geometry

For a recovery aircraft at 140 kts and an altitude of 500 ft, the simulation (below) indicates that 10 seconds after line engagement the HotGlobe is at the recovery aircraft's speed and is being pulled behind it. A maximum of 3 g's is experienced by the HotGlobe. Thus, the recovery aircraft experiences a pulling drag of three times the HotGlobe's weight, or less than 60,000 lbs. While this would definitely slow the aircraft down at the instant of engagement, for a large aircraft such as the C-17 this drag force is less than the extra thrust available from its engines.

A similar simulation, not shown, indicates that the recovery aircraft can be flying at 200 kts provided its altitude is increased to 1,000 feet, along with the recovery line length. This increases maximum load factor to about 3.5 g's, still well within acceptable limits. Detailed trade studies will be required to determine the optimal recovery conditions considering both HotGlobe vehicle impacts and survivability of the recovery aircraft.

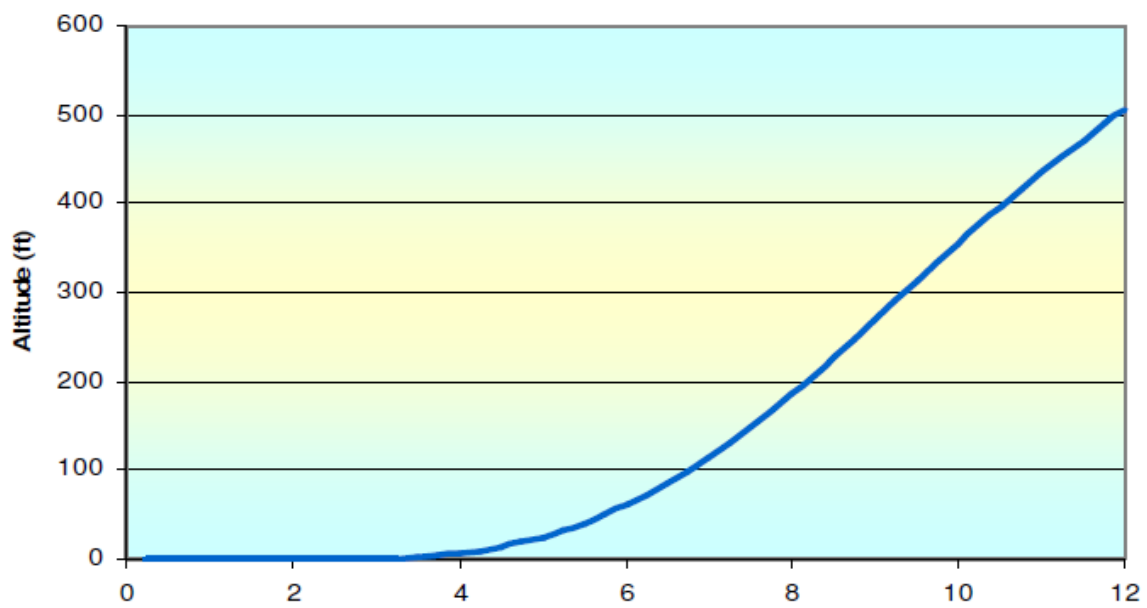
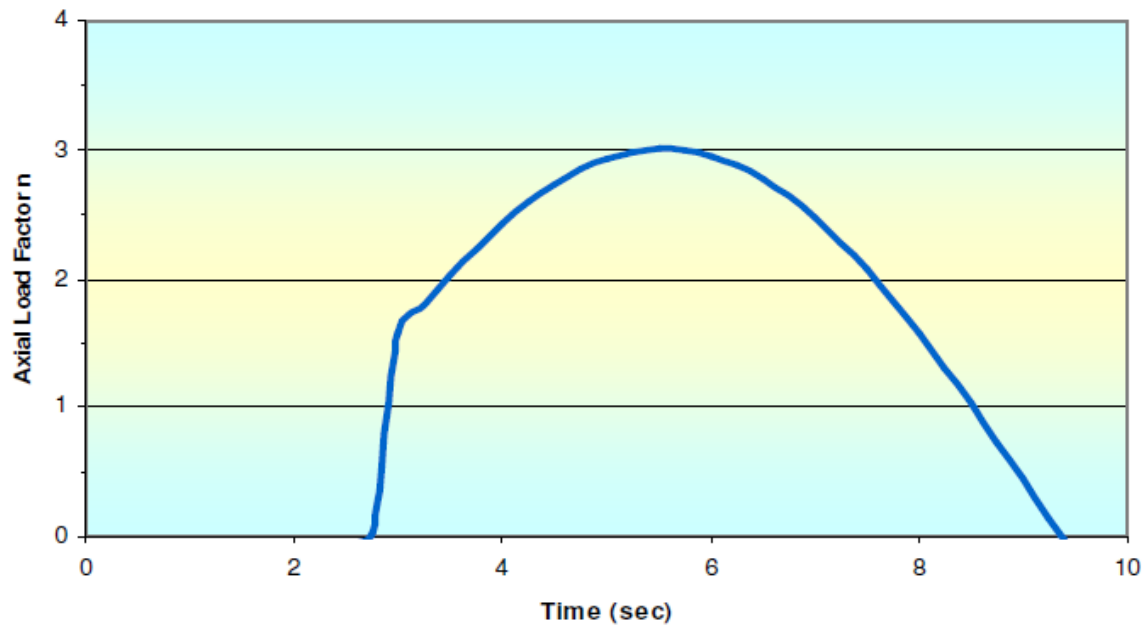


Figure 16. Near-Term Global Transport Weights

Table 15. Near-Term Global Transport Weights

	Weight lbs	Loc ft	Moment ft-lbs		Weight lbs	Loc ft	Moment ft-lbs
STRUCTURES	5389		180332	EQUIPMENT	5943		68741
Wing (inner panel)	136	47.0	6383	Flight Controls (EMA)	539	42.0	22654
Wing (outer panel)	54	52.4	2846	Instrumentation	150	5.0	750
Wing (carry-through)	56	44	2480	Wiring	270	34.0	9165
Tails	148	52.4	7763	Electrical (Power)	46	34.0	1564
Fuselage	1267	30.0	37999	Avionics - Fwd Bay	160	4.0	638
Passenger comp.	500	28.0	14000			51.0	0
Body Flaps	64	54.9	3523	Avionics - Thermal Mgmt	412	30.0	12360
		31.3	0	Battery	162	5.0	808
			0	Life Support	2256	5.5	12408
Gear Doors&Wells	527	33.6	17716	Parasail & Fulton	1849	4	7394.511
Landing Gear	1055	33.6	35431	RCS System	100	10	1000
TPS	1582	33.0	52193	(% We Allowance)	8.6		
			0	Empty Weight Allowance	999	22.7	22717
PROPULSION	285		15077	TOTAL WEIGHT EMPTY	12615	22.7	286867
Engines (OMS)	285	52.9	15077				
			0	USEFUL LOAD	6385		
			0				0
			0	Check sum=0	0	0.0	0
			0	RCS Propellant	760	17.8	13528
			0	OMS Propellant	1425		0
			0	Payload	4200	15.3	64260
			0				
			0	TAKEOFF GROSS WEIGHT	19000	19.2	364655

	Weight	Install.	Weight
Parasail	1165	1.2	1398
Fulton system buildup:			
Lifted weight	19000		
Load factor	10.00		
Total load	190000		
Material Strength	83520000		
Material density	60.56		
Line X-section	0.002275		
Line length	500		
Line weight (4)	276		
Balloon & canister	20		
Helium tank	20		
Structure & Misc	60		
Total Fulton System	376	1.2	451

Weights for this near-term HOT EAGLE Global Troop Transport are estimated above including the Fulton Recovery System and Parasail. Total loaded weight is 19,000 lb, and empty weight is 12,615 lb.

All in all, this near-term global troop transport concept appears feasible and practical. Whether it is affordable for its intended missions, including the cost of its launch booster, will require further study which includes a mission value assessment.

7.4 Global Troop Transport – Rocket Lander

The HOT EAGLE Global Transport concept described above relies upon a gliding parasail landing. This may prove unsurvivable in certain mission scenarios, or it may limit available landing zones. A minimum ground roll of about 100 feet of unobstructed and nearly-flat terrain is required. This assumes a perfect touchdown right on the spot – in reality, it would probably be necessary to add another 100 ft for touchdown dispersion.

A variant of the above design was created with the parasail removed and belly landing rockets added. These are placed in a cluster of four around the center of gravity and are based upon XCOR engine designs developed for the HOT EAGLE demonstrator, described in a later section. Two LOX tanks are located in back, balanced by two CH₄ tanks forward near the troop compartment. The resulting design is shown below*. To accommodate the addition of rocket engines and propellant, the total vehicle weight was increased to 25,000 lb.

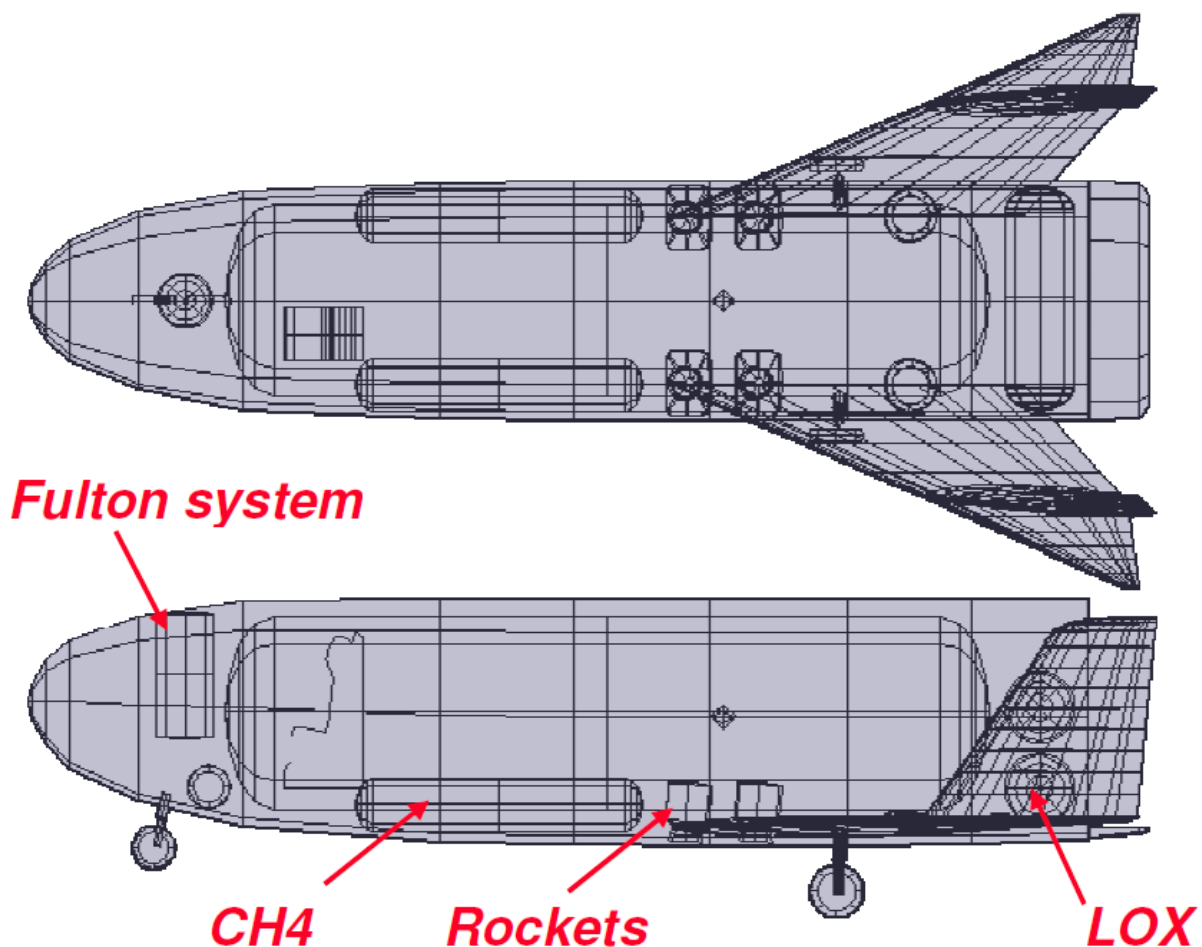


Figure 17. Global Troop Transport – Rocket Lander

* Referred to as “HOTGLOB1” in data file naming

For landing, the propellant tanks are sized for 45 seconds at maximum thrust assuming a 10% margin of thrust over weight. This should be sufficient for a computer-controlled transition from gliding flight (250 kts) to a vertical touchdown. Flight experience with the DC-X suggests that despite the high exhaust velocity of a rocket engine, landings on dirt and other unprepared surfaces are possible without excessive erosion of the surface or debris impact damage on the vehicle. Further study and test is required.

Note that in the event of a landing rocket failure the vehicle can make a gliding landing, provided that a long enough runway can be found.

The Fulton Recovery System shown in the nose is used for extraction. Simulation analysis would be virtually identical except that the load exerted on the recovery aircraft would be increased proportional to the increased weight, but still within reasonable limits. Vehicle weights are detailed in Table 16.

Table 16. Global Transport Rocket Lander Weights

	Weight lb	Loc ft	Moment ft-lb		Weight lb	Loc ft	Moment ft-lb
STRUCTURES	5594		186755	EQUIPMENT	5038		86380
Wing (inner panel)	136	47.0	6383	Flight Controls (EMA)	692	42.0	29082
Wing (outer panel)	54	52.4	2846	Instrumentation	150	5.0	750
Wing (carry-through)	56	44	2480	Wiring	270	34.0	9165
Tails	148	52.4	7763	Electrical (Power)	46	34.0	1564
Fuselage	1267	30.0	37999	Avionics - Fwd Bay	160	4.0	638
Passenger comp.	500	28.0	14000	Avionics - Engine Bay	329	51.0	16755
Body Flaps	64	54.9	3523	Avionics - Thermal Mgmt	412	30.0	12360
Tanks	205	31.3	6423	Battery	162	5.0	808
			0	Life Support	2256	5.5	12408
Gear Doors and	527	33.6	17716	Fulton	463	4	1850.122
Landing Gear	1055	33.6	35431	RCS System	100	10	1000
TPS	1582	33.0	52193	(% We Allowance)	7.9		
			0	Empty Weight Allowance	934	26.2	24424
PROPULSION	1262		37997	TOTAL WEIGHT EMPTY	12828	26.2	335556
Landing Engines (4)	624	30.0	18721				
Mount & Misc Install	140	30.0	4200	USEFUL LOAD	12172		
Engines (OMS)	285	52.9	15077	Land Propellant	5097		0
			0	Check sum=0	0	0.0	0
			0	RCS Propellant	1000	17.8	17800
			0	OMS Propellant	1875		0
Prop Pressurization	91		0	Payload	4200	15.3	64260
Propellant Insulation	122		0				
			0	TAKEOFF GROSS WEIGHT	25000	16.7	417616

7.5 Super Global Troop Transport

The global troop transport concepts described above offer substantial capability, but depend upon the availability and survivability of a recovery aircraft for extraction. In certain scenarios this would be limiting. To attain self-extraction capability in most likely operational scenarios requires a vertical or short takeoff much like that of the tilt rotor V-22. In aircraft, such ability

imposes substantial weight and complexity penalties on the vehicle. Any attempt to add aircraft- style vertical flight equipment to a launch vehicle would probably be fruitless.

Instead, the inherent high thrust-to-weight ratio of rocket engines can be applied to provide vertical takeoff capability. Several options were defined and are described below including belly rockets and vertical-attitude takeoff.

The other problem is the need to provide substantial egress range for such a vehicle. While it would be simpler to use the same thrust mechanism used for vertical takeoff to provide thrust for forward flight, this is not necessarily the only approach. Rocket engines are notoriously inefficient compared to aircraft engines, so perhaps aircraft engines could be added to the system for egress flight.

After qualitative study and a lot of concept sketching, it was concluded that such an approach would probably be too complicated and would create a monstrosity of a design. This conclusion should be revisited in a later study, but with the available funding it was not possible to design and study all options, so this author's judgment as to the most likely approach was followed.

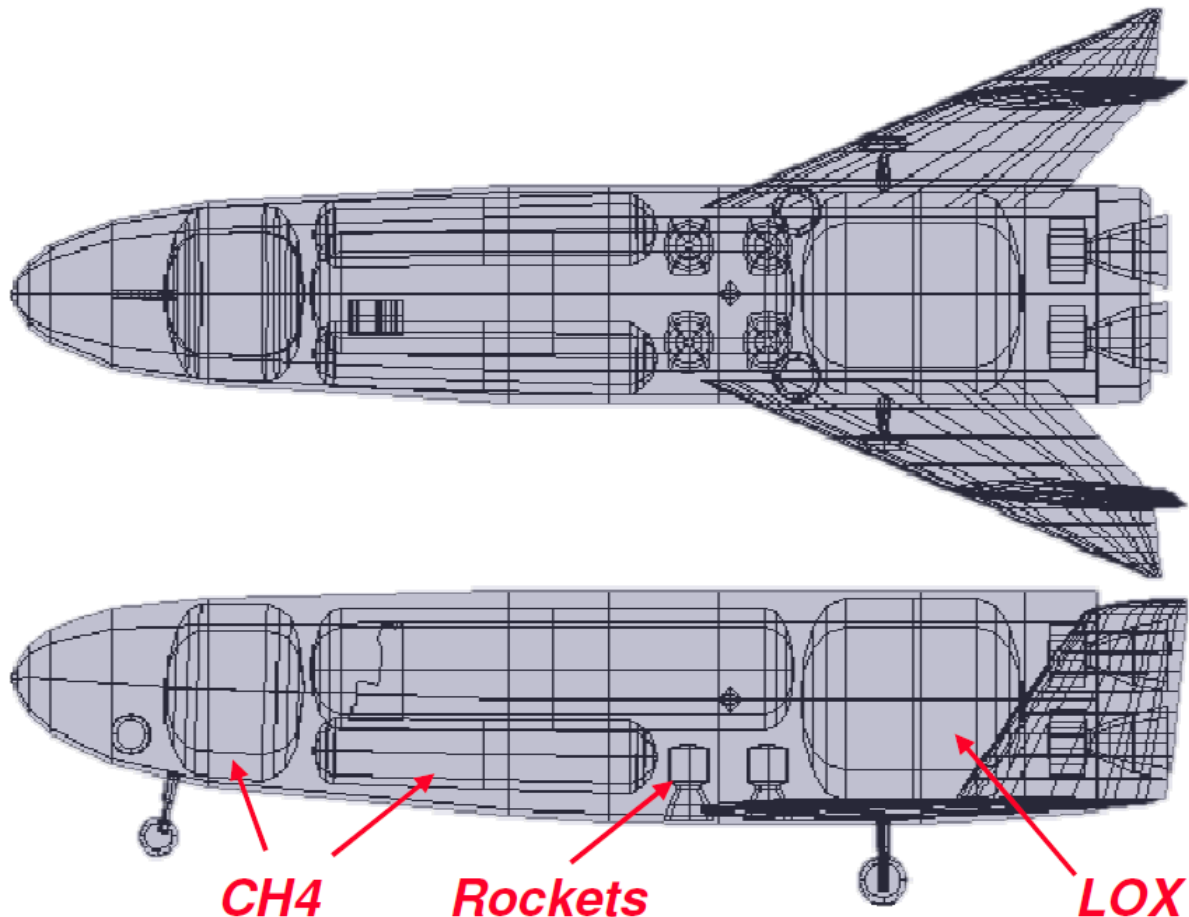


Figure 18. Super Global Troop Transport – Rocket Land and Egress

Preliminary sizing estimates indicated that a vehicle about the same size as the HOT EAGLE Reusable Upper Stage would be required, so that 73,000 lb GLOW design was used as the starting point for the “Super Global Troop Transport” design, shown above*. This required only slight changes to the fuselage mold lines. The troop compartment is narrower but longer than the RUS payload bay, so the forward propellant tank had to be shortened. Part of its methane was relocated to two new tanks along side the troop compartment, yielding the same total volume, requiring slight reshaping to the lower fuselage. Vectoring belly rockets were added near the center of gravity – otherwise the design is identical to the RUS such that the two systems could be an “A” and a “B” model off the same production line. Weight estimates for this design are provided below, followed by design data for all three global troop transports.

Table 17. Super Global Transport Weights

	Weight lb	Loc ft	Moment ft-lb		Weight lb	Loc ft	Moment ft-lb
STRUCTURES	5747		195253	EQUIPMENT	5620		117722
Wing (inner panel)	205	47.0	9655	Flight Controls (EMA)	1169	42.0	49113
Wing (outer panel)	85	52.4	4451	Instrumentation	150	5.0	750
Wing (carry-through)	90	44	3967	Wiring	595	34.0	20218
Tails	237	52.4	12420	Electrical (Power)	46	34.0	1564
Fuselage	1380	30.0	41390	Avionics - Fwd Bay	213	4.0	851
Door & Bay Cutout	227	28.6	6489	Avionics - Engine Bay	329	51.0	16755
Body Flaps	71	54.9	3908	Avionics - Thermal Mgmt	412	30.0	12360
Integral Tanks	777	31.3	24335	Battery	162	5.0	808
			0	Life Support	2256	5.5	12408
Gear Doors and Wells	221	33.6	7409	Misc Equipment	0	4	0
Landing Gear	441	33.6	14818	RCS System	289	10	2894.876
TPS	2012	33.0	66411	(% We Allowance)	2		
			0	Empty Weight Allowance	292	32.1	9378
PROPULSION	3234		155934	TOTAL WEIGHT EMPTY	14893	32.1	478287
Engines (8)	1956	52.9	103480				
Mount & Misc Install	642	50.7	32570	USEFUL LOAD	58107		
			0	Start & Residual Prop	639	31.3	20000
			0	Boost Propellant	39983	31.3	1251461
			0	RCS Propellant	396	17.8	7048
			0	Land Propellant	12089		0
Prop Pressurization	360	31.3	11272	Payload	5000	28.6	143000
Propellant Insulation	275	31.3	8612				
			0	TAKEOFF GROSS WEIGHT	73000	26.0	1899796

* Referred to as “HOTGLOB2” in data file naming

Table 18. Global Troop Transport Comparative Design Data

	HOTGLOBE	HOTGLOB1	HOTGLOB2
W-gross	19000	25000	73000
W-empty	12615	12828	14893
W-payload	4200	4200	4200
W-misc UL	2185	7972	13124
W-propellant	0	0	40783
PMF	0.0%	0.0%	55.9%
# engines	0	4	4
T per engine	0	7000	20000
T/W	0.0	1.1	1.1
Length	35	35	57.3
Diameter	7.5	7.5	10.8

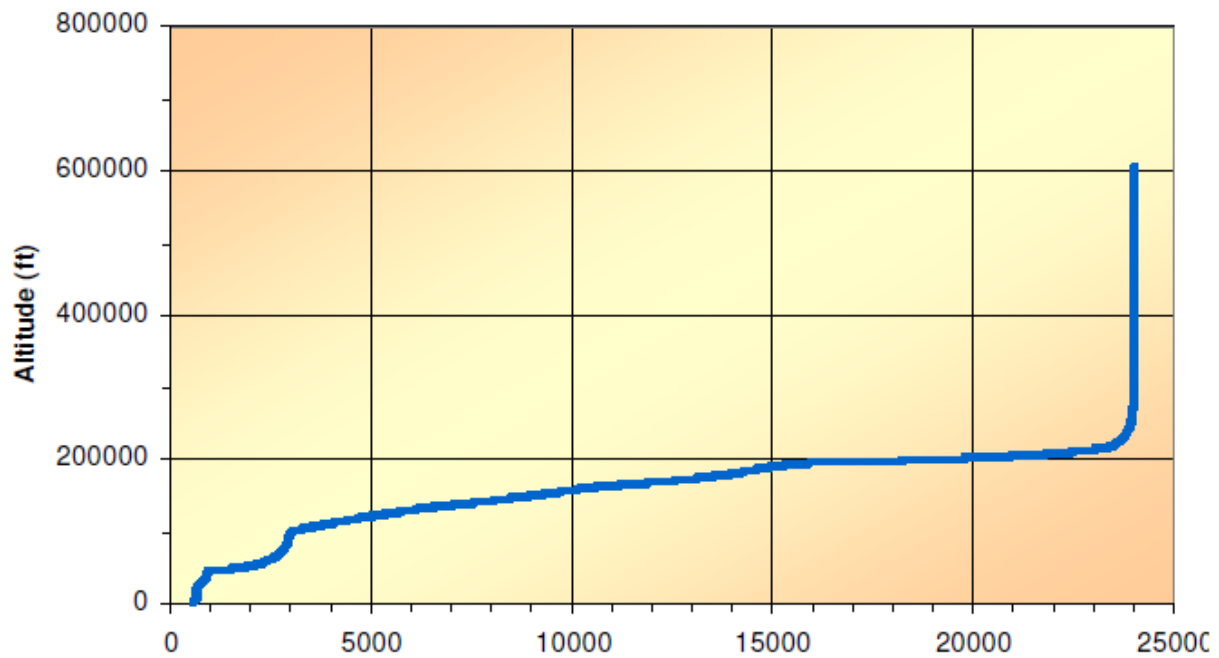
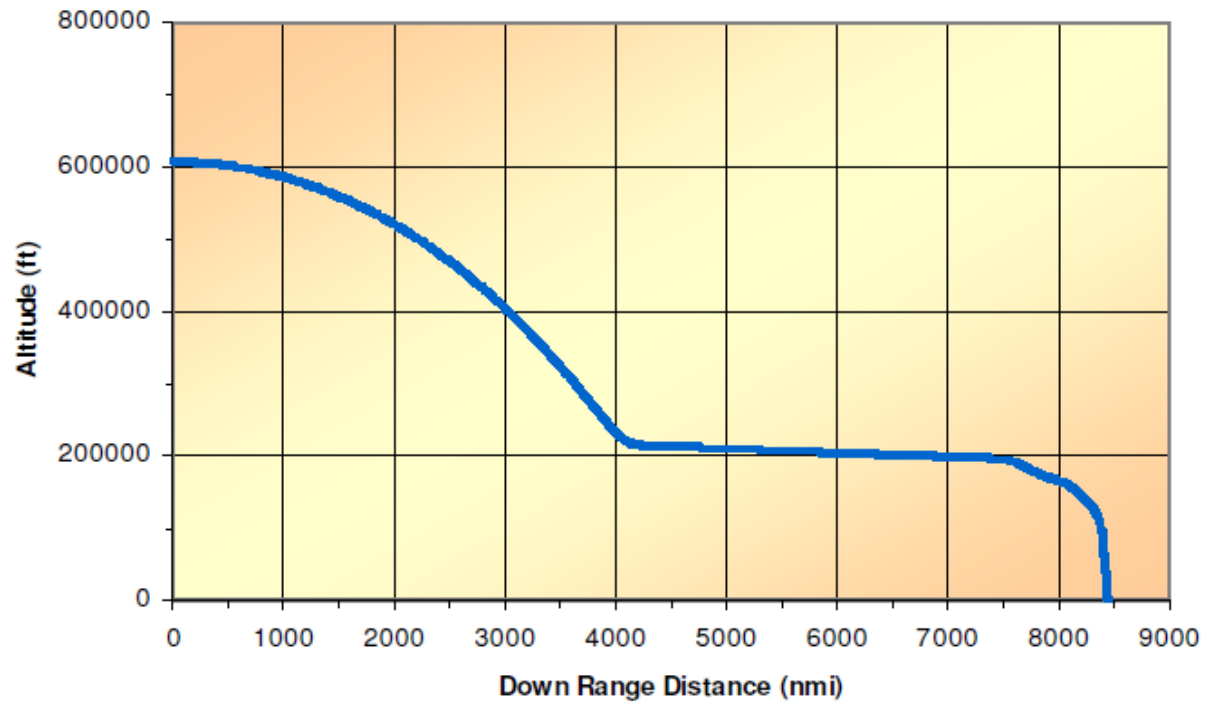


Figure 19. HotGlobe2 Reentry Trajectory Analysis

Reentry trajectory analysis is shown in Figure 19. Propellant for the vertical landing was estimated by assuming 45 seconds at full thrust ($T/W=1.12$). This is probably about 1 minute of actual firing time since much of the time the engines will be at less than full thrust.

For egress takeoff it was assumed that the belly rockets would fire alone for 4 seconds to clear the ground, at which point the main rockets would begin to fire and the nose would be raised. The belly rockets would continue for another 6 seconds, or 10 seconds in all, as the vehicle accelerates on main engine thrust. This was used to calculate liftoff propellant totaling 4200 lb, and all propellant remaining was used for egress flight analysis.

The available propellant for fly out is 35,778 lb. One option is to essentially fly out like a rocket powered airplane, cruising on rocket thrust and wing lift. An analysis of vehicle drag and thrust indicates that best cruise occurs at about 425 kts at 30,000 feet. This requires cruising on one engine, and that at 50% thrust. Assuming that at that condition an Isp of 270 seconds is attained, the HotGlobe2 gets a range of 150 nmi. This assumes a dead stick landing since all propellant is used during cruise.

Another option is to fly out like a rocket, boosting nearly vertically and following a ballistic trajectory after taking off on the belly rockets. Best range seems to occur with engine burnout at a 30 degree climb angle, occurring at 165,000 ft and 4800 fps. Counting reentry gliding, this gives a total range of 230 nmi range. Again, a dead-stick landing is required but should not be a problem for a specialized mission vehicle.

Intermediate options were also studied, climbing on rocket thrust at lower flight path angles then gliding. These attained less range than either option above apparently due to the high atmospheric drag.

Another recover option favored by this author is to use rocket thrust to get a reasonable distance away from the hostile fire zone, then rendezvous with a modified retrieval aircraft. This aircraft would be outfitted with a boom much like the refueling boom on a KC-135, but much stronger, and would be maneuvered into a receptacle on the top of the Global Troop Transport vehicle. Then the recovery aircraft (possibly a B-1 or C-17) would tow the Global Troop Transport vehicle to a recovery base where it would be released to make a dead stick landing. This is illustrated in Figure 20.

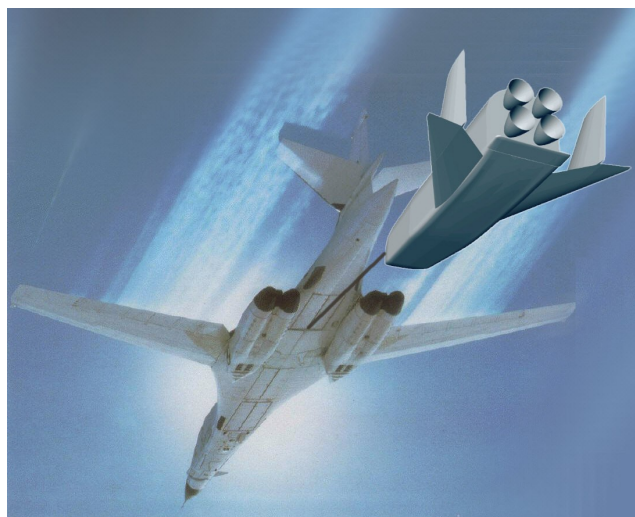


Figure 20. Towed Recovery Scheme

Vertical attitude landing alternatives were also investigated for these Global Troop Transport concepts, and should have roughly similar weights and capabilities. However, it seems difficult to provide a tail-mounted landing gear that is broad and robust enough to permit safe landings on a wide variety of unprepared surfaces, especially in mountainous terrain. It would be catastrophic for the vehicle to tip over after engine shutdown. Also, getting the troops in and out of a vertical-attitude landing design would be difficult – the front seat is at least 25 feet off the ground!

One approach for a vertical-attitude landing design uses external carriage of the troop compartment, much like the external payload shroud concept alternative for the RUS. When this lands in a vertical attitude, the payload pod pivots down to the ground so that the troops can egress as if stepping out of a parked automobile. During transition, though, the entire vehicle would be prone to tip over so a foot, looking somewhat like the fork on a forklift, would first pivot downward and rest on the ground. This is shown below, and is roughly estimated to add 400 to 600 lb to the total empty weight. This concept was not pursued further under the current contract funding, but would be an interesting follow-on study.

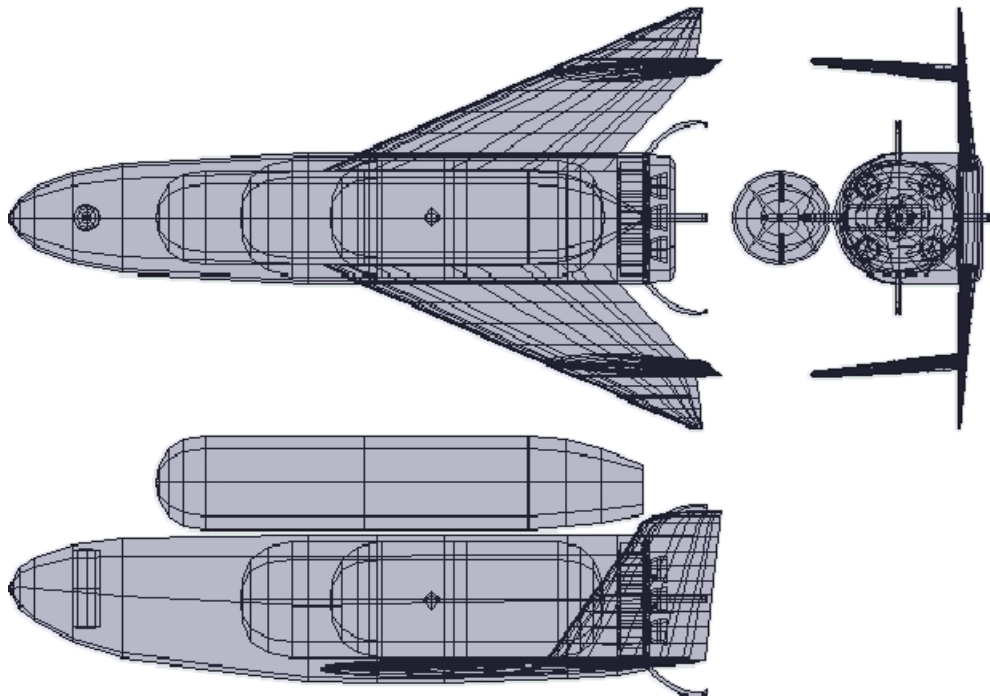


Figure 21. Global Troop Transport Vertical Attitude Lander – External Troop Compartment

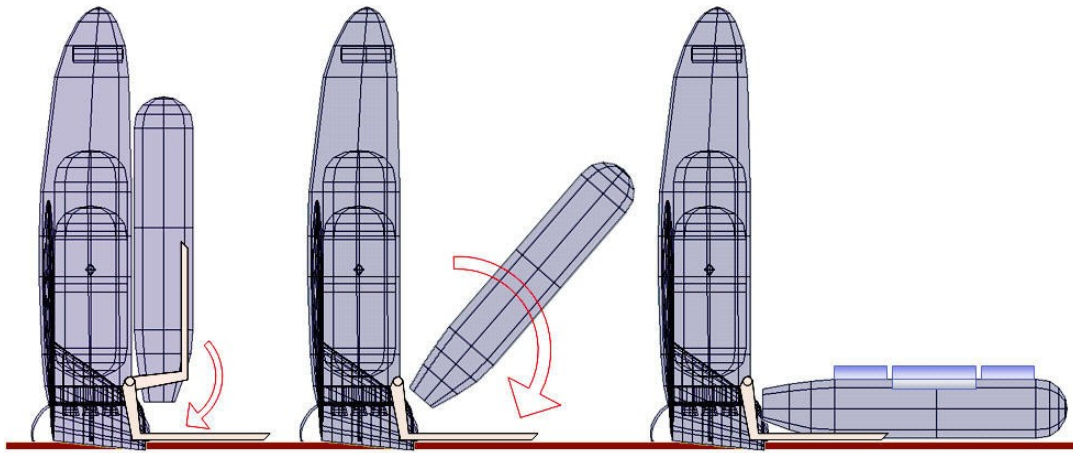


Figure 22. Vertical Attitude Lander Troop Compartment Deployment

7.6 Global Range Troop Transport Summary and Conclusions

The Phase One study results show that, wild as it sounds, there are both near-term and far-term options for a HOT EAGLE Global Range Troop Transport system capable of inserting a Marine Rifle Squad to an unprepared location anywhere on the globe within less than an hour, and safely recovering them after their mission is complete. The cost would be large, but the operational rewards potentially enormous.

8. HOT EAGLE DEMONSTRATOR

8.1 Design Requirements

A key element of the HOT EAGLE program will be a technology and concept demonstration effort. This will include a ground-based structures demonstration followed by a flight demonstration vehicle capable of replicating all HOT EAGLE system flight envelope points and validating key technologies. The HOT EAGLE Demonstrator* vehicle design was based on the RUS and HotGlobe designs above, sized to permit self-launch for flight envelope expansion followed by boost to reentry speeds on a 1st stage launch vehicle. Successful completion of the HOT EAGLE Demonstrator program would mature relevant technologies, explore high-payoff system concepts, and significantly reduce the risk of developing the desired operational capabilities described above.

Many of the emerging technologies for Reusable Access to Space could be tested with the HOT EAGLE Demonstrator vehicle. Some of them have to do with reusability itself, such as reusable auxiliary power sources (batteries, APU's, etc...), durable and/or flightline-replaceable TPS, accessible and maintainable avionics, non-expendable igniters, and coking-free rocket engines, turbopumps, and RCS thrusters. Some test technologies are related to the desire to reduce the logistics trail, such as non-pyrotechnic actuation and avoidance of monopropellants in RCS and APU systems.

Other technologies are enablers for improved operations and reduced design size and cost. These include the potential use of a high angle-of-attack reentry profile, which has been shown to reduce heating which in turn reduces TPS cost and weight. High- α reentry also reduces sonic boom. The HOT EAGLE Demonstrator will probably be fabricated from composite materials much like a modern fighter aircraft, relying upon its TPS for thermal protection. This offers weight and cost savings, and also reduces demonstrator design and fabrication time.

To maximize value as a technology demonstrator, an unallocated payload weight of 2000 pounds is assumed in all weight and performance calculations below. This weight allocation could be additional technologies for testing, specialized test equipment, telemetry, or eventually some sort of operational payload if appropriate.

To allow self-launch for early flight test, the demonstrator vehicle must be designed with rocket engines capable of operating under sea level conditions and the thrust must be sufficiently in excess of GLOW to allow a safe liftoff. These are described below. To allow boost on an existing launch vehicle, the demonstrator vehicle weight must be kept low enough that sufficient performance can be attained.

A tabulation of current and recent stages (shown below) was used to identify candidate launchers for a HOT EAGLE demonstration vehicle. Be advised that this data comes from a variety of sources including the internet, and some of the "data" is educated guesswork (including much of the Space-X Falcon-V data).

* Referred to as "HE-DEMO" in data file naming

This data indicates that a Titan stage would be a good candidate for launching a demonstrator vehicle. However, Titan flight hardware is basically unavailable. Lockheed indicates that it would be prohibitively expensive to attempt to use the Titan, and recommends the solid propellant Athena instead. This would provide ample throw-weight margin and must be considered a leading candidate.

The Delta first stage would also be an excellent candidate. Since its launch thrust is just barely over the stage-alone weight, solid booster zero stages are required. This adds cost to the test mission, but total cost may be competitive anyway. The maximum possible weight of a HOT EAGLE test vehicle carried by a Delta would depend on the number of solid boosters added, and could reach in excess of 90,000 lb to an altitude of 100 nmi, depending on the configuration selected.

Table 19. Candidate Demo Booster Weight and Performance Data

Stage	Propellant Weight lbs	Propellant Type	Average Propellant Specific Gravity	Propellant Feed	Stage-Alone Weight lbs	Isp (vac)	Ideal DeltaV fps	Propellant Mass Fraction	Typical Payload lbs	Total Stage Thrust	1st Stage Available Lift Weight (ROM)
Delta 6925 Stage 2	13,400	N2O4/ Aerozine 50	1.04	pressure	15,331	319	21,278	87.4%	4,000	9,815	
Delta 6925 Stage 1	211,300	LOX/RP-1	0.98	pump	223,800	295	27,383	94.4%	4,000	244,100	-49,443
Titan II Stage 2	59,000	N2O4/ Aerozine 50	1.04	pressure	65,000	308	23,611	90.8%	4,200	100,000	
Titan II Stage 1	260,000	N2O4/ Aerozine 50	1.04	pump	269,000	287	31,372	96.7%	4,200	474,000	69,571
Sea Launch Stage 2	178,000	LOX-RP-1	0.98	pump	198,000	350	25,816	89.9%	30,000	191,000	
Sea Launch Stage 1	703,000	LOX-RP-1	0.98	pump	778,000	337	25,364	90.4%	30,000	1,779,000	492,714
Saturn IB Stage 1	889,000	LOX/RP-1	0.98	pump	980,000	263	20,111	90.7%	45,000	1,848,937	
Saturn IB Stage 2	233,000	LOX-H2	0.42	pump	255,000	425	33,504	91.4%	45,000	231,440	
Titan IV Stage 2	77,200	N2O4/ Aerozine 50	1.04	pump	87,000	312	21,919	88.7%	48,000	106,150	
Titan IV Stage 1	340,000	N2O4/ Aerozine 50	1.04	pump	359,000	283	26,759	94.7%	48,000	551,000	34,571
Saturn V Stage 3	238,000	LOX-H2	0.42	pump	263,000	425	32,179	90.5%	200,000	231,440	
Saturn V Stage 2	993,000	LOX-H2	0.42	pump	1,071,000	425	35,821	92.7%	200,000	1,157,200	
Saturn V Stage 1	4,584,000	LOX/RP-1	0.98	pump	4,872,000	265	24,114	94.1%	200,000	8,682,573	1,329,838
Athena/Castor120	107380	Solid	1.7	Solid	116,644	229	18,663	92.1%		360,420	140,799
Space-X Falcon 1 1st	42300	LOX/RP-1	0.98	pump	45,580	310	26,248	92.8%	1480	77,000	9,420
Space-X Falcon 1 2nd	14100	LOX/RP-1	0.98	pump	14,700	327	33,653	95.9%	1480	7,000	
Space-X Falcon V 1st	211500	LOX/RP-1	0.98	pump	227900	310	26,248	92.8%	9240	385,000	47,100
Space-X Falcon V 2nd	70500	LOX/RP-1	0.98	pump	73500	310	31,903	95.9%	9240	77,000	

Another good candidate is the Space-X Falcon V, with a first-stage throw-weight estimated at 47,000 lbs. However, it would be an unwise choice at this point since even Falcon I has yet to fly as this is written. Space-X is reluctant to release definitive data on Falcon V since its design is still being revised. But, being based largely on proven technologies there is high confidence of both versions being successfully flown and produced, so it should remain a viable candidate until a final decision must be made.

Thus, it appears that all likely candidates for first-stage boost of a HOT EAGLE demonstrator vehicle can be accommodated provided that the demonstrator weight, including any required

payload adapter, fairing, and interface hardware, is kept below 47,000 lb.

Other considerations affect the desired demonstrator weight. Cost will be somewhat proportional to weight, so it would be desirable to have the demonstrator as small as possible, consistent with demonstration objectives. Prior Micro-X studies had demonstrator designs ranging from 15,000 to 30,000 lbs. Based upon the capabilities attained by those vehicles, a weight well below the 47,000 lbs maximum derived above was assumed.

The small size and tailored technical objectives of the HOT EAGLE Demonstrator make it affordable and timely – first flight could occur in as little as 30 months. Testing of the HOT EAGLE Demonstrator would occur incrementally, beginning with self-launch and envelope expansion. This would minimize risk as well as the up-front commitment of financial resources. The initial flights could be done without an installed thermal protection system (TPS), validating the propulsion system and the chosen landing method. TPS would then be added, with high-Mach, high temperature flights in the upper atmosphere as well as exoatmospheric flight using an initial booster.

8.2 HOT EAGLE Demonstrator Analysis

The demonstrator designs described below were analyzed using the same methods and data as for the other concepts, with a few notable differences. Propulsion design was again done by XCOR Aerospace Inc, as described in their separate report, but their demonstrator engine designs were not adjusted for future technologies since it is hoped to begin the demonstrator development program in the near future.

Similarly, weights were again calculated by a detailed build-up method, leveraged from the work done by Convergence Engineering, USL, UDRI, and XCOR. However, these were not adjusted for future technologies for the same reason.

Aerodynamics is similar to that of the other designs due to the geometric similarity, recalculated to account for the smaller size and slightly different shaping.

8.3 HOT EAGLE Demonstrator Configuration Concepts

The HOT EAGLE Demonstrator (HE-Demo) was configured as a subscale version of the Reusable Upper Stage, and also resembles the similar Global Troop Transport vehicle concept. These concepts all feature a highly-swept wing with vertical tails near the tips. Outboard of the vertical tails are all-moving elevons for pitch authority.

Both vertical and horizontal landing versions of the demonstrator were defined. These have the same external configuration – as described above, the horizontal tails required for stability are large enough to act as wings and provide a reasonable stall speed (168 kts). These concepts are therefore virtually identical except for landing gear, and were all designed to the maximum GLOW of 25,000 lb. This gives a length of 27.6 ft., with a span of 16.6 ft and body diameter of 6.4 ft.

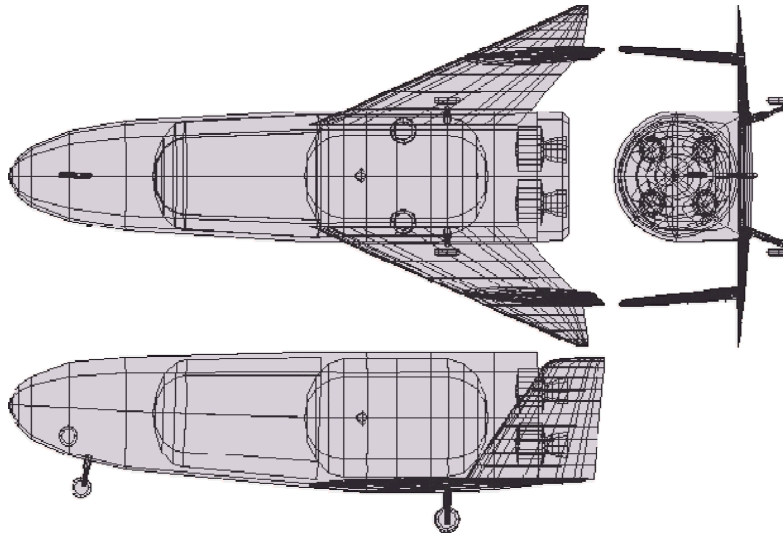


Figure 23. HOT EAGLE Demonstrator External Three-View (HL)

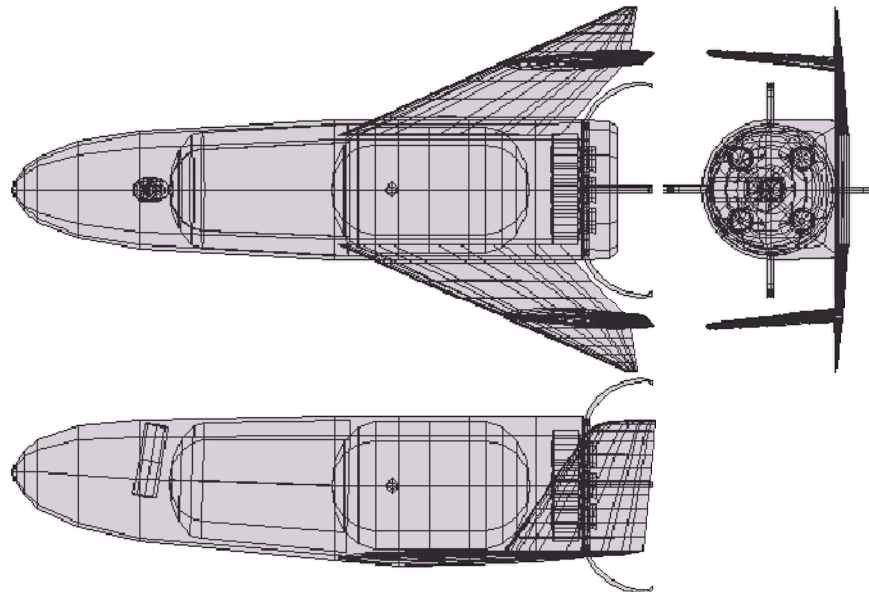


Figure 24. HOT EAGLE Demonstrator External Three-View (VL)

Table 20. HOT EAGLE Demonstrator Design Data

	HE-DEMO	HE-DEMVL
W-gross W-	25000	25000
empty W-	6939	7051
payload W-	2000	2000
misc UL	629	1341
W-propellant	15433	14608
PMF	61.7%	58.4%
# engines	4	5
T per engine	8750	7000
T/W	1.4	1.4
Length	27.6	27.6
Diameter	6.4	6.4
WI and/Wo	0.38	0.42
Stall kts	168	180
Approach kts	194	207

Table 21. HOT EAGLE Demonstrator Tail and Reference Geometries

	Wing-Inner	Wing-out	Tails	TrapWing
Area Sref	110	15	27	128
Aspect Ratio	1.2	1.59	1.3	2.14
Taper Ratio	0.42	0.08	0.44	0.13
Sweep (LE)	66.3	66.3	35	66.3
Sweep (c/4)	62.703	60.146	28.839	62.467
Airfoil	NACA 64A-010	NACA 64A-010	NACA 64A-010	NACA 64A-010
Thickness t/c	0.06	0.06	0.099	0.06
Dihedral	3	3	85	3
Twist	0	0	0	0
Span	11.489	4.884	5.925	16.551
Root Chord	13.485	5.688	6.33	13.688
Tip Chord	5.664	0.455	2.785	1.779
Mean Chord	10.097	3.811	4.782	9.253
Y-bar	2.481	0.874	2.578	3.076

The landing gear of the horizontal landing concept is similar to that on the Space Shuttle. The vertical landing concept uses gear legs which are curved and retract into the fuselage base area forming a ring around the engines. The mechanically-simple retraction is via a single trunnion for each gear leg. This gear arrangement provides a wide total gear spread for greater tip-over resistance. Since the gear retracts into the base of the fuselage, there are no doors penetrating the thermal protection system. Also, the gear legs attach directly to the engine mounts, providing a structurally efficient load path.

The landing strategy for the vertical landing HOT EAGLE Demonstrator relies upon simple, proven technology to convert from forward gliding flight to a tail-first, vertical landing. A small drogue chute is fired upwards from the nose. When it opens, it pulls the nose up causing a complete aerodynamic stall. The vehicle pivots roughly 180 degrees to a tail-first attitude, being

pulled and stabilized by the parachute, at which point the engines are restarted for deceleration and landing. This turnover scheme was dynamically simulated in the Micro-X Phase 4 contract by subcontractor Universal Space Lines, where it was found that a reasonably-sized drogue chute could in fact facilitate a rapid and predictable turnover maneuver, with acceptable loads and transients.

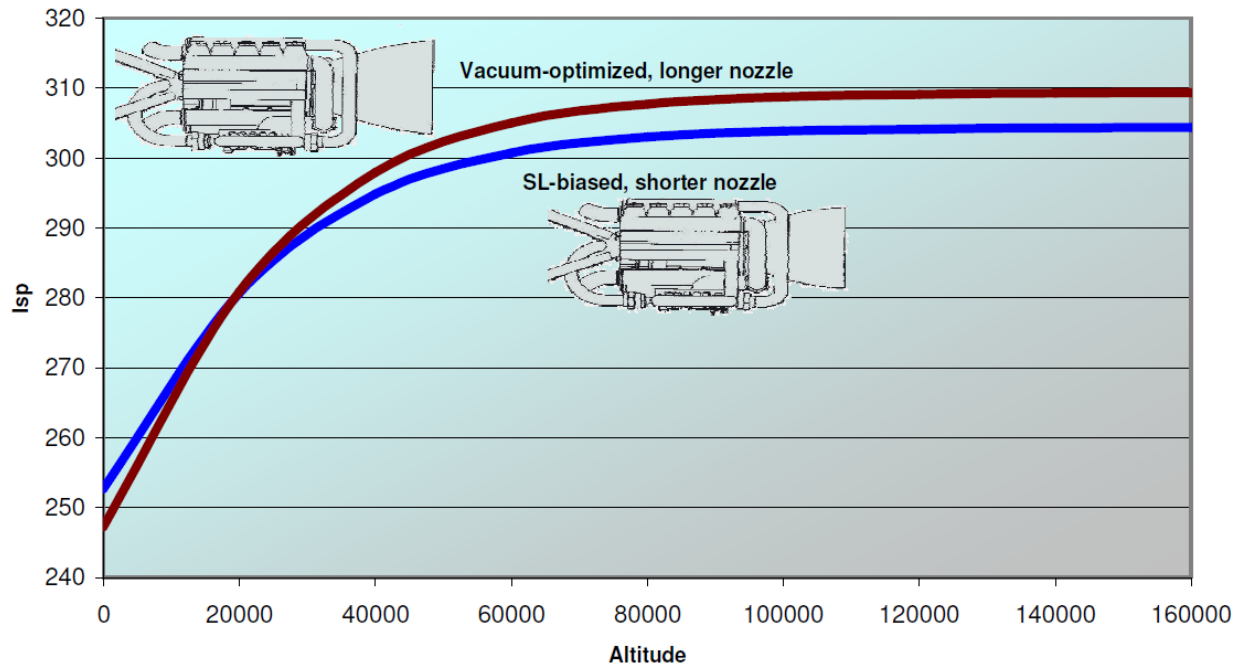


Figure 25. Impact of Sea Level Bias on Isp (XCOR)

The RUS concept as described above does not require engine operation at sea level unless a vertical powered landing is to be performed. Since an engine biased for sea level operation has poorer performance at higher altitudes (see figure above), this imposes a penalty on a vertical landing version that has to be included when ultimately making the HL vs. VL selection.

However, it may be advantageous for the demonstrator to use a vertical landing in any case since this provides an abort capability early in the flight test program, when the demonstrator is self-launched for envelope expansion. For example, a few seconds after liftoff there may be some indication of trouble. A VL capability would allow the vehicle to quickly set back down, whereas an HL demonstrator would have to continue to accelerate until a safe gliding speed could be reached, and the vehicle would have to position itself for an emergency landing on a runway.

Demonstrator weights were calculated by a detailed build-up method, leveraged from the work done by Convergence Engineering, USL, UDRI, and XCOR. Since the demonstrator is to be built in the near-future, no adjustments for future technologies were made. The weights below represent the CRC team's collective judgment of the likely resulting weights, assuming sufficient resources are applied to do a reasonably good job of optimizing structure and systems, and that "requirements creep" does not rear its ugly head.

Table 22. HOT EAGLE Demonstrator Weights (HL)

	Weight lb	Loc ft	Moment ft-lb		Weight lb	Loc ft	Moment ft-lb
STRUCTURES	3091		53166	EQUIPMENT	2325		34663
Wing (inner panel) Wing	111	22.3	2478	Flight Controls (EMA)	757	20.0	15140
(outer panel) Wing	46	25.8	1194	Instrumentation Wiring	14	4.0	55
(carry-through)	52	19.7	1025	Electrical (Power)	381	18.0	6862
Tails	133	26.0	3467	Avionics - Fwd Bay	46	5.0	230
Fuselage	725	15.0	10878	Avionics - Engine Bay	106	4.7	500
			0	Avionics - Thermal Mgmt	329	23.8	7819
Body Flaps Integral	43	26.6	1138	Battery	412	5.0	2060
Tanks	588	15.7	9233		162	5.0	808
			0			6.2	0
Gear Doors and Wells	153	17.2	2625	Misc Equipment	0		0
Landing Gear	305	17.2	5250	RCS System	119	10	1189.675
TPS	934	17.0	15878				
			0	(% We Allowance)	5		
				Empty Weight Allowance	330	17.4	5758
PROPULSION	1192		27340	TOTAL WEIGHT EMPTY	6939	17.4	120927
Engines (4)	712	25.7	18299				
Mount & Misc Install	175	24.3	4253	USEFUL LOAD	18061		
			0	Start & Residual Prop	379	15.7	5946
			0	Boost Propellant RCS	15433	15.7	242294
			0	Propellant	250	10.0	2500
			0	Land Propellant			0
			2041	Payload	2000	15.3	30600
Prop Pressurization	130	15.7	2748				
Propellant Insulation	175	15.7	0				
				TAKEOFF GROSS	25000	16.1	402267

Table 23. HOT EAGLE Demonstrator Weights (VL)

	Weight lbs	Loc ft	Moment ft-lbs		Weight lbs	Loc ft	Moment ft-lbs
STRUCTURES	3030		56019	EQUIPMENT	2425		35283
Wing (inner panel)	111	22.3	2478	Flight Controls (EMA)	757	20.0	15140
Wing (outer panel)	46	25.8	1194	Instrumentation	14	4.0	55
Wing (carry-through)	52	19.7	1025	Wiring	381	18.0	6862
Tails	133	26.0	3467	Electrical (Power)	46	5.0	230
Fuselage	725	15.0	10878	Avionics - Fwd Bay	106	4.7	500
			0	Avionics - Engine Bay	329	23.8	7819
Body Flaps	43	26.6	1138	Avionics - Thermal Mgmt	412	5.0	2060
Integral Tanks	588	15.7	9233	Battery	162	5.0	808
			0	Pitchover Chute	100	6.2	620
			0	Misc Equipment	0		0
Landing Gear	397	27.0	10729	RCS System	119	10	1189.675
TPS	934	17.0	15878	(% We Allowance)	5		
			0	Empty Weight Allowance	336	17.9	6019
PROPULSION	1260		29087	TOTAL WEIGHT EMPTY	7051	17.9	126409
Engines (5)	780	25.7	20046				
Mount & Misc Install	175	24.3	4253	USEFUL LOAD	17949		
			0	Start & Residual Prop	363	15.0	5446
			0	Boost Propellant	14608	7.0	102254
			0	RCS Propellant	250	15.7	3925
			0	Land Propellant	728	15.7	11427
Prop Pressurization	130	15.7	2041	Payload	2000	15.3	30600
Propellant Insulation	175	15.7	2748				
			0	TAKEOFF GROSS WEIGHT	25000	11.2	280061

Note that the vertical landing variant has about the same empty weight but requires a set aside of 728 lb of landing propellant. This leaves less propellant for boost, reducing performance. This contradicts the previous Micro-X results wherein the vertical landing design had a substantial empty weight reduction which made up for the extra landing propellant. The reason for this change is simple – in the Micro-X design the VL version only had small tails while the HL version required the addition of wings. As described above, it was learned that the small tails were inadequate and that both versions required much larger tails. These tails are so large that they act as wings for horizontal flight, so additional wing area is not required.

Trajectory analysis results for the HOT EAGLE Demonstrator are shown below (HL version, the VL would have slightly less performance). This shows the performance attainable from a ground launch assuming the shorter, SL-biased nozzles. Two alternative trajectories are shown, one a shallower launch and the other more-vertical. An altitude of nearly 300,000 feet and a speed of 3700 fps are attained, illustrating the performance potential of this design and its ability to perform envelope expansion and technology test via self-launch from the ground. Following that are the trajectory analysis results for the HOT EAGLE Demonstrator when boosted by a first stage, in this case the SpaceX FalconV. In the absence of better information,

available information was used to infer an ability to carry the HE-DEMO to a release condition of 300,000 ft and 9,000 fps. From these release conditions, the demonstrator can attain a final altitude of 450,000 ft and a velocity of 18,000 fps. Larger boosters should readily exceed these release conditions, enabling the HOT EAGLE Demonstrator to boost itself to a 100 nmi orbit.

These trajectory results indicate that the HOT EAGLE Demonstrator as described above can readily meet its test objectives and provide realistic testing throughout the desired flight envelope.

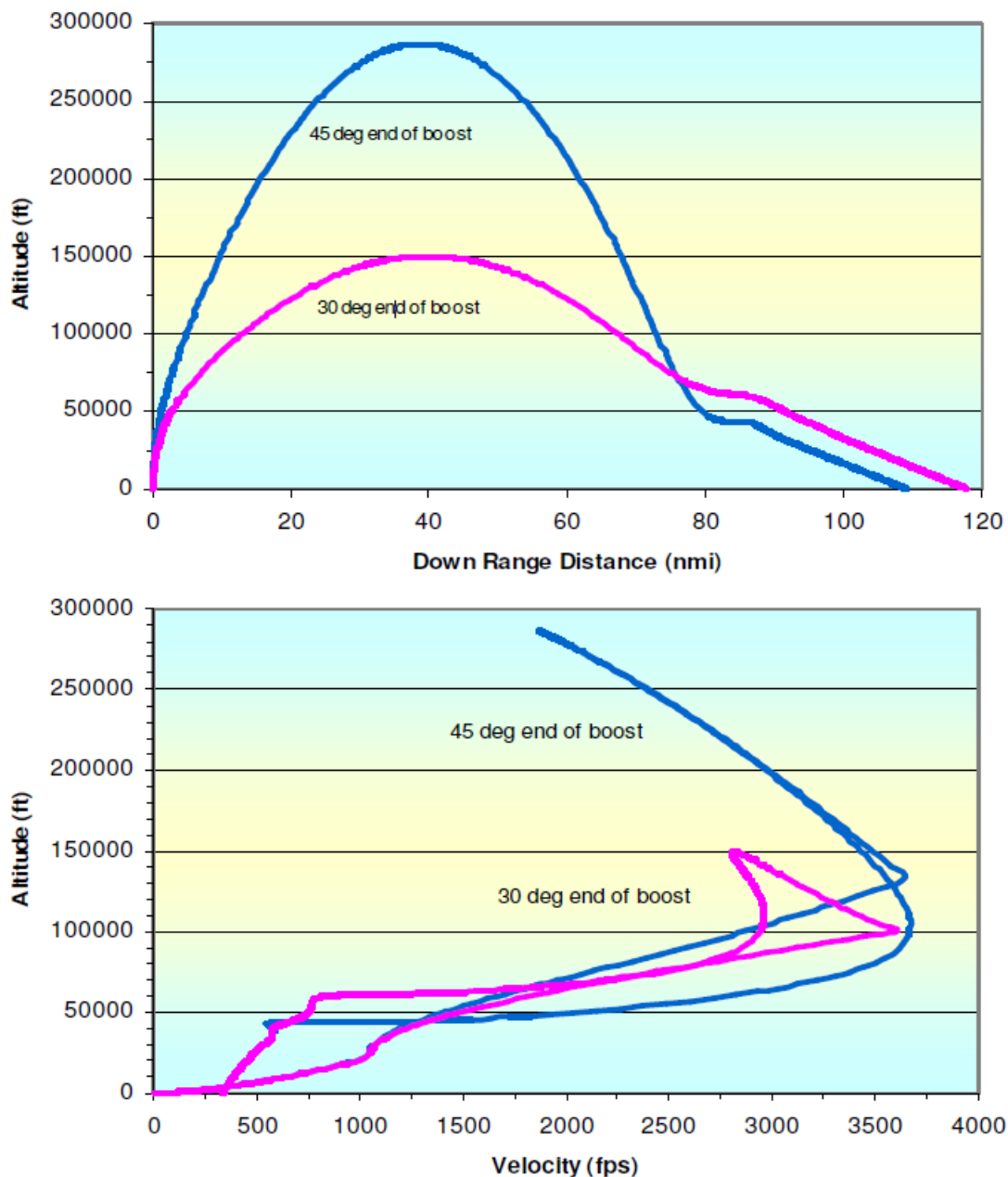


Figure 26. HOT EAGLE Demonstrator Self-Launch Trajectory Analysis

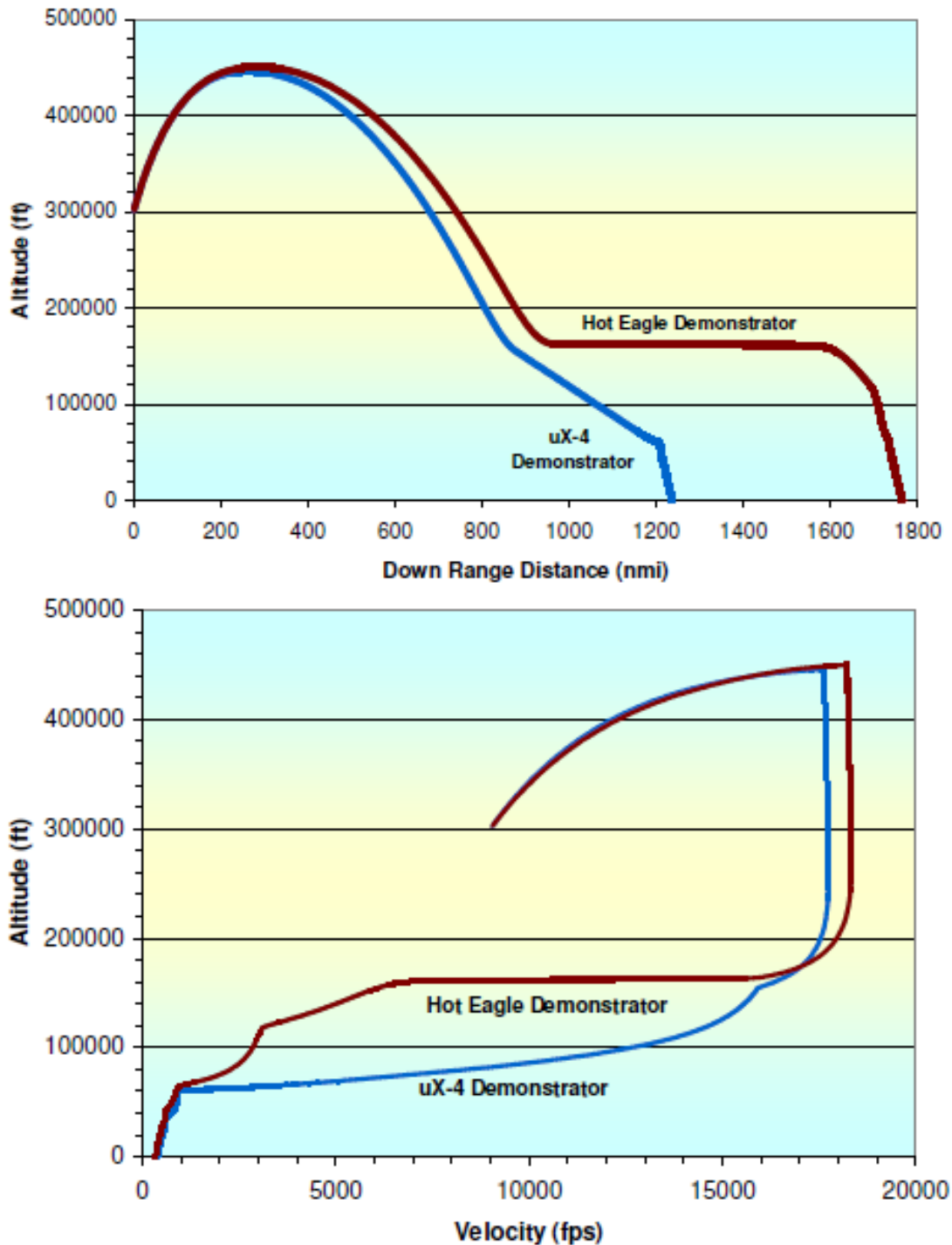


Figure 27. HOT EAGLE Demonstrator Trajectory Analysis – FalconV Launch

8.4 HOT EAGLE Demonstrator Cost and Schedule Estimate

A tentative schedule for the HOT EAGLE demonstrator program is shown below. This includes demonstrator design, fabrication, and test, as well as a near-term structural article fabrication and test effort. The schedule begins with the continuation of concept development studies through the end of FY06 to mature the design and address certain areas of concern. Starting in

FY07, a structural test article (see below) would be designed and fabricated for test at government facilities at WPAFB. This would be similar to the eventual flight-capable structure, and would include TPS in certain regions for testing in the 2009 timeframe. At the end of 2009, the flight demonstrator program would begin in earnest with a contract award. PDR would occur 8 months later, followed by CDR, fabrication, and checkout. Flight tests would begin in 2012. Engine development would occur in parallel with vehicle development.

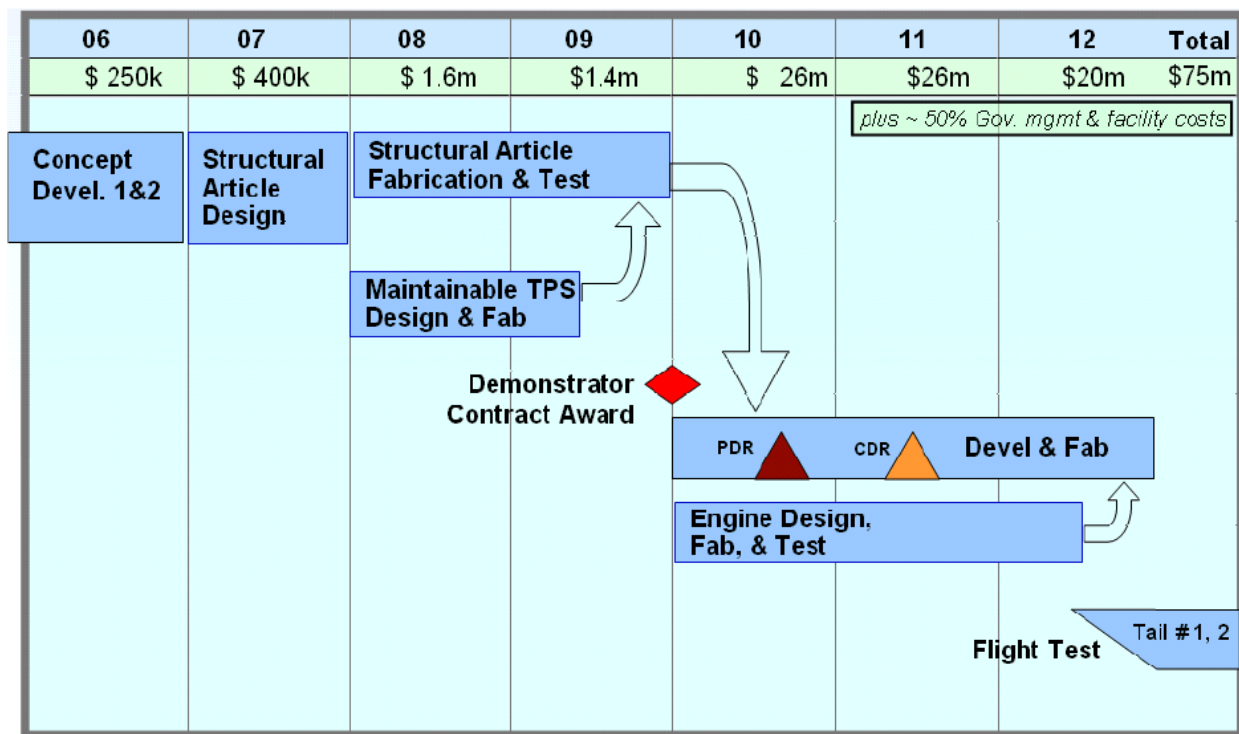


Figure 28. Tentative Program Schedule

A key part of this program is the structural test article to be built for ground testing of the structure, tanks, and TPS. This article would be full size and complete, but would be somewhat simplified compared to the actual flight hardware to save cost and accelerate the schedule. For example, the structure would not include all attachment fittings and hard points. Structural thicknesses would not be fully optimized for expected flight loads, instead relying upon a reduced amount of optimization with constant skin thicknesses over fairly large regions. However, the basic geometry would be identical to the expected flight hardware and the flight structure would later be built on the same molds and tooling, after further design optimization and incorporation of lessons-learned.

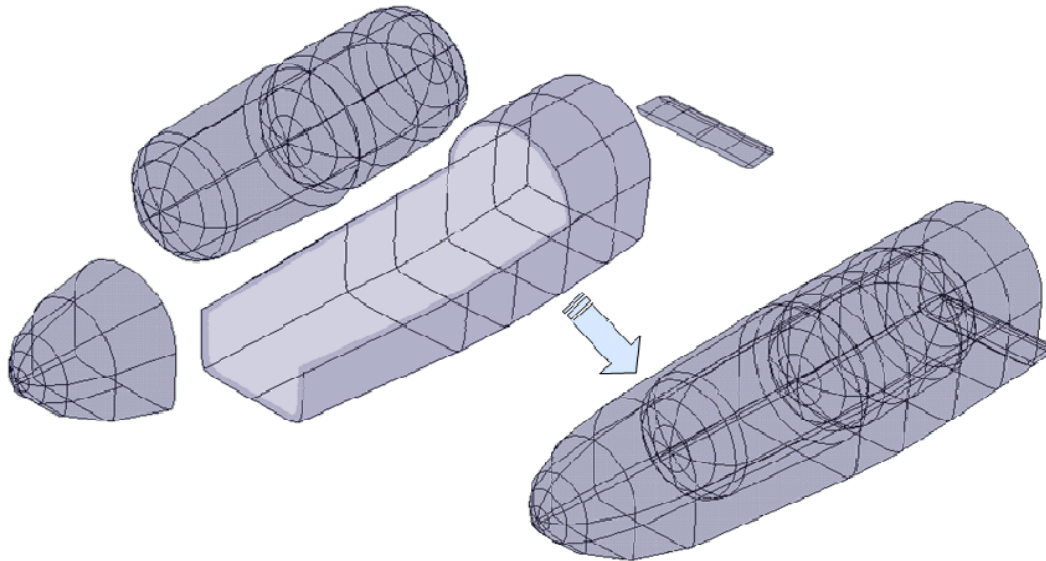


Figure 29. Near-term Structures Demonstrator

The overall structural concept for the HOT EAGLE demonstrator fuselage as conceived by CRC and Convergence Engineering is shown above. The fuselage is built in three main sections – nose cap, integral tanks, and fuselage slipper containing the engine and wing mounts. These are bonded together forming a strong, light, and affordable structure. Wings and tails are built up from top and bottom skins plus one-piece waffle box substructure sections, bonded together as described in the Micro-X final report³ then bonded into the slipper section in a form-fitting recess (not shown).

Testing of the resulting structure article would begin with pressure and cryogenic testing of the integral tanks. Next, simulated air, inertial, propulsion, actuation, and landing gear loads would be applied using the facilities at WPAFB. This would include a reasonable amount of fatigue testing as well. Localized TPS testing would occur using the WPAFB heating and acoustic generation capabilities. Finally, landing gear would be simulated and drop tests conducted.

Completion of this ground structural testing would increase confidence and reduce risk for the subsequent flight test program. Another complete vehicle structure would be built, incorporating further optimization and design detailing, into which the systems, propulsion, avionics, and other flight equipment would be installed. Flight test could commence in 2012 or earlier, with front-loaded funding. To save up-front expenses, certain technologies and components could be left off the vehicle for initial flight testing then added later after basic flight envelope expansion has been completed. For example, the real TPS is only required for high Mach and reentry flights. Early flights could be done with dummy TPS made of expanded foam or similar material.

Costs for this demonstration program in the areas of propulsion, subsystems, and structures were estimated by component cost buildup carried out by the CRC subcontractors as described in their separate project reports. These estimates were then brought together by CRC and combined with historical and expert opinion estimates for other costs, plus management reserve and project management and overhead. Results are shown below, and total about \$3.4m for the

structure demonstrator and about \$72 million for the flight demonstrator. To this must be added government-side costs for technical activities, management, and test facility and operations costs, which should add about 50% to the estimates below.

Table 24. Cost ROM

	\$k
Concept design, analysis, and simulation	\$4,000
Airframe design and fabrication	\$7,500
Propulsion development, fabrication, and test	\$20,000
Flight Control and other software	\$4,000
Subsystems design and fabrication	\$3,000
System integration and test	\$2,000
TPS design and fabrication	\$8,000
Facilities design and fabrication	\$4,000
Flight test	\$2,000
Project Management (10%)	\$5,450
Management reserve (20%)	\$11,990
Total	\$71,940

Table 25. Structural Test Article Cost ROM

	\$k
Concept design refinement	\$50
Airframe design and fabrication	\$1,922
Propulsion - interface def	\$20
Flight Control - interface def	\$10
Subsystems - interface def	\$20
Cryo tank technical support	\$50
TPS test design and fabrication	\$250
Test equip design and fabrication	\$200
Test support (~2 people, 20 days)	\$60
Project Management (10%)	\$258
Management reserve (20%)	\$568
Total	\$3,408

9. SUMMARY AND CONCLUSIONS

The HOT EAGLE Phase One study has defined vehicle concepts in three types – Reusable Upper Stage, Global Troop Transport, and Demonstrator. The Reusable Upper Stage will place a payload of about 5,000 lb into a 100 nmi orbit after boost on an HLV/ARES-class vehicle. The Global Troop Transport will deliver an entire Marine Rifle Squad to any spot in the world in less than an hour, and then allow them to egress to safety once their mission is complete. The Demonstrator will validate technologies and vehicle concepts to attain these operational objectives. While clearly these HOT EAGLE operational systems are DARPA-hard, the analysis above indicates that they are feasible with the aggressive application of emerging technologies. The HOT EAGLE Demonstrator will reduce the risk and help guide the program to success.

The next step in the HOT EAGLE program should be a second round of vehicle definition, analysis, optimization, and systems studies. While HOT EAGLE was fortunate to leverage from the prior Micro-X studies by CRC, this benefit was insufficient to assume that the HOT EAGLE designs are done and ready for fabrication. The immediate follow-on study should include the following activities:

- Design analysis of external payload configuration
- Detailed review of options for moving cg forward to reduce tail size
- Rescrub of RUS-VL assumptions and analysis
- Rescrub of tank approach (liner vs. linerless, materials)
- Study of engine alternatives
- Refined CFD on selected configuration with goals to minimize tail size, heating, loads, and risk
- Dynamic simulation with control actuation modeled to validate system stability and fine-tune allowable gains
- Design & integration of baseline TPS with attachments, including vendor buy-in and quotes
- Configuration baseline selection and refinement
- Refinement of structure and systems designs, development of vendor detailed cost quotes for flight-worthy demonstrator fabrication

Following those efforts the design should be mature enough to proceed into the structural demonstrator design activities, then on to the flight test vehicle.

10.REFERENCES

- 1 Raymer, D., "X-VTOL Spacecraft Conceptual Design Study (Final Report)", Conceptual Research Corporation, Los Angeles, CA, 4/9/03
- 2 Raymer, D., "MicroDemonstrator Rocket Design Study (Phase Two Final Report)", Conceptual Research Corporation, Los Angeles, CA, 11/25/03
- 3 Meyer, D., Wells, C., & Raymer, D., "MicroDemonstrator Rocket Airframe Preliminary Design & Analysis (Phase Three Final Report)", Conceptual Research Corporation, Los Angeles, CA, 02/03/04
- 4 Raymer, D., "MicroDemonstrator Rocket-Powered Technology Demonstrator Design Study (Phase Four Final Report)", Conceptual Research Corporation, Los Angeles, CA, 5/31/05
- 5 Raymer, D., "Micro-X Rocket Powered Technology Demonstrator Design Study (Phase Five Final Report)", Conceptual Research Corporation, Los Angeles, CA, 10/21/05
- 6 Bryan Munro, B., and Zanzig, J., , "Stability Characteristics of MicroX Preliminary Design Concepts", Report AMI 0541 IR, Analytical Methods Inc., Redmond, WA, 10/04/2005
- 7 Isakowitz, S., et al., International Reference Guide to Space Launch Systems, Third Edition, AIAA, Washington D.C., 1999
- 8 Encyclopedia Astronautica (www.astronautix.com)
- 9 Raymer, D., *AIRCRAFT DESIGN: A Conceptual Approach*, American Institute of Aeronautics and Astronautics, Washington, D.C., Third Edition 1999
- 10 Sutton, G., *Rocket Propulsion Elements (5th ed.)*, John Wiley & Sons, 1986
- 11 Bate, R., et. al., *Fundamentals of Astrodynamics*, Dover, NY, 1971
- 12 Griffin, M., & French, J., *Space Vehicle Design*, American Institute of Aeronautics & Astronautics, Reston, VA, 1991
- 13 Koelle, H. (ed.), *Handbook of Astronautical Engineering*, McGraw-Hill, 1961

11.APPENDICES

The following table is a side-by-side comparison of key design data for the main HOT EAGLE concepts described above. Note that the “HOTGLOBE” and “HOTGLOB1” designs are geometrically similar to the small Demonstrator, whereas the “HOTGLOB2” is virtually identical to the RUS geometry.

Table 26. Summary and Comparison of HOT EAGLE Concept Design Data

	Demonstrator		Reusable Upper Stage			Global Range Troop Transport		
	Horizontal Landing	Vertical Landing	H-Land, Mid-Bay	H-Land, Front-Bay	V-Land, Front-Bay	Parasail + Fulton	BellyJets+ Fulton	Belly & Rear Jets
	HE-DEMO	HE-DEML	HE-RUS	HE-RUS2	HE-RUSVL	HOTGLOBE	HOTGLOB1	HOTGLOB2
W-gross	25000	25000	73000	73000	73000	19000	25000	73000
W-empty	6939	7051	10353	10115	10314	12615	12828	14893
W-payload	2000	2000	5000	5000	5000	4200	4200	4200
W-misc UL	629	1341	1201	1204	2503	2185	7972	13124
W-propellant	15433	14608	56446	56681	55183	0	0	40783
PMF	61.7%	58.4%	77.3%	77.6%	75.6%	0.0%	0.0%	55.9%
# engines	4	5	4	4	5	0	4	4
T per engine	8750	7000	20000	20000	16000	0	7000	20000
T/W	1.4	1.4	1.1	1.1	1.1	0.0	1.1	1.1
Length	27.6	27.6	57.3	57.3	57.3	35	35	57.3
Diameter	6.4	6.4	10.8	10.8	10.8	7.5	7.5	10.8
Wland/Wo	0.38	0.42	0.23	0.22	0.24	1.00	1.00	0.44
Stall kts	168	180	135	132	138	225	225	186
Approach kts	194	207	155	152	158	258	258	214

This table shows the systems and avionics weights as estimated by USL and described in their report. This was based on the previous Micro-X 4 demonstrator design layout, but with estimated HOT EAGLE Demonstrator operational conditions and loadings. These values as shown in the first column were adjusted by CRC to the conditions and assumptions of the various HOT EAGLE vehicles. Adjustments included vehicle size (scale), technology assumptions, and mission peculiarities. Revised values are in shaded cells. All of these estimates are debatable and should be revisited in a later study when the system characteristics of the various HOT EAGLE concepts are further detailed.

APPENDIX A: XCOR – HOT EAGLE Report

A1. EXECUTIVE SUMMARY

XCOR Aerospace was asked to define propulsion systems for HOT EAGLE demonstrator and operational vehicles, define and assess propulsion technologies, determine propulsion penalties of vertical landing capability, and derive a cost estimate and schedule for development of the propulsion system concept.

The primary challenge in defining the HOT EAGLE propulsion system has been the range of system options considered: for ground takeoff the throttling requirement for vertical landing is a modest penalty; for upper stage mission the requirement to tolerate sea-level operation significantly degrades performance and puts a premium on high Isp.

XCOR defined thrust, specific impulse, propellant allowance for start-up and chill-down, and propellant mixture ratio, and estimated external dimensions and mass for engines, pumps, actuators, and other rocket propulsion components based on engineering judgment. Analyses were made of engines for HOT EAGLE demonstrators with both vertical landing and horizontal landing. As a result, we determined that there is a substantial performance penalty for a vertical landing system. In an upper-stage mission high Isp is essential, and the only way to get high Isp is high expansion, which leads to engines that cannot operate at sea level; this in turn requires unpowered horizontal landing. A vertical landing vehicle suffers **both** the penalties of throttling and the somewhat lower take-off weight due to smaller engines.

Trade space assessed methane versus kerosene fuels for the propellant. The compelling performance (seven percent increase in Isp) and cryogenic (kept at near-LOX temperature) advantages of methane resulted in CRC directing us to focus on it.

We examined several means for lowering propulsion system mass and/or increasing performance. Aluminum could lower the mass of the combustion chamber's inner layer by about 60%, resulting in a three- to five-percent reduction in total engine weight.

Carbon fiber composite can optimize the pressure jacket in larger engines by reducing the mass of the jacket. Ceramic matrix composites can be made into very thin nozzles, which offer a 60-65% reduction in nozzle extension mass and provides a 20-25% reduction in engine mass for engines with large vacuum nozzles. Since XCOR has been developing a piston motor and pump assembly for about three years, and is currently working on third generation prototype hardware that we expect to deploy in an operational engine in 2006, this is our reference technology for the baseline engine. Chamber pressure for the baseline engines is 600 psi because we know we can get long-life reusable chambers at this pressure and we have completed cooling and pump-drive analysis. Higher chamber pressure involves a major development program that would extend over many years.

We estimate a \$7 million, three-year program that culminates in readiness for production of the flight demonstrator engines.

A2. OVERVIEW

The HOT EAGLE program called for studies of a vehicle with a reusable upper-stage and expendable lower stage that could also deliver strategic equipment or a small squad of Marines to any point on the globe – even the most hard-to-reach location – within hours of deployment (See Appendix A: Alternative Concepts for the Global Insertion Mission). The combination of missions to be performed by HOT EAGLE resulted in some of XCOR's configuration choices, such as the trade between vertical and horizontal landing and LOX-methane (CH₄) and LOX-kerosene propellant.

Under the contract terms and statement of work (SOW) as accepted by Conceptual Research Corporation (CRC), XCOR's tasks for this project were to:

- Define propulsion systems for HOT EAGLE demonstrator and operational vehicles based on thrust and throttling requirements specified by Conceptual Research Corporation (CRC), for pump-fed LOX/methane and LOX/kerosene engines. This definition includes thrust, specific impulse, propellant allowance for start-up and chill-down, and propellant mixture ratio. We estimated external dimensions and mass for engines, pumps, actuators, and other rocket propulsion components based on engineering judgment, interpolation and extrapolation from past XCOR engine design efforts, including our DARPA SCAMP study, which was for LOX-methane stages using XCOR rocket engines and piston pumps.
- Define and qualitatively assess applicable propulsion technologies and concepts, with commentary based on engineering experience and a metric assessment of figure-of-merit parameters such as reliability, development risk, performance, weight, and technology readiness.
- Evaluate the propulsion penalties of vertical landing capability by comparing estimated system weights for non-throttled engines to throttled engines meeting CRC throttling targets. This comparison was based on engineering judgment and did not involve new engine design efforts.
- Provide estimated development cost and schedule for the selected propulsion system concept. This did not include vendor quotes as we do not have sufficient detail to issue an RFQ, but was established from our engineering judgment.

In an earlier report we completed initial estimates on the propulsion systems for the HOT EAGLE demonstrator and operational vehicles based on thrust and throttling requirements specified by Conceptual Research Corporation, and assessed the propulsion penalties of vertical landing capability. In this final report, we reiterate those data, and provide concept drawings and estimates for the Demonstrator HL and VL engines, as well as drawings and initial estimates for the Operational engine.

A3. PROPULSION SYSTEMS

XCOR investigated the feasibility of propulsion systems for pump-fed LOX/methane and LOX/kerosene engines for the HOT EAGLE demonstrator and operational vehicles based on the requirements outlined by CRC.

The primary challenge in defining the HOT EAGLE propulsion system has been the range of system options considered. For ground takeoff the throttling requirement for vertical landing is a modest penalty. For an upper stage mission, the requirement to tolerate a sea-level landing operation significantly degrades. LOX-CH₄ or LOX-kerosene systems require approximately one second of full LOX (and CH₄ if used) flow for each engine to chill-down and start-up. This allowance must be made for VTHL launch and VTVL launch and landing.

Another challenge is in increasing chamber pressure. Typically, we have shied away from this in our engine work because it reduces reusability. However, research exists on how to build long-life, reusable high pressure engines, and, because the XCOR team put together some of these concepts when they worked at another company, we believe the problem is solvable. Nevertheless, long-life, reusable high pressure engines are much less mature systems than the moderate-pressure reusable engines we have been developing the past few years. This technology is not appropriate for a demonstrator, but we could make some estimates of what might be achievable in this direction and start painting a picture of where some R&D investments might be made and how much weight might be reduced.

A3.1 Propellant

Trade space issues involved the use of LOX-methane (CH₄) or LOX-kerosene. Our assessment found that maintenance was not a factor:

- Kerosene tends to coke in cooling passages, and create other problems in reusable engines. However, modern, clean kerosenes may not have this issue.
- Methane has possible sulfur-corrosion issues.

However, methane has compelling performance advantages. It is seven percent higher in Isp than kerosene, and can be stored at near-LOX (cryogenic) temperature, eliminating the need for insulation between tanks. This also prevents CH₄ boiloff during ground holds, since the LOX tank provides cooling for the CH₄ tank.

When the trade space was completed CRC directed us to focus on methane. With this determined it should be noted that “RP” methane is not part of the current logistics supply yet, instead LNG is widely available. XCOR is part of a working group which will define RP-grade LNG/Methane soon.

Propellant boiloff is a concern for cryogenic propellants such as LOX or methane. Depending on how much insulation we carry, boiloff will likely be one- to two-percent of tank mass per hour. During the mission, this is probably not significant. However, for an operationally responsive spacelift, the customer may desire a vehicle which can sit in a ready-to-launch state for extended periods, waiting for mission authorization, a tight launch window, or to launch in response to an external event. In such a case, we can sit, indefinitely, in a ready-to-launch state as long as the tanks are insulated and boiloff is periodically replenished from ground facilities.

By leaving a little extra tank volume, the time between replenishment is extended. For example, if we have 1.5% per hour boiloff, leaving an extra six percent tank volume allows us to go for four hours between replenishment activities. Tank insulation is typically foam. If it is structural (as in a composite tank) it needs to be approximately five pounds per cubic foot. If the tanks are not structurally connected to the aeroshell, then a lower density foam in the two pounds per cubic foot range can be used. XCOR has typically employed 1 to 1.5 inches of insulation thickness to eliminate icing completely.

For axisymmetric tanks, which only need to drain when the primary acceleration loads are aft, we would expect about one percent residual oxidizer, and approximately two percent residual fuel. This assumes a propellant management system where the O:F ratio is adjusted to burn both propellants dry nearly simultaneously. Such a system requires propellant quantity sensors in the tank and an appropriate piece of software in the flight computer. In addition, the ullage pressurization gases remain as residual weight in the tank.

In all circumstances to date, XCOR has used helium pressurant. The pressure required for this operation will be set by the pump net positive suction head (NPSH). These types of pumps are still in development at XCOR. For preliminary design purposes, we suggest 45 psia ullage pressure for LOX or methane, with 25 psia ullage pressure for kerosene.

A3.2 Nozzles

The HOT EAGLE program requires high performance vacuum nozzles that will expand the exhaust to low exit pressure, gaining extra thrust. For this study XCOR compared sea level landing nozzles to those usable only at high altitude. Sea level nozzles are short and must not expand the exhaust below approximately one-third atmosphere exit pressure, while vacuum nozzles face no such limitation. XCOR did assess various “altitude compensating” nozzles which were not included in the baseline due to low technical maturity or penalties in vacuum performance.

It should be noted that conventional nozzle shape is only optimized for a fixed operational point and since specific impulse increases with an increase of the nozzle size an extendible nozzle is attractive. Extendible nozzles (Figure A-1) provide altitude compensation, and in vacuum allow for higher performance by applying higher nozzle expansion area ratio. Nozzle exit pressure can be decreased with a high-area-ratio nozzle to enable combustion gas to expand more. However, the high-area-ratio nozzle will buckle at or near sea-level due to the low pressure inside the nozzle.

There are two technologies that achieve high vacuum Isp in a sea-level operable engine:

1. A translating, or jettisonable, nozzle extension, which suffers approximately 10% Isp penalty at sea level; at TRL 4-5.
2. Liquid injection separation control, which suffers approximately 5% Isp penalty at sea level; at TRL 3-4.



Figure A-1. Extendible Nozzle for Altitude Compensation

Other altitude-compensating nozzles suffer performance penalties in the critical vacuum phase:

- Aerospike, or expansion-deflection, nozzles (Figure A-2) lose several percent I_{sp} , and have major uncertainties in sea-level operation that pose significant program risk.
- Dual-bell concepts (Figure A-3) could cut vacuum I_{sp} loss to one to two percent, but these technologies are not very mature.

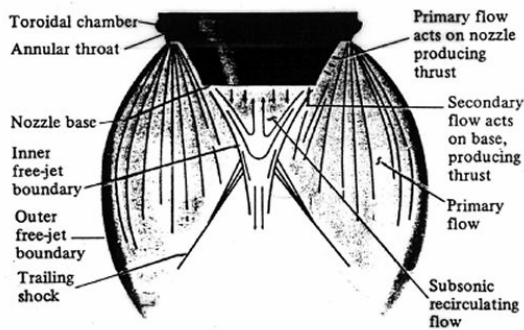


Figure A-2. Diagram of an Aerospike Nozzle



Figure A-3. Dual Bell Nozzle Test

A3.3 Demonstrator Vehicles

We have been assuming fairly conservative engines for the demonstrator, with no breakthroughs and a cost-constrained development environment. We have estimated the performance cost of vertical landing versus a horizontally landed system. Since a reusable upper stage would primarily fly in vacuum we could use significantly larger nozzles, and this has significant impact on the specific impulse. Given a 25,000 lbm takeoff weight, we assumed a constant T/W ratio of 1.4:1. In some cases this is required for engine-out margin. However, our own trajectory experience suggests that for performance reasons you would probably not want to go much below that even in cases where engine-out capability is not needed.

A3.3.1 Demonstrator VL Engine

To determine the consequences of vertical landing for the propulsion system, we looked at three engines, with both LOX-methane and LOX-kerosene propellant (six in total).

Based on our assessments, a VTVL vehicle will require a cluster of five, 7,000 lbf sea level engines, which are able to throttle to 72% with Pexit (exit jet pressure) at least one third bar and 12:1 expansion. Each engine will have a 156 lb mass and approximately 18 inch diameter

package with an overall length of approximately 39 inches. At the engine's head end, the gimbal tripod and actuators may extend somewhat further than the 18 inch diameter.

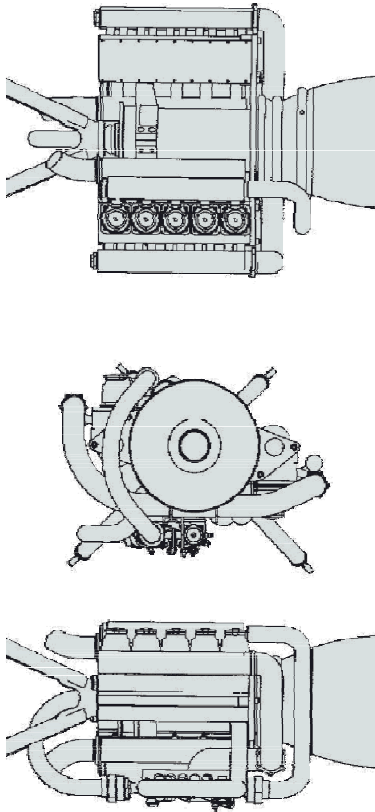


Figure A-4. Concept Drawing of the Demonstrator VL Engine

The technical requirements for a pump-fed LOX-methane and/or LOX-kerosene demonstrator VTVL engine in a HOT EAGLE vehicle based on thrust and throttling requirements specified by Conceptual Research Corporation include:

- An integrated pump, valve, and engine assembly.
- A nozzle short enough for sea-level operation when throttled.
- Capability of throttling to 72% of full thrust.
- Operator ability to select any engine in the five-engine cluster to provide thrust for vertical landing.
- Chamber pressures at max throttle of 577 psi (lower than HL engines due to higher injector drop to allow throttling).
- XCOR's existing piston-pump technology, which has similar performance to turbomachinery of this size (for long-life and low cost).
- 7,000 lbf thrust at sea level, 8,432 lbf in vacuum.
- ISP of 253 sec at sea level, 304 sec in vacuum.
- 156 lbm each, 780 lbm for a five engine cluster.

A3.3.2 Demonstrator VTHL Engine

For the Demonstrator VTHL engine, we recommend a cluster of four engines with a total mass of 712 lb, and Pexit of one third bar at 15:1 expansion. Each engine will have 8,750 lbf sea level thrust, no throttling capability, and an 178 lb engine mass. The engine package will be approximately 18 inch diameter and have an overall length of approximately 42 inches. As with the VL, the gimbal tripod and actuators may extend somewhat out of 18 inch diameter at the engine's head end.

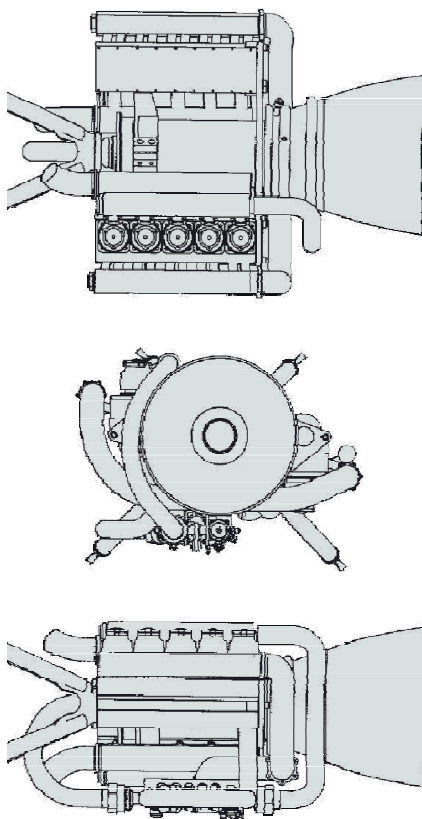


Figure A-5. Concept Drawing of the Demonstrator HL Engine

The technical requirements for a pump-fed LOX-methane and/or LOX-kerosene VTHL demonstrator engine in a HOT EAGLE vehicle based on thrust and throttling requirements specified by Conceptual Research Corporation (CRC) include:

- An integrated pump, valve, engine assembly.
- A nozzle short enough for sea-level operation.
- Four, non-throttling, packaged engines to allow step-throttling on ascent for G management.
- Chamber pressure is 600 psi, and is based on mature technology (for long-life).
- XCOR's existing piston-pump technology, which has similar performance to turbomachinery of this size (for long-life and low cost).
- 8,750 lbf thrust at sea level, and 10,947 lbf in vacuum.
- ISP is 247 sec at sea level, and 309 sec in vacuum.
- Mass is 178 lbm for each engine, and 712 lbm for cluster of four engines.
- Overall this propulsion system has nine percent lower mass and one-and-one-half percent higher vacuum ISP than the VL design. These are both a win for HL.

A3.4 Operational HL Vehicle

In an earlier report, XCOR surveyed a number of possible technologies summarizing strengths and weaknesses of the HOT EAGLE systems. For the operational vehicle, we assumed an initial mass at ignition of 75,000 lbm, and that the engines for the vehicle only needed to operate in vacuum. This assumption allowed us to design for much higher performance vacuum nozzles. We considered the number of engines desired based on weight, packaging, and engine-out capabilities. Finally, we explored the possibility of using separate landing engines to enable a vertical belly landing for the global transport mission.

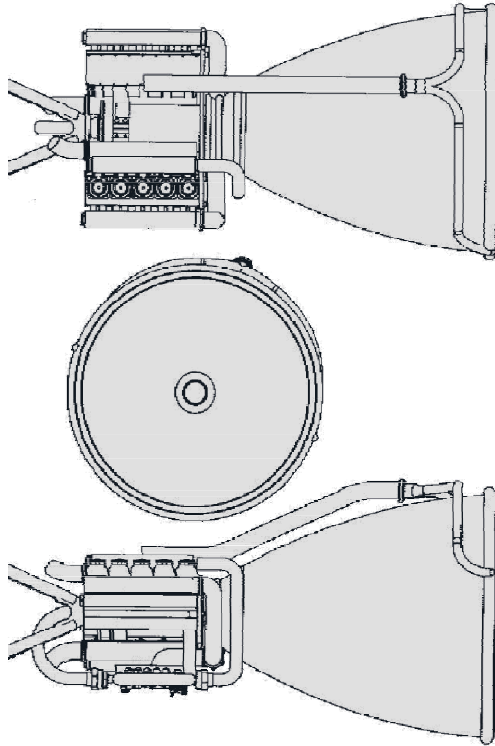


Figure A-6. Concept Drawing of Operational HL Engine Based on XCOR's Analyses

The technical requirements for a pump-fed LOX-methane and/or LOX-kerosene HL operational engine in a HOT EAGLE vehicle based on thrust and throttling requirements specified by Conceptual Research Corporation include:

- Four engines for packaging and to allow step-throttling on ascent.
- Engines not throttled.
- 600 psi chamber pressure, which is the same as HL demonstrator.
- XCOR's existing piston-pump technology, which has similar performance to turbomachinery of this size (for long-life and low cost).
- 20,000 lbf vacuum thrust, which is not usable below approximately 100 kft, and is most suitable for larger operational vehicle.
- ISP 347 sec vacuum
- A mass of 385 lbm for each engine, and 1,540 lbm for four engine cluster.
- 12% higher ISP than an HL with ground takeoff, and 14% higher ISP than VL that uses boost engines for landing.

A4. APPLICABLE PROPULSION TECHNOLOGIES AND CONCEPTS

For the HOT EAGLE operational system, we have enough time to mature applicable technologies to enhance vehicle performance. However, there is NO technology offering significant improvement in I_{SP} without other compromises. For example:

- High I_{SP} comes from high expansion ratio – big nozzles and/or small throats
- Big nozzles require innovative packaging in reusable system.
- Small throats come from high chamber pressure.

Below is a summary of technologies XCOR considered for application to the HOT EAGLE engines. Each technology includes a brief discussion of its status and potential benefits. These technologies are each incrementally applied to a basic piston pump-fed, concentric-shell combustion chamber with tube-bundle nozzle.

For comparison purposes, each technology includes ratings for Performance, Cost, and Technical Readiness (TRL) on a one to ten scale, with 10 as the best and one as the least desirable:

- Performance is on a scale where 10 is a 30% weight reduction or five percent I_{SP} gain.
- Cost is a subjective estimate of life-cycle cost with 10 the lowest and one the highest cost.
- TRL values reflect NASA/DOD designations.

A4.1 Aluminum Combustion Chamber

Combustion chambers are typically made of copper or stainless steel. However, we use a baseline of copper with aluminum outer shell because aluminum has high thermal conductivity and strength, lower density, and is light weight. By using aluminum in the chamber and injector, we could lower the mass of the combustion chamber's inner layer by about 60%, which would result in a 3%-5% reduction in total engine weight.

These chambers have been tested in XCOR's lab at low pressure, but have not yet been implemented in flight. We are not aware of any programs that have reached flight ready status for an aluminum chamber at 600 psi or greater pressure, which is the baseline for larger engines.

No breakthroughs are required, but there are some issues to solve:

- Cooling design must be more robust to keep wall temperature within aluminum limits.
- Aluminum is flammable in high pressure oxygen, so we need a careful injector design to avoid oxidizing streaks.

Performance: 2, Cost: 9, TRL: 4

A4.2 Carbon-Fiber Composite Chamber Jacket

The pressure jacket in larger engines is usually sized based on strength due to pressure stresses, stiffness due to the bending stresses of gimbaling, and the minimum gauge required for fittings and manifolds. We can optimize each of these properties by switching from structural metals to carbon fiber composite.

The difference in coefficient of thermal expansion (CTE) between composite and metallic materials makes bonded designs difficult. However, the chamber-saddle-jacket design that XCOR has used to maximize chamber life permits thermal expansion by disconnecting the inner and outer layer of the combustion chamber. A carbon-fiber composite chamber jacket offers about 50% reduction in mass of the jacket compared to aluminum, for a 0.5%-1% reduction in total engine mass.

Performance: 1, Cost: 9, TRL: 4

A4.3 Ceramic-Matrix Composite (CMC) Nozzle Extension

XCOR's reference design for the nozzle extension uses a tube-bundle metallic nozzle, which is a mature technology for reusable engines. As an example, it was used in the DC- X's RL-10 engines. Nozzles are under relatively low pressure stresses and are therefore sized primarily by minimum gauge. At the same time, the nozzle extension must incorporate cooling. While baseline engine weights use metallic nozzles, our investigation demonstrates that ceramic matrix composites (CMC) have much lower density and can be radiation cooled, which allows them to be simple shells. If CMC nozzles can be made in very thin shells, they could offer a 60-65% reduction in nozzle extension mass that provides a 20-25% reduction in engine mass for engines with large vacuum nozzles.

Eliminating oxidation is the fundamental challenge with CMC nozzle extensions. When you burn fuel and oxidizer, the overall mixture is reducing, there is more fuel than oxidizer, but there are always eddies and streaks where there is a bit of extra oxidizer. Carefully balancing the fuel/oxidizer mixture ratio near the nozzle wall to ensure a reducing environment, combined with the use of oxidation-resistant coatings could make CMC nozzles practical in a reusable engine and offer substantial engine mass reduction.

CMC nozzles are flying today; issues for HOT EAGLE are:

- Can reusable nozzles be made in thin shells of 0.03-inch thickness or are such nozzles too fragile for reusable systems?
- Can the oxidation resistance of these nozzles be made rugged enough to keep the nozzle intact during reentry?
- Can the radiative nozzle start close to throat (i.e., at low expansion ratio)?

Performance: 10, Cost: 6, TRL: 5

A4.4 Piston Motor/Pump Assembly

XCOR has been developing a piston motor/pump assembly for about three years, and is currently working on third generation prototype hardware that we expect to deploy in an operational engine in 2006. Therefore this is our reference technology for the baseline engine.

In large engines, piston pumps are a bit heavier than conventional turbopumps, but for the engine size that HOT EAGLE requires, piston pumps are competitive with turbopumps by weight, and are far lower in cost and more durable. Piston pumps do require maintenance from time to time, but this consists of replacing seals at a modest cost in labor and parts. However, relative to piston pumps, existing turbopumps have short life and are major contributors to

engine operating cost. Indeed, with the exception of the RL- 10, turbopump assemblies typically require major overhaul on a scale of tens of flights.

Replacement cost of turbopumps is typically millions of dollars. Piston pumps, while less mature, should have somewhat longer life between overhaul, and the overhaul is a replacement of soft goods at negligible parts cost. The replacement cost of the entire piston pump assembly is on order of 5% of the turbopump assembly. Therefore, in a program driven by life cycle cost such as HOT EAGLE, the piston pump should be the baseline. As the piston pump matures we expect weight reduction of 20-25%, making them comparable to turbopumps in this size range.

A4.5 Higher Chamber Pressures

Chamber pressure is a design choice for engines that has a dramatic effect on the size of a rocket engine. However, an increase in chamber pressure tends to slightly reduce engine weight. Increasing chamber pressure, by itself, does not increase Isp, but a higher chamber pressure engine can fit a higher expansion nozzle in the same space. Even with the effects of higher expansion, increasing chamber pressure only slightly increases Isp. However, as this is almost the only way to increase Isp at all, it is worth considering.

We have derived the baseline engines to be 600 psi. Based on our cooling and pump- drive analysis to date, we are certain that we can get long-life reusable chambers at this pressure. The operational engines might be 600 psi, or we might increase this to somewhere between 750 to 900 psi since, combined with optimizing injectors, we can gain 3 to 4% Isp (355-360 sec).

If we were to increase the pressure beyond this, for instance in the 1,000 to 3,000 psi range, then we should expect these engines to have shorter chamber life and hence a higher life- cycle cost. Higher chamber pressure causes heat flux increases, which create thermal stresses within the engine materials. This would prevent the use of materials such as aluminum that offer more promising weight reductions.

There is a suite of technologies for ultra-high pressure engines (4,000+ psi), which employ transpiration cooling to get long life, and we may be able to make transpiration cooled chambers from aluminum making them weight competitive with lower pressure chambers. Additionally, this higher pressure is very suitable for a piston pump because piston pump mass scales very slowly with pressure.

However, this approach requires significant research. It would be a whole new engine technology, where virtually every piece of the engine would have to be developed from scratch and necessitates moving the HOT EAGLE program from RL-10 to SSME operability. While the resulting engine would be nice to have, there are probably less costly and more reliable ways to gain performance for a vacuum-stage HOT EAGLE. Since this would be a major development program extending over many years; we judged this to be beyond the scope of HOT EAGLE.

Performance: 7, Cost: 2, TRL: 4

A5. PROPULSION PENALTIES OF VERTICAL LANDING

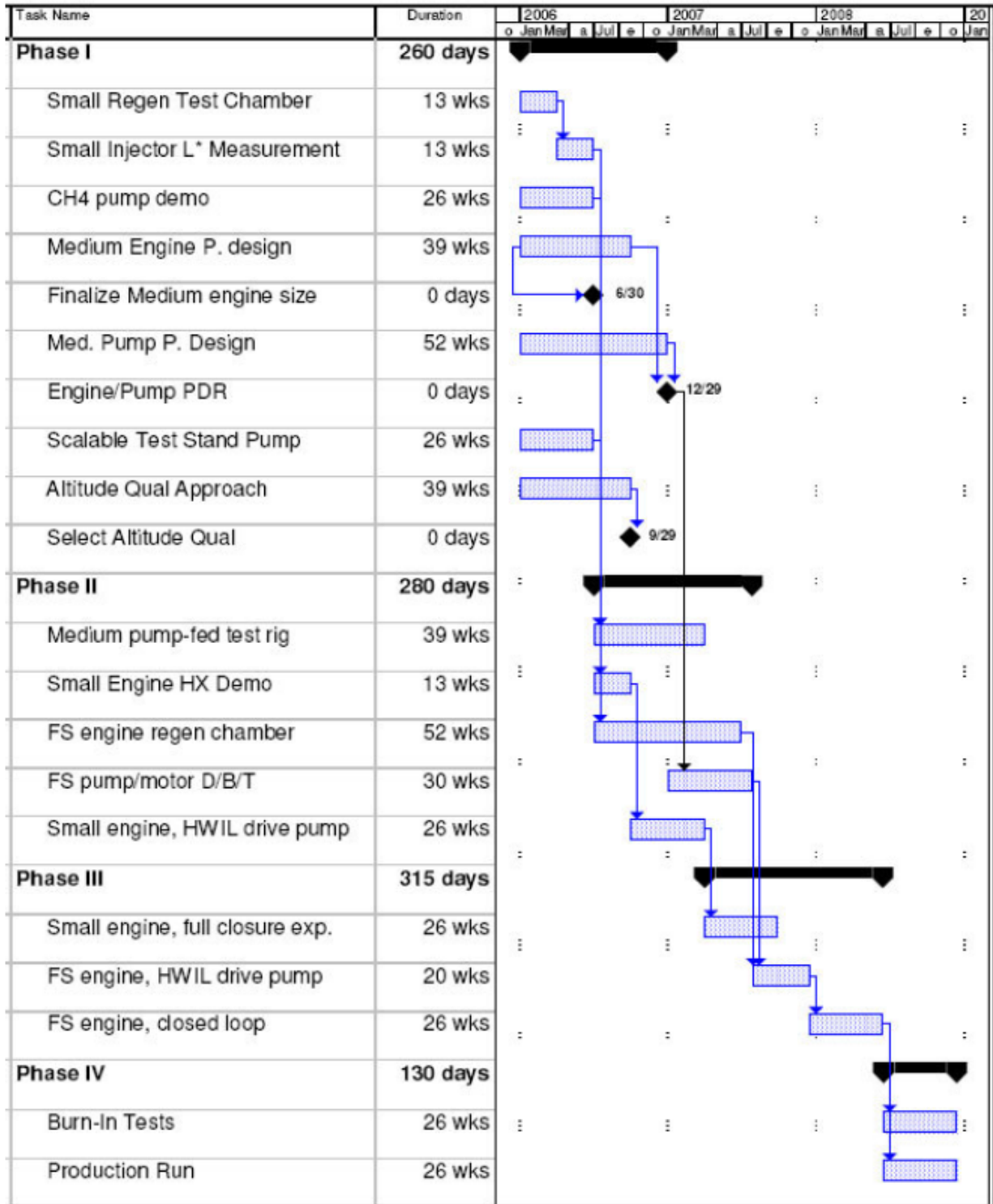
Vertical landing vehicles require throttled engines, which imposes a slight penalty in I_{sp} and engine weight, described above in section on engines. Also, because the engine must operate at sea level as well as out of the atmosphere, vertical landing vehicles suffer a substantial penalty in I_{sp} , on the order of twelve percent. Constraining the nozzle for sea level operation imposes penalties discussed above under nozzles.

The combined effect of the above means that a vertical landing system's I_{sp} is penalized by about 14%. This would be even higher if fewer than five engines are used because they would have to throttle more deeply and have an even higher I_{sp} penalty from throttling.

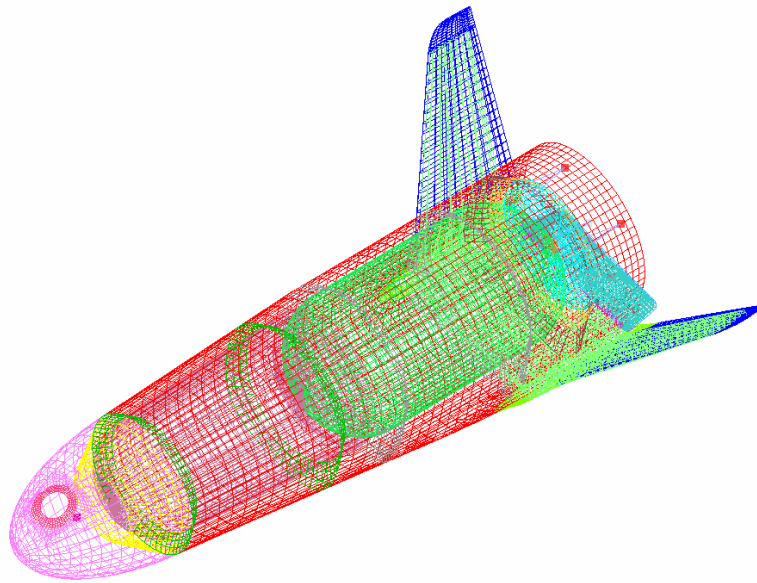
The reason horizontal landing vehicles do not have this problem is not because they land horizontally, it is because they do not need to operate the engines inside the atmosphere. A powered horizontal lander would have almost the same I_{sp} as a powered vertical lander. Most horizontal landing versions use unpowered landing, which means that they can use vacuum-optimized engines with higher I_{sp} .

A6. DEVELOPMENT COST AND SCHEDULE

XCOR's final task is a rough order of magnitude (ROM) schedule and cost estimate for the HOT EAGLE engines. We have looked only at the Demonstrator engine, since the technologies for the Operational engine have not yet been selected. We estimate a \$7 Million, three year program culminating in readiness for production of flight demonstrator engines.



APPENDIX B:
Preliminary Structural Analysis



SUBMITTED TO

Daniel P. Raymer, Ph.D. President, Conceptual Research Corp.
PO Box 5429
Playa del Rey, CA 90296

By Subcontractor Convergence Engineering Corp.
1638 Finch Drive, Gardnerville, NV 89410 Performed by

Dave Crockett

Dr. Rory R. Davis, P.E.

Osprey Technologies, LLC

Convergence Engineering Corp.

2655 W. Oak Grove, Chandler, AZ 85224

15 November 2005

HOT EAGLE Preliminary Structural Analysis 11-15-2005 Convergence Engineering Corp.

TABLE OF CONTENTS

B1.	INTRODUCTION	85
B2.	FINITE ELEMENT MODEL	87
B2.1	Model, Design, and Analysis Assumptions.....	87
B2.2	Model Geometry and Configuration.....	87
B2.3	Material Properties	88
B2.4	Primary Structures	90
B2.4.1	Nosecone	90
B2.4.2	Fuselage.....	91
B2.4.3	Wing and Wing Carry-Through	91
B2.4.4	Payload Cone.....	95
B2.4.5	Engine Bulkhead and Cone Assembly	97
B2.4.6	Rear Aero Flap	98
B2.4.7	Propellant Tanks.....	98
B2.5.	Mass Properties	100
B3.	TRADE STUDIES.....	101
B3.1	Propellant Tank Material Selection	101
B4.	ANALYSIS.....	104
B4.1	Analysis Load Cases.....	104
B4.2	Local Analysis	105
B4.2.1.	Propellant Tank	105
B4.3	Vehicle Analysis.....	109
B4.3.1	Ground Handling Horizontal Lift Load Case.....	109
B4.3.2	Ground Handling Vertical Lift Load Case.....	110
B4.3.3	Launch Load Case.....	112
B4.3.4	Powered Flight: Exo-Atmospheric.....	121
B4.3.5	Re-Entry Load Case	125
B4.3.6	Chute Deployment Load Case.....	132
B4.3.7	Vehicle Landing Load Case	136
B4.3.8	Demonstration Vehicle Launch Load Case.....	140
B5.	TPS TRADE STUDY AND ANALYSIS.....	148
B6.	SUMMARY AND CONCLUSIONS	151
B7.	REFERENCES	152
	APPENDIX BA: Tsai-Wu Failure Criteria.....	153
	APPENDIX BB: Loads Document.....	155
BB.1	Other important notes:	157

LIST OF FIGURES

Figure	Page
Figure B-1. FEM with Top Level Dimensions.....	88
Figure B-2. Primary Structures and Components Included in the Model	88
Figure B-3. Nosecone with Parachute Door Opening (0° Ply Direction Shown)	93
Figure B-4. Design Concept for Steel Ring around the Chute Door Opening.....	93
Figure B-5. Fuselage Section (0° Ply Direction Shown).....	94
Figure B-6. Modeling of the Wing Skin and Wing Carry-through (0° Ply Direction Shown).....	95
Figure B-7. Payload Cone with Forward Bi-mese Attach Lug (0° Ply Direction Shown).....	96
Figure B-8. Nosecone/Payload Cone/Fuselage Interface Joint	97
Figure B-9. Engine Support Structure (0° Ply Direction Shown)	97
Figure B-10. Model Details of the Rear Flap.....	98
Figure B-11. Model Details of the Propellant Tanks	100
Figure B-12. Model Details for Propellant Tank Analysis	106
Figure B-13. Tsai-Wu Survey Plot of the Liner and External Shell for the Thermal and Pressure Load.....	107
Figure B-14. von Mises Stress in the Foam Core for the Thermal and Pressure Load Case	107
Figure B-15. Tsai-Wu Stress Survey Plot of Composite Structure for the Thermal-only Load Case.....	108
Figure B-16. von Mises Stress in the Foam Core for the Thermal-only Load Case	108
Figure B-17. Deflection of the Vehicle with a 4 g Horizontal Lift	109
Figure B-18. Resultant Displacement of Structure during Horizontal Lift	110
Figure B-19. Tsai-Wu Stress Survey Plot of the Composite Structures during Horizontal Lift	110
Figure B-20. Deformed Geometry Plot of the Vehicle for a Vertical Lift.....	111
Figure B-21. Resultant Displacement Contour Plot of the Vehicle for a Vertical Lift.....	111
Figure B-22. Tsai-Wu Stress Survey Plot of the Composite Structures during Vertical Lift	112
Figure B-23. Vehicle Cp Plot from CFD Analysis for M = 2.0 and AOA = 2.0	113
Figure B-24. Vehicle Aero Load Pressure Profile for q=1200 psf, M=2.0 and AOA=2.0	113
Figure B-25. Aero Load Pressure Profile on Vehicle's Wing for q=1200 psf, M=2.0 and AOA=2.0.....	114
Figure B-26. Boundary Conditions and Loads on Model for Launch Loads Analysis.....	115
Figure B-27. Pressure Profile in Propellant Tanks.....	115
Figure B-28. Deformed Geometry Plot of the Vehicle for the Launch Load Case.....	116
Figure B-29. Resultant Displacement Contour Plot for the Launch Load Case	117
Figure B-30. Tsai-Wu Stress Survey of the Vehicle Composite Structures for the Launch Load	118
Figure B-31. Tsai-Wu Stress Survey of the Vehicle's Propellant Tanks for the Launch Load Case.....	118
Figure B-32. Tsai-Wu Stress Survey of Vehicle Composite Structures without the Propellant Tanks.....	119
Figure B-33. Tsai-Wu Stress Survey of Vehicle Composite Structures without Propellant Tanks.....	119
Figure B-34. Tsai-Wu Stress Survey of Wing Waffle and Wing Carry-through Composite Structures	120
Figure B-35. Tsai-Wu Stress Survey of Vehicle Engine Support and Payload Cone Structures	120

Figure B-36. Boundary Conditions on Model for Powered Flight Analysis.....	121
Figure B-37. Pressure Profile in Propellant Tanks.....	122
Figure B-38. Deformed Geometry Plot of the Vehicle for Powered Flight.....	122
Figure B-39. Resultant Displacement Contour Plot of the Vehicle for Powered Flight.....	123
Figure B-40. Resultant Displacement Contour Plot of Engine Support Structure for Powered Flight.....	123
Figure B-41. Tsai-Wu Stress Survey of the Vehicle's Composite Structures for Powered Flight.....	124
Figure B-42. Tsai-Wu Stress Survey of the Engine Support Structure for Powered Flight.....	124
Figure B-43. Vehicle Cp Plot from CFD Analysis for $M = 25.0$ and $AOA = 70.0$	125
Figure B-44. Vehicle Aero Load Pressure Profile for $q=190$ psf, $M=25.0$ and $AOA=70.0$	126
Figure B-45. Vehicle Aero Load Pressure Profile for $q=190$ psf, $M=25.0$ and $AOA=70.0$	126
Figure B-46. Boundary Conditions on Model for Re-entry Loads Analysis	127
Figure B-47. Pressure Profile in Propellant Tanks.....	127
Figure B-48. Deformed Geometry Plot of the Vehicle for Re-entry Loads.....	128
Figure B-49. Deformed Geometry Plot of the Vehicle's Wing for Re-entry Loads	128
Figure B-50. Resultant Displacement Contour Plot for Re-entry Loads	129
Figure B-51. Tsai-Wu Stress Survey of the Vehicle's Composite Structures for Re-entry	129
Figure B-52. Tsai-Wu Stress Survey of the Vehicle's Composite Structures for Re-entry Loads.....	130
Figure B-53. Tsai-Wu Stress Survey of the Vehicle's Composite Structures for Re-entry Loads.....	130
Figure B-54. Tsai-Wu Stress Survey of the Vehicle's Wing Waffle and Wing Carry-through Section.....	131
Figure B-55. Tsai-Wu Stress Survey of the Vehicle's Wing Waffle and Wing Carry-through Section.....	132
Figure B-56. Chute Deployment Force Applied to the FEM.....	133
Figure B-57. Pressure Profile in Propellant Tanks.....	133
Figure B-58. Deformed Geometry Plot of the Vehicle during Chute Deployment	134
Figure B-59. Resultant Displacement Contour Plot of the Vehicle during Chute Deployment	134
Figure B-60. Tsai-Wu Stress Survey of Vehicle's Composite Structures during Chute Deployment.....	135
Figure B-61. Tsai-Wu Stress Survey Plot of the Nosecone during Chute Deployment	135
Figure B-62. Landing Gear Geometry during Landing.....	136
Figure B-63. Vehicle Velocity and Acceleration Profiles during Landing.....	137
Figure B-64. Reaction Force on Landing Gear during Landing	137
Figure B-65. Resultant Displacement Plot of the Vehicle's Aft Skirt Region for Landing Loads.....	138
Figure B-66. Tsai-Wu Stress Survey of the Vehicle's Composite Structures during Landing..	139
Figure B-67. Tsai-Wu Stress Survey Plot of the Vehicle's Aft Skirt Region during Landing ..	140
Figure B-68. Vehicle Cp Plot from CFD Analysis for $M = 2.0$ and $AOA = 2.0$	141
Figure B-69. Vehicle Aero Load Pressure Profile for $q=1200$ psf, $M=2.0$ and $AOA=2.0$	141
Figure B-70. Aero Load Pressure Profile on Vehicle's Wing for $q=1200$ psf, $M=2.0$ and $AOA=2.0$	142
Figure B-71. Boundary Conditions and Loads on Model for Demonstrator Launch Loads Analysis.....	142

Figure B-72. Pressure Profile in Propellant Tanks.....	143
Figure B-73. Deformed Geometry Plot of the Vehicle for Demonstrator Launch.....	143
Figure B-74. Resultant Displacement Contour Plot of the Vehicle for Demonstrator Launch..	144
Figure B-75. Deflection Contour Plot of Engine Support Structure for the Demonstrator Launch.....	144
Figure B-76. Tsai-Wu Stress Survey of Vehicle's Composite Structures for the Demonstrator Launch.....	145
Figure B-77. Tsai-Wu Stress Survey of Vehicle's Composite Structures for the Demonstrator Launch.....	145
Figure B-78. Tsai-Wu Stress Survey of Vehicle's Composite Structures for the Demonstrator Launch.....	146
Figure B-79. Tsai-Wu Stress Survey of Vehicle's Composite Structures for the Demonstrator Launch.....	146
Figure B-80. Tsai-Wu Stress Survey of Vehicle's Composite Structures for the Demonstrator Launch.....	147
Figure B-81. Tsai-Wu Stress Survey of Vehicle's Composite Structures for the Demonstrator Launch.....	147
Figure B-82. Mechanical TPS Attach Concept.....	150
Figure BA-1. Tsai-Wu Failure Envelope Compared with Three Other Failure Criteria	154

LIST OF TABLES

Table	Page
Table B-1 Analysis Assumptions and Rationale	87
Table B-2. Mechanical Material Properties Used in the Analysis.....	90
Table B-3. Ply Schedule for All Primary Structures.....	91
Table B-4. Vehicle Mass Properties	101
Table B-5. Results of Material Trade Study for the Propellant Tanks	103
Table B-6. Vehicle Analysis Matrix	104
Table BB-1. Vehicle Load Cases.....	155

B1 INTRODUCTION

Convergence Engineering and Osprey Technologies have completed a preliminary structural analysis of the HOT EAGLE space vehicle as currently proposed by Dr. Daniel Raymer of Conceptual Research Corporation [1, 2, 3].

This work was performed under subcontract to Conceptual Research Corporation in support of its "HOT EAGLE" design study of a reusable upper stage for an HLV/ARES-class reusable lower stage. The CRC study also includes a manned Global Transport system based on the HOT EAGLE vehicle concept to perform certain high-value objectives in high-response operational scenarios, and includes the design definition of a subscale technology demonstrator sized appropriately to allow flight on an existing first- stage booster. The CRC study effort was funded by USAF-AFRL/VA and structured as a subcontract from the University of Dayton Research Institute.

This task continued and expanded the previous Micro-X structural tasks, assessing the effects of design and environmental details of the HOT EAGLE demonstrator design. This included structural design, FE stress analysis, and weight and cost estimation. Loading conditions were developed and analyzed, from launch to landing, for HOT EAGLE operational scenarios. Thermal Protection System (TPS) attachment concepts were also studied.

This effort is a continuation of the Micro-X previously analyzed [4]. In fact one of the assumptions going into this analysis is that the Micro-X finite element model (FEM) is used as a baseline for the HOT EAGLE analysis. The most significant modification to the model was in the propellant tank configurations. In the Micro-X design the tanks were separate and internal to the vehicle. For HOT EAGLE the tanks are combined into a single pressure vessel with one internal bulkhead. The tank diameters were also increased to match the outer mold line (OML) of the vehicle so that they now act as a primary structure capable of taking the vehicle's axial, bending, and shear loads.

Like the Micro-X, HOT EAGLE utilizes 5 liquid propulsion engines each providing 8200 lbf sea level thrust. The propellant system consists of liquid oxygen as the oxidizer and liquid methane as the fuel. The vehicle is capable of carrying a payload of 2000 lbm. All of the vehicle's primary structures are of an aluminum honeycomb sandwich core construction with carbon/epoxy facesheets.

Analysis and design of the vehicle is based on specific load cases time-lined with its operation: ground handling, launch, flight, re-entry, parachute deployment after reentry, and finally a vertical landing on 4 deployable support legs. One additional load case involved ground launch of a demonstrator vehicle. Here the demonstrator is assumed a single stage sub-orbital vehicle. The various load cases analyzed provided a design basis for the vehicle's primary structures. This included material selection, composite material lay-ups, and estimates of structural mass properties.

Also, contained within this report, are two trade studies involving propellant tank and thermal protection system (TPS) design. The propellant tank trade study was done to identify possible candidate materials and configurations. The TPS trade study involved a top level analysis of two

different mounting schemes for two different systems. Analysis of the down selected tank design was accomplished.

Given the preliminary nature of the design, numerous assumptions were used. These included load estimates, mounting configurations, and mass distribution. These are documented in the sections that follow. Given the preliminary state of loads definition, operational environment, and system requirements, this report can be taken as nothing more than preliminary. However, it does show that the HOT EAGLE structural design is feasible, low risk, and within the mass estimates currently baselined.

B2. FINITE ELEMENT MODEL

The vehicle's structural analysis was done using finite element analysis. The finite element model was built using EMRC's DISPLAY-IV preprocessor. Their solver, NISA II Version 12, was used for the solution phase. Display-IV was again used for post processing of results.

B2.1 Model, Design, and Analysis Assumptions

A number of assumptions went into the analysis of this vehicle. Some of the assumptions are based on design details of referenced documents (Section 7) and others are based on the authors' experience within the launch industry.

Table B-1 outlines the assumptions that went into the analysis with appropriate rationale.

B2.2 Model Geometry and Configuration

For this analysis all loading is assumed symmetric about the vehicle's pitch plane, Figure B-1. The model includes all primary structures and components, Figure B-2.

The finite element model uses two types of shell elements (composite and general shell), solid elements, and point mass elements.

The finite element model has approximately 60,000 degrees of freedom. It was run in a linear static mode on a PC-based platform using EMRC's NISA Solution II solver. Composite modeling includes the linear orthotropic material properties of the directional laminates selected.

Additional model details are covered in the following sections.

Table B-1, Analysis Assumptions and Rationale

Assumption	Rationale
Individual Engine Thrust is 8200 lbf	Per uX4 Baseline [3]
Payload Mass of 2000 lbm	HOT EAGLE Loads Document [Appendix B]
Tsai-Wu failure criteria used for composite materials. Interaction term $F_{12} = -.5$	Industry acceptable standard, polynomial expression allows rapid post processing of stress results, values > 1.0 indicate ply failure. Results spot checked using Hashin-Rotem failure criteria.
Actual model loads are increased 1.5 from baseline loads.	Provides for more rapid post processing of results to see if margins are satisfied. Note that Tsai-Wu failure criteria is a 2nd order polynomial. For ground handling load cases the loads were increased 2.0 times for the additional safety margins required when personnel are typically involved.
No deflection requirement on the wing or other structures	Current emphasis is design for strength
Full model analysis and loads assumes symmetry in the pitch plane.	Good for preliminary level of effort. Localized analysis modeled loading in all directions.

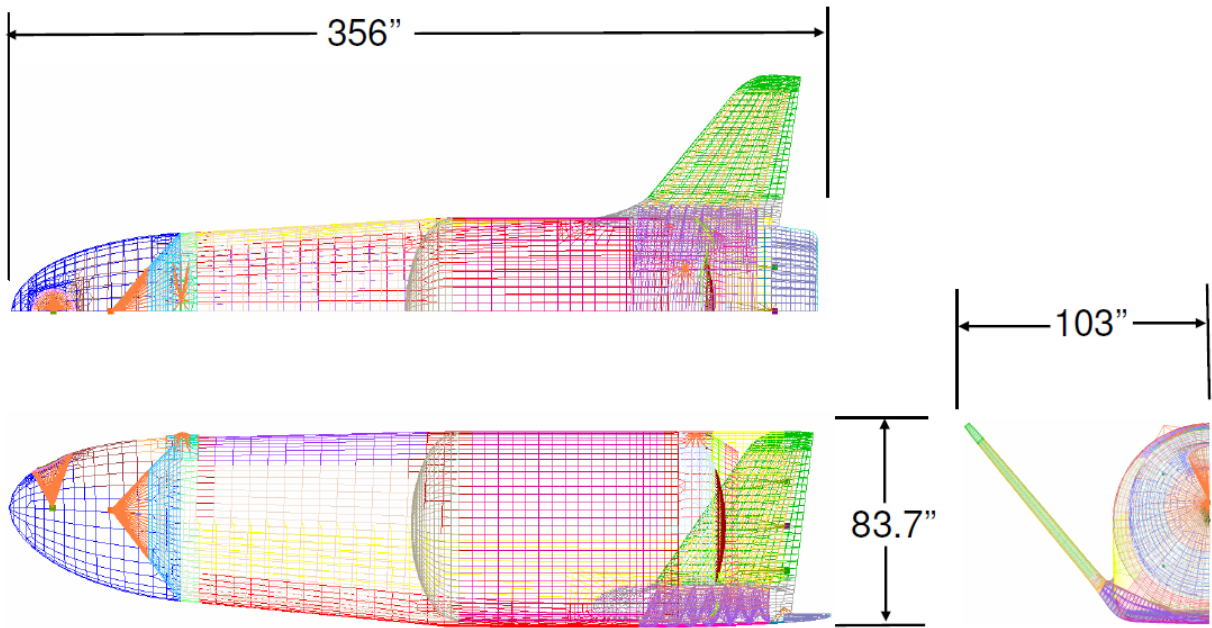


Figure B-1. FEM with Top Level Dimensions

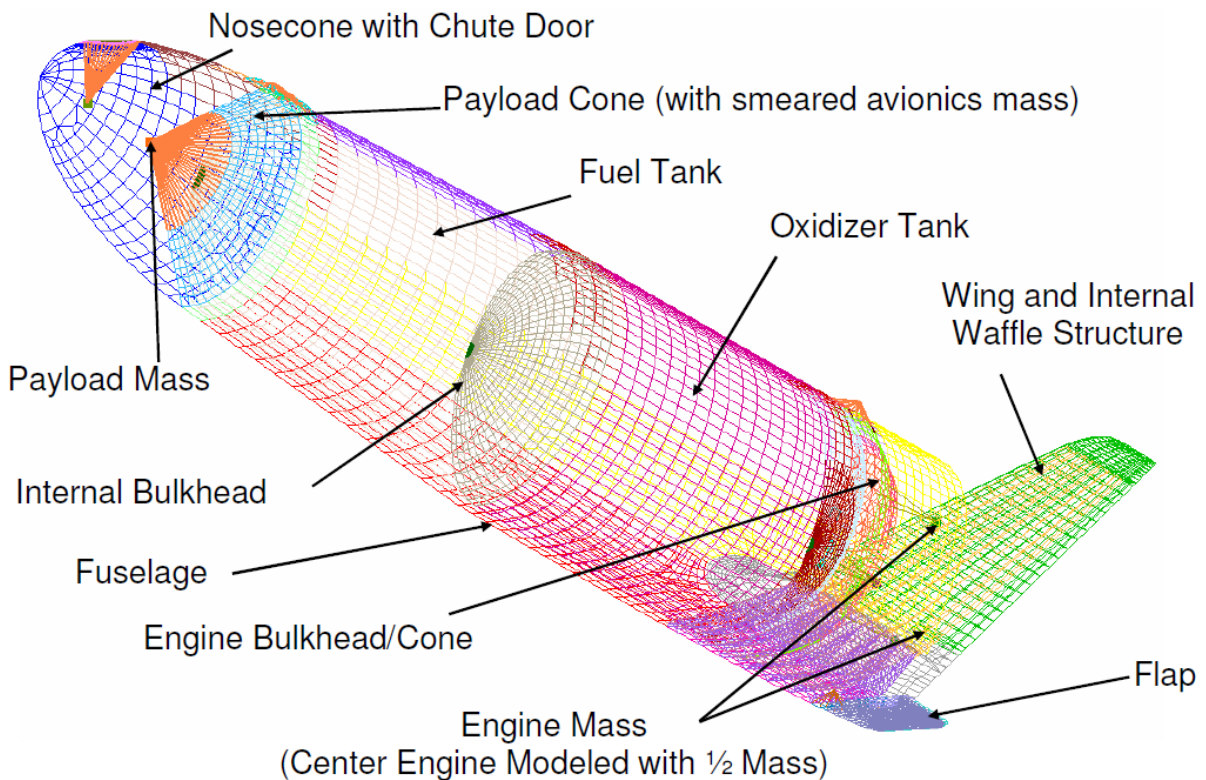


Figure B-2. Primary Structures and Components Included in the Model

B2.3 Material Properties

All primary structures within the vehicle are constructed of composite materials to take advantage of their strength and stiffness-to-weight ratio. Sandwich core construction was chosen

over a skin and stringer design as a means to improve buckling, bending, and stiffness margins without significantly increasing mass.

The sandwich structure facesheets are constructed of a unidirectional carbon/epoxy tape. Tape provides more flexibility in design and is stronger than a woven cloth. The tape material baselined for this design is an M40J fiber. This fiber was selected for several reasons.

- It is a high modulus fiber (although on the low end) which provides additional buckling margins and vehicle stiffness
- Has good material strengths
- Made by Toray and readily available. Historically, various types of carbon fiber have come under short supply, frustrating program costs and schedules. Careful monitoring of future supplies is good risk reduction
- Reasonable cost (i.e., it is half the cost of an IM7 fiber, which has a lower modulus)

No attempt was made at selecting a particular epoxy system for the matrix. Generally most good toughened epoxies would work well in this application. Some of the ones that have heritage in the launch industry are Hexcel's 8552, Bryte's EX-1522, and Cytec's 977. However, the composite industry is quite dynamic. New materials are constantly being developed capable of higher strengths, temperatures, and at lower costs than today's materials. It is the author's recommendation that at some point when the mission and technical requirements become defined for the vehicle a materials trade study be conducted.

It should be noted that higher temperature capability resins are available, one of the better being Maverick MM10.8, which can sustain temperatures toward 500 °F. Convergence (CEC) is currently studying MM10.8 in the context of JSF aircraft structure usage, for AFRL Wright Patterson Propulsion Directorate. But in their current state of development, they are quite brittle, difficult to use in design for high durability, and are very expensive. For good reliability and low program risk, more conventional toughened resins such as those above must still be recommended, and TPS must be designed to keep laminate temperatures tolerable (350 °F or less). On the other hand, the current state of development of these resins should be monitored for possible incorporation when warranted.

Table B-2. Mechanical Material Properties Used in the Analysis

	M40J/Epoxy Tape	IM7/Epoxy Cloth	Glass/PTFE Cloth	1/4" 5052- .001 2.3psf core	Rohacell 51W Foam Core
EX (psi)	2.73E+07	1.00E+07	3.40E+06	1.00E+02	1.09E+04
EY (psi)	1.10E+06	1.00E+07	3.40E+06	1.00E+02	
EZ (psi)	1.10E+06	1.00E+06	8.00E+05	1.25E+05	
NUXY	3.50E-01	1.00E-01	1.00E-01	4.99E-01	3.50E-01
NUXZ	3.50E-01	3.00E-01	3.00E-01	4.99E-01	
NUYZ	3.50E-01	3.00E-01	3.00E-01	4.99E-01	
GXY (psi)	8.00E+05	7.00E+05	3.00E+05	1.00E+02	
GXZ (psi)	8.00E+05	7.00E+05	3.00E+05	1.30E+04	
GYZ (psi)	5.00E+05	7.00E+05	3.00E+05	1.30E+04	
DENS (lbm/in^3)	6.10E-02	6.10E-02	9.70E-02	1.80E-03	1.88E-03
FXC (psi)	9.15E+04	9.50E+04	4.50E+04		116
FXT (psi)	2.72E+05	9.80E+04	4.50E+04		232
FYC (psi)	1.00E+04	9.50E+04	4.50E+04		116
FYT (psi)	8.00E+03	9.80E+04	4.50E+04		232
FZC (psi)	1.00E+04	1.00E+04	1.00E+04		116
FZT (psi)	8.00E+03	8.00E+03	8.00E+03		232
FSXY (psi)	9.20E+03	1.60E+04	1.60E+04		116
FSXZ (psi)	9.20E+03	1.60E+04	1.60E+04		116
FSYZ (psi)	5.00E+03	1.20E+04	1.20E+04		116
Thickness (in)	5.00E-03	1.50E-02	1.00E-02		

In areas of core ramp downs, close-outs, and bolted joints a carbon cloth material is used. Here a standard IM7 8-harness weave cloth is used. This fiber is typically used for woven goods. It has excellent strength and significant aerospace heritage.

The specified areal weight for the tape and cloth materials gives a ply thickness of .005 inch and .015 inch, respectively. Table B-2 lists properties of the composite materials used in the analysis.

B2.4 Primary Structures

With the exception of the propellant tanks, all of the vehicles primary structures are constructed of composite materials identified in Section B2.3. This section describes the construction of each of the primary structures. As a summary, Table B-3 lists the ply schedules for lay-up of the various structures.

B2.4.1 Nosecone

Figure B-3 shows the modeling details of the nosecone. The nosecone is a single structure of sandwich core construction. It uses a .75-inch aluminum honeycomb core with .035-inch carbon/epoxy facesheets. The section around the parachute deployment tube ramps down the core to a monolithic lay-up with additional plies for added strength. The total doubler section thickness is .190 inch. The inside row of elements of the doubler region model a pay-out eye of

4130 steel for chute deployment, Figure B-4.

Summary of the nosecone's ply schedules are shown in Table B-3.

B2.4.2 Fuselage

Figure B-5 shows the modeling details of the vehicle's fuselage. The fuselage uses a sandwich core construction. The core is .75-inch aluminum honeycomb with .035-inch carbon/epoxy facesheets. The fuselage- to-wing transition area uses a .5-inch core and .065-inch facesheets. To account for the larger bending loads from the rear aero flap and its actuator, the aft end of the fuselage ramps up to a 1-inch core with .065-inch facesheets. Summary of the fuselage's ply schedules are shown in Table B-3.

B2.4.3 Wing and Wing Carry-Through

The vehicle's wing and internal structure, Figure B-6, are constructed of a monolithic lay-up of carbon/epoxy. The wing skin is .040 inch thick and the wing waffle is .045 inch. The purpose of the wing waffle is to react the shear loads between the wing skins in a bending mode. They also transfer the wing load into the wing carry-through located in the aft fuselage section. The wing skin is attached to the wing waffle by means of a secondary bonding operation.

Table B-3. Ply Schedule for All Primary Structures

Structure	Ply Schedule	Thickness
Nosecone		
Primary Section	[0/45/0/90/0/-45/0/core]s	.035 Facesheet .750 Core
Chute Doubler	[(0)c/(45)c/(0)c/(45)c/0/45/0/90/0/-45/0]s	.190
Top Section Reinforcement	[0/90/45/90/0/90/0/90/0/-45/0/0/core]s	.065 Facesheet .750 Core
Local Reinforcement for Bi-Mese Lug	[cloth-quasi buildup /0/90/45/90/0/90/0/90/0/-45/0/0/core]s	.110 Facesheet .750 Core
Fuselage		
Fuselage Bottom	[0/45/0/90/0/-45/0/core]s	.035 Facesheet .750 Core
Fuselage Sidewall	[0/45/0/90/0/-45/0/core]s	.035 Facesheet .750 Core
Flap Actuator Reinforcement	[(0)c/(45)c/0/45/0/90/0/-45/0/core]s	.065 Facesheet 1.00 Core
Wing Transition	[(0)c/(45)c/0/45/0/90/0/-45/0/core]s	.065 Facesheet .500 Core
Wing Carry-Through	[0/45/0/90/0/-45/0/core]s	.035 Facesheet .750 Core
Aft Strut Reinforcement	[(02/902)2/0/(45)c/0/30/-30/90/45/-45/core]s	.095 Facesheet .750 Core
Landing Leg Reinforcement	Cloth-Quasi buildup for 0.500" monolithic pad, taper to [cloth-quasi buildup / (0)c/(45)c/(0)c/(45)c/0/45/0/90/0/-45/0/core]s	.500 Pad .250 Facesheet .750 Core
Wing		
Wing Skin	[0/30/-30/90]s	.040
Wing Waffle	[(45)c/(45)c/(45)c]	.045
Wing Carry-Through		
Top Skin	[0/30/-30/90]s	.040

Structure	Ply Schedule	Thickness
Waffle	[(45)c/(45)c/(45)c]	.045
Payload Cone		
Primary Section	[0/30/90/-30/0/core]s	.025 Facesheet .500 Core
Bolt Ring (Nosecone/Fuselage)	Quasi-isotropic lay-up with cloth and uni	.260
Engine Support Structure		
Bulkhead	[(0)c/(45)c/0/45/-45/90/90/-45/45/0/core]s	.070 Facesheet 2.00 Core
Bulkhead Cutout Doubler	[(0)c/(45)c/(0)c/(45)c/(0)c/(45)c/0/45/-45/90/90/-45/45/0/(0)c/(45)c/core]s	.160 Facesheet 2.00 Core
Conical Section	[0/30/90/-30/0/core]s	.025 Facesheet .375 Core
Bulkhead/Cone Transition	[(0)c/(45)c/0/30/90/90/-30/0/core]s	.060 Facesheet .375 Core
Propellant Tanks		
Oxidizer Bottom Section	Liner/Core/[0/903/45/0/-45/903/0]	.080 Facesheet 1.50 Core
Oxidizer Top Section	Liner/Core/[0/902/0/90/-45/90/45/0/-45/90/45/90/0/902/0]	.110 Facesheet 1.50 Core
Fuel Bottom Section	Liner/Core/[90/0/90/45/-45/90/0/90]	.055 Facesheet 1.50 Core
Fuel Top Section	Liner/Core/[0/90/02/90/0/90/45/-45/90/02/90/02/90/0]	.100 Facesheet 1.50 Core
Local Reinforcement (Bi-Mese and Mid Tank Top Section)	Liner/Core/[03/902/03/90/-453/90/453/0/-453/90/453/90/03/902/0]	.190

“c” = cloth material (vs. unidirectional tape)

“s” = symmetric lay-up

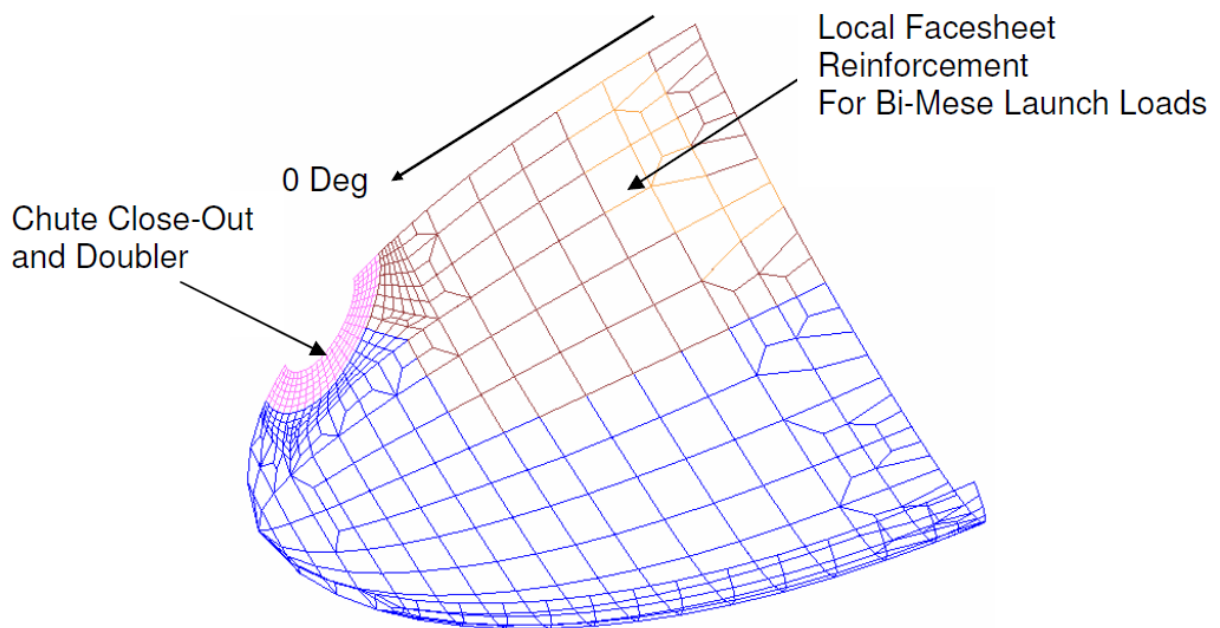


Figure B-3. Nosecone with Parachute Door Opening (0° Ply Direction Shown)

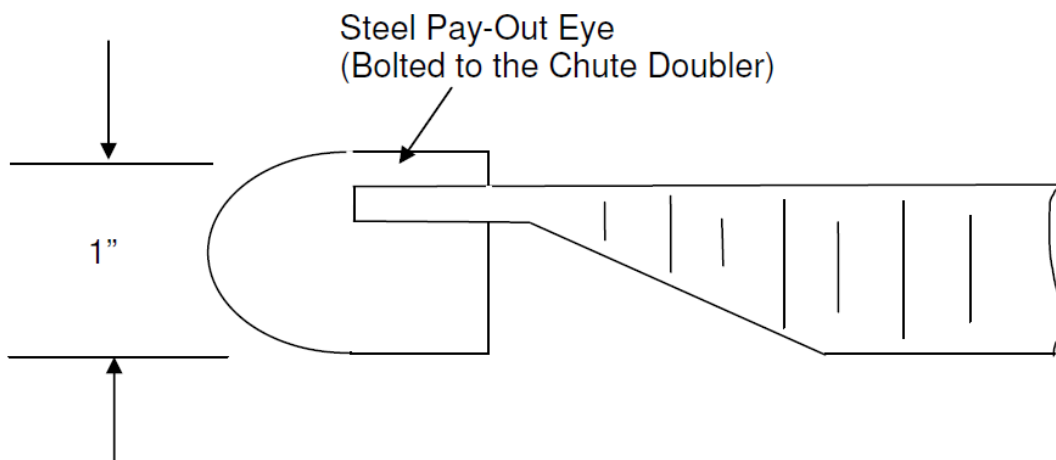


Figure B-4. Design Concept for Steel Ring around the Chute Door Opening

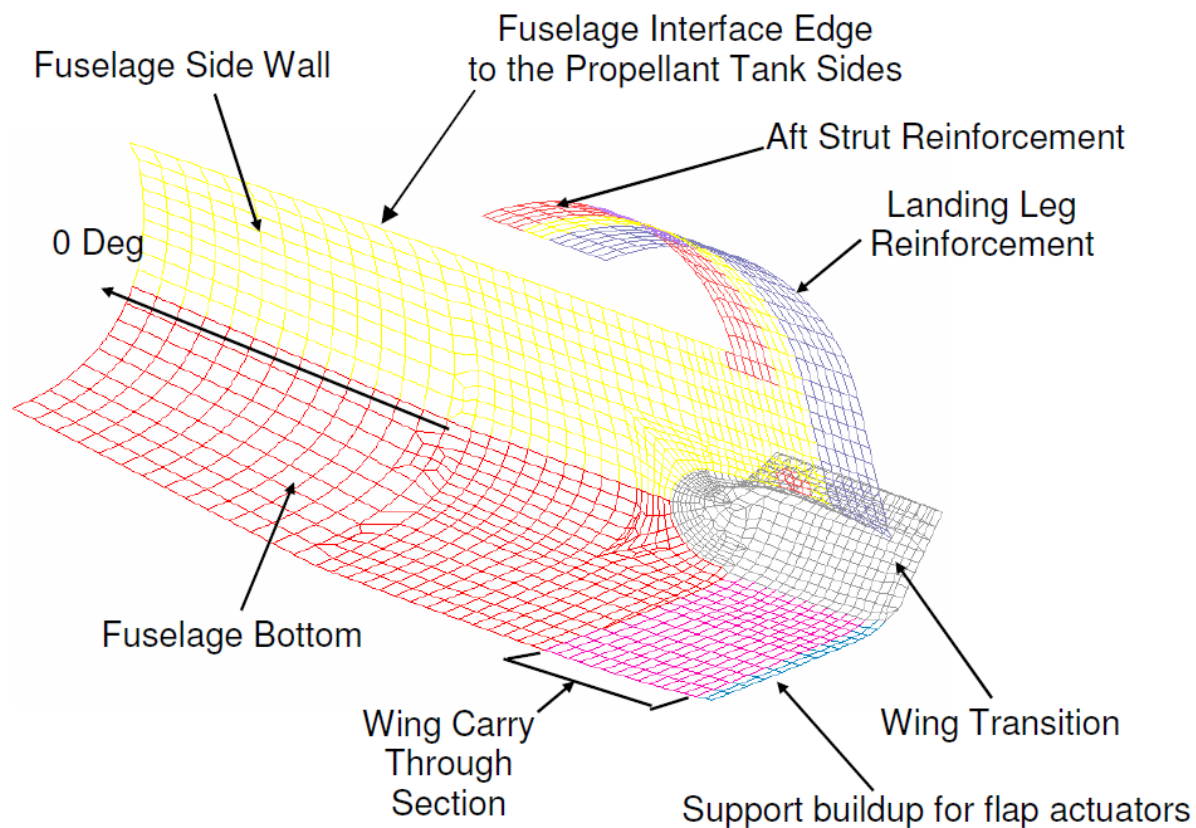


Figure B-5. Fuselage Section (0° Ply Direction Shown)

The wing carry-through is constructed of the same waffle configuration and lay-up as the wing's internal structure. To avoid the bottom aft portion of the oxidizer tank the carry-through section has a conformal shape. The carry-through's internal structure is closed out with a bonded top skin plate constructed of carbon/epoxy 0.040 inch thick. For the bottom close-out, wing carry-through is bonded to the aft section of the fuselage.

Summary of the wing's ply schedules are shown in Table B-3.

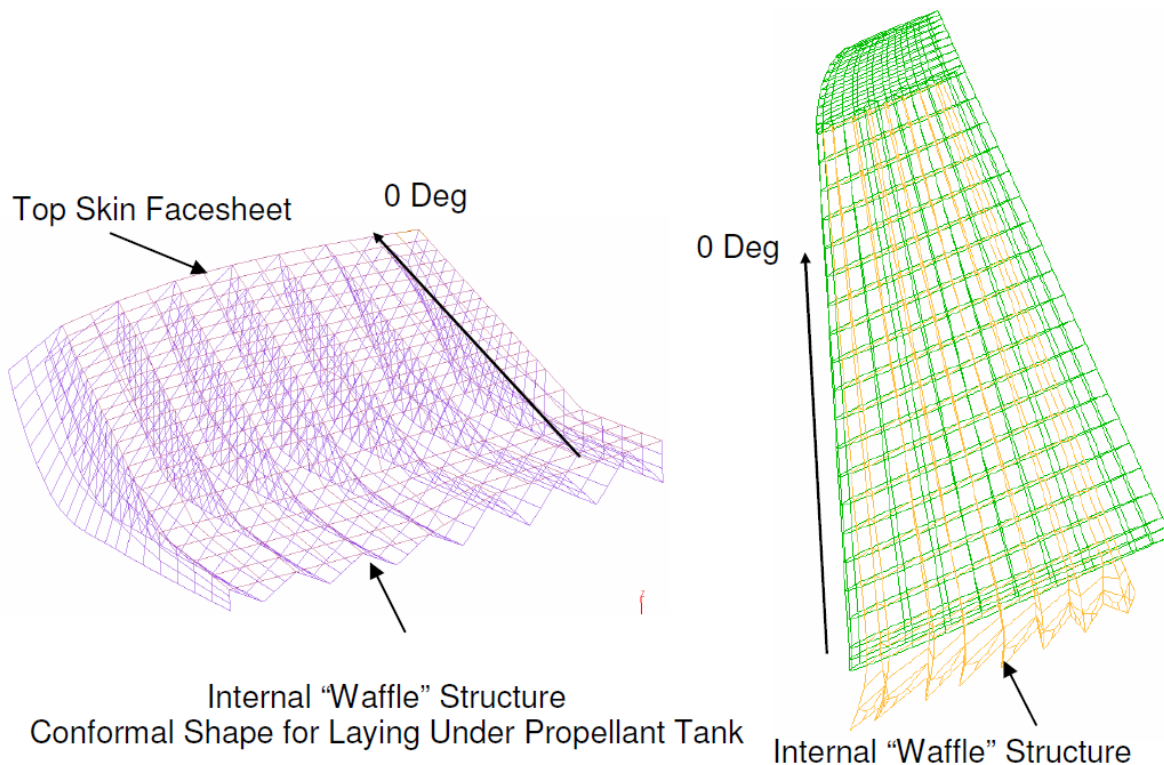


Figure B-6. Modeling of the Wing Skin and Wing Carry-through (0° Ply Direction Shown)

B2.4.4 Payload Cone

The payload cone, Figure B-7, was sized to accommodate a standard SAAB Erickson 38-inch payload separation system. This is a standard separation system used within the launch industry for payloads in this vehicle's weight class. The design of the payload cone does allow an option to use a standard 16-inch separation system but was not analyzed here.

It is assumed that the vehicle's avionics' will be attached to the payload cone, either directly or on an attached avionics deck. The configuration of the cone and the volume available make it an ideal location for mounting of electronic boxes and other avionic components. For modeling purposes at this preliminary stage non-structural mass was added to the payload cone to account for the avionics.

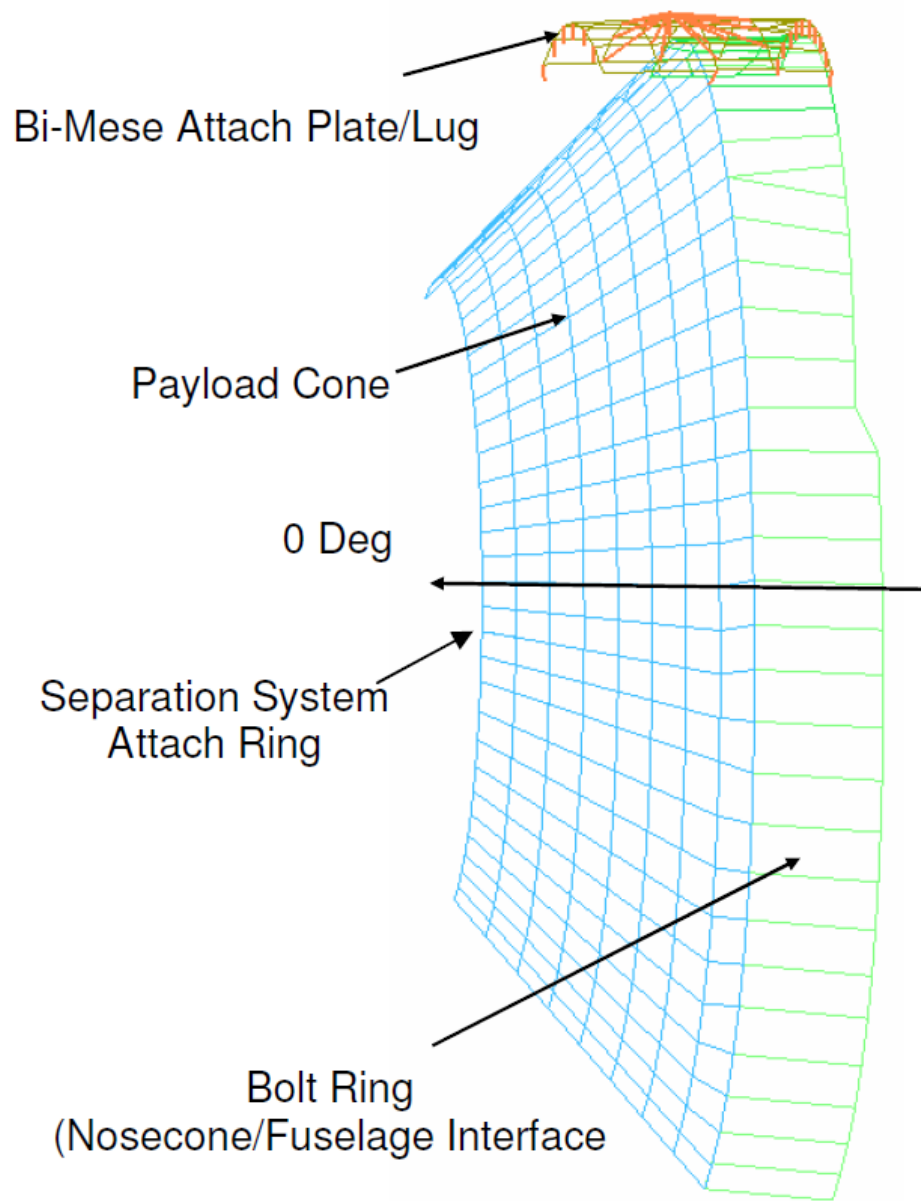


Figure B-7. Payload Cone with Forward Bi-mese Attach Lug (0° Ply Direction Shown)

The payload cone is a sandwich construction. It uses a .5-inch aluminum honeycomb core with .025-inch carbon/epoxy facesheets.

Figure B-8 illustrates the design concept for interface of the payload cone and nosecone to the vehicle's fuselage section. One advantage of this design is it allows for separate integration and encapsulation of the payload prior to integration with the vehicle.

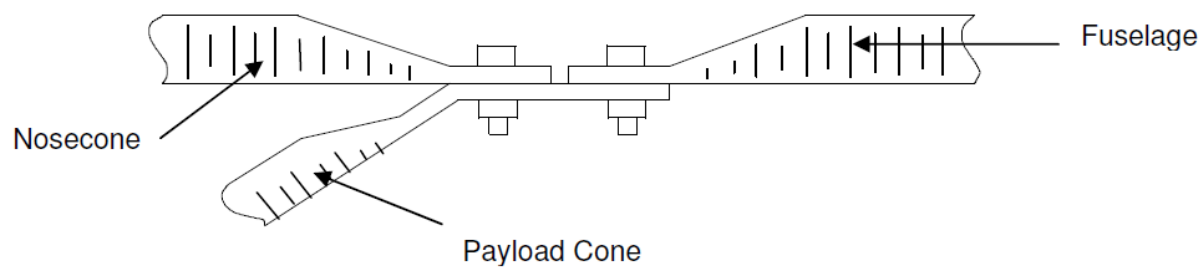


Figure B-8. Nosecone/Payload Cone/Fuselage Interface Joint

Summary of the payload cone's ply schedules are shown in Table B-3.

B2.4.5 Engine Bulkhead and Cone Assembly

The five engines are attached to an engine bulkhead which is attached to the aft end of a conical structure, Figure B-9. The engines are modeled using point mass elements. These elements are then tied to the bulkhead structure by means of spar elements. The engine mass (c.g.) is located 21 inches aft of the engine bulkhead. The spar elements are a simplified representation of the engine gimbal and attachment structure. Vectoring actuators are not included in this model due to lack of definition.

The engine conical section transfers loads from the engine bulkhead to the fuselage. The slot in the bottom section of the conical section is there to prevent interference with the wing waffle and wing transition section. It also serves as a pass-through for control cables and tubing.

The engine bulkhead is constructed of 2-inch aluminum honeycomb core and .070-inch carbon/epoxy facesheets. For additional strength doublers around cutouts and pass-throughs in the bulkhead facesheets are reinforced to a thickness of .160 inch. Summary of the engine bulkhead and cone's ply schedules are shown in Table B-3.

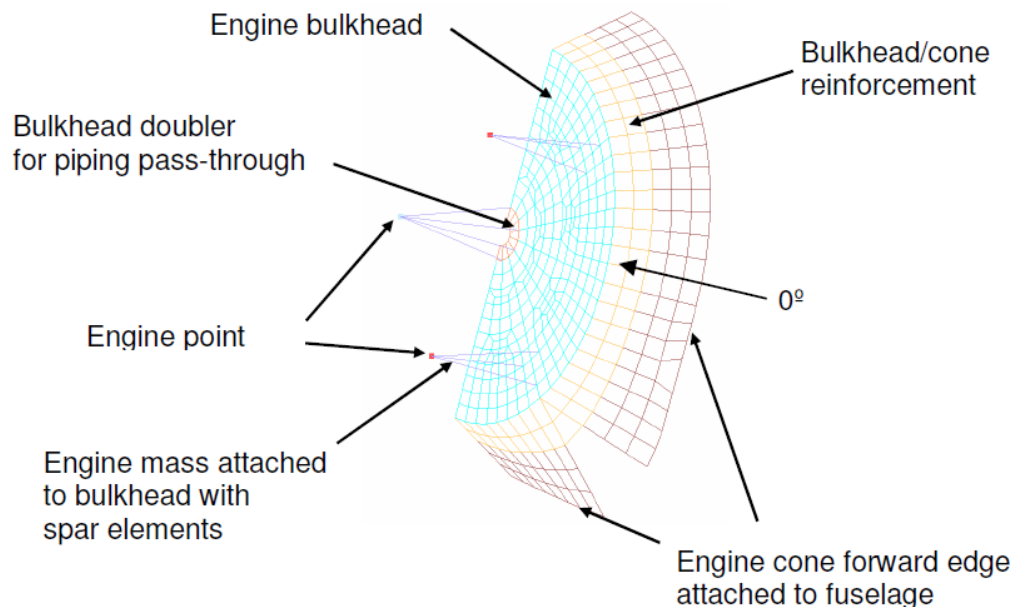


Figure B-9. Engine Support Structure (0° Ply Direction Shown)

B2.4.6 Rear Aero Flap

The rear flap is modeled as hinged at the aft edge of the fuselage. The design assumes an actuator attached to the bottom aft end of the fuselage. The actuator ram end is attached to a bracket mounted on the top aft edge of the flap, Figure B-10.

The flap is constructed of Rohacell foam shaped to the needed configuration with an overwrap of carbon/epoxy plies. The facesheet thickness over the core is .050 inch. On the forward edge the facesheet thickness is increased to .110 inch to better redistribute the loads from the actuator brackets and hinges.

Summary of the aero flap skin's ply schedules are shown in Table B-3.

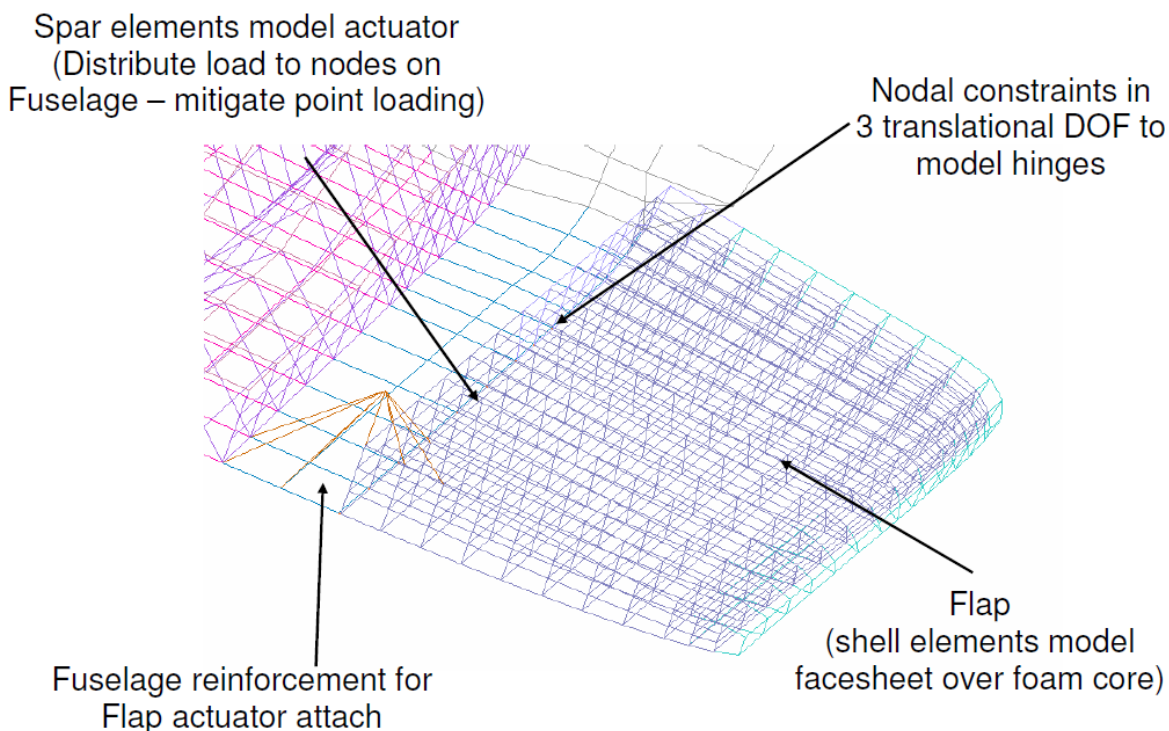


Figure B-10. Model Details of the Rear Flap

B2.4.7 Propellant Tanks

Unlike the Micro-X, HOT EAGLE utilizes a more efficient usage of its propellant tank structure. Rather than having two separate pressure vessels to contain the propellants, HOT EAGLE uses a single pressure vessel with an internal bulkhead, Figure B-11. This has two distinct advantages. The first is replacing two pressure end domes with a single internal dome that does not require design to the higher pressure of the propellant tanks. Thus structural mass is reduced. The other advantage is a more efficient usage of the vehicle's internal volume.

The internal bulkhead design works well for HOT EAGLEs propellant combination. The oxidizer, LOX, and the fuel, liquid methane, have cryo temperatures that are nearly identical (-290 °F). Thus insulating material in the internal bulkhead is not critical.

Another feature that was incorporated into the HOT EAGLE design was to change the configuration of the propellant tanks from an internal non-primary structure to a contributing primary structure of the vehicle. Using the tanks internal pressure helps to improve vehicle buckling margins without the addition of structural mass. Carbon fiber tends to be almost twice as strong in tension as in compression. Thus designing structures to produce more tensile loads improves the vehicle's structural efficiency and reduce overall mass.

To change the tanks from the Micro-X internal tank design to HOT EAGLE's primary structure design required the tanks outside diameters to be increased to the OML of the vehicle. This allowed removal of the top section of the fuselage. The fuselage now only resides on the bottom half of the vehicle extending half way up the sides of the propellant tanks. This section of the fuselage is retained to provide a conformal fairing for the bottom of the vehicle and to provide a plenum for running of propellant lines, electrical cables, and other miscellaneous items.

Other unique features of the propellant tank design are placement of the insulating material internal to the tank rather than external and use of compression molded composite bosses instead of metal. Although compression molded boss ends have not been utilized in pressure vessels, the concept is feasible based on DC-X technology and manufacturing practice, and is low risk here due to relatively benign external tank temperatures via the use of internal insulation. The DC-X did successfully develop and use LOX ball valves made of compression molded carbon/epoxy. HOT EAGLE could further develop this technology for reduction of propellant tank weight.

For HOT EAGLE, the propellant tanks insulating material is placed between the tanks' internal liner and the external carbon/epoxy shell. This has three advantages. The first is it forms a sandwich structure which is a more efficient design (for buckling and bending loads) than a single thick monolithic shell lay-up. The second is the tanks' outer surfaces are part of the primary structure thus allowing easy attachment and interface with other structures. Working around external insulation is eliminated. The third advantage to placing the insulating foam internal is that it mitigates the risk of damage.

The internal liner for the propellant tanks is constructed of a glass 8H weave with PTFE or other fluouopolymer as a matrix. Use of a thermoplastic in place of a thermoset matrix is to mitigate microcracking issues at cryo temperatures. The glass fiber is used in place of carbon fiber for chemical compatibility, especially with LOX.

Section B3.1 provides more information addressing the trade studies that went into selection of the current tank design.

Due to budget constraints and limited time for analysis, the HOT EAGLE tanks were not sized to accommodate the same propellant load as the Micro-X. By moving the tank diameter out to the vehicle's OML and then combining the tanks into a single pressure vessel significantly increased the tank volumes. However, for this analysis the intent was to keep the same propellant load as the Micro-X. To accomplish this, the densities of the propellants were reduced accordingly to give the same mass but for a larger volume of the Micro-X. This then allowed inertial loads to be applied to the vehicle that were representative of those in the Micro-X. More is discussed on this modeling item in the appropriate load cases analyzed in Section B4.

Additional nonstructural mass is added to the tanks to account for internal structures such as baffles and external materials such as piping, brackets, and insulation. Breakdown of mass properties is given in Section B2.5.

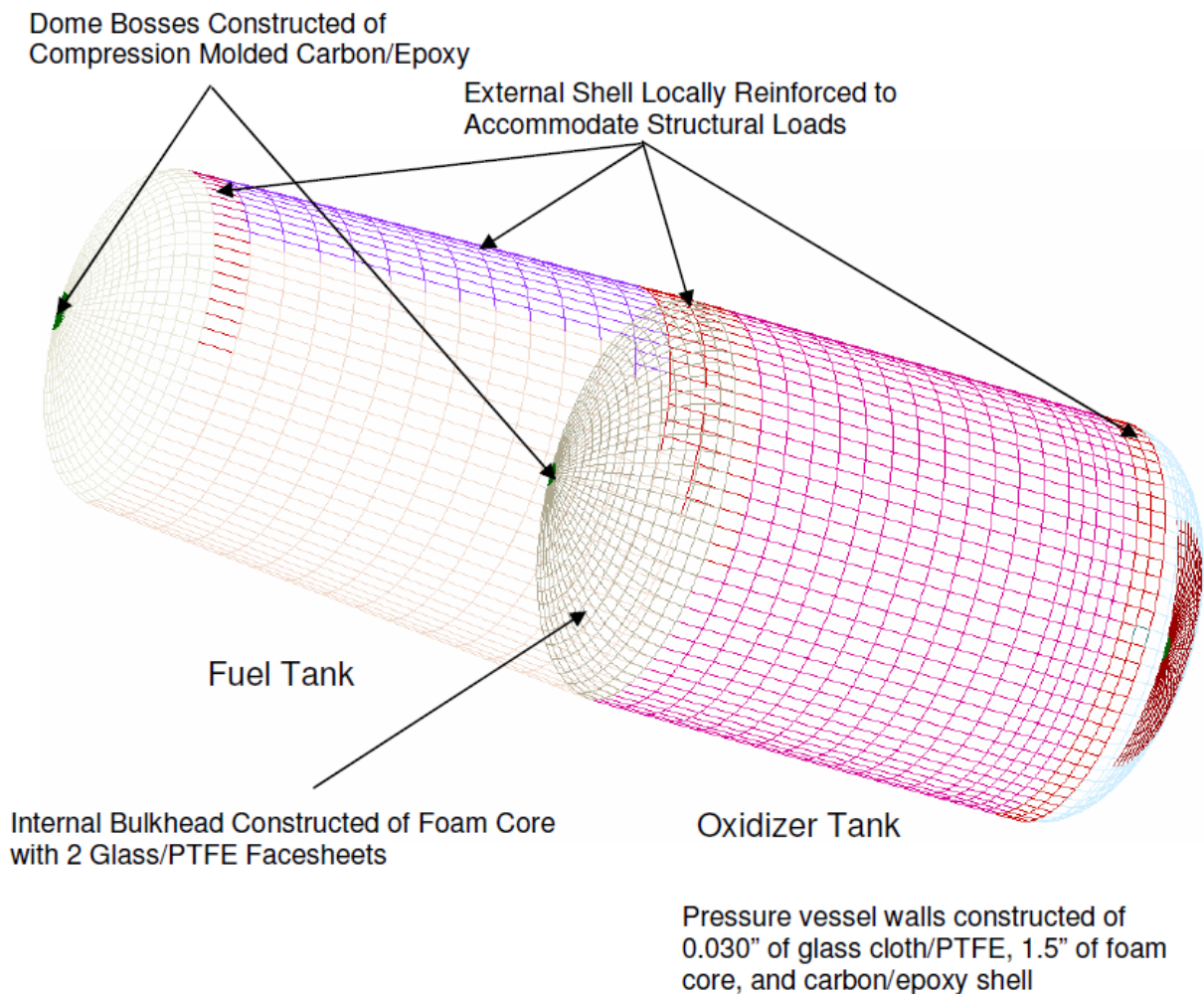


Figure B-11. Model Details of the Propellant Tanks

B2.5. Mass Properties

Table B-4 provides a mass breakdown of the vehicle. Structure mass properties were calculated from their respective lay-up or construction via the FE model. Contingency was added to account for non- structural mass and other items not modeled elsewhere.

Table B-4. Vehicle Mass Properties

Item	Mass	Basis/Comments
Structures		
Nosecone Structure	104.3	Calculated from FEA model which included a 20% increase in material densities.
Fuselage	440.0	Calculated from FEA model which included a 20% increase in material densities.
Wing	77.8	Calculated from FEA model which included a 20% increase in material densities.
Wing Carry Through	51.1	Calculated from FEA model which included a 20% increase in material densities.
Flap	22.4	Calculated from FEA model which included a 20% increase in material densities.
Payload Cone/Doubler	31.9	Calculated from FEA model which included a 20% increase in material densities.
Engine Bulkhead/Cone	71.1	Calculated from FEA model which included a 20% increase in material densities.
CH4/LOX Tank	674.0	Single pressure vessel with internal bulkhead separating fuel and oxidizer. Construction is glass/PTFE liner, 1.5" Rohacell 51W foam core, carbon/epoxy overwrap. Design for 40 psi MEOP. Includes composite boss ends. Calculated from FEA model which included a 20% increase in material densities.
Total Structural Mass	1473	
Non-Structural Masses		
		Masses below are assumptions used to provide loading conditions for structural analysis and may not exactly match the final weights estimates for these components.
TPS	623.0	Ref Timothy Fry's TPS Analysis Summary Spreadsheet 9/13/05 for lightest option
Baffles, Plumbing	80	Value carried over from Micro-X Analysis
Engines (5)	820	Raymer D., 8/20/04,"Rocket Micro-X Demonstrator Design Study"
Avionics (summation)	1232	Raymer D., 4/9/03, "X-VTOL Spacecraft Conceptual Design Study" minus parachute
Parachute	50	Raymer D., 4/9/03, "X-VTOL Spacecraft Conceptual Design Study"
Propellant		
LOX	15412	Raymer D., 8/20/04,"Rocket Micro-X Demonstrator Design Study"
Methane	4403	Raymer D., 8/20/04,"Rocket Micro-X Demonstrator Design Study"
Payload	2000	Per Loads Document Appendix B
Inert Vehicle Weight	4278	Mass of vehicle without propellant or payload
GLOW	26093	

B3. TRADE STUDIES

B3.1 Propellant Tank Material Selection

The design concept for HOT EAGLE's propellant tanks is a single pressure vessel with an internal bulkhead. Design of this internal bulkhead is simplified by the vehicle using two propellant fluids that have similar cryogenic temperatures. Both the oxidizer (liquid oxygen) and fuel (liquid methane) have cryogenic temperatures near -290 °F. Given the proposed tank configuration the next step was to select material or materials capable of meeting the vehicles structural requirements as well as the requirements for storing cryogenic materials.

The use of cryogenic propellants requires the use of an insulating material. For LOX tank applications insulation thickness typically varies from 0.375 to 1.5 inches. For this trade study and subsequent vehicle analysis an insulation thickness of 1.5 inches is assumed. Note that reducing the insulation thickness by half would reduce the mass of the vehicle an additional 200 lbm.

Now placement of the insulation can either be on the exterior of the tank, which is typical, or it can be placed internal to the pressure vessel structural shell. The latter has several advantages. Being internal to the structural shell, the insulation is protected from external processes or events that could damage it. The external or structural shell is not subjected to the large changes in temperature that it would see if it were internal to the insulation. And lastly, by having the propellant tank structural shell external to the insulation provides for a structural surface to simplify attachment of other structures and mitigates localized heat leak paths for attached structures.

For this trade study materials were investigated that could be used for either concept in location of the insulation and had some heritage to cryogenic tank application. Table B-5 shows the materials investigated. Stainless steel and aluminum were both investigated given their heritage in this application. Composite materials were also included given their recent application to cryo tank applications. Examples include propellant tanks for X-33 and X-34.

The trade study was done assuming a pressure vessel designed for 100 psi operation, 286-inch length and 76-inch diameter, with hemispherical domes and internal bulkhead. The pressure vessel also had a structural requirement for a 3.0 Min-lbf bending and a 50 kip axial load. Total tank volume was 684 ft³. For this trade no structural requirement was levied on the internal bulkhead. The intent here is to identify materials that could meet the structural requirements of the pressure vessel.

A spreadsheet was setup using superposition to calculate stresses from combined pressure, bending, and axial loads. For each tank material or combination of such, appropriate thicknesses were calculated based on material strength. Table B-5 summarizes the results.

Table B-5. Results of Material Trade Study for the Propellant Tanks

Design Description	Mass (lbm)	Wall Thick.	Comments
301 SS ¾ Hard	832	.032	Flight Heritage. Use in liquid H2 tanks
Linerless T1000 Carbon/Epoxy. Solid Wall.	144	.035	New technology. Linerless high risk. Carbon compatibility with LOX could be issue
Linerless S-Glass/Epoxy. Solid	392	.060	New technology. Linerless high risk
Aluminum-Lithium 2195. Solid Wall.	442	.054	Flight Heritage. Material selected by NASA for Ultra-Light Weight tank applications.
Aluminum-Lithium Liner with T1000 fiber hoop wrap. Solid wall	341	.044	CTE concerns between aluminum and carbon overwrap, need to autofrettage for full strength
T1000 Carbon/Epoxy. 1.5" Rohacell 51W foam core. Fiberglass/PTFE liner.	174 (430 lbm with foam core)	.035	New technology.

Results of the trade show that the composite tank design with the glass/PTFE liner and internal foam core to be of the best option for HOT EAGLE. Use of this material and configuration will result in development of propellant tanks with potentially the lowest mass (if core can be reasonably optimized) and the most acceptable risk. Other advantages to this material selection are the compatibility of the fiberglass/PTFE liner to the LOX and methane. The PTFE (Teflon) or other fluoropolymer thermoplastic matrix material also has the advantage of mitigating the micro-cracking issue found in thermoset matrix materials.

Since the structural shell or membrane is not subjected to cryogenic temperatures (internal foam core insulation), a thermoset material (stronger than a thermoplastic) can be used with the carbon fiber. Concerns with micro-cracking in this layer becomes much less of an issue.

B4. ANALYSIS

B4.1 Analysis Load Cases

To verify design margins the vehicle was analyzed for a number of load cases each representative of a specific operation or flight condition, Table B-6. Analysis included key ground operations, vehicle launch, exo-atmospheric flight, parachute deployment, and landing. Two other load cases were analyzed. One was a local analysis of the propellant tanks to identify minimum required material lay-up. The other was an analysis of HOT EAGLE as a ground launch demonstrator.

Table B-6. Vehicle Analysis Matrix

Load Case	Axial g Load	Lateral G Load	Propellant Tanks	Aero	Engine Thrust	Comments
Vehicle Horizontal Lift	No	2.0g	No propellant, no pressure, no temperature	No	No	Lift g's increased by 2.0 for additional ground handling margins
Vehicle Vertical Lift	2.0g	No	No propellant, no pressure, no temperature	No	No	Lift g's increased by 2.0 for additional ground handling margins
Vehicle Launch as Upper Stage.	8.0g	3.0g	Full Propellant Mass, 40 psi tank press, -292°F temp internal, 40°F temp external structure	CFD Cp plot, q=1200 psf, M=2, alpha	No	Attach to launch vehicle in Bi-Mese config. No fairing.
Powered Flight (Demo Unit)	3.0g	3.0g	20% Propellant Mass, 40 psi tank press, -292°F temp internal, 40°F temp external structure	CFD Cp plot, q=1200 psf, M=2, alpha	8200 lbf per engine	Assumes load case for ground launch with max q.
Powered Flight (Exo-Atm)	3.0g (Limit by Engine Throttle)	3.0g	20% Propellant Mass, 40 psi tank press, -292°F temp internal, 40°F temp external structure	No	8200 lbf per engine	
Re-entry	3.0g	4.0g (based on aero reaction)	20% Propellant Mass, 40 psi tank press, -292°F temp internal, 40°F temp external structure	CFD Cp plot, q=190 psf, M=25, alpha =70	No	
Chute Deployment	Reaction to deployment force	Reaction to deployment force	20% Propellant Mass, 40 psi tank press, -292°F temp internal, 40°F temp external structure	No	No	Chute deployment force of 5000 lbf

Load Case	Axial g Load	Lateral G Load	Propellant Tanks	Aero	Engine Thrust	Comments
Landing	Reaction to decel leg forces	No	20% Propellant Mass, 40 psi tank press, -292°F temp internal, 40°F temp external structure	No	No (Limited by 3g axial, conservative)	5950 lbf on each leg, 204 kip-in moment, landing approach v=10 ft/sec. Engine off on touchdown puts more reacting force in legs.

B4.2 Local Analysis

B4.2.1. Propellant Tank

A local analysis of the propellant tanks was conducted to validate the design concept and to verify the minimum required structural lay-up of the composite material.

As identified in Section B3.1 for the propellant tank trade study, the internal liner for the propellant tanks is a fiberglass/thermoplastic cloth material. For this design an 8 harness weave cloth having a ply thickness of 0.01 inch is assumed. The liner lay-up is [0/45/0] with 0 degrees being aligned with the tanks' axial direction. This produces a liner thickness of 0.030".

The tanks' foam core consists of 1.5 inches of Rohacell 51W. This thickness of foam core is assumed to give frost free conditions on the tanks exterior shell. A minimum temperature for the shell is assumed to be 40 °F.

The exterior or structural shell of the pressure vessel is constructed of a carbon/epoxy unidirectional tape. The tape's thickness is 0.005 inch. It is assumed that the tank's outer wrap will be done using either filament winding or fiber placement. Thus the domes will have a helical wrap giving an average thickness of 0.080 inch. Buildup will be thicker around the 1" thick composite bosses. The bosses are used as both part of the filament winding/fabrication process and to provide access to the propellant through fitting ports.

The cylindrical portion of the propellant tank will consist of a series of hoop and helical wraps. A ± 45 deg layer is included for torsional loads. The ply schedule for the outer wrap is [0/90/90/0/90/45/- 45/90/0/90/90/0] to produce a shell thickness of 0.060 inch. Note that this is a minimum thickness. To accommodate vehicle loads during flight operations the propellant tanks are locally reinforced to thicker values, Table B-5.

Figure B-12 shows the FEM used to conduct the analysis. Given the tanks axisymmetric nature only one circumferential row of elements was used for the analysis. For clarity Figure B-12 shows additional elements.

Analysis of the tanks included a thermal gradient due to the internal cryo fluid (-292 °F) and external surface conditions (40 °F). Structural loading was a combination of 60 psi for tank operation (including a 1.5 safety factor) and additional pressure loading due to the inertial effects of the propellant on the aft dome from vehicle launch. A maximum 12 gs was assumed. This included a 1.5 safety factor. This inertial pressure assumed LOX as the fluid given its density being nearly 3 times that of the methane. No attempt was made to refine the load and use a

pressure gradient for the inertia load. To be conservative a total 135 psi internal pressure was applied.

Two load cases were analyzed. The first is a flight condition with both thermal and pressure loads. The second is a ground condition with thermal load only. This case was run to investigate the potential tensile stress the foam core would see as a result of liner shrinkage from thermal contraction. On the ground during fill or in a vented condition there is no internal pressure to push the liner back out against the foam core. Thus there is a potential for a delamination or separation.

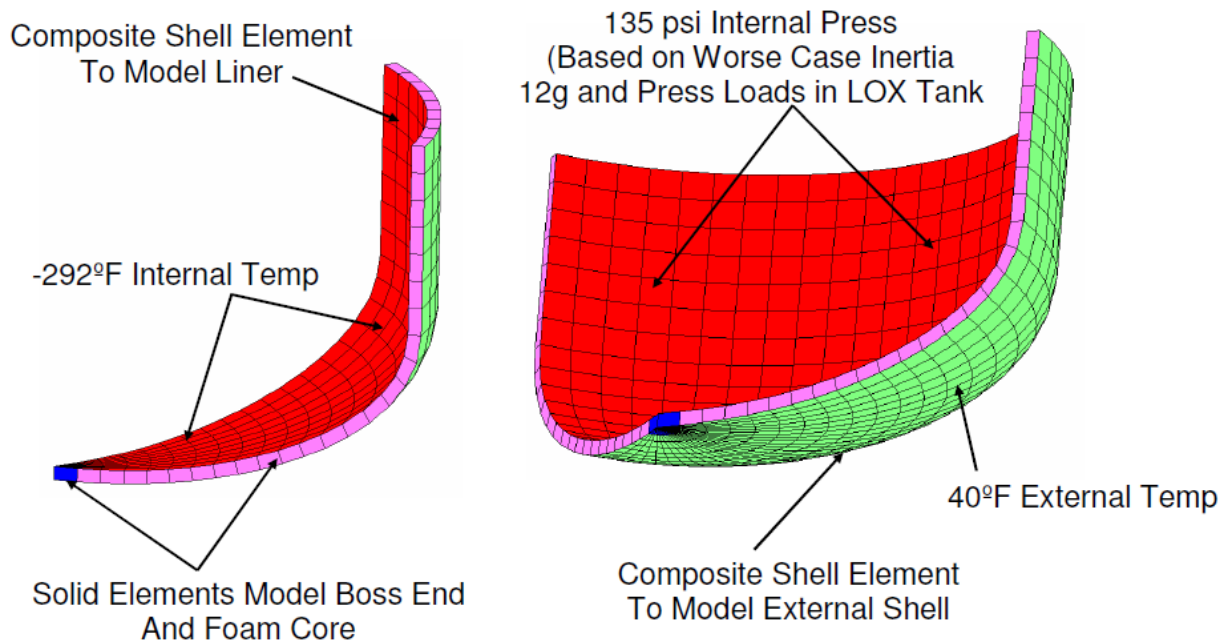


Figure B-12. Model Details for Propellant Tank Analysis

Figures B-13 to B-16 show the results of the analysis. The Tsai-Wu stress survey plots (Figures B-13 and B-14) are all showing values <1.0 . Thus, the tank's composite structures (liner and external shell) are showing safety factors greater than 1.5.

The Rohacell 51W foam has a strength of 232 psi. Figure B-14 is showing a localized failure of the foam in the cylinder-to-dome transition region for the flight condition. This is not surprising as this current tank design is not optimized for a dome profile that would produce a geodesic-isotenoid stress state in the dome shell fibers. By doing so would eliminate the bending being seen in this transition region which is causing the foam to fail. To define the optimum shape for the domes, and possibly locally tailor the laminates requires non-linear analysis that is out-of-scope of this analysis effort. Also, the ground condition is acceptable, with large margin.

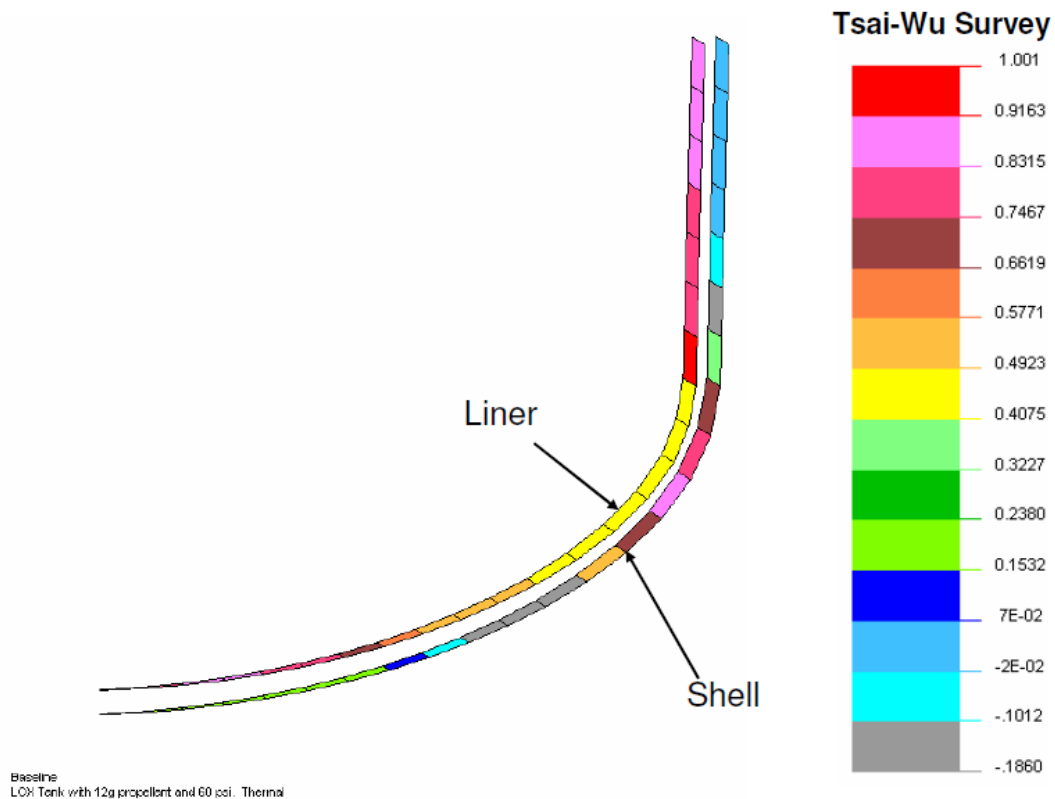


Figure B-13. Tsai-Wu Survey Plot of the Liner and External Shell for the Thermal and Pressure Load

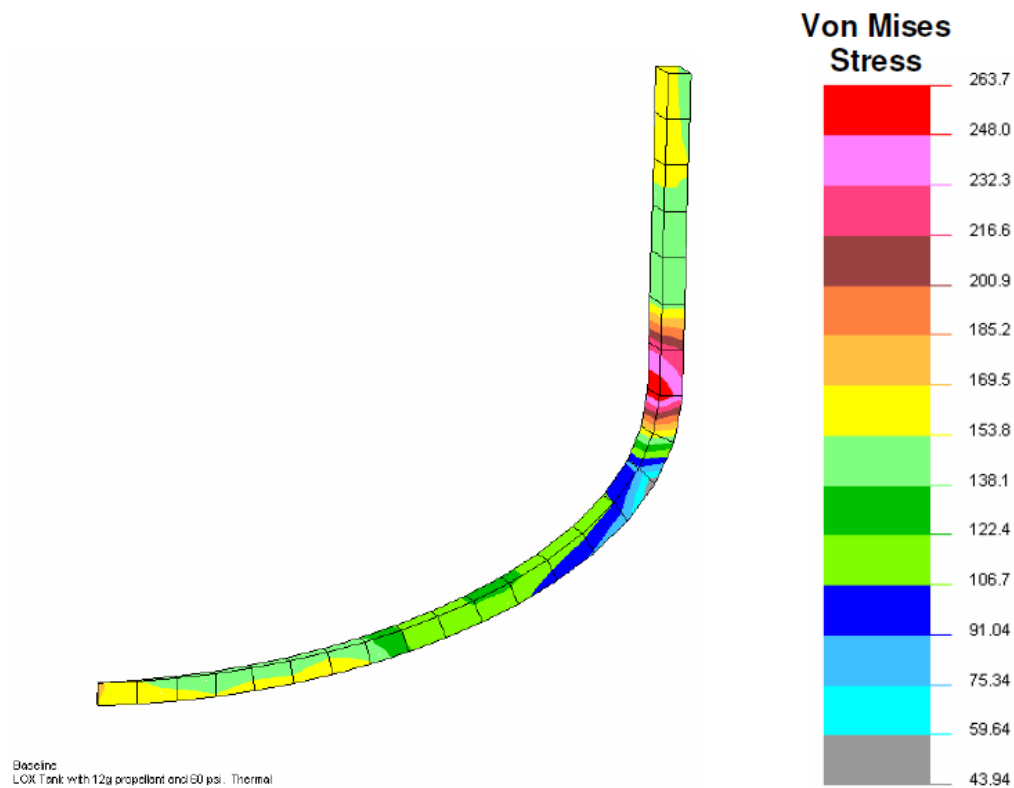


Figure B-14. von Mises Stress in the Foam Core for the Thermal and Pressure Load Case

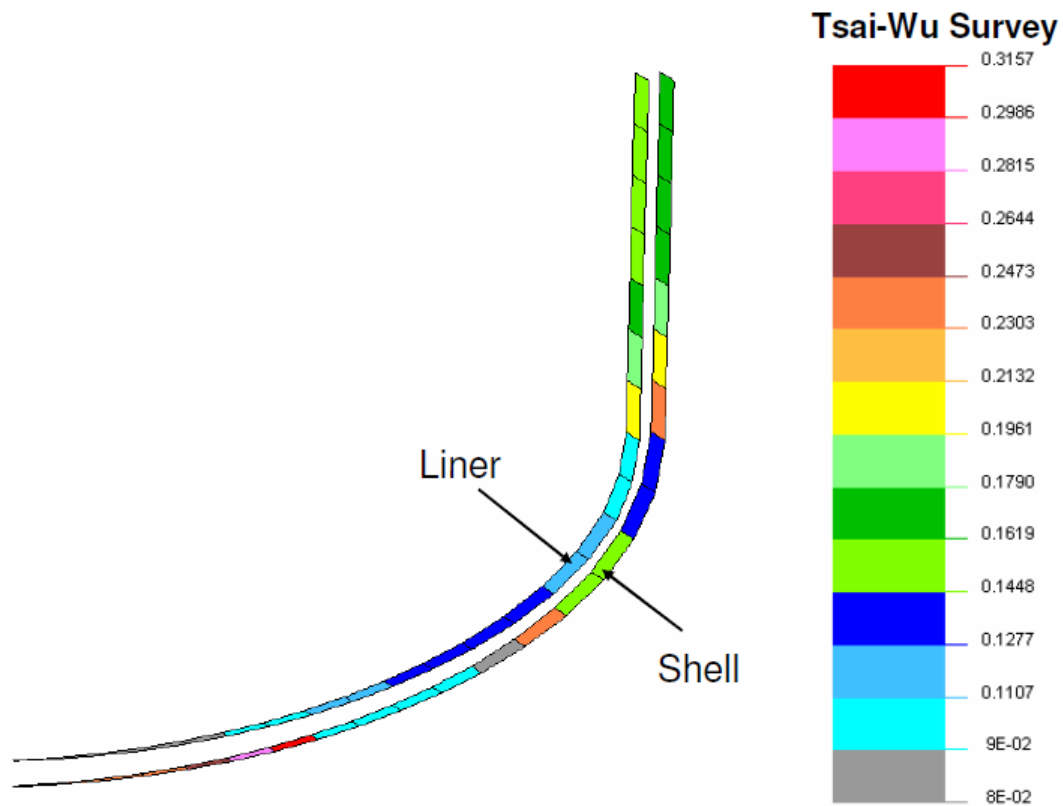


Figure B-15. Tsai-Wu Stress Survey Plot of Composite Structure for the Thermal-only Load Case

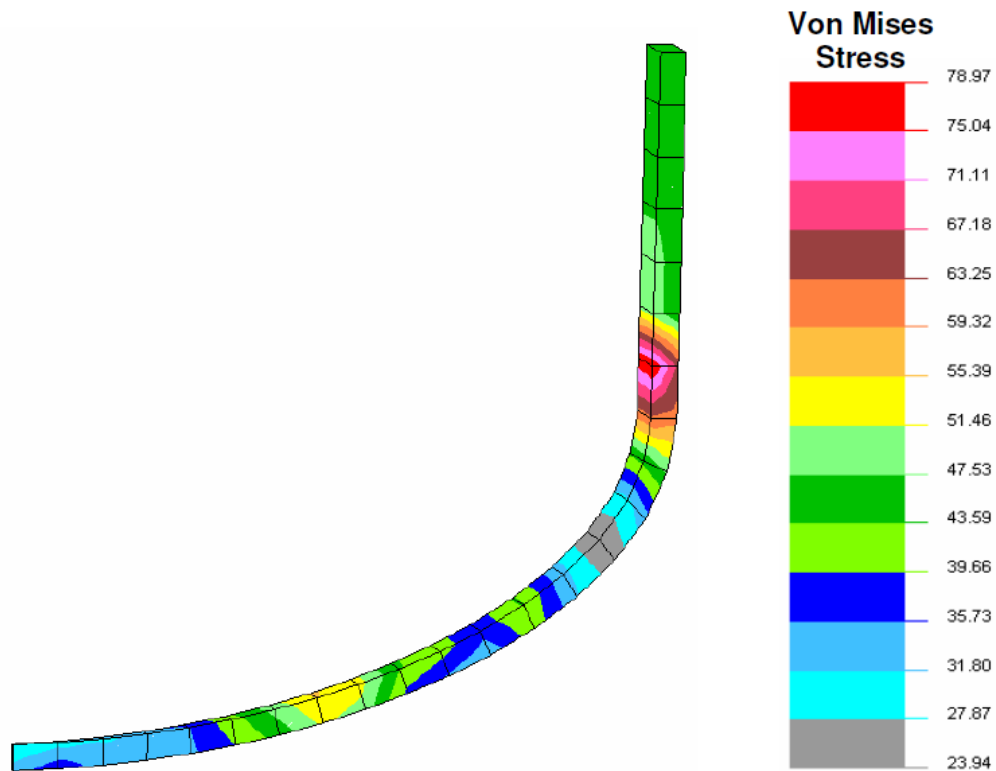


Figure B-16. von Mises Stress in the Foam Core for the Thermal-only Load Case

B4.3 Vehicle Analysis

The following sections provide details and results of the vehicle analysis as defined in Table B-6.

B4.3.1 Ground Handling Horizontal Lift Load Case

In ground handling the vehicle is assumed secured in a horizontal position sitting in an integration cart or dolly. To position the vehicle in a launch configuration requires it to be horizontally lifted then broken over to vertical. This is assumed done with a dual hook crane and spreader bars. Vehicle lift points are shown in Figure B-17. The forward section is lifted at side attach points on the payload cone/nose cone/fuselage interface joint, Figure B-19. Straps run between swivels mounted to the vehicle and up to a spreader bar. The straps are long enough to clear the nose cone during breakover to vertical. The aft attach point is a swivel mounted into the joint at the engine cone/fuselage joint.

For the horizontal lift load case it is assumed the propellant tanks are empty. This is typical field practice. Loading on the vehicle is a 4 g lateral load (in direction of gravity). 2 gs are assumed for transient loads as lift starts and stops and an additional 2 gs are added for a minimum safety factor. Typically ground operations, especially lifts, use higher safety factors than flight given safety concerns.

Figures B-17 and B-18 show deformed geometry and resultant displacement contour plots. These figures show little deformation of the vehicle during a horizontal lift operation.

Figure B-19 is a Tsai-Wu survey plot of the composite structures. Tsai-Wu values less than 0.2 indicate good structural safety margins (all >2.0).

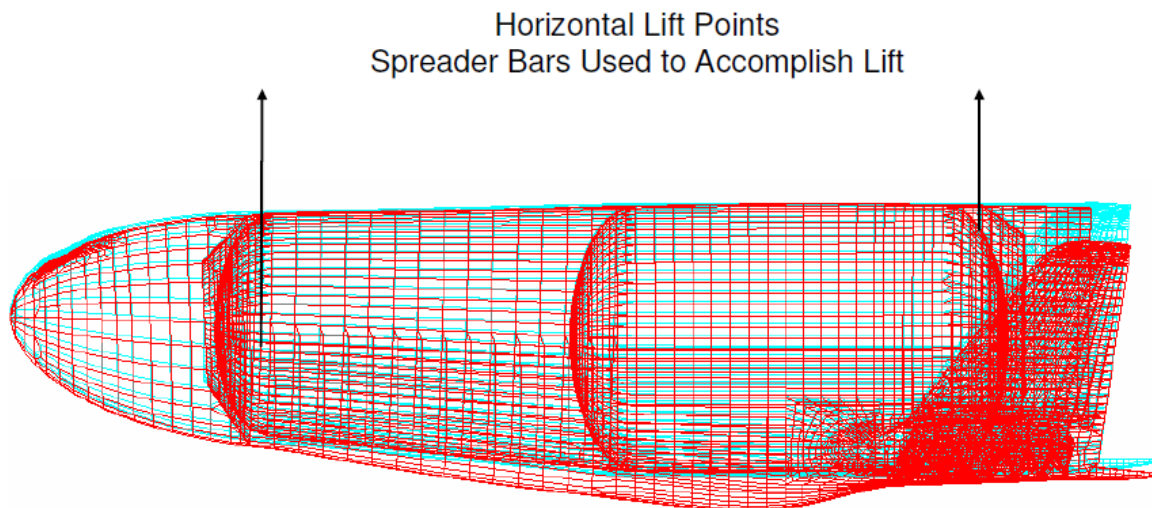


Figure B-17. Deflection of the Vehicle with a 4 g Horizontal Lift

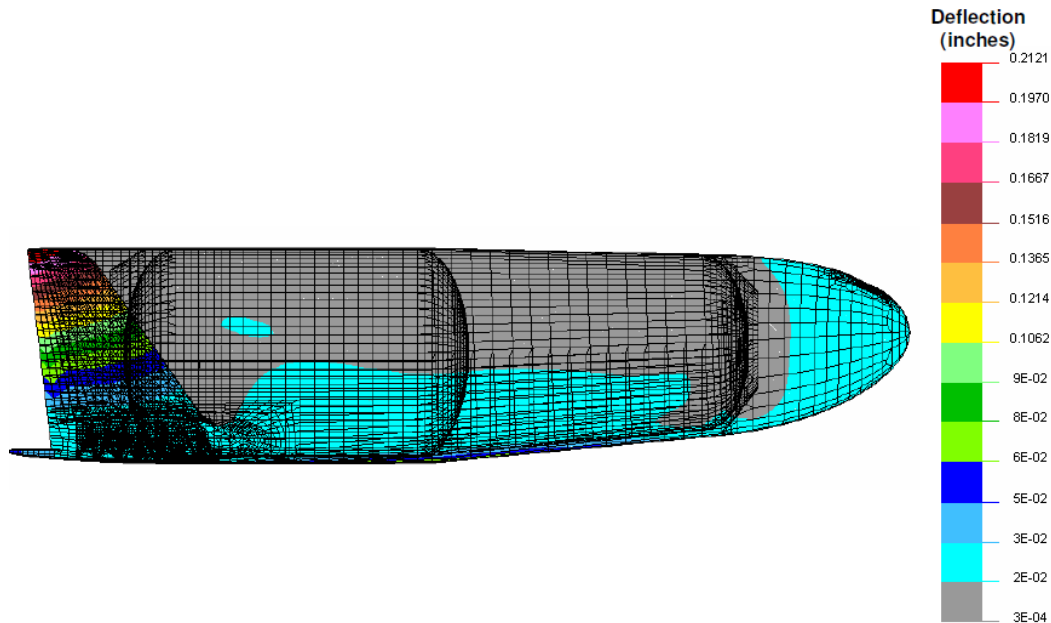


Figure B-18. Resultant Displacement of Structure during Horizontal Lift

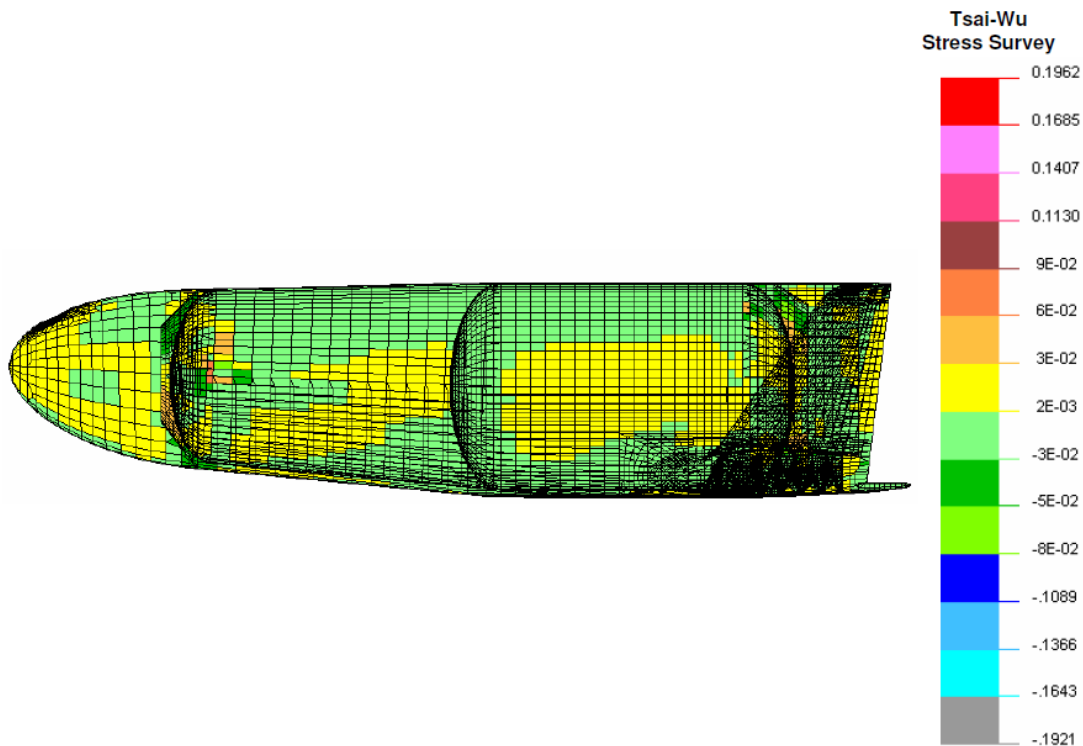


Figure B-19. Tsai-Wu Stress Survey Plot of the Composite Structures during Horizontal Lift

B4.3.2 Ground Handling Vertical Lift Load Case

After horizontal lift the vehicle is broken over to the vertical position. In the vertical position all of the weight of the vehicle is suspended from the straps attached to a swivel on the forward sides of the vehicle. As in the horizontal lift load case a 4 g axial load is applied and the propellant tanks are empty.

Figures B-20 and B-21 show deformed geometry and resultant displacement contour plots. These figures show little deformation of the vehicle during a vertical lift operation.

Figure B-22 is a Tsai-Wu survey plot of the composite structures. With Tsai-Wu values below 1.0 all structural safety margins are >2.0 .

Vertical Lift Point
 Spreader Bars Used to Accomplish Lift

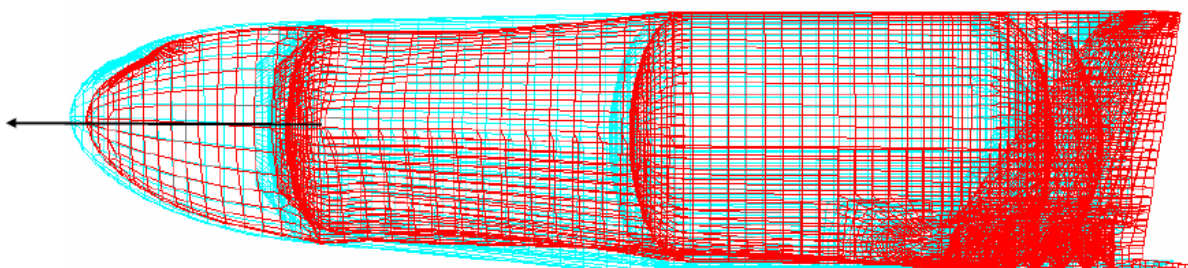


Figure B-20. Deformed Geometry Plot of the Vehicle for a Vertical Lift

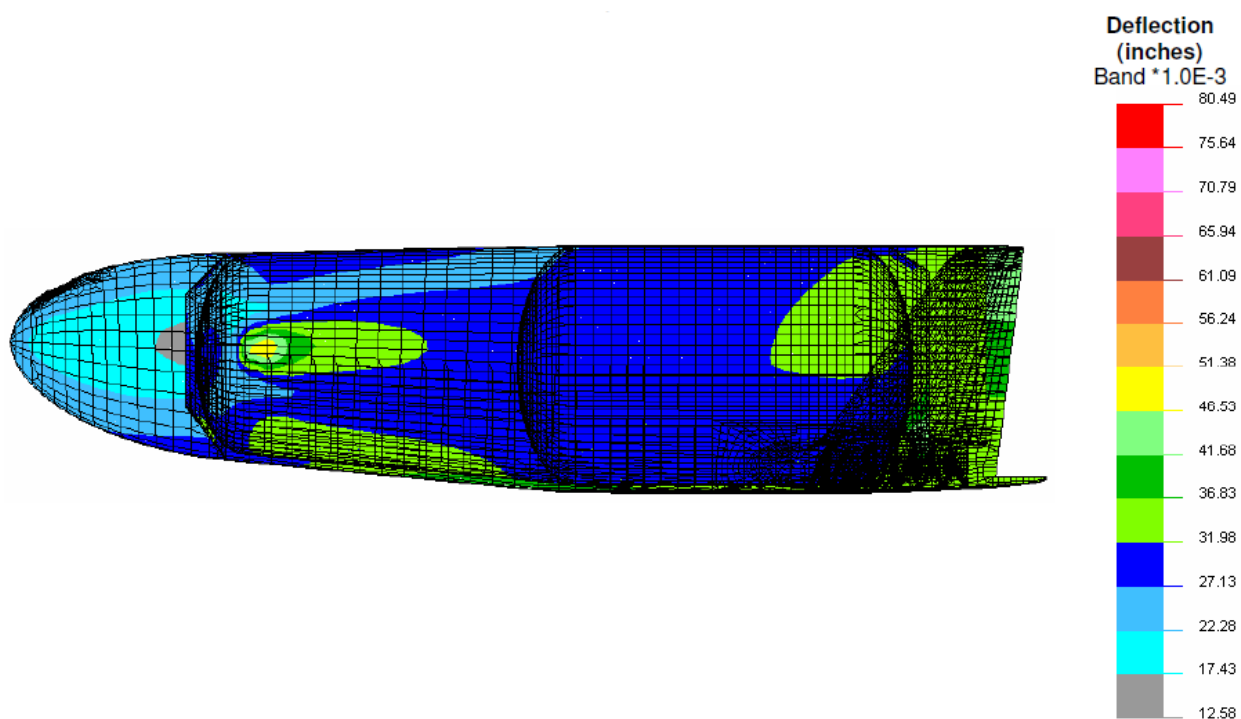


Figure B-21. Resultant Displacement Contour Plot of the Vehicle for a Vertical Lift

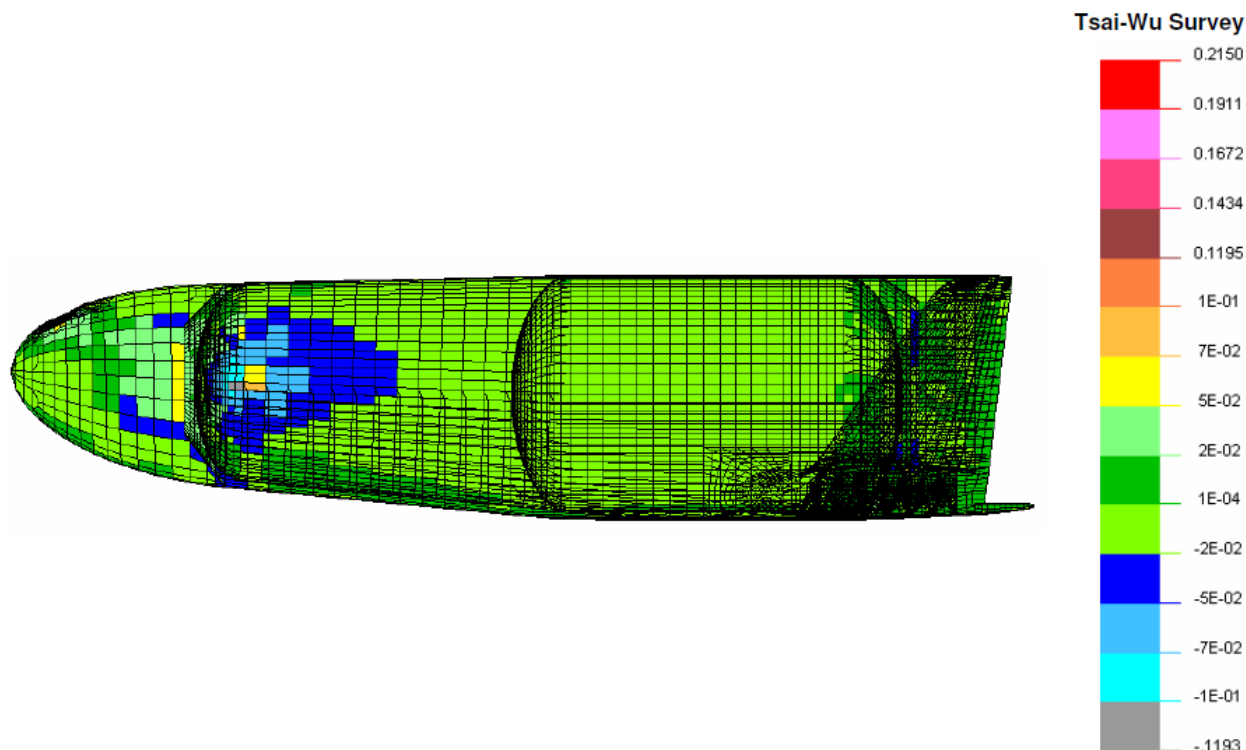


Figure B-22. Tsai-Wu Stress Survey Plot of the Composite Structures during Vertical Lift

B4.3.3 Launch Load Case

The launch load case models that time in flight where HOT EAGLE is being carried as an upper stage on a boost vehicle. HOT EAGLE is attached to the booster by a bi-mese attach configuration. During boost phase launch the maximum structural loads typically occur in the transonic region as the vehicle passes through its maximum dynamic pressure (max q). For this load case max q is assumed to be 1,200 psf [5]. The pressure profile on the vehicle is taken from the Cp plots generated by CFD analysis. For this load case the Micro-X Cp plot for M=2.0 with and AOA=2.0 is used, Figure B-23. From the Cp values in Figure B-23 a pressure profile is mapped onto the vehicle, Figure B-24 and B-25. The relationship to calculate panel pressures is:

$$P = q C_p + P_{inf} \quad (1)$$

where

P_{inf} = absolute pressure at altitude

For this analysis P_{inf} is set to zero. This is conservative in that it sets the pressure differential between the inside of the vehicle and the outside to 0.0, which maximizes the compressive structural loads on the vehicle (in this case worst positive C_p is much larger than negative). During vehicle ascent there is always some positive internal pressure to the vehicle (typically about 3.0 psi higher than ambient) as a result of the vehicle's restricted venting capabilities. Later detailed design should consider additional cases of non-zero internal pressure possibilities.

As part of defining safety margins using the Tsai-Wu failure criteria, the aeroloads shown in Figures B-24 and B-25 include a 1.5 increase in pressure.

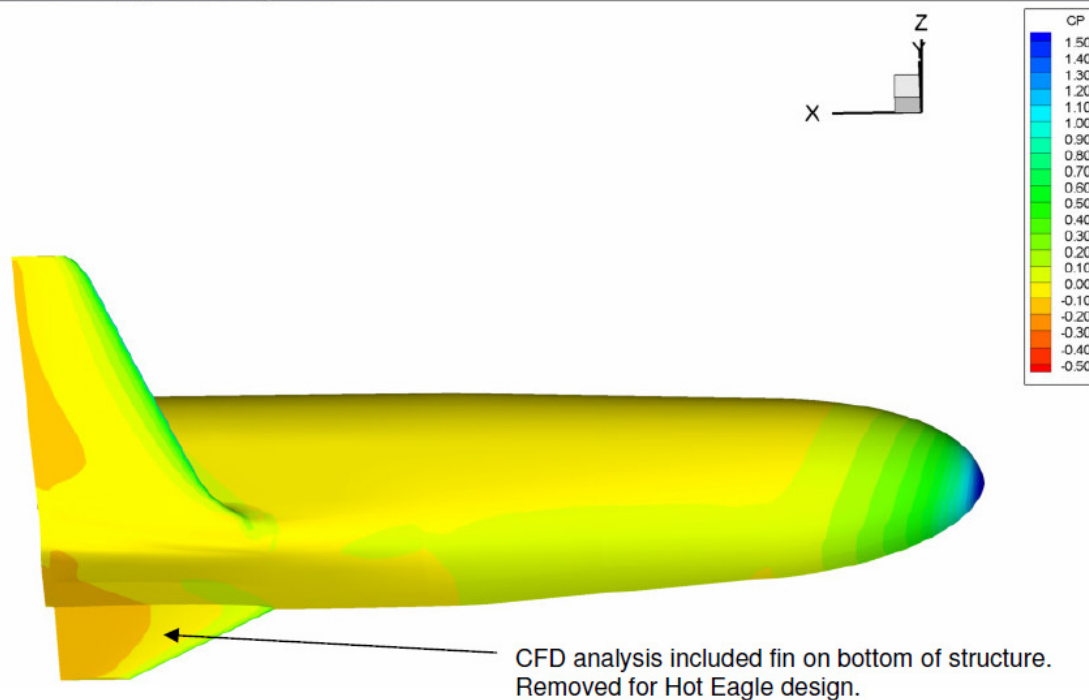


Figure B-23. Vehicle Cp Plot from CFD Analysis for $M = 2.0$ and $AOA = 2.0$

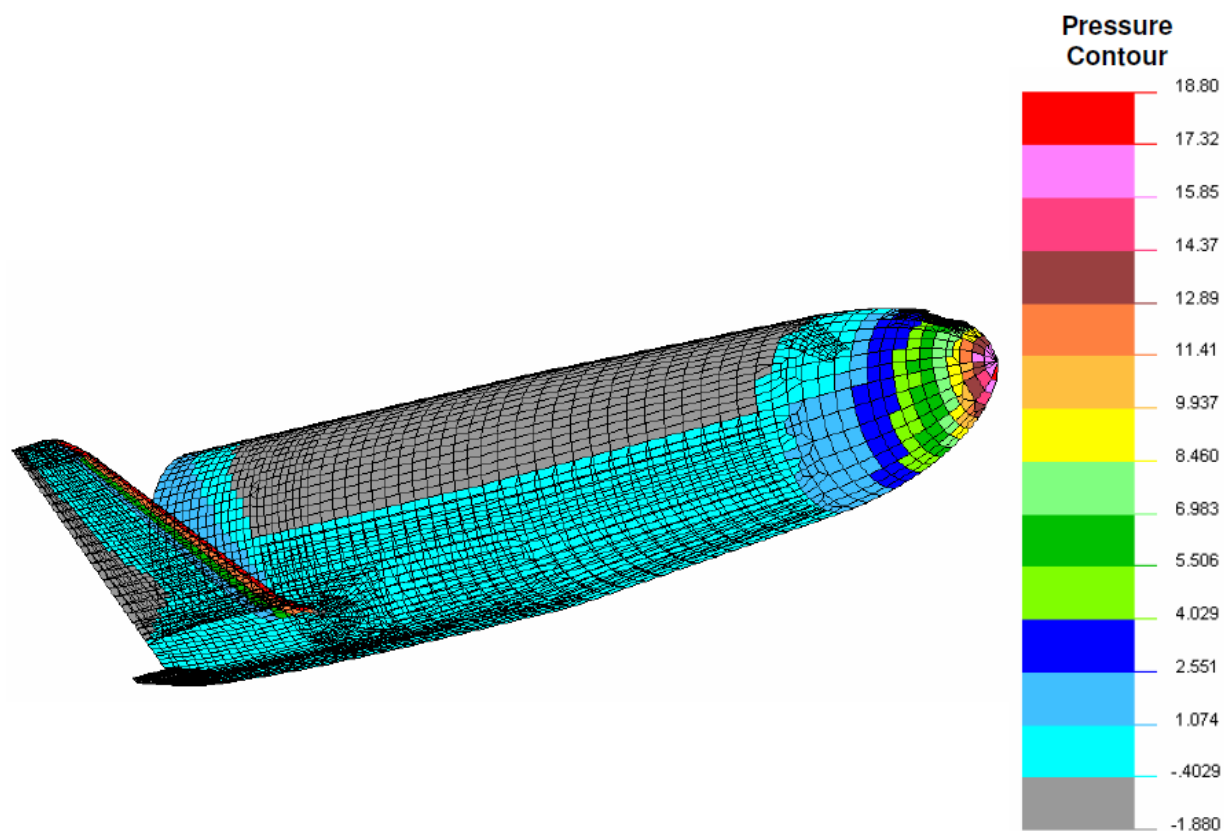
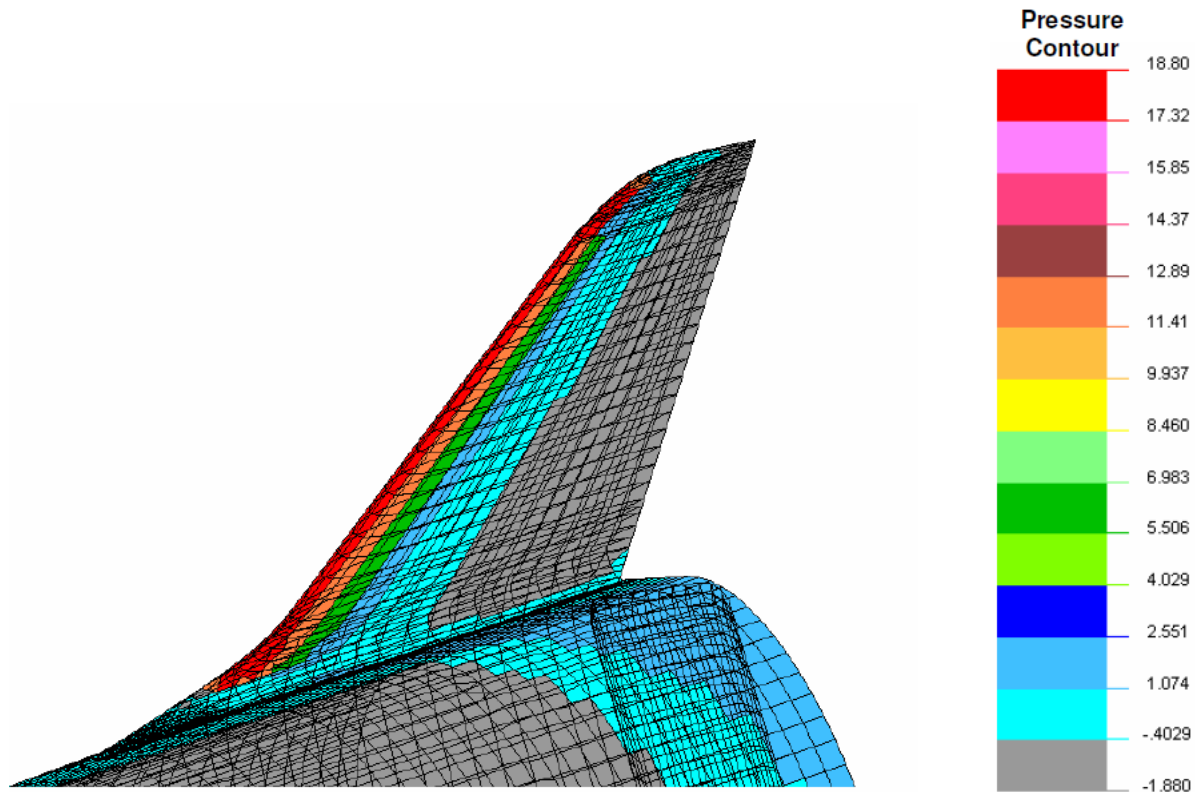


Figure B-24. Vehicle Aero Load Pressure Profile for $q=1200$ psf, $M=2.0$ and $AOA=2.0$
(Pressure loads shown include an additional 1.5 increase for safety margin.)



*Figure B-25. Aero Load Pressure Profile on Vehicle's Wing for $q=1200$ psf, $M=2.0$ and $AOA=2.0$
(Pressure loads shown include an additional 1.5 increase for safety margin.)*

Aside from the aero loads, inertia loads were also applied to the model per Table B-6. These loads were also increased an additional 1.5 times to facilitate the use of the Tsai-Wu failure criteria. Figure B-26 illustrates the inertia loads applied to the vehicle and how the model was constrained to simulate the bi-mese attach.

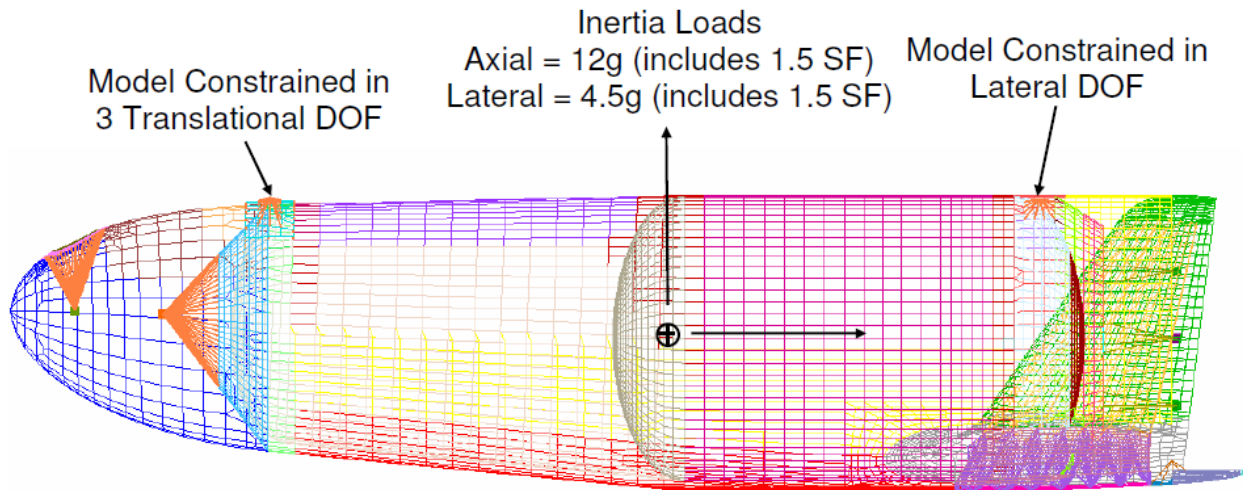
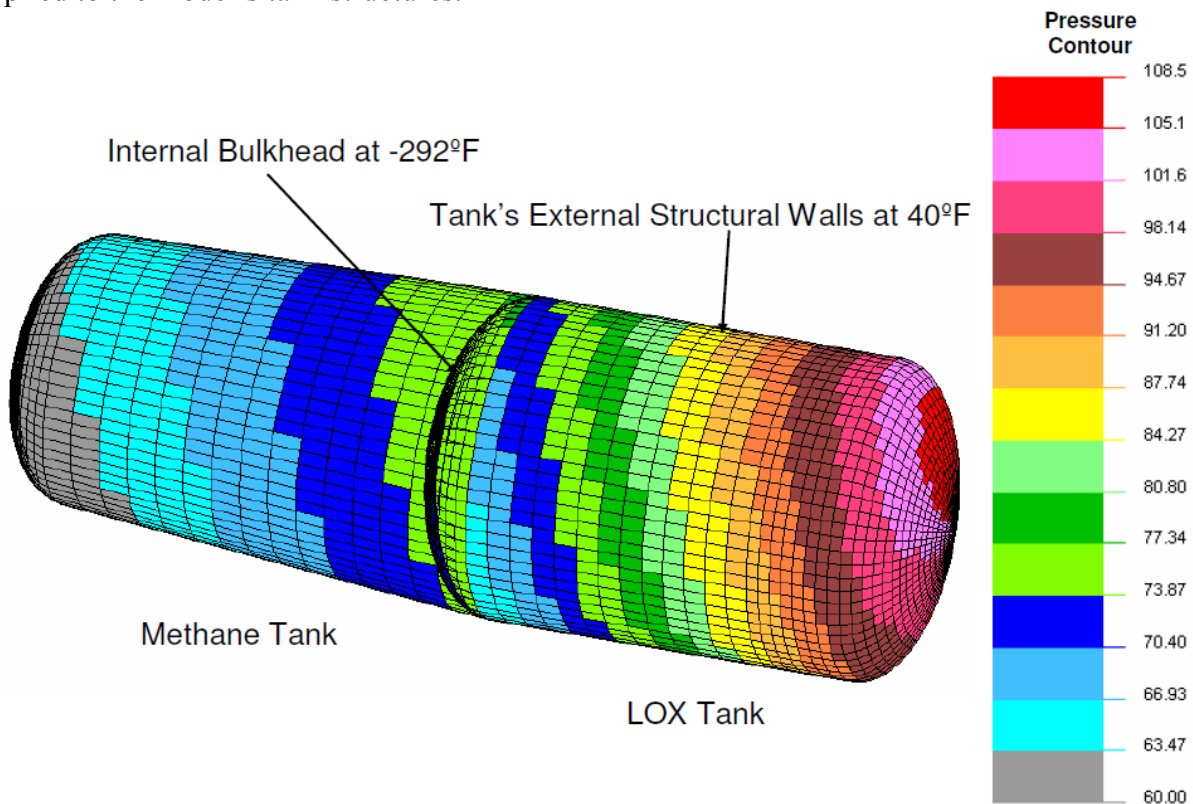


Figure B-26. Boundary Conditions and Loads on Model for Launch Loads Analysis

For the vehicle launch load case the propellant tanks are assumed full. To simulate the inertia effects of the propellant in the propellant tanks a pressure gradient was calculated based on the inertia load, density of the propellant (scaled per Section B3.1 for the same Micro-X propellant load), and the axial length (depth) of the propellant in each tank. This gradient was then added to the tanks blowdown pressure of 40 psi. These pressures were then scaled an additional 1.5 for safety margin verification using Tsai-Wu. Figure B-27 shows the pressure and thermal loads applied to the model's tank structures.



*Figure B-27. Pressure Profile in Propellant Tanks
(Pressure loads shown include an additional 1.5 increase for safety margin.)*

Figures B-28 through B-35 show results of the analysis. Figures B-28 and B-29 are deformed geometry and resultant displacement contour plots of the vehicle for 1.5 times applied loads. Maximum deflection is occurring at the wing tip, which is expected.

Figures B-30 through B-35 show the Tsai-Wu stress survey plots of the composite structures. With a 1.5 times safety factor on applied launch loads, all composite structures are showing positive margins. But, this required local addition of structure at the bi-mese attach points, which costs significant weight.

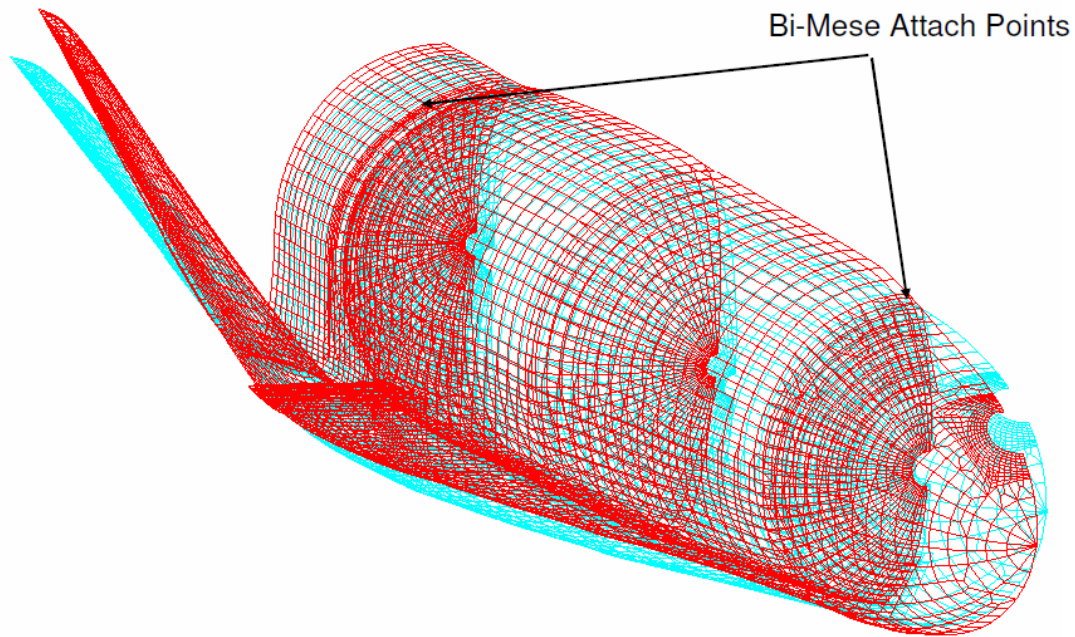


Figure B-28. Deformed Geometry Plot of the Vehicle for the Launch Load Case

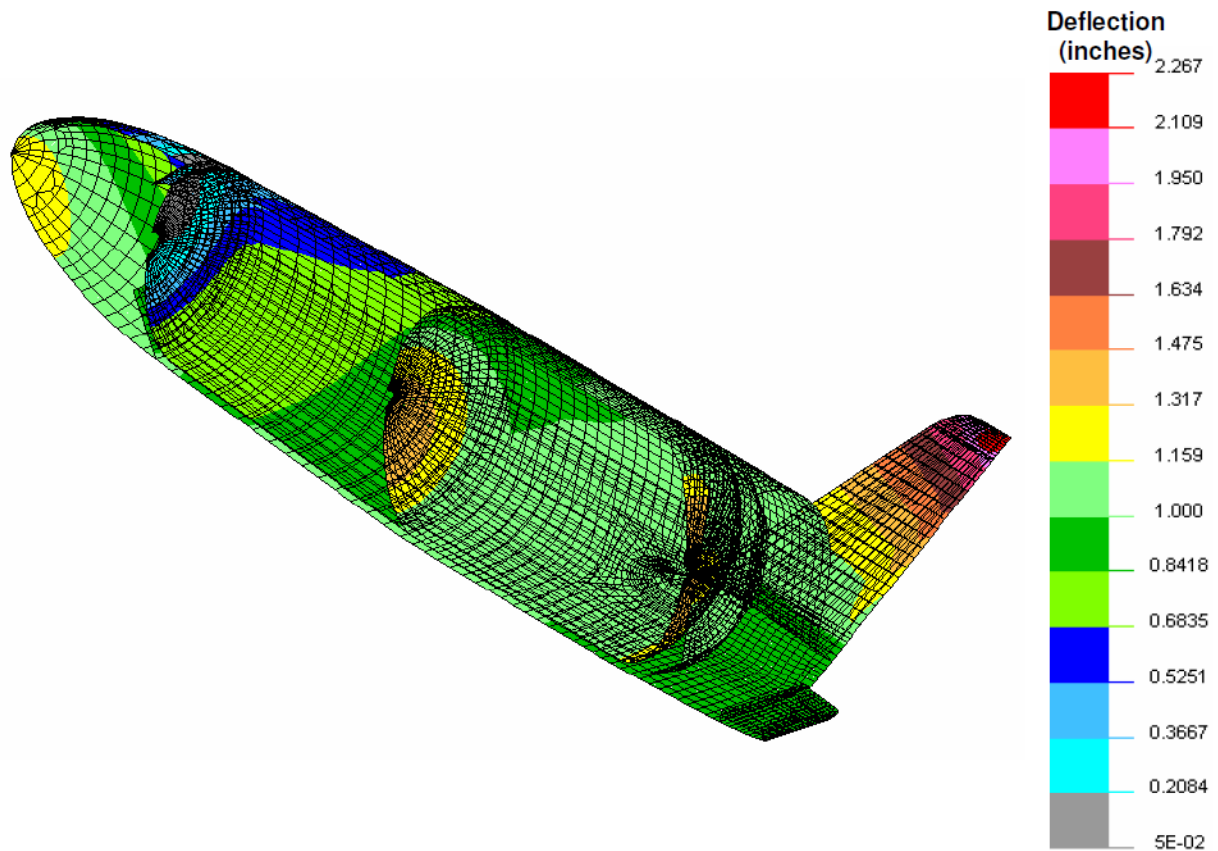


Figure B-29. Resultant Displacement Contour Plot for the Launch Load Case

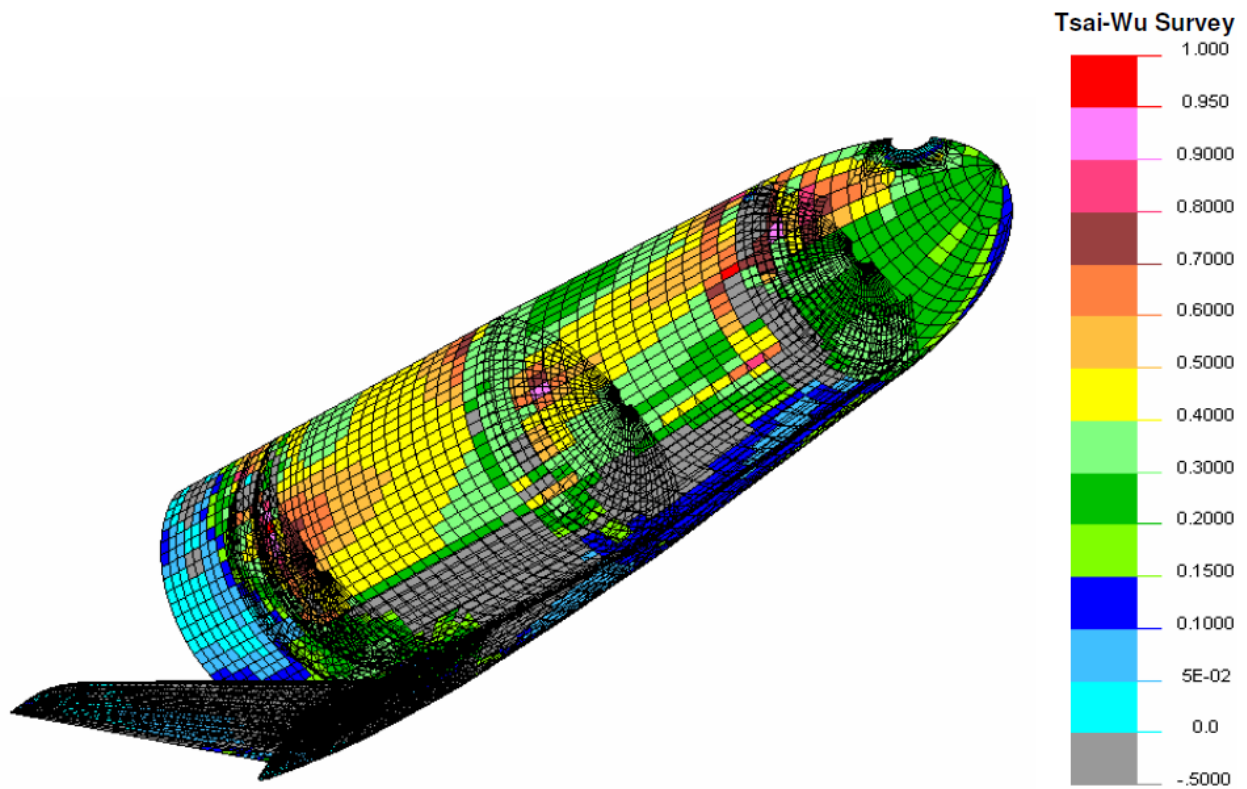


Figure B-30. Tsai-Wu Stress Survey of the Vehicle Composite Structures for the Launch Load

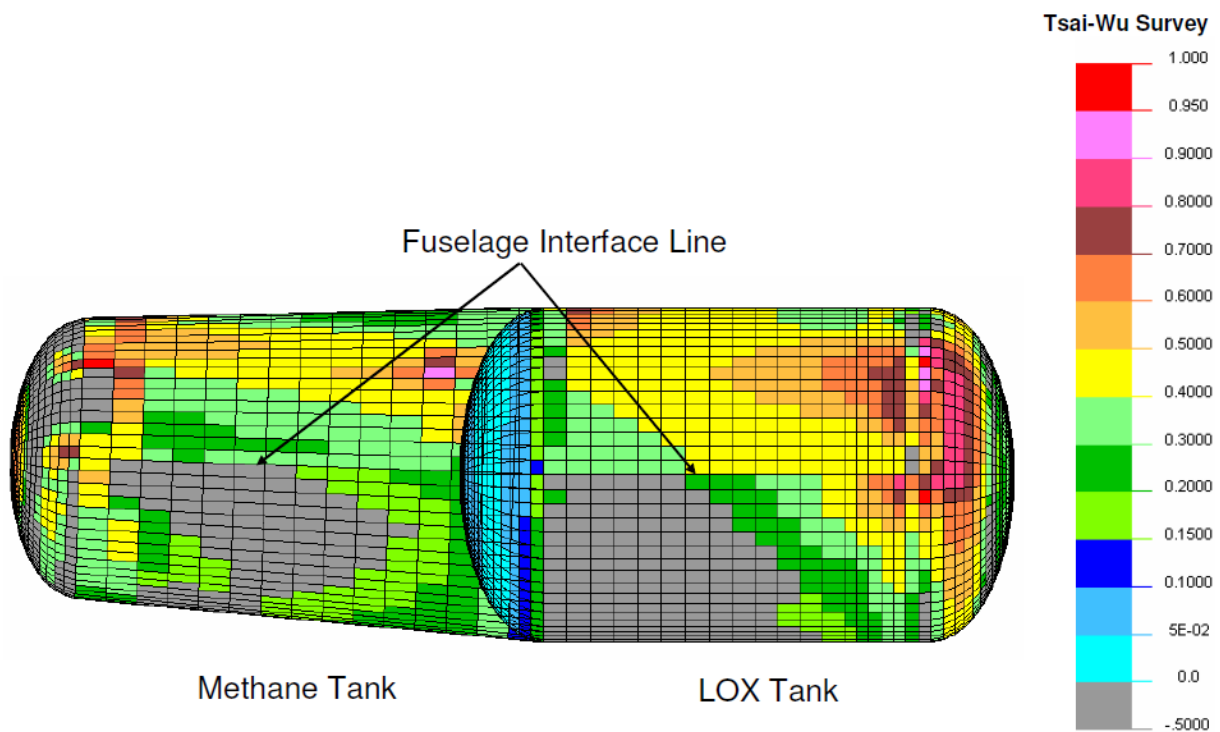


Figure B-31. Tsai-Wu Stress Survey of the Vehicle's Propellant Tanks for the Launch Load Case

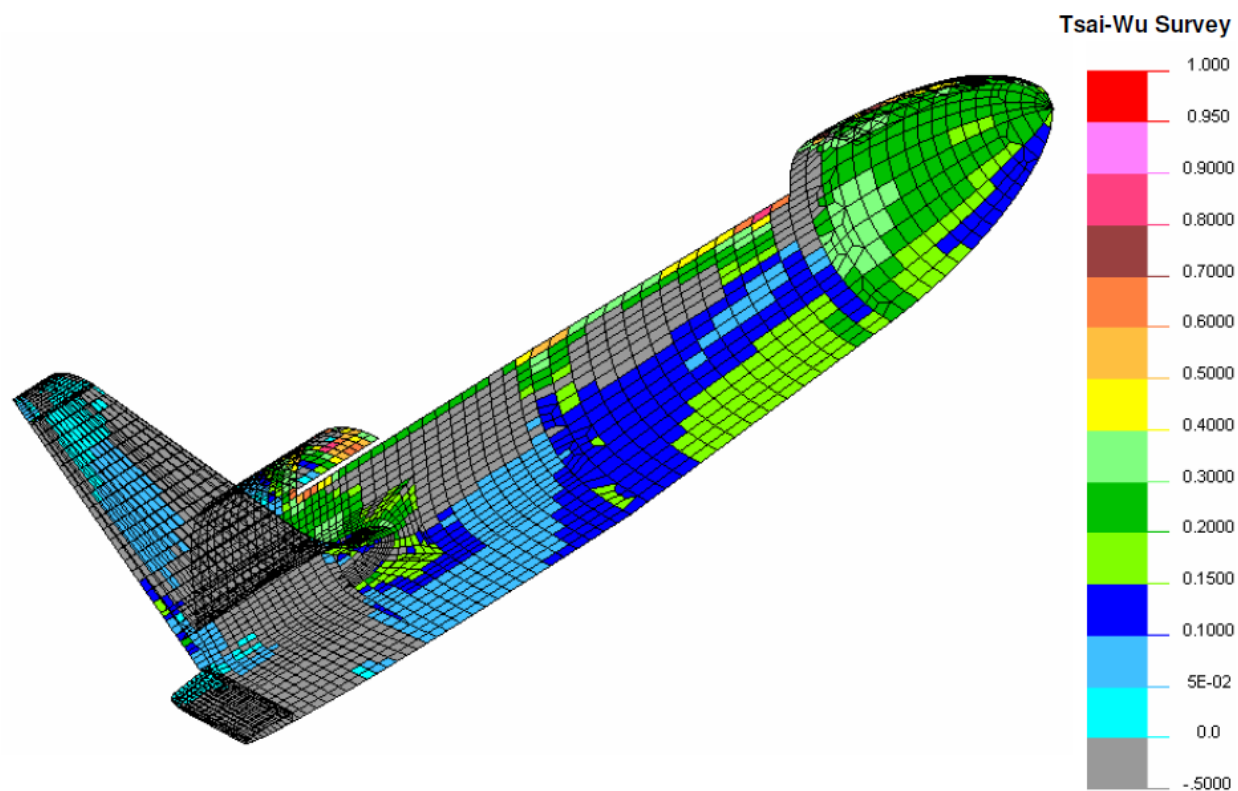


Figure B-32. Tsai-Wu Stress Survey of Vehicle Composite Structures without the Propellant Tanks

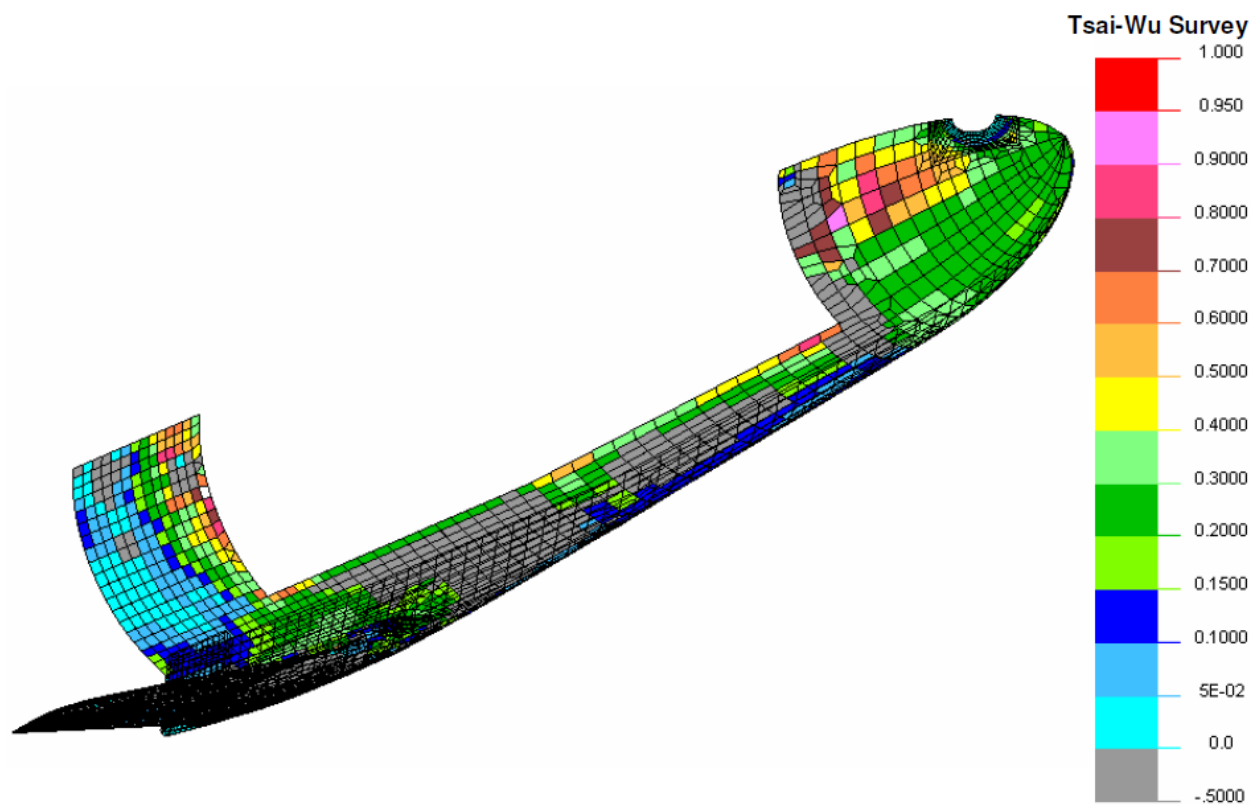


Figure B-33. Tsai-Wu Stress Survey of Vehicle Composite Structures without Propellant Tanks

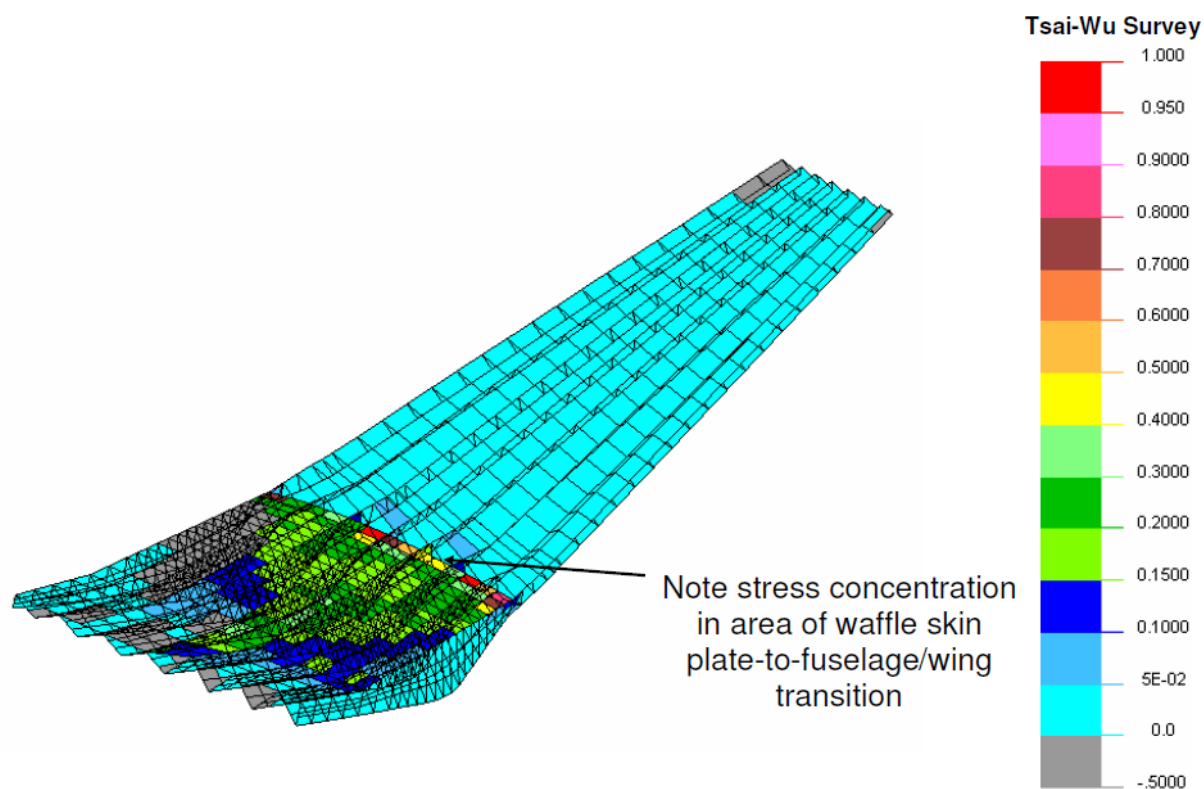


Figure B-34. Tsai-Wu Stress Survey of Wing Waffle and Wing Carry-through Composite Structures

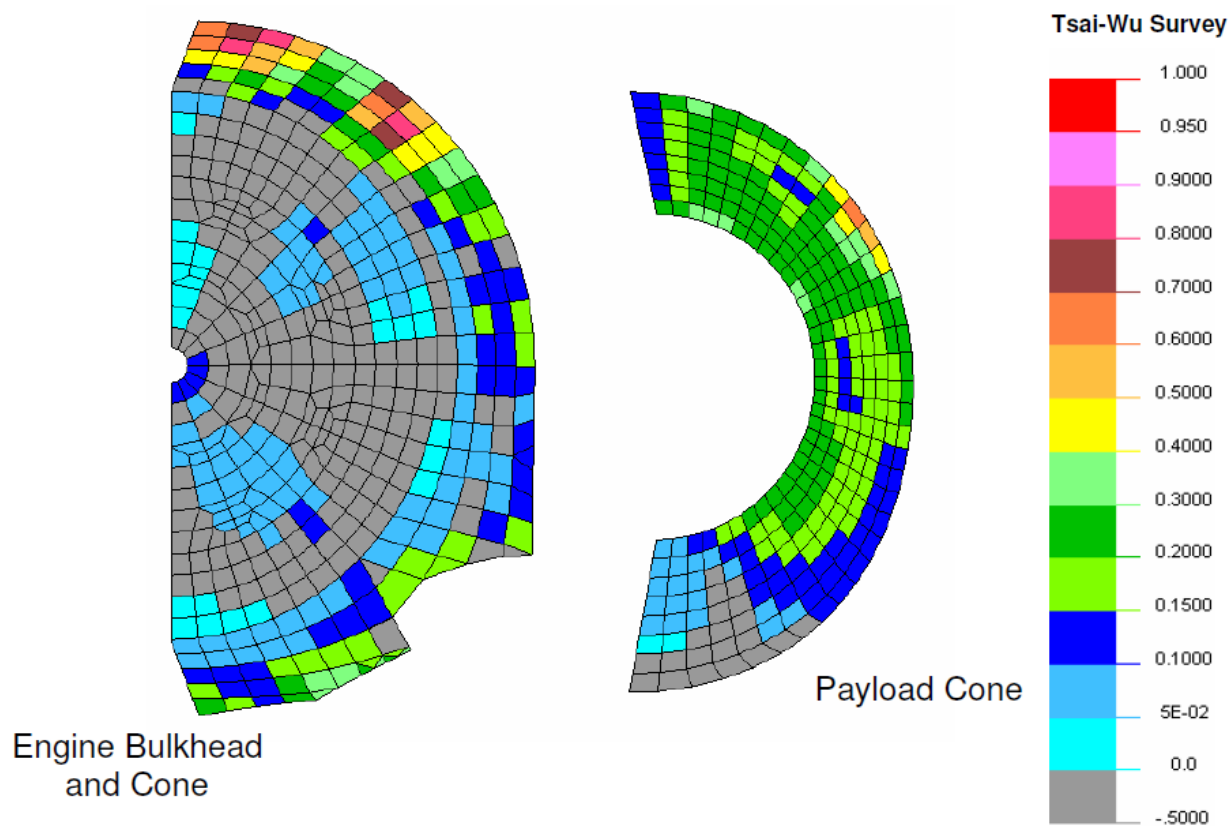


Figure B-35. Tsai-Wu Stress Survey of Vehicle Engine Support and Payload Cone Structures

B4.3.4 Powered Flight: Exo-Atmospheric

At some point after boost phase launch the vehicle is separated from the launch vehicle. It is assumed that HOT EAGLE will be exo-atmospheric for its engine operation. Thus for this load case there are no aero loads on the vehicle. Table B-6 outlines the loads applied for this analysis. Figure B-36 shows the loads reacting on the vehicle and the applied boundary conditions. Propellant tanks are assumed 20% full, Figure B-37. Inertia loading is applied to the propellant in the same manner as was done in the launch load case, Section B4.3.3, but for the lower level of fluid.

For this load case the engines had to be throttled back to prevent exceeding the axial inertia load of 3g. The center engine was turned off and the other engines throttled back to 93% power.

For this load case the vehicle is in a free flight condition (that is no boundary constraints to hold it) Static finite element analysis of a model that is not fixed in space is not a straight forward task. NISA does have the capability for inertial relief analysis, or automatic force balance for this kind of condition. To prevent rigid body motion requires that the model have some level of constraint or balancing of forces that keeps it from flying off the paper. To accomplish this, this analysis was done through a series of iterations equivalent to inertial relief analysis.

To prevent rigid body motion, two additional constraints were added to the model, two nodes, one on the forward end of the vehicle and one on the aft end. The forward node was constrained in all 3 translational DOF. The aft node was constrained only in the vehicle's pitch direction. Several iterations were conducted varying inertia loads to reduce the reaction forces on these nodes to a small value (< 100 lbf). Essentially what was done was to balance all of the applied forces on the vehicle with reacting inertia loads.

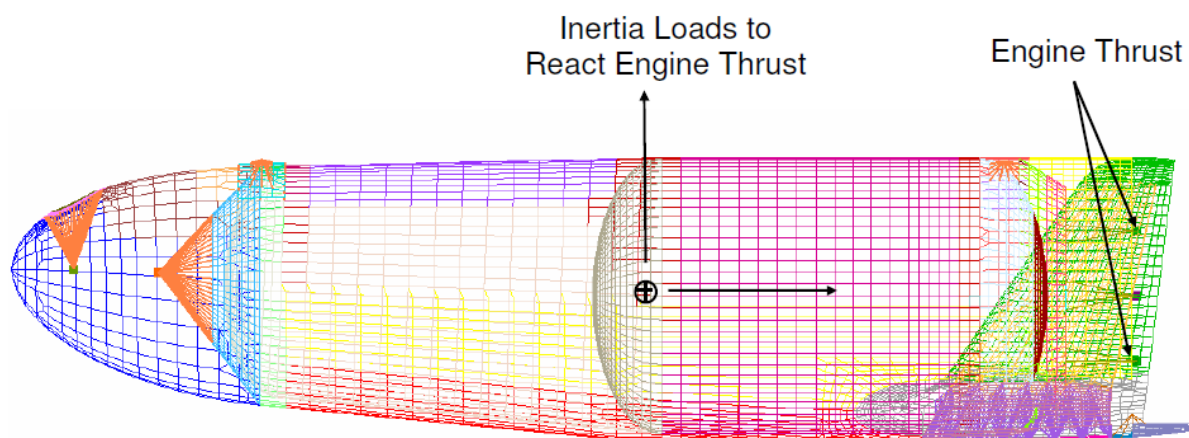
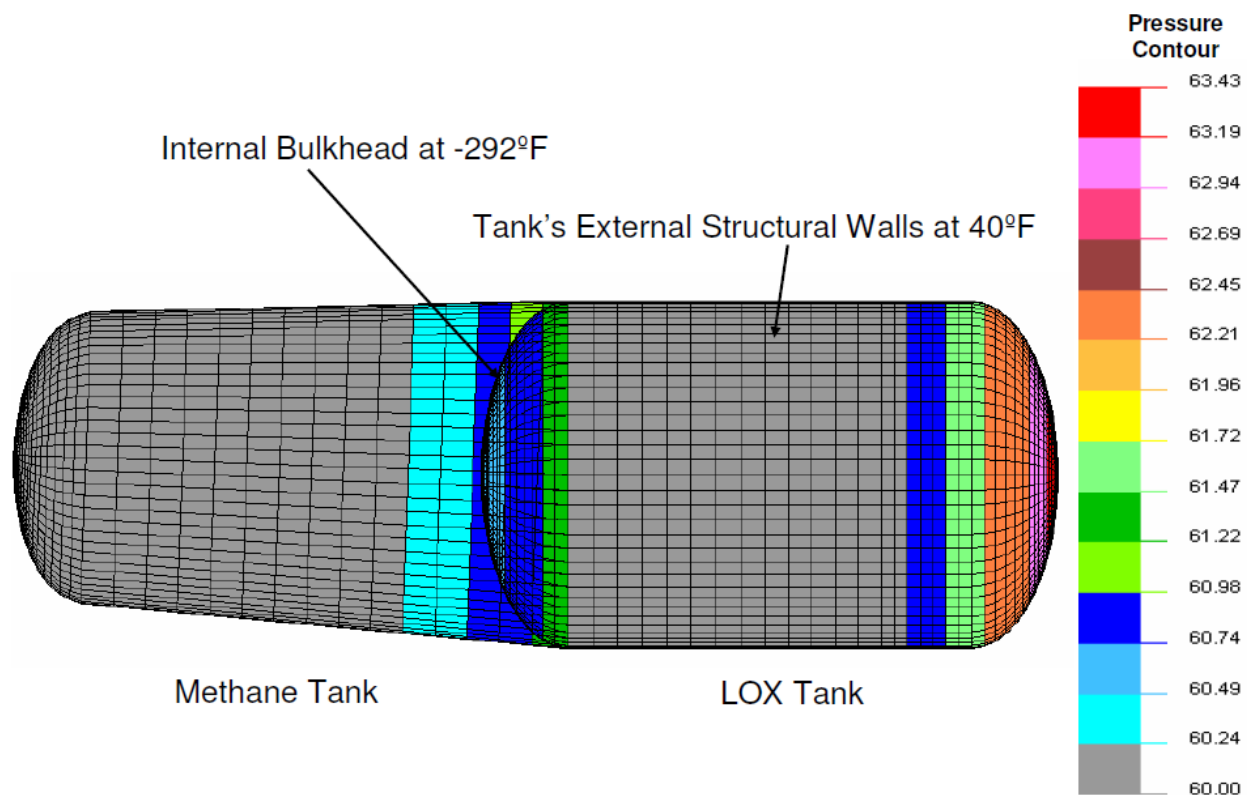


Figure B-36. Boundary Conditions on Model for Powered Flight Analysis



*Figure B-37. Pressure Profile in Propellant Tanks
(Pressure loads shown include an additional 1.5 increase in loads for safety factor.)*

Figures B-38 through B-42 show results of the analysis. Figures B-38 and B-39 are deformed geometry and resultant displacement contour plots of the vehicle for 1.5 times applied loads. Figure B-40 is showing resultant deflection of the engine support structure. Here the maximum deflection 0.22 inch.

Figures B-41 and B-42 show the Tsai-Wu stress survey plots of the composite structures. With a 1.5 times applied launch loads all composite structures are showing positive margins. This case was relatively benign, and did not require design iteration.

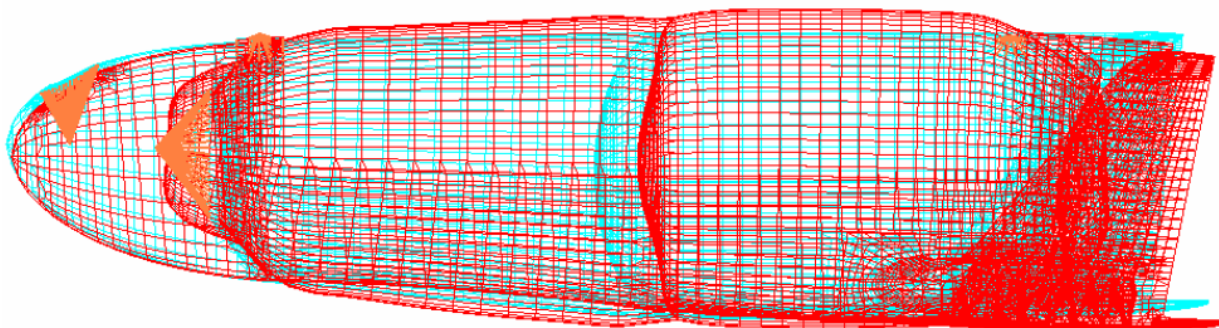


Figure B-38. Deformed Geometry Plot of the Vehicle for Powered Flight

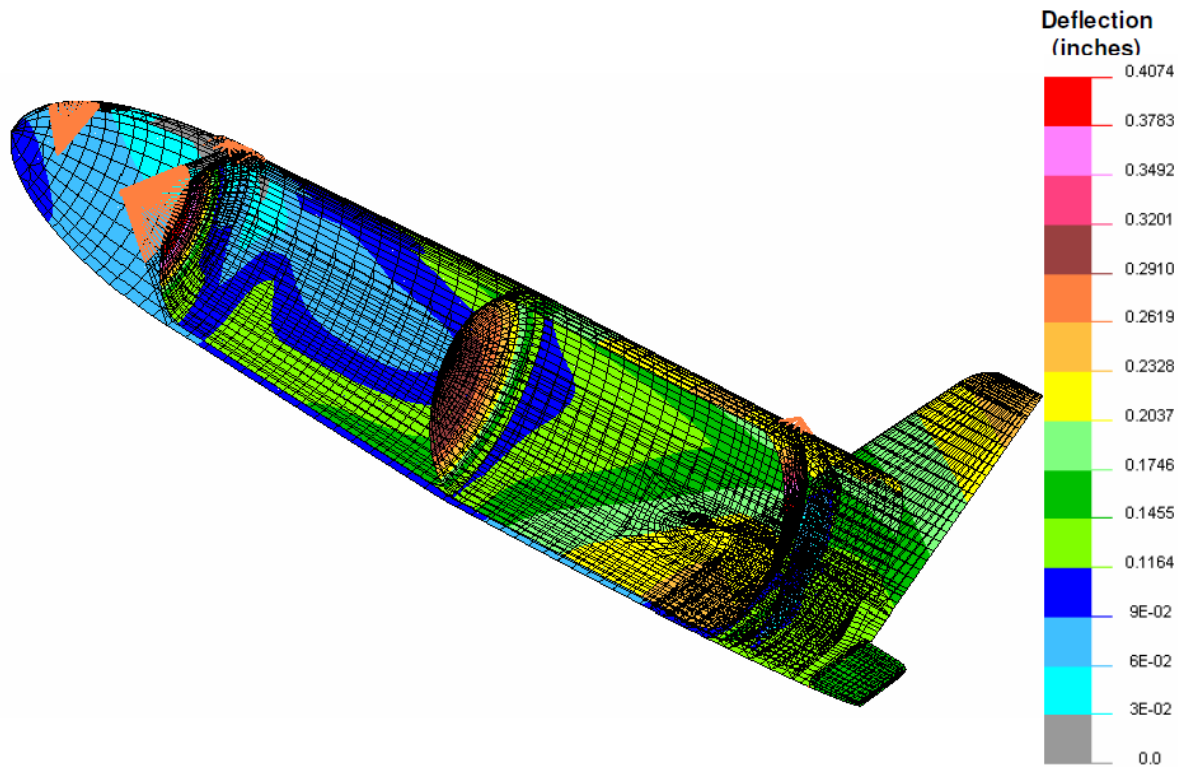


Figure B-39. Resultant Displacement Contour Plot of the Vehicle for Powered Flight

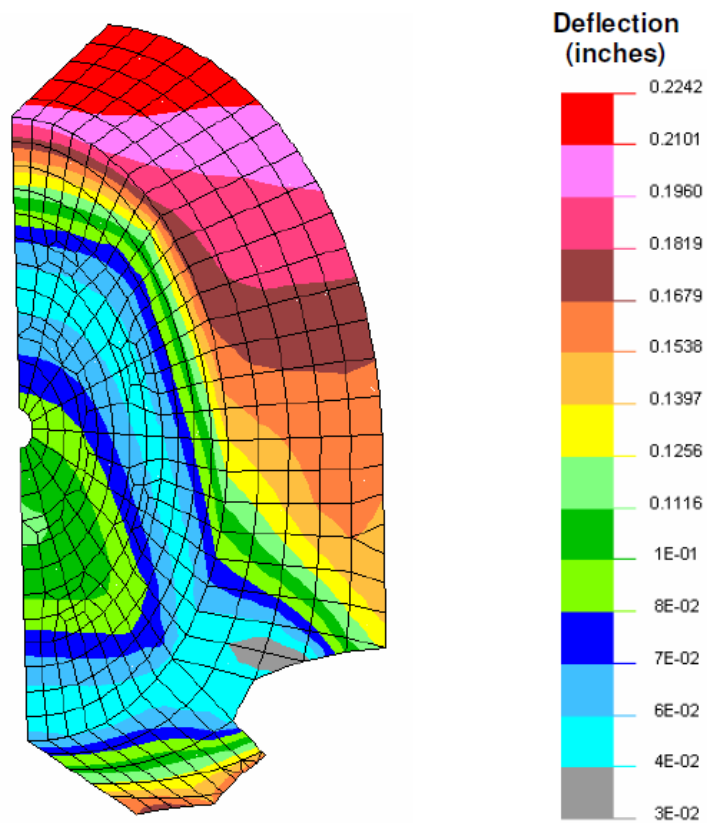


Figure B-40. Resultant Displacement Contour Plot of Engine Support Structure for Powered Flight

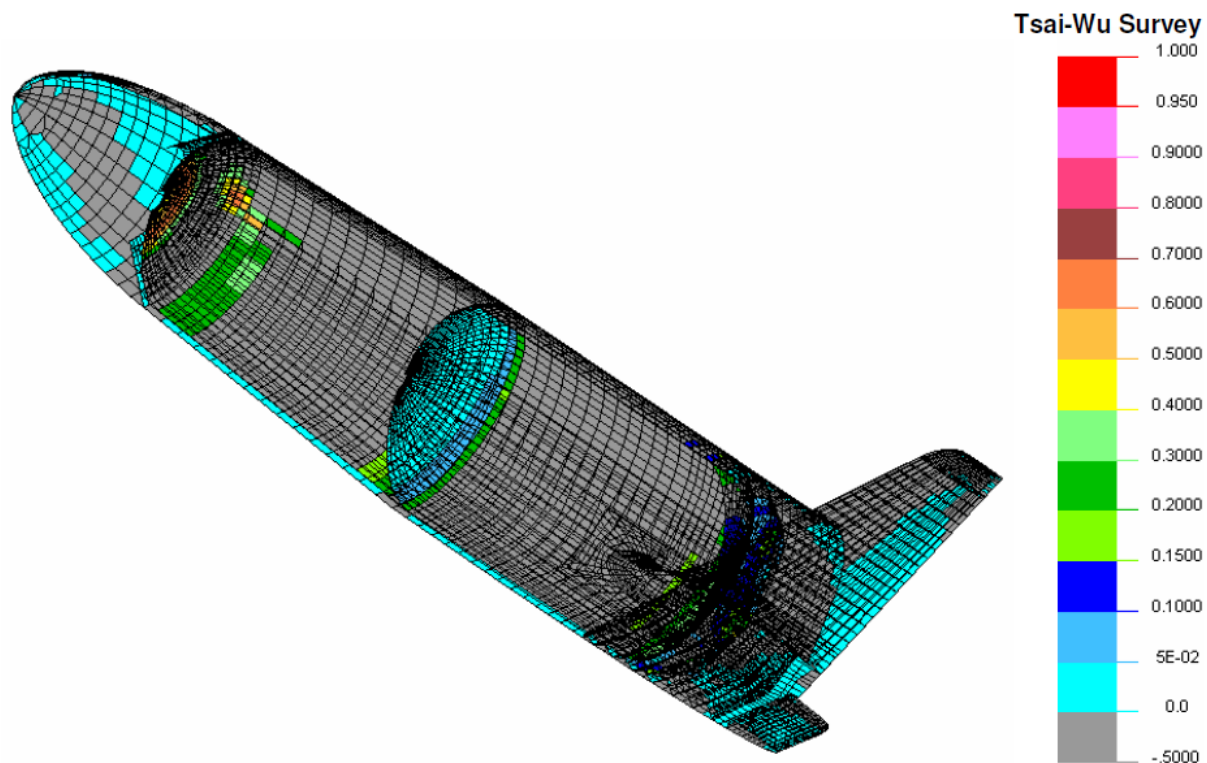


Figure B-41. Tsai-Wu Stress Survey of the Vehicle's Composite Structures for Powered Flight

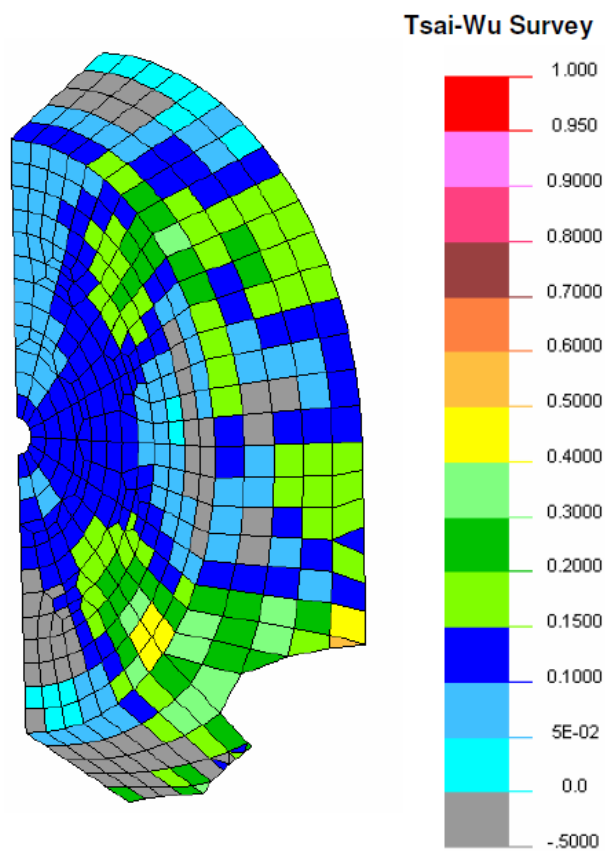


Figure B-42. Tsai-Wu Stress Survey of the Engine Support Structure for Powered Flight

B4.3.5 Re-Entry Load Case

At the early stage of its re-entry HOT EAGLE will be at a very high angle-of-attack. As it begins to slow down in the atmosphere it will have tendency to pitch down. For this load case it is assumed that the vehicle is at $M = 25$ with an $AOA = 70$ deg. Dynamic pressure is assumed 190 psf. Other loads are as defined in Table B-6.

The pressure profile for re-entry aero loads is taken from the C_p plots generated by CFD analysis. For this load case the Micro-X C_p plot for $M = 25.0$ with and $AOA = 70.0$ is used, Figure B-43. From the C_p values in Figure B-43, a pressure profile is mapped onto the vehicle in the same manner as was done for the launch load case, Figure B-44 and B-45. As part of defining safety margins using the Tsai-Wu failure criteria the aero loads shown in Figures B-44 and B-45 include a 1.5 increase in pressure

In the first iteration of this analysis it was realized that the aero load forces were putting such a large forward pitch force on the vehicle that the model could not be realistically constrained. To counteract this force a pressure was applied to the wing's aileron, Figure B-45. Figure B-46 shows the other loads and boundary conditions applied to the model for this analysis. Figure B-47 shows loads in the propellant tanks.

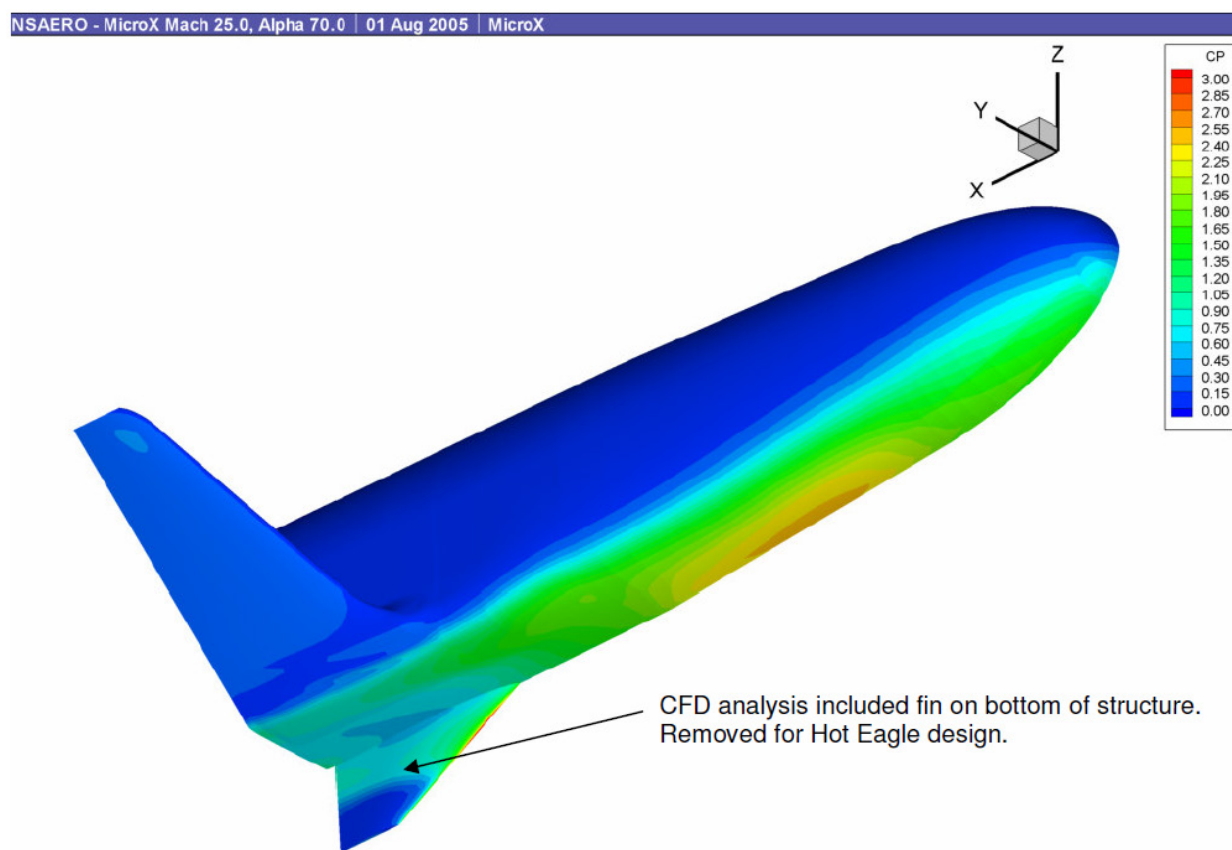


Figure B-43. Vehicle C_p Plot from CFD Analysis for $M = 25.0$ and $AOA = 70.0$

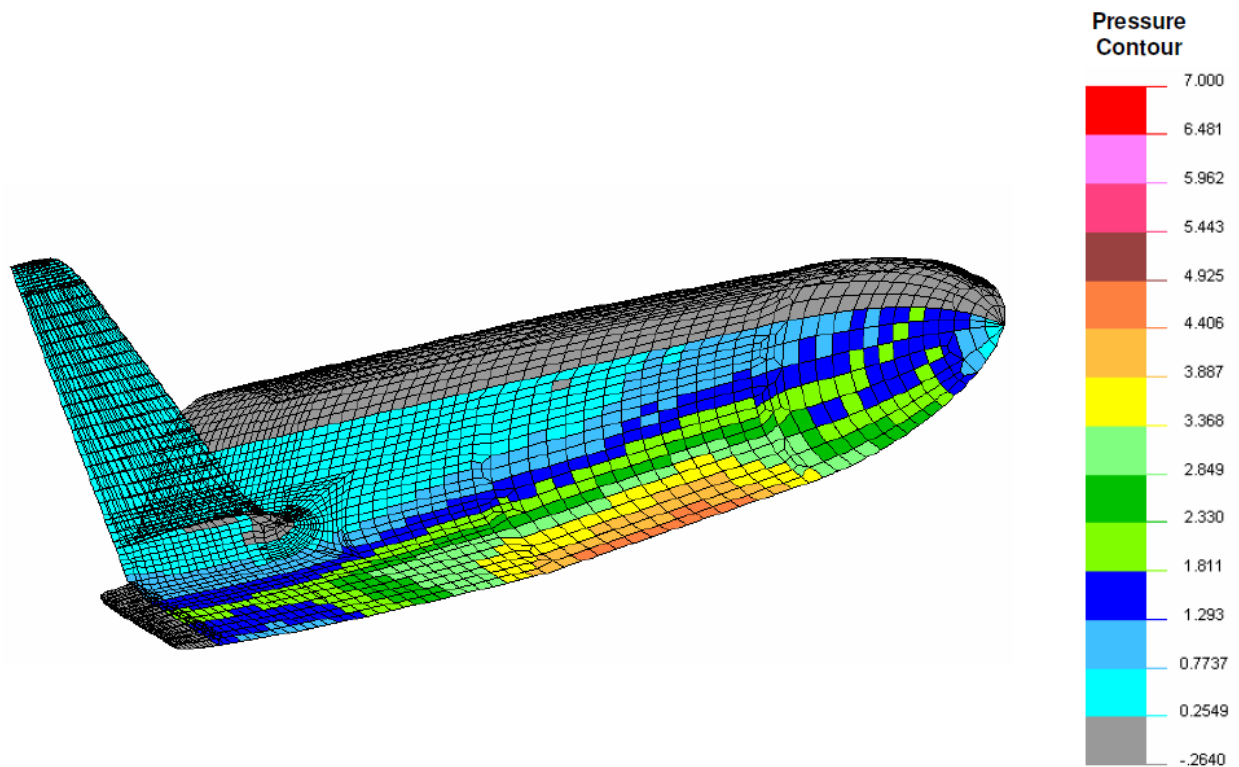


Figure B-44. Vehicle Aero Load Pressure Profile for $q=190$ psf, $M=25.0$ and $AOA=70.0$
(Pressure loads shown include an additional 1.5 increase for safety margin.)

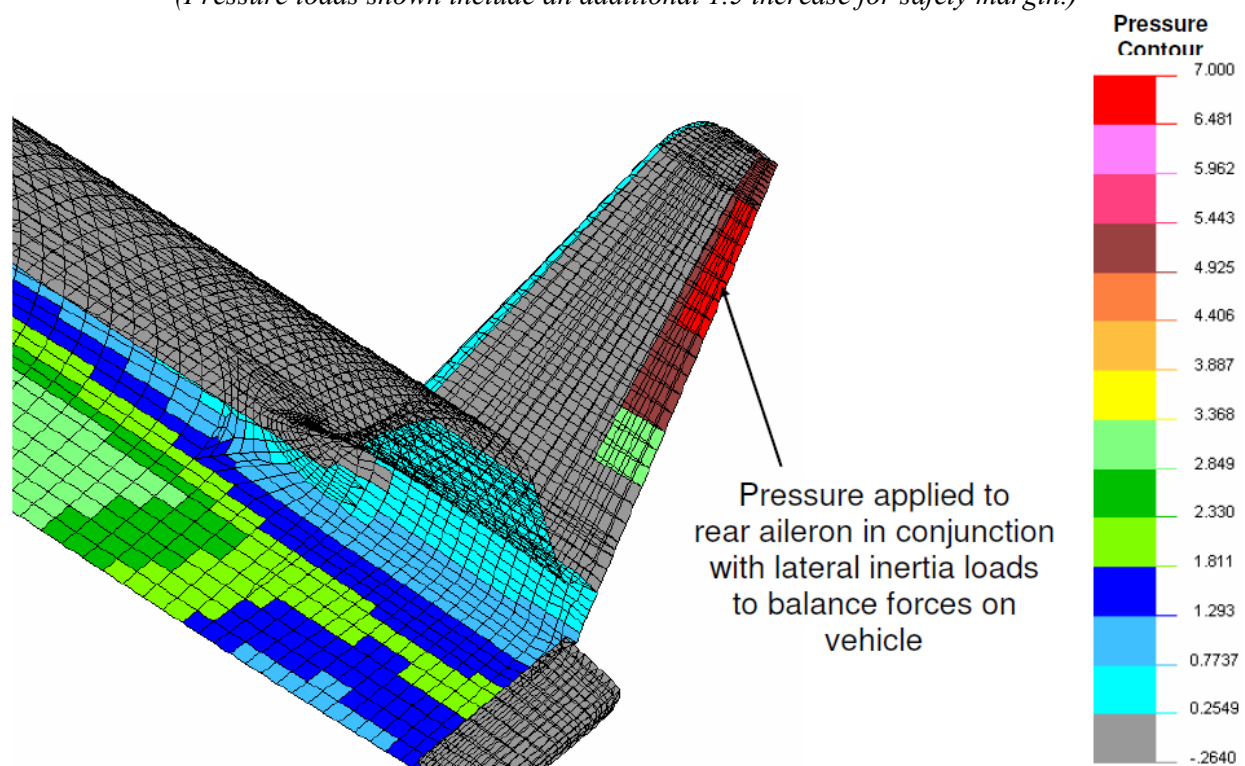


Figure B-45. Vehicle Aero Load Pressure Profile for $q=190$ psf, $M=25.0$ and $AOA=70.0$
(Pressure loads shown include an additional 1.5 increase for safety margin.)

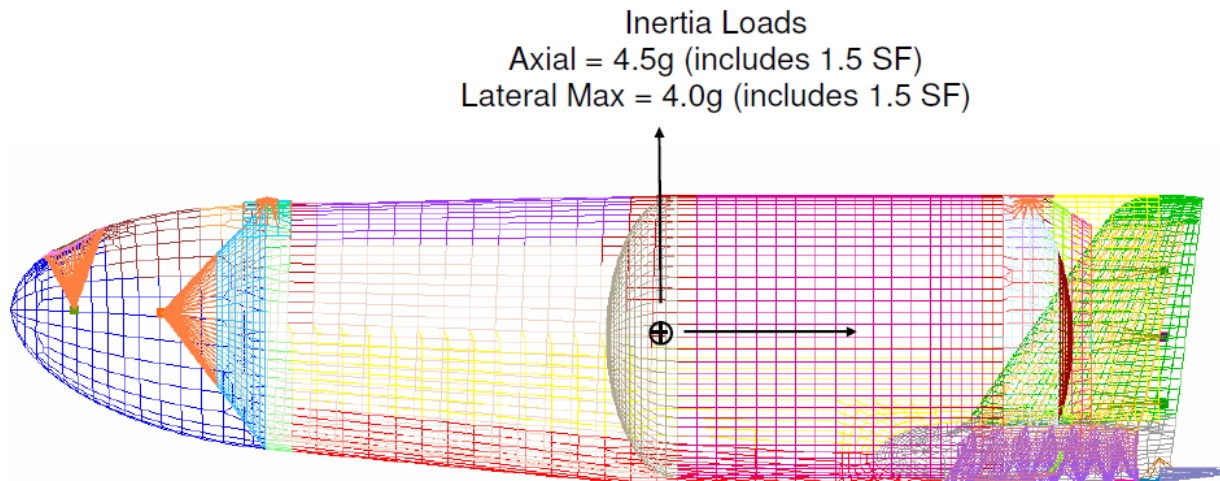


Figure B-46. Boundary Conditions on Model for Re-entry Loads Analysis

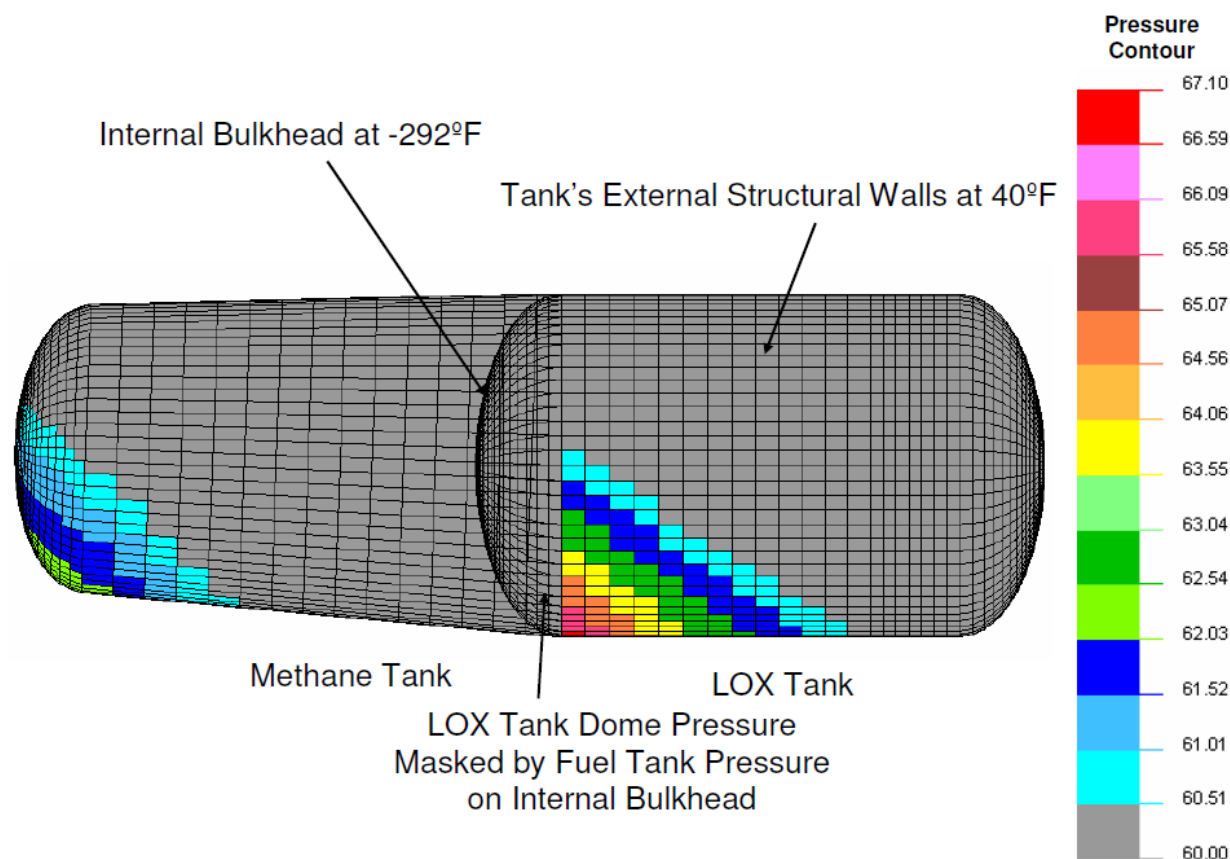


Figure B-47. Pressure Profile in Propellant Tanks
 (Pressure loads shown include an additional 1.5 increase for safety margins.)

Figures B-48 through B-54 show results of the analysis. Figures B-48 and B-49 are deformed geometry plots of the vehicle. Figure B-49 is showing a large downward deflection of the wing (2.6 inches). This is a result of the pressure applied to the wings aileron to counteract the large aero force wanting to pitch the vehicle down.

Figure B-50 is a resultant displacement contour plot of the vehicle for 1.5 times applied loads. Maximum deflection is occurring at the wing tip, which is expected.

Figures B-51 through B-54 show the Tsai-Wu stress survey plots of the composite structures. With a 1.5 times applied launch loads all composite structures are showing positive margins.

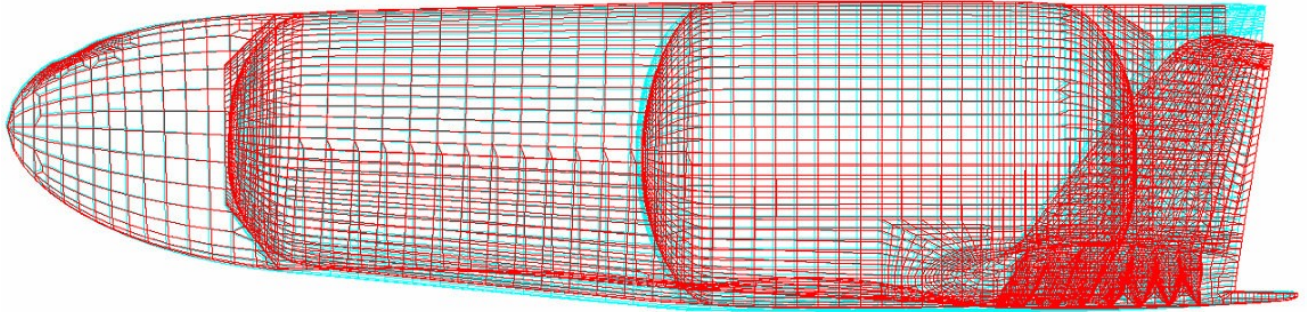


Figure B-48. Deformed Geometry Plot of the Vehicle for Re-entry Loads

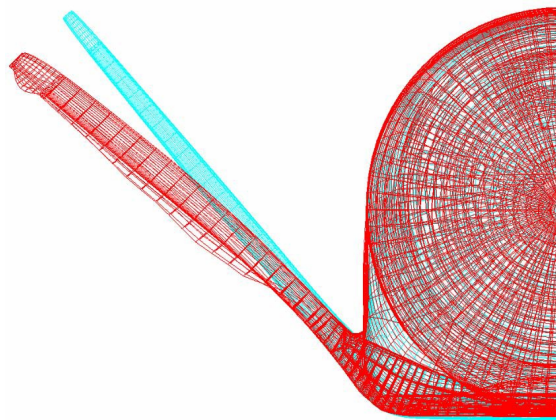


Figure B-49. Deformed Geometry Plot of the Vehicle's Wing for Re-entry Loads

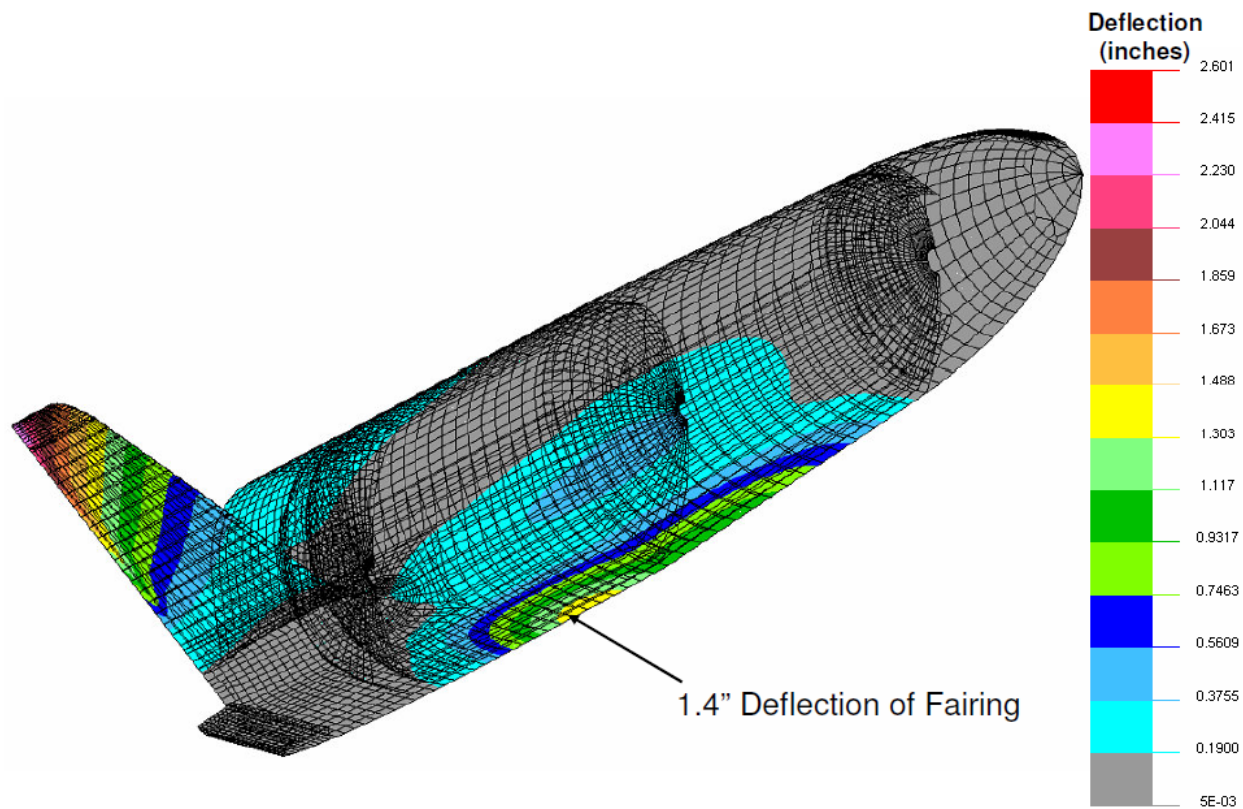


Figure B-50. Resultant Displacement Contour Plot for Re-entry Loads

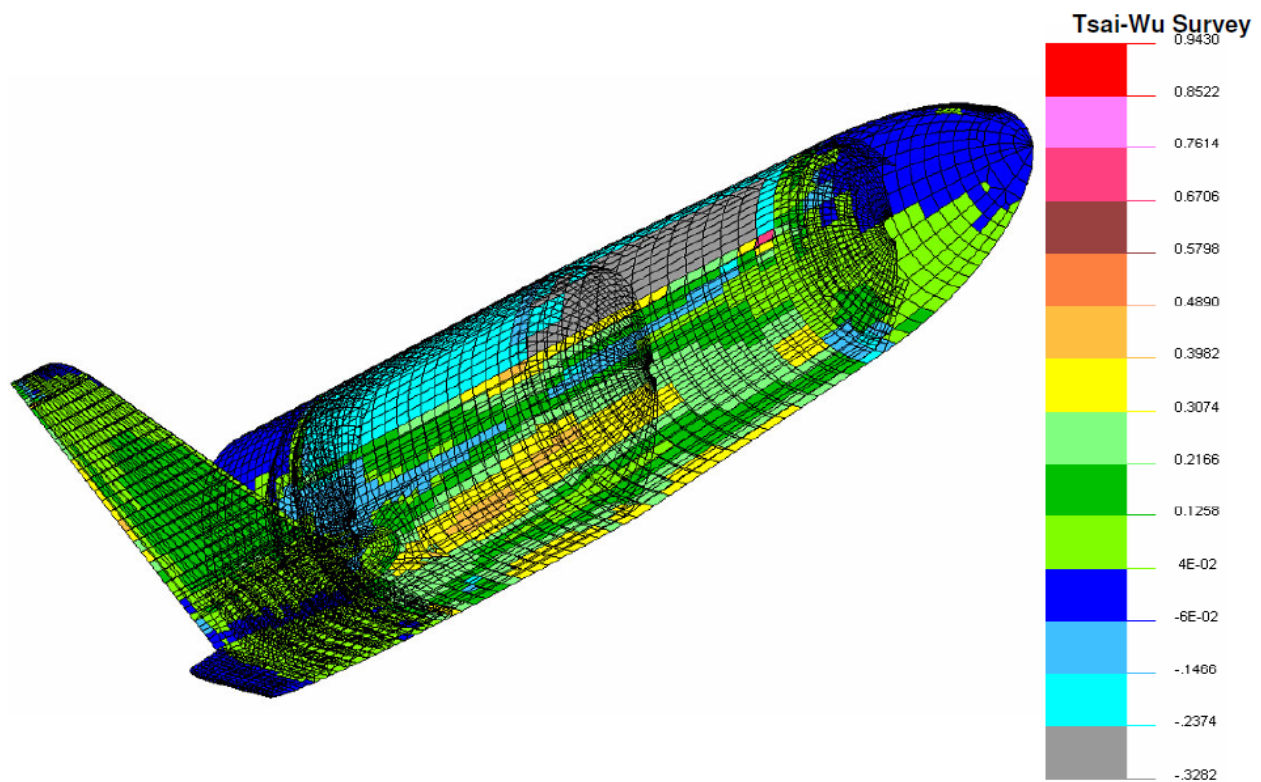


Figure B-51. Tsai-Wu Stress Survey of the Vehicle's Composite Structures for Re-entry

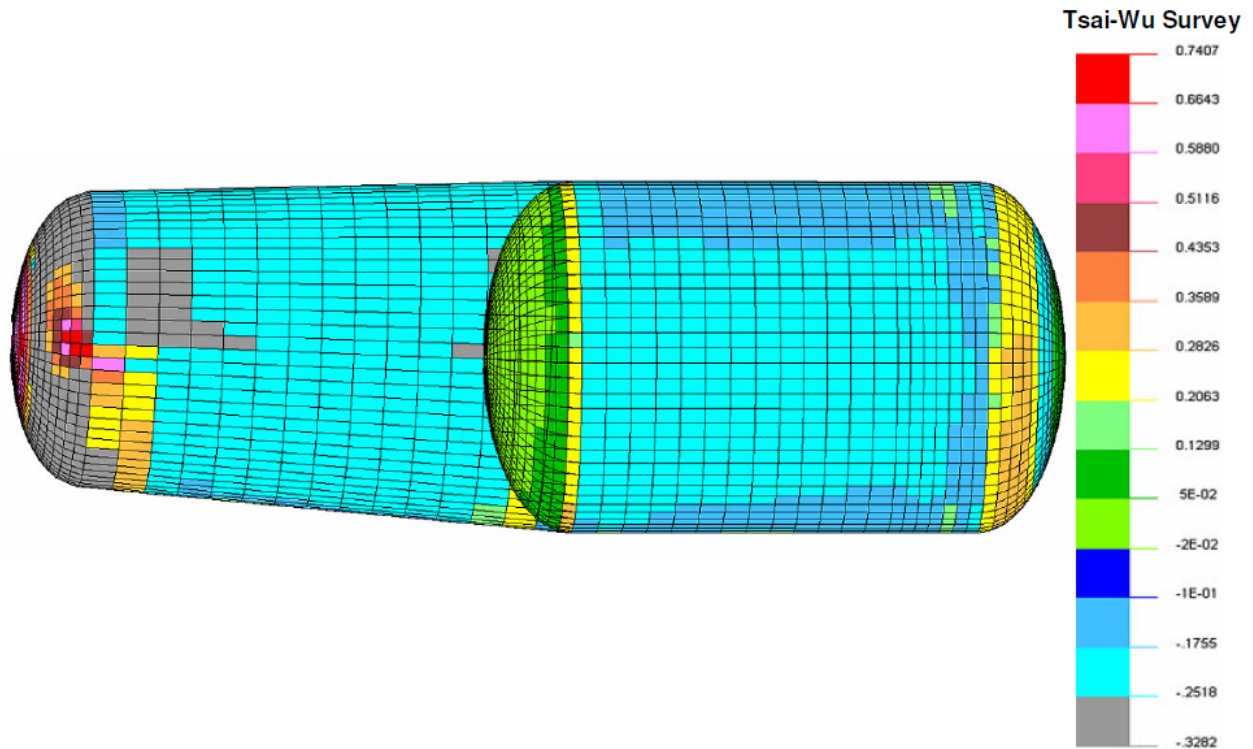


Figure B-52. Tsai-Wu Stress Survey of the Vehicle's Composite Structures for Re-entry Loads

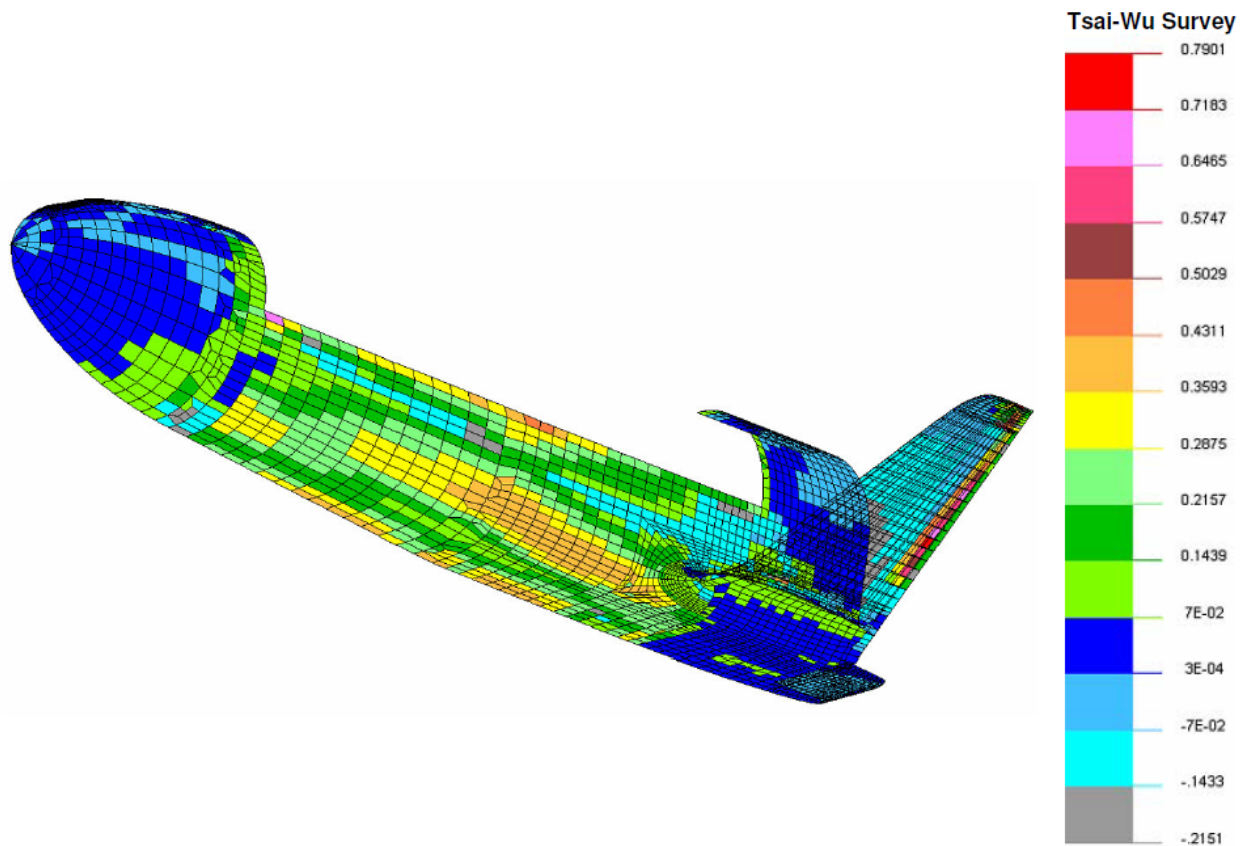


Figure B-53. Tsai-Wu Stress Survey of the Vehicle's Composite Structures for Re-entry Loads

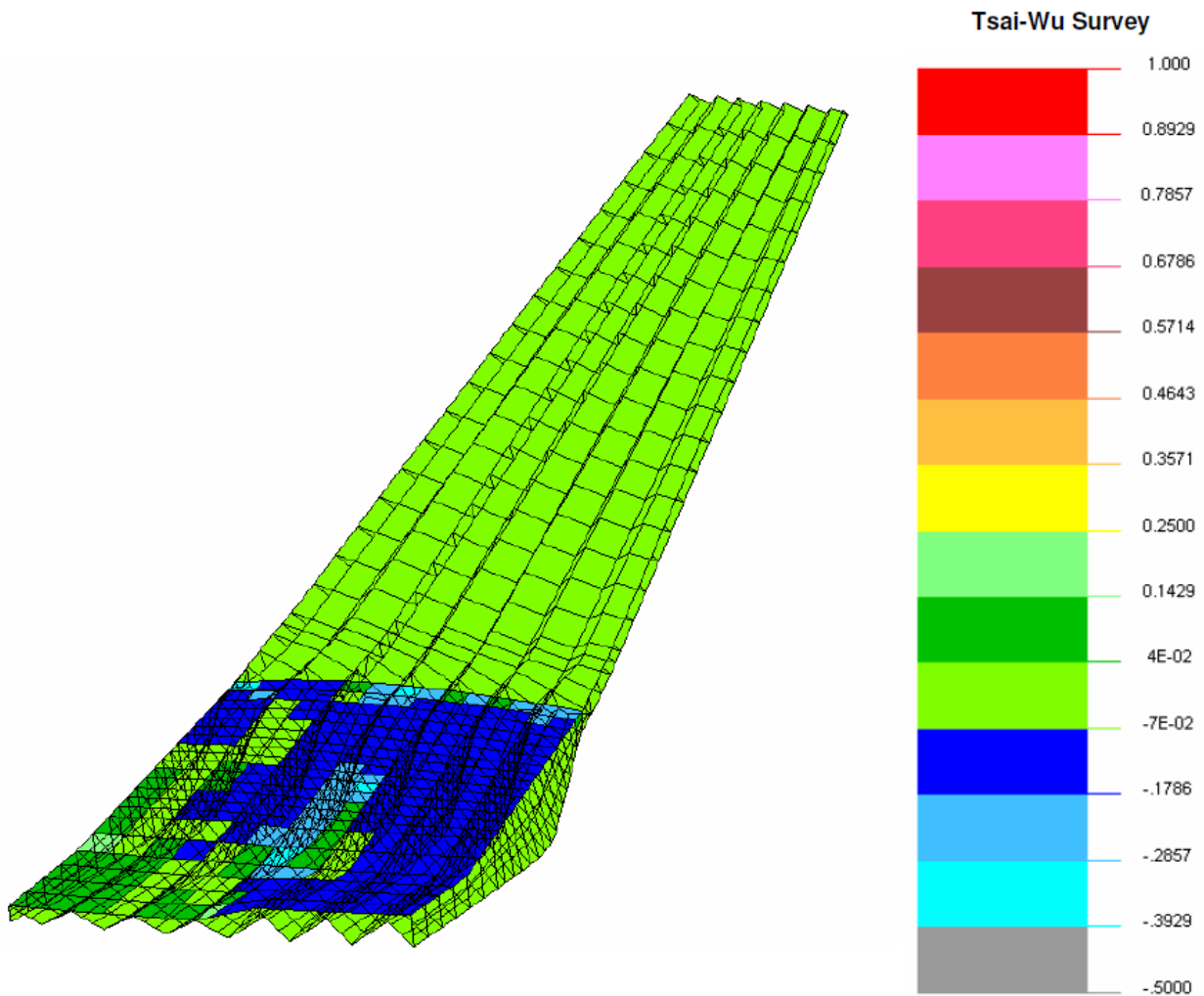


Figure B-54. Tsai-Wu Stress Survey of the Vehicle's Wing Waffle and Wing Carry-through Section

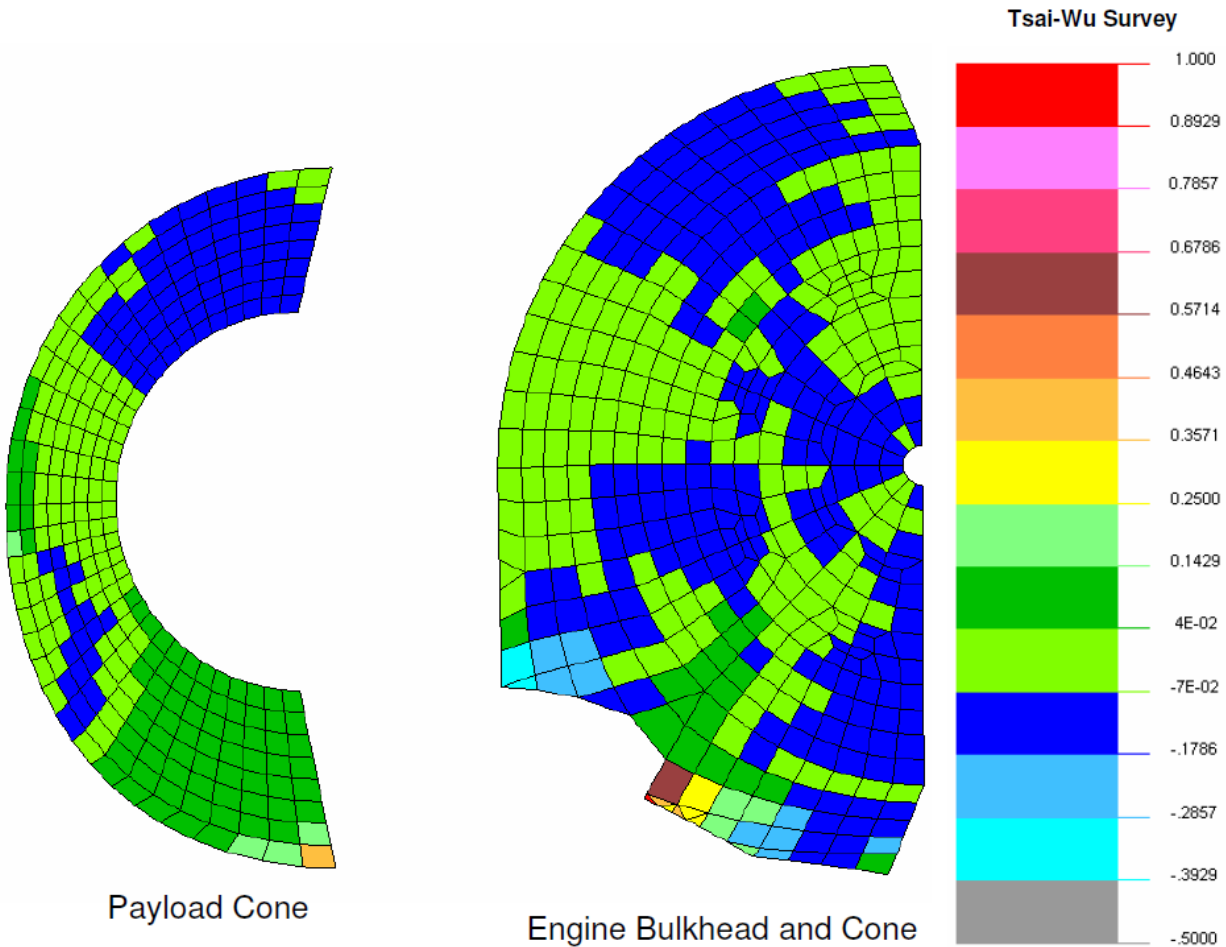


Figure B-55. Tsai-Wu Stress Survey of the Vehicle's Wing Waffle and Wing Carry-through Section

B4.3.6 Chute Deployment Load Case

After reentry the vehicle deploys a parachute to position the vehicle for firing its engines to slow its descent. The maximum force the chute imparts on the vehicle is 5,000 lbf. For this analysis it is assumed that the chute deploys and produces a maximum force on the vehicle at a 30-degree angle to the vehicle's centerline. To account for a 1.5 safety factor and only half the vehicle modeled, the applied force is 3,750 lbf. Figure B-56 illustrates the loads and boundary conditions on the vehicle.

Figure B-47 shows loads on the propellant tank. A 20% propellant load is assumed.

To restrict rigid body motion this analysis was conducted in the same iterative manner that the re-entry load case was done. Two nodes were constrained in the model in the same manner as previous.

However the nodes were positioned in the mid and aft section of the vehicle. Intent was to stay away from the nosecone area and not skew results. With the nodes constrained, inertia loads, including rotational, were applied about the vehicle's c.g. to react against the chute forces. The rotational inertia load was iterated until the two constrained nodes' reaction forces were <100

lbf. This analysis methodology actually simulates the large rotational inertia forces the vehicle would see during chute deployment.

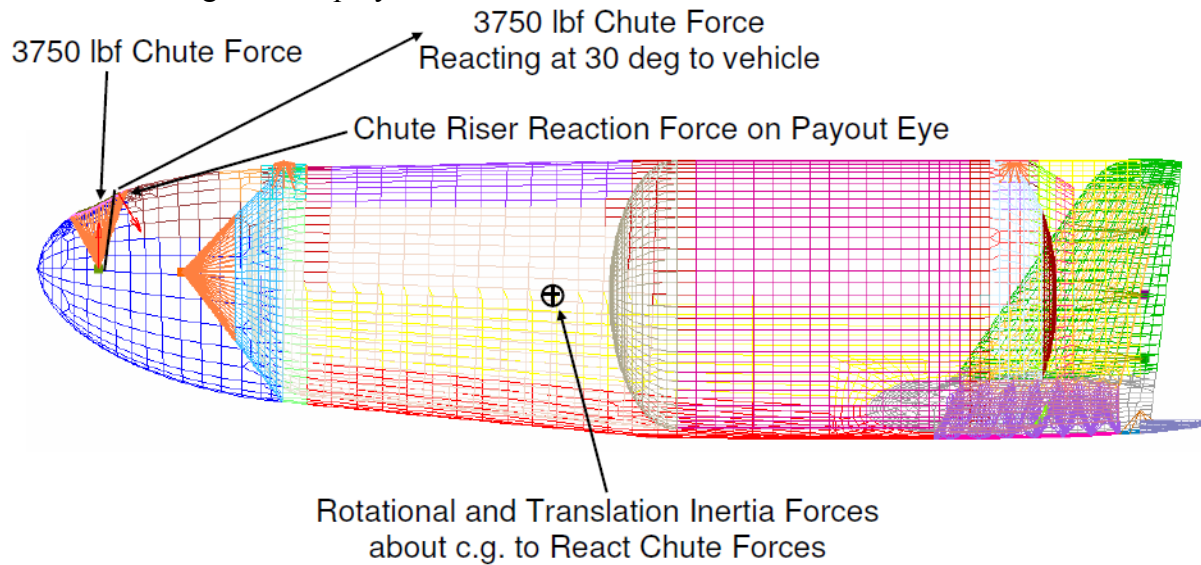


Figure B-56. Chute Deployment Force Applied to the FEM

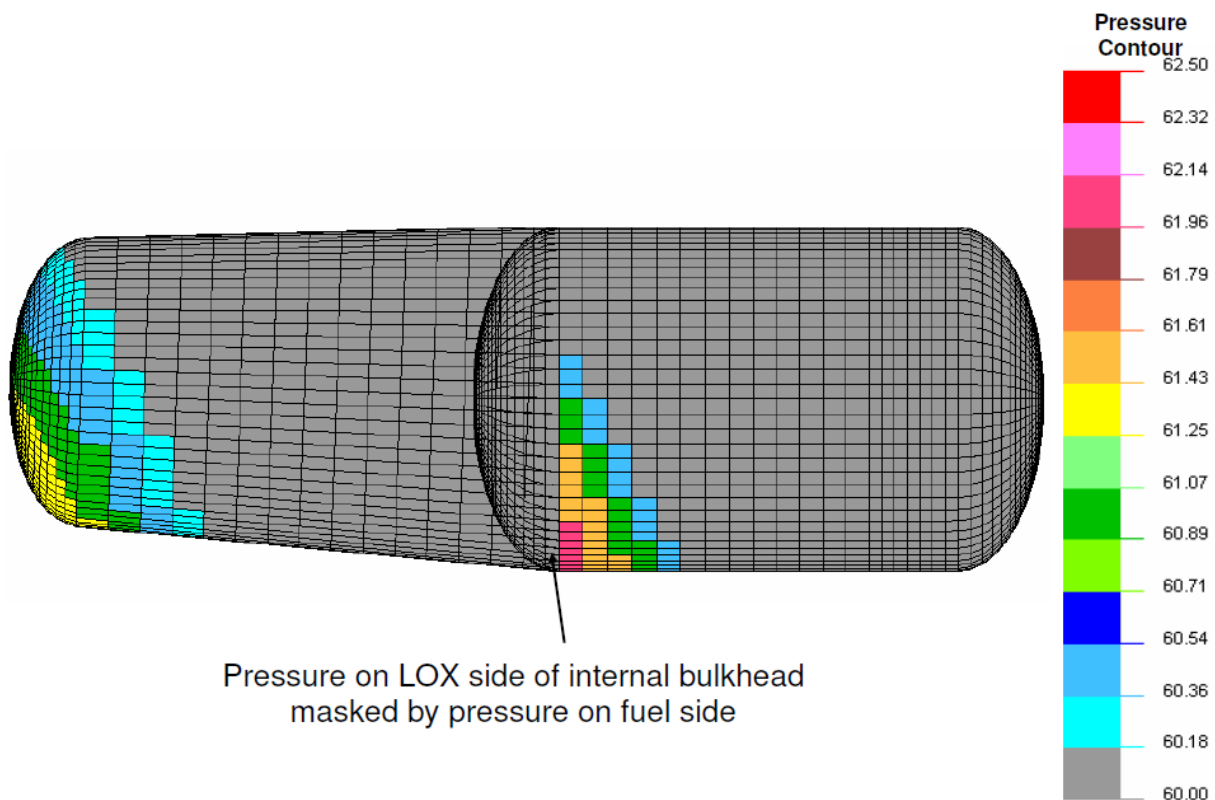


Figure B-57. Pressure Profile in Propellant Tanks
(Pressure loads shown include an additional 1.5 increase for safety margin.)

Figures B-58 through B-61 show results of the analysis. Figures B-58 and B-59 are deformed geometry resultant displacement plots of the vehicle.

Figures B-60 and B-61 show the Tsai-Wu stress survey plots of the composite structures and nose cone. With a 1.5 times applied launch loads all composite structures are showing positive margins.

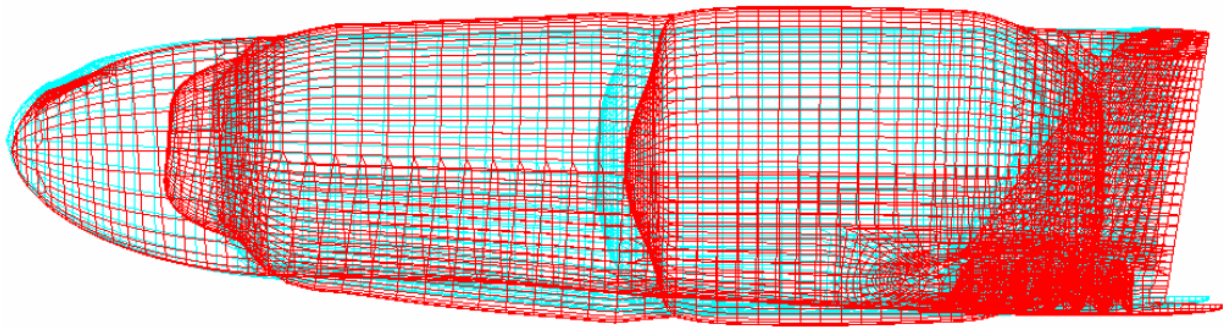


Figure B-58. Deformed Geometry Plot of the Vehicle during Chute Deployment

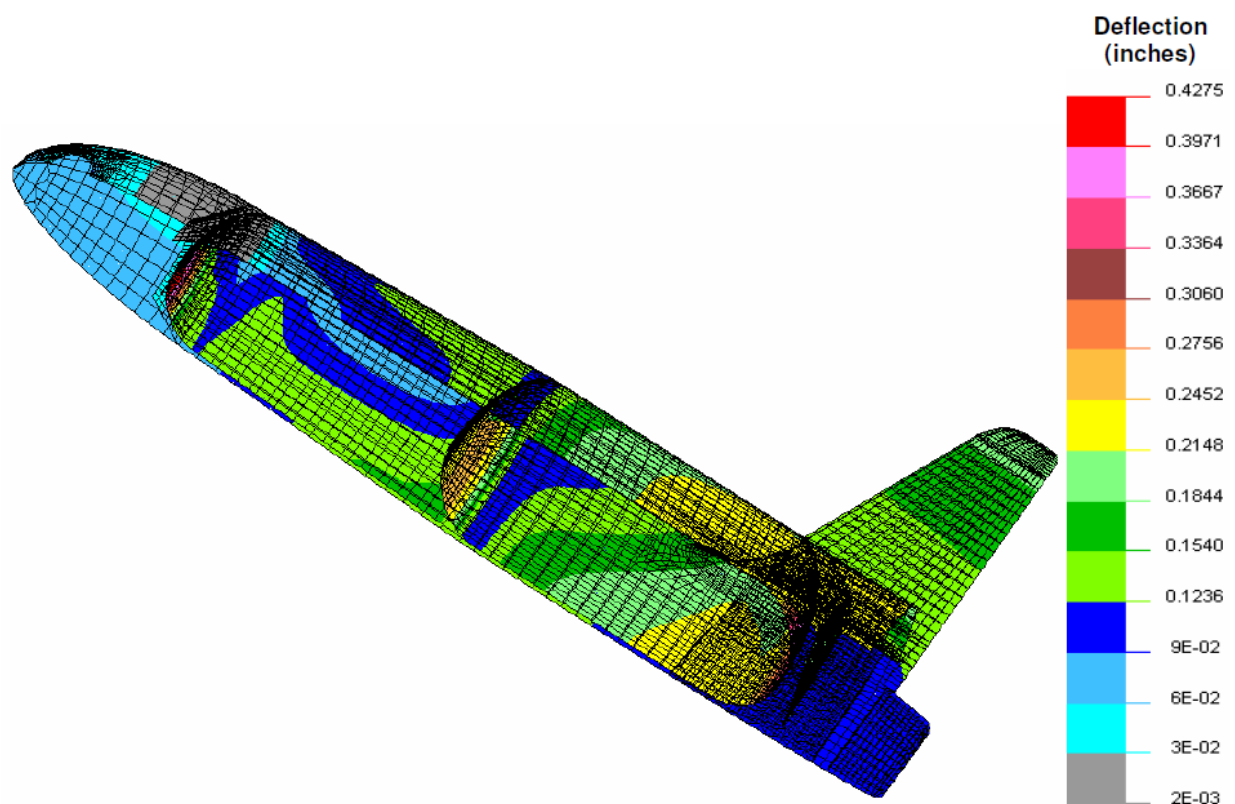


Figure B-59. Resultant Displacement Contour Plot of the Vehicle during Chute Deployment

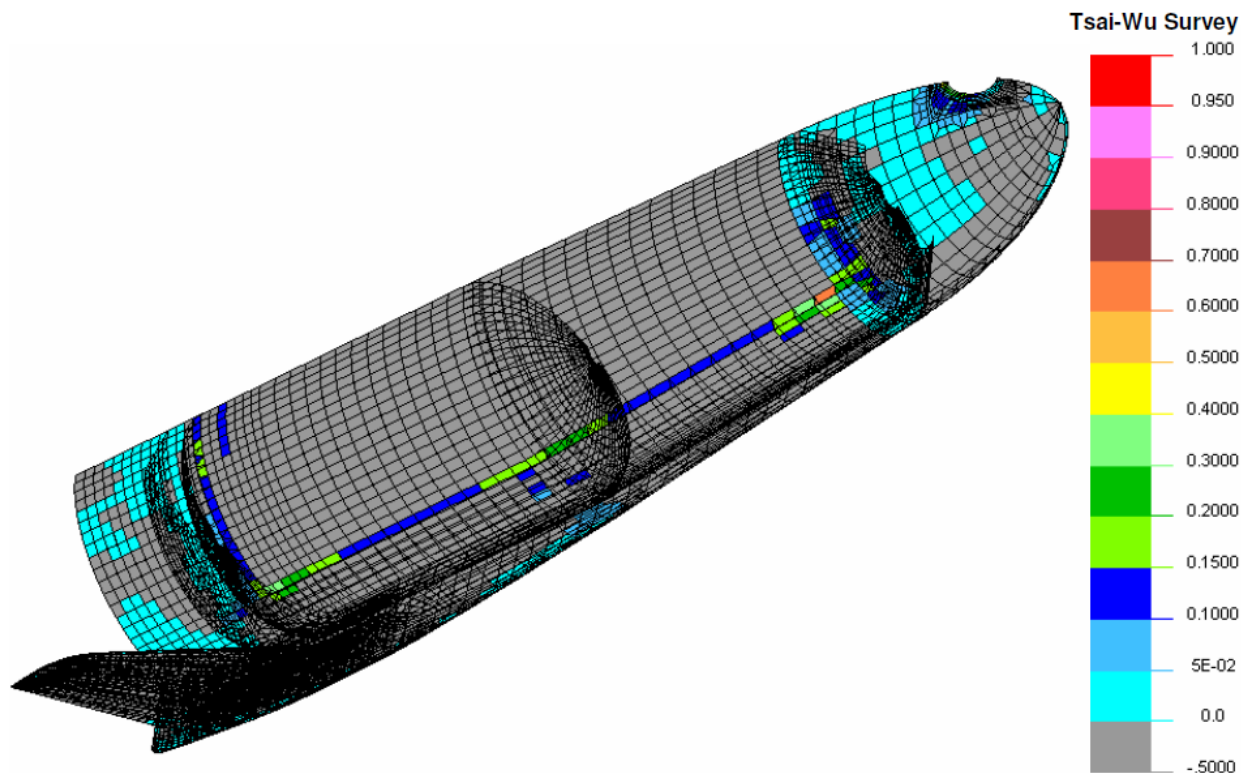


Figure B-60. Tsai-Wu Stress Survey of Vehicle's Composite Structures during Chute Deployment

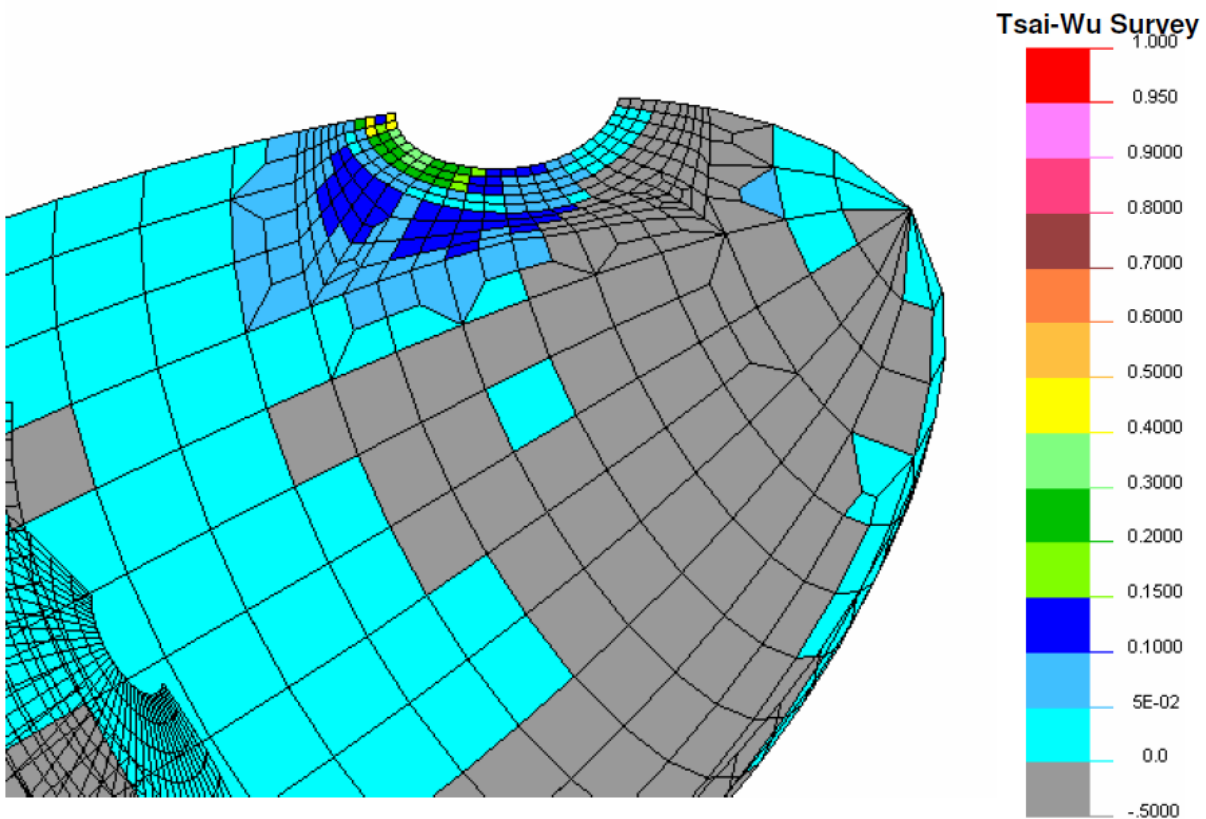


Figure B-61. Tsai-Wu Stress Survey Plot of the Nosecone during Chute Deployment

B4.3.7 Vehicle Landing Load Case

The vehicle is designed for a vertical landing. Prior to touching down, four gear legs are deployed. These legs are designed as a spring/damper system. To minimize the responsive g loads the system uses a substantial amount of deflection and undamped compression to store the vehicle's kinetic energy, Figure B-62. The stored energy is then released by damped tension using unidirectional shock absorbers. Construction of the legs is 6061-T6 4.0 x 4.0 x 0.375 rectangular structural tubing (sized by this analysis).

Assumptions for the design are:

- 10,100 lbf vehicle weight at landing (2,525 lbf per leg) Spring $k=17,500$ lbf/in
- Damper $c=1.0E6$ lbf-s/in in extension only Load is evenly distributed between all four legs
- Conceptual geometry only – revision for packaging/deployment is likely

Results of the dynamic analysis of the vehicle's velocity and deceleration are shown in Figure B-63. Leg loading as a function of time is shown in Figure B-64. Summary of the landing loads on each leg system are a maximum 5950 lbf (2525 lbf per leg weight) and a maximum bending moment in-plane with the leg of 203,800 in-lbf (this assumes vehicle attachment is above the actuator upper pivot). In landing, the legs will deflect 18 inches. Results show oscillations are well damped and g levels kept within reason.

A calculated max bending moment in the aluminum tube at the actuator attach of 142,800 in-lbf produces a safety factor of 1.52 against yield. A substantial safety factor is warranted at this stage.

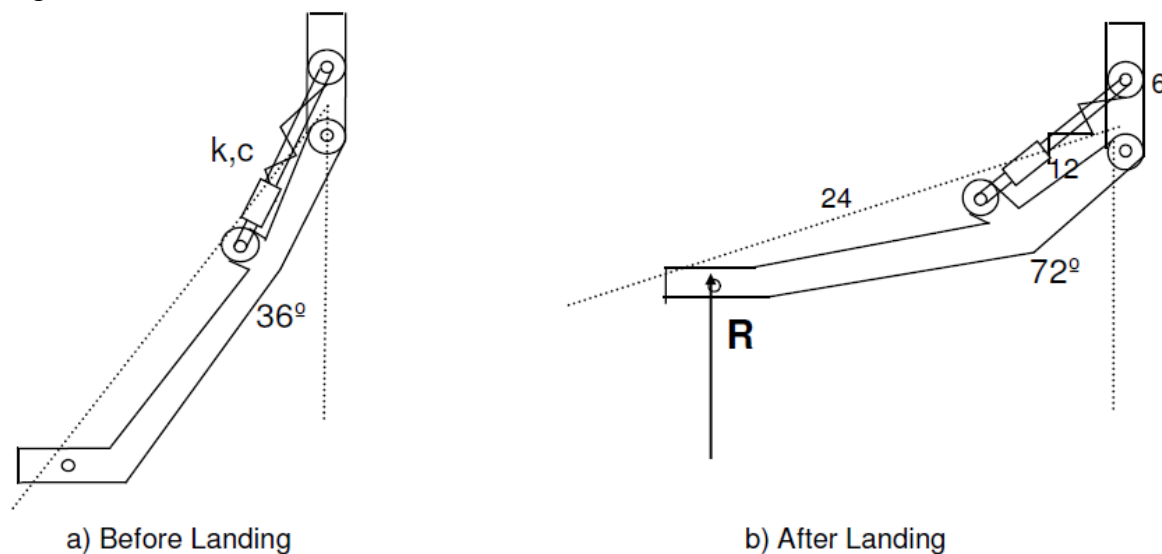


Figure B-62. Landing Gear Geometry during Landing

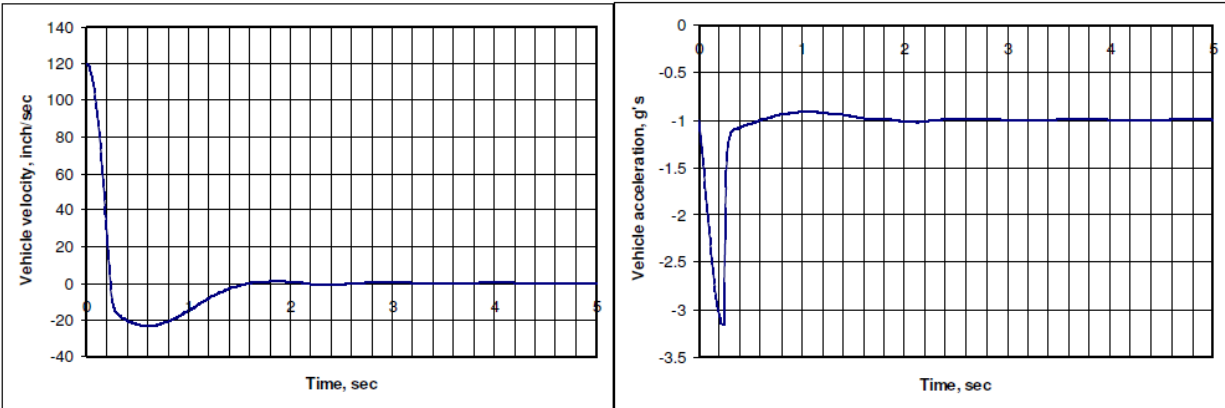


Figure B-63. Vehicle Velocity and Acceleration Profiles during Landing

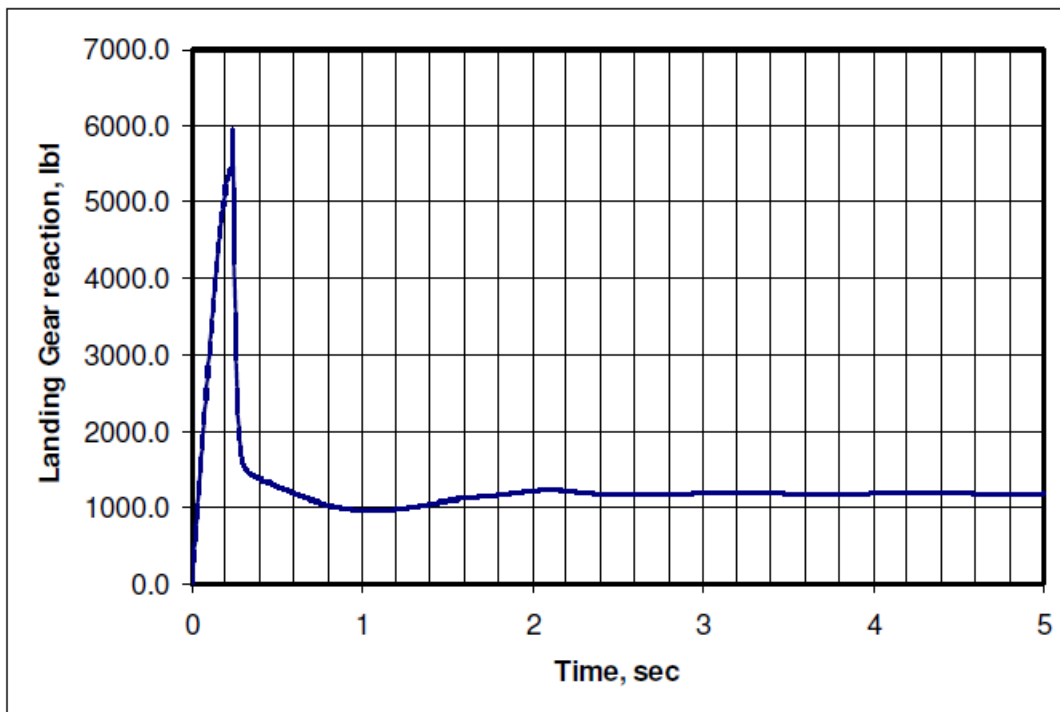


Figure B-64. Reaction Force on Landing Gear during Landing

Results of the localized leg analysis are then used as an applied load in the vehicle's finite element model. Figure B-65 shows the assumed position for mounting of the landing legs. Figure B-66 shows that for the applied leg loads on the skirt it will rotate out a maximum of .30 inch.

Figures B-66 and B-67 are Tsai-Wu stress survey plots of the composite structures. All Tsai-Wu values are <1.0 showing that structural safety factors are greater than 1.5.

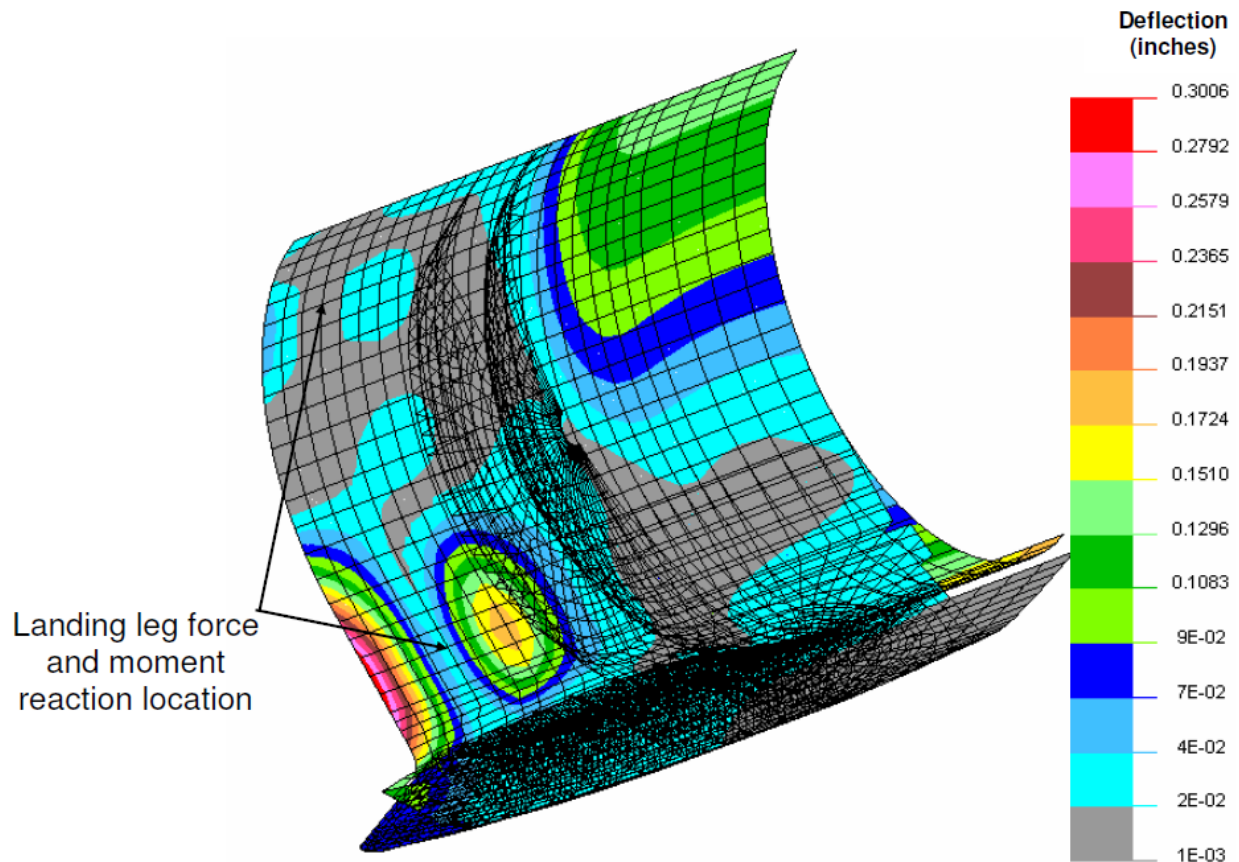


Figure B-65. Resultant Displacement Plot of the Vehicle's Aft Skirt Region for Landing Loads

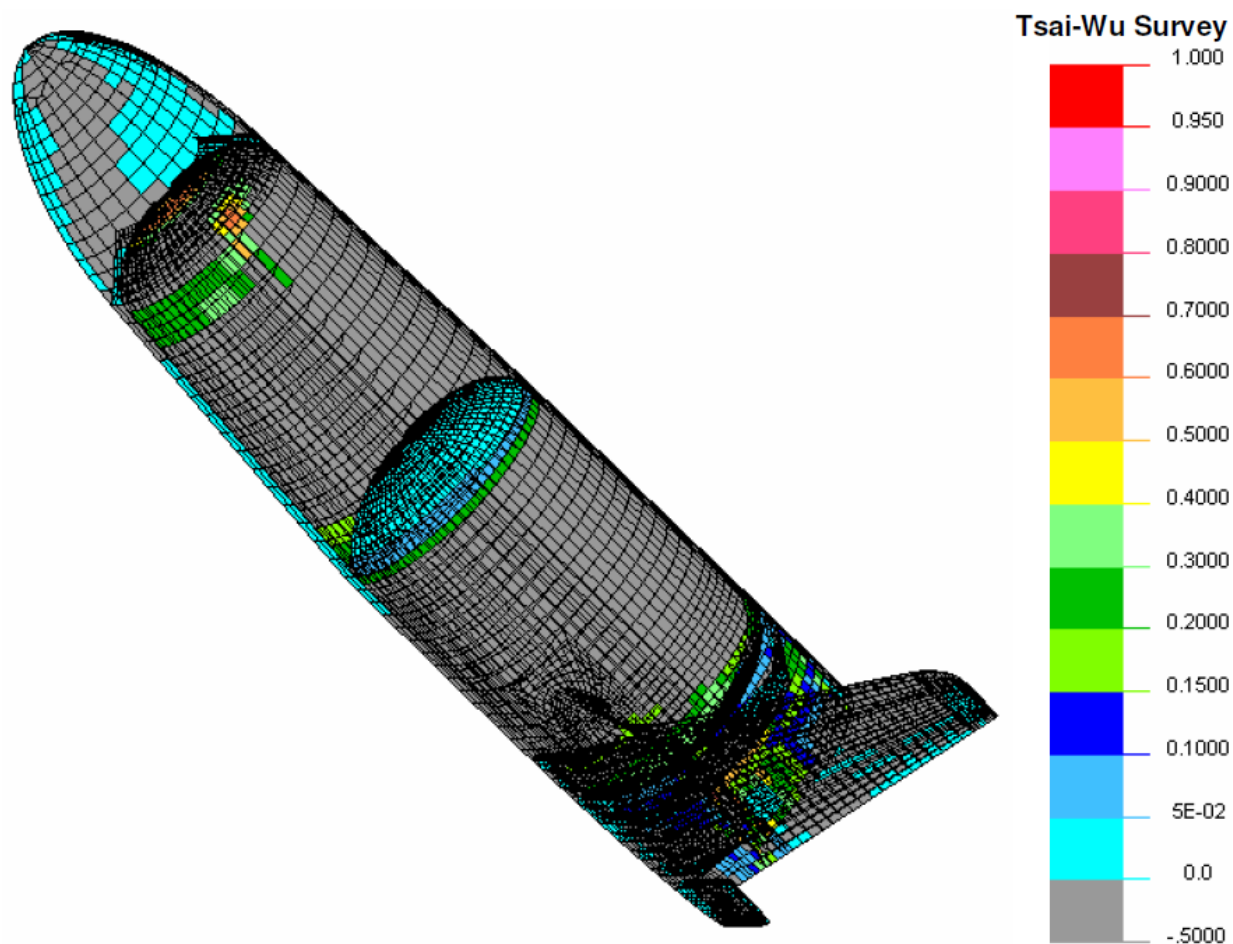


Figure B-66. Tsai-Wu Stress Survey of the Vehicle's Composite Structures during Landing

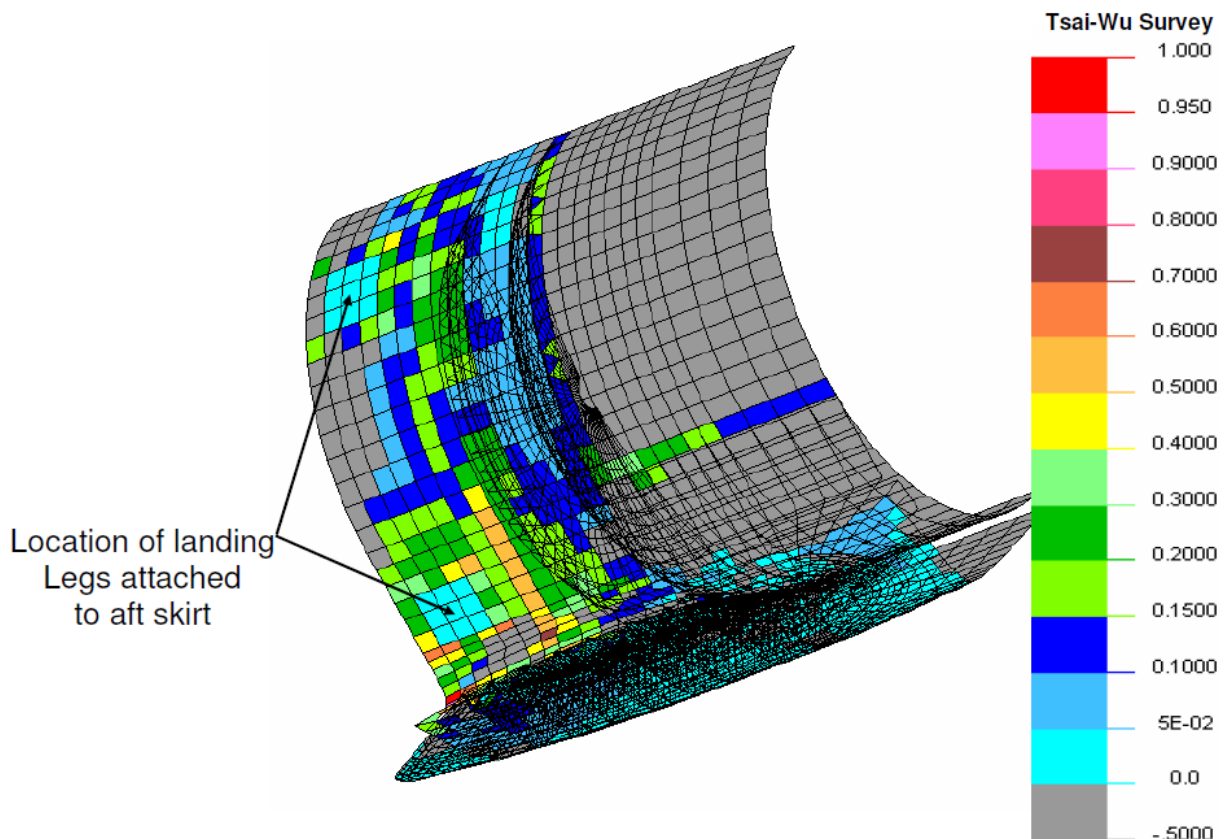


Figure B-67. Tsai-Wu Stress Survey Plot of the Vehicle's Aft Skirt Region during Landing

It should be noted that the landing loads were substantial, and reinforcement at the aft end of the fuselage, near the engine cone, was required, costing significant weight. Further optimization of load path here is warranted in detailed design, in conjunction with detailed packaging of the landing legs for deployment and stowage.

B4.3.8 Demonstration Vehicle Launch Load Case

The demonstrator launch load case assumes that HOT EAGLE is a single stage sub-orbital vehicle. Worst case structural loading on the vehicle will occur at max dynamic pressure. This analysis assumes that the pressure profile is identical to that used in the bi-mese launch case, Section B4.3.3. Summary of the loads on the vehicle for this analysis are outlined in Table B-6.

Figures B-68 through B-70 show the C_p plot from the CFD analysis and the subsequent pressure profile applied to the vehicle. Figure B-71 shows the other loads and boundary conditions applied to the model for this analysis. Figure B-72 shows loads in the propellant tanks.

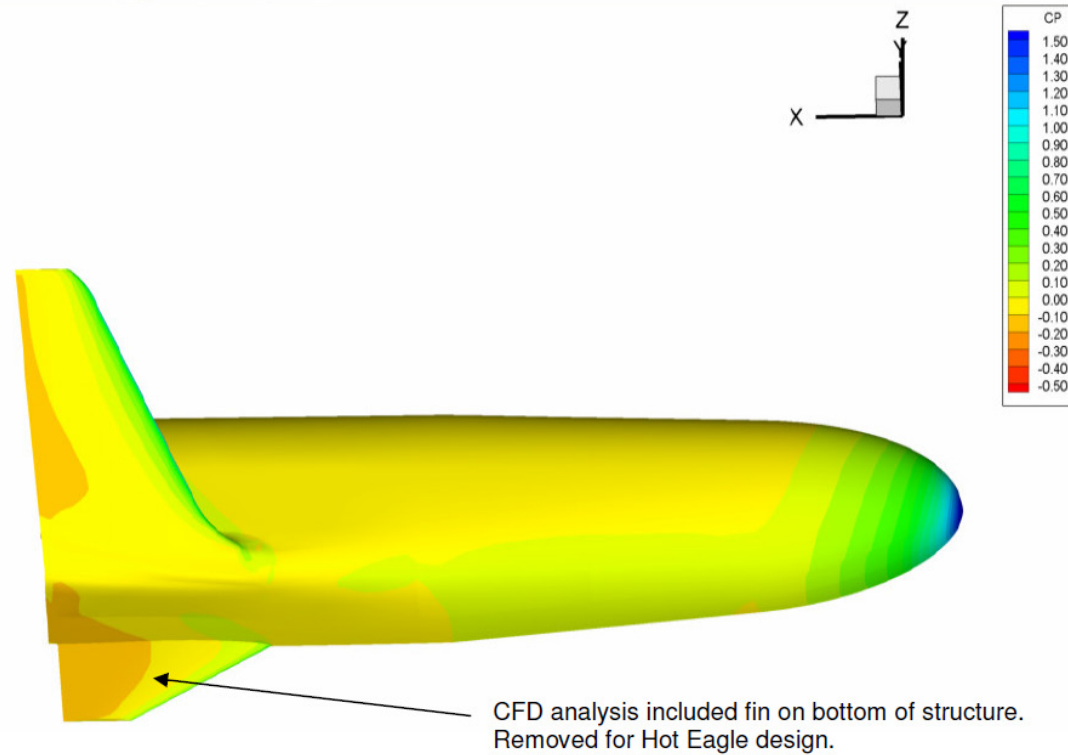


Figure B-68. Vehicle Cp Plot from CFD Analysis for $M = 2.0$ and $AOA = 2.0$

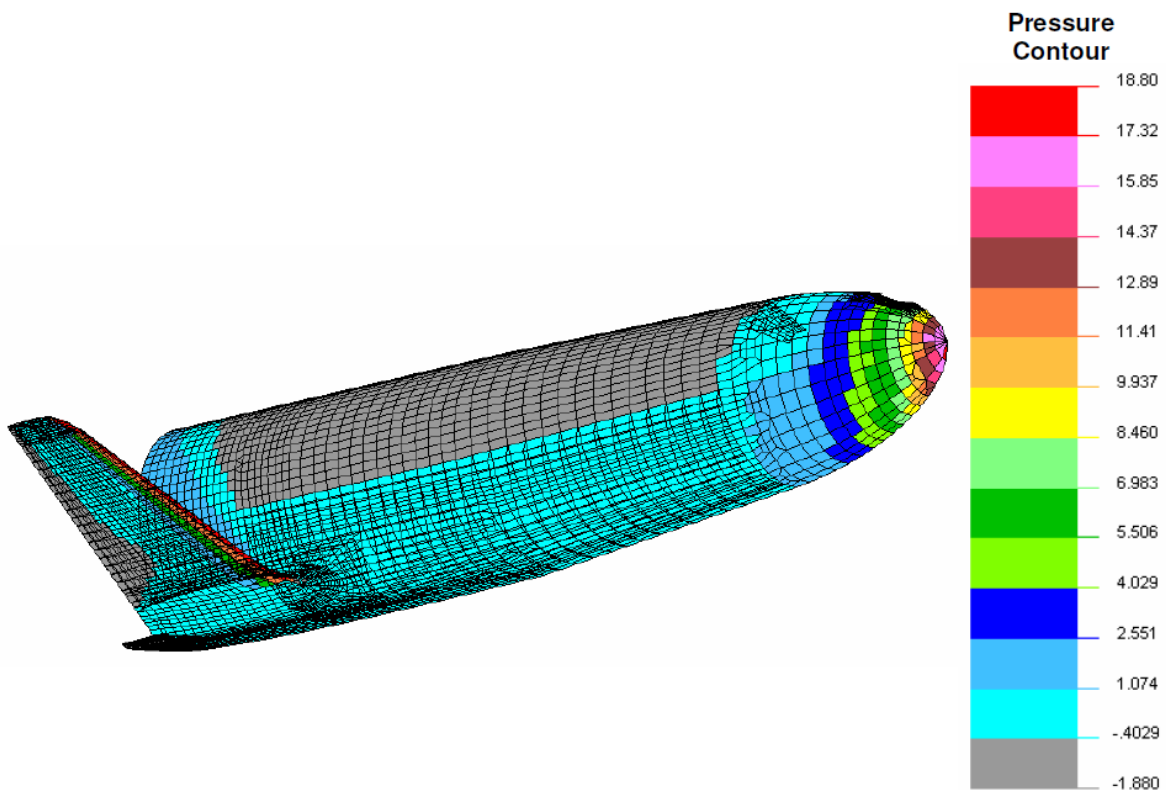
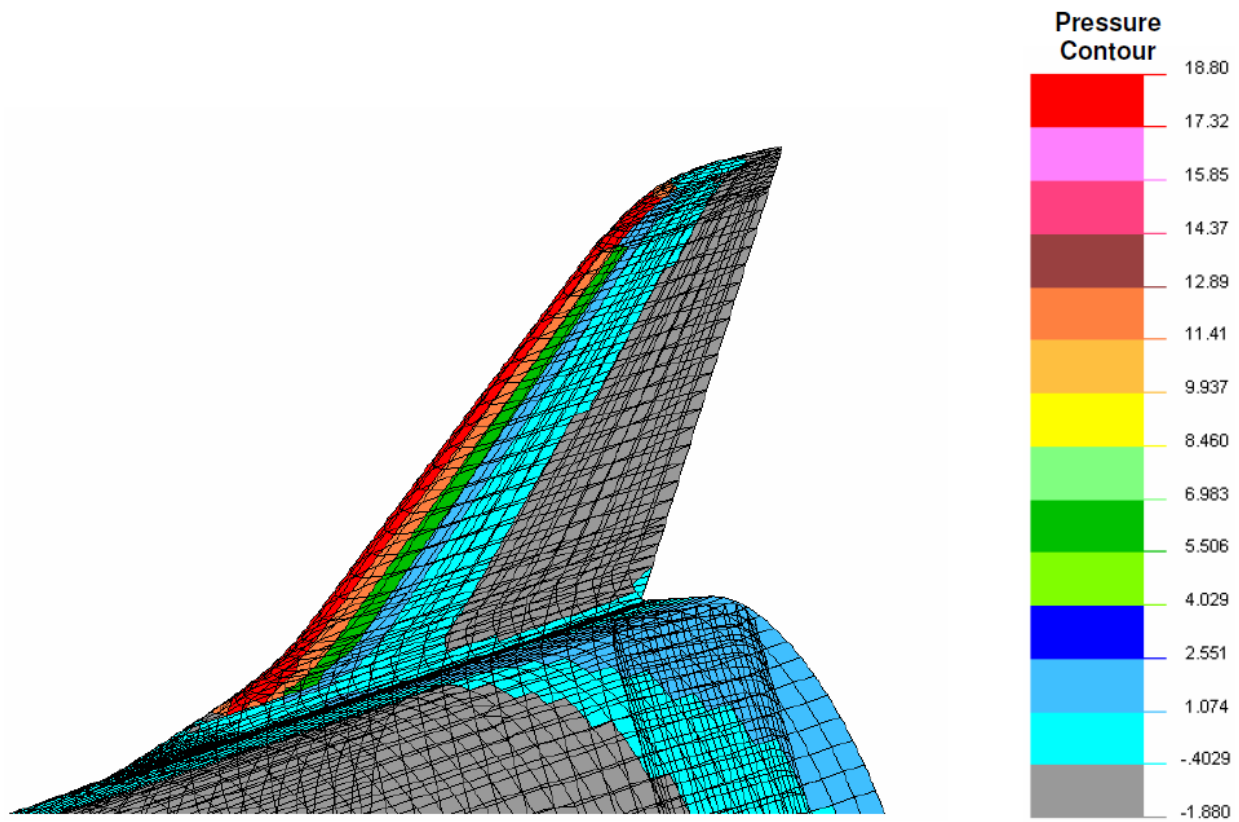


Figure B-69. Vehicle Aero Load Pressure Profile for $q=1200$ psf, $M=2.0$ and $AOA=2.0$ (Pressure loads shown include an additional 1.5 increase for safety margins.)



*Figure B-70. Aero Load Pressure Profile on Vehicle's Wing for $q=1200$ psf, $M=2.0$ and $AOA=2.0$
(Pressure loads shown include an additional 1.5 increase for safety margin.)*

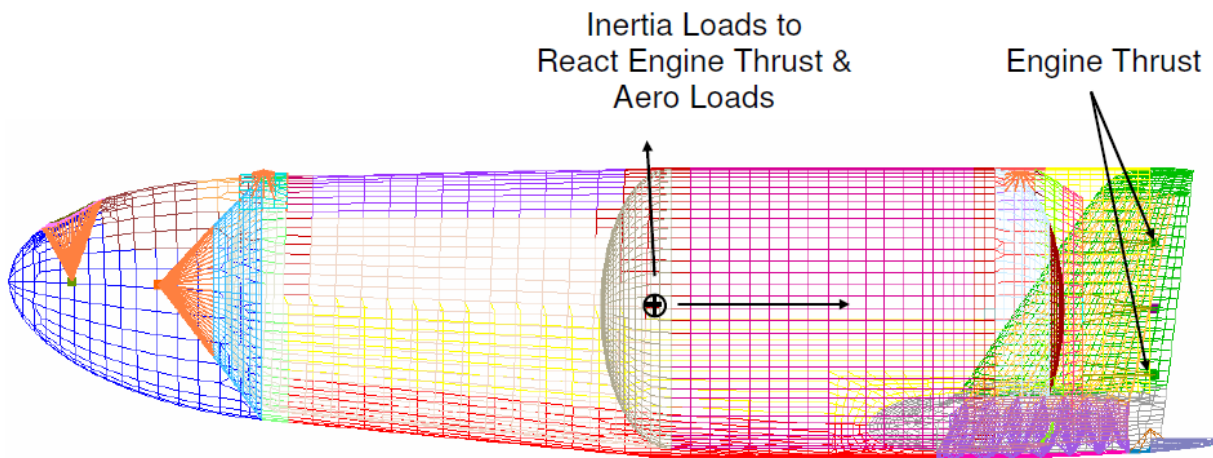
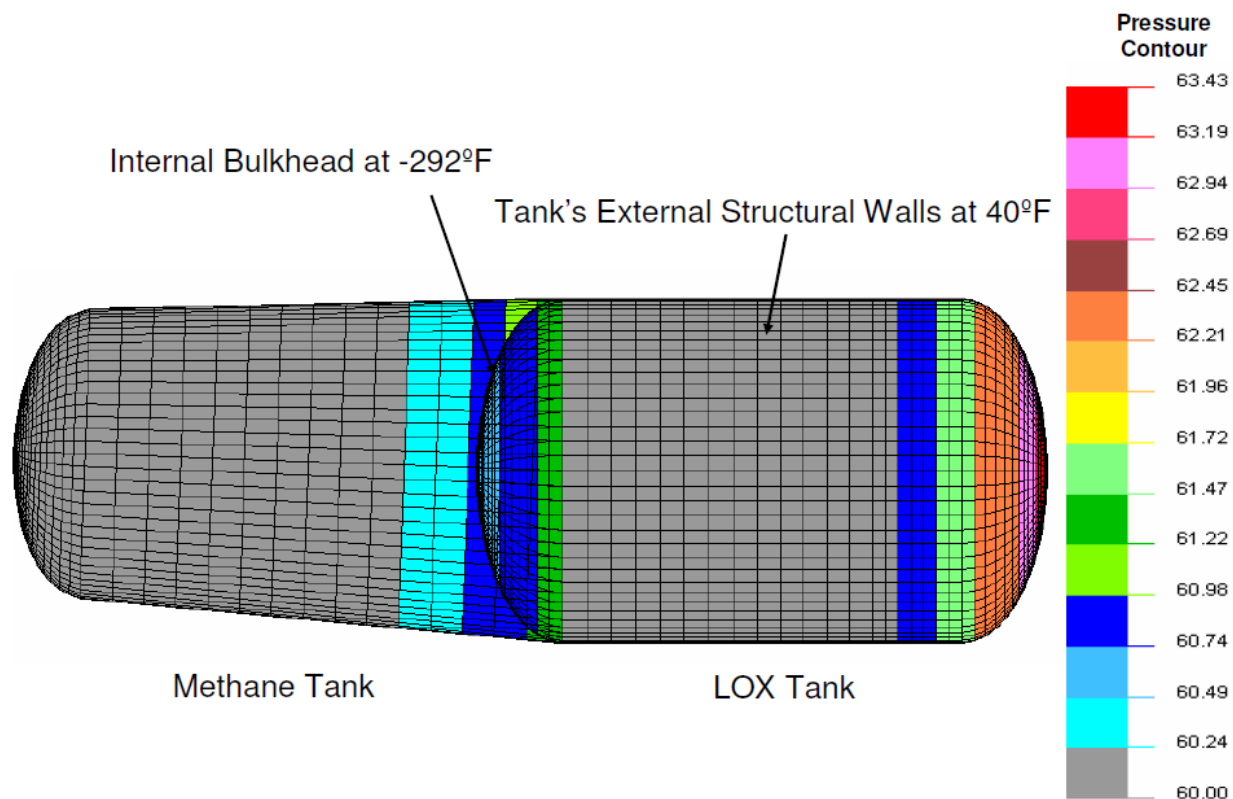


Figure B-71. Boundary Conditions and Loads on Model for Demonstrator Launch Loads Analysis



*Figure B-72. Pressure Profile in Propellant Tanks
(Pressure loads shown include an additional 1.5 increase for safety margins.)*

Figures B-73 through B-81 show results of the analysis. Figures B-73 and B-74 are deformed geometry and resultant displacement plots of the vehicle. Figure B-75 is a resultant displacement plot of the engine support structure. With all engines on, the center of the bulkhead can deflect up to 0.5 inch.

Figures B-76 through B-81 show the Tsai-Wu stress survey plots of the composite structures. With a 1.5 times factor on applied launch loads, all composite structures are showing positive margins. Note that the engine bulkhead panel is designed near-optimal for all engines firing.

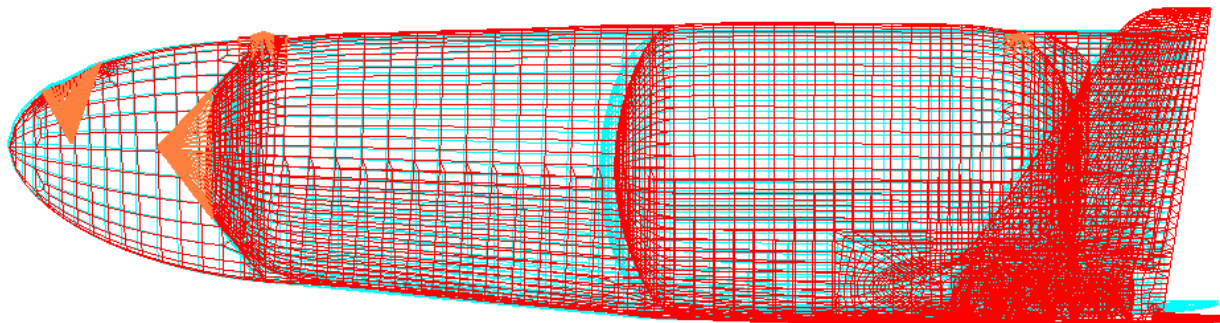


Figure B-73. Deformed Geometry Plot of the Vehicle for Demonstrator Launch

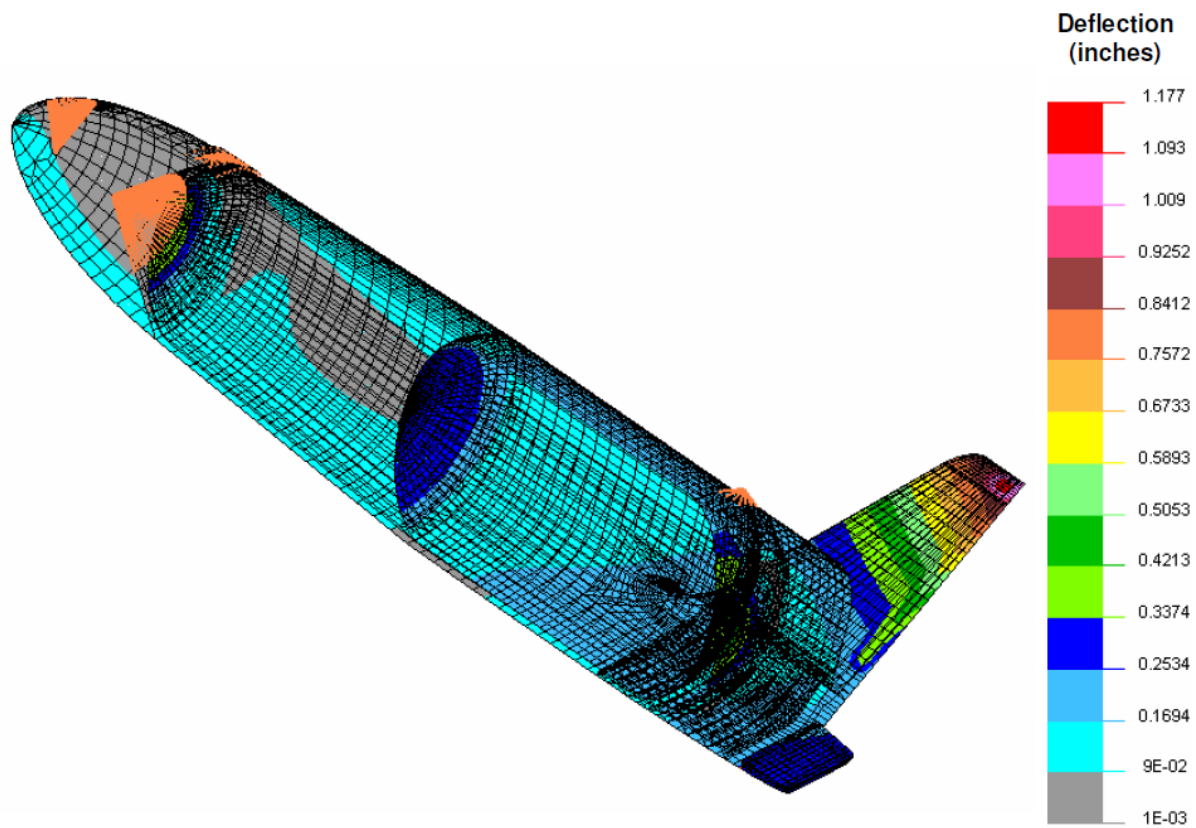


Figure B-74. Resultant Displacement Contour Plot of the Vehicle for Demonstrator Launch

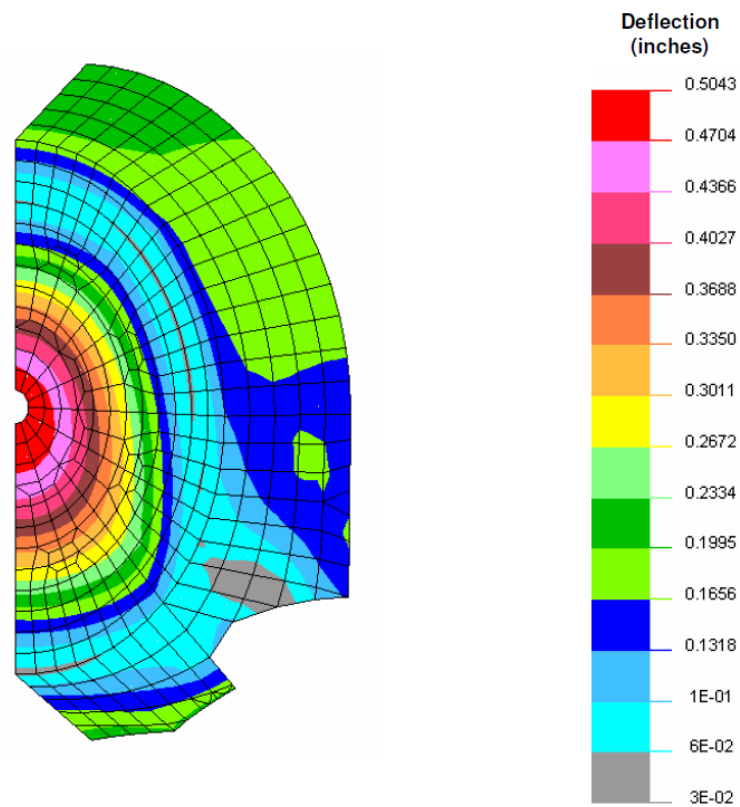


Figure B-75. Deflection Contour Plot of Engine Support Structure for the Demonstrator Launch

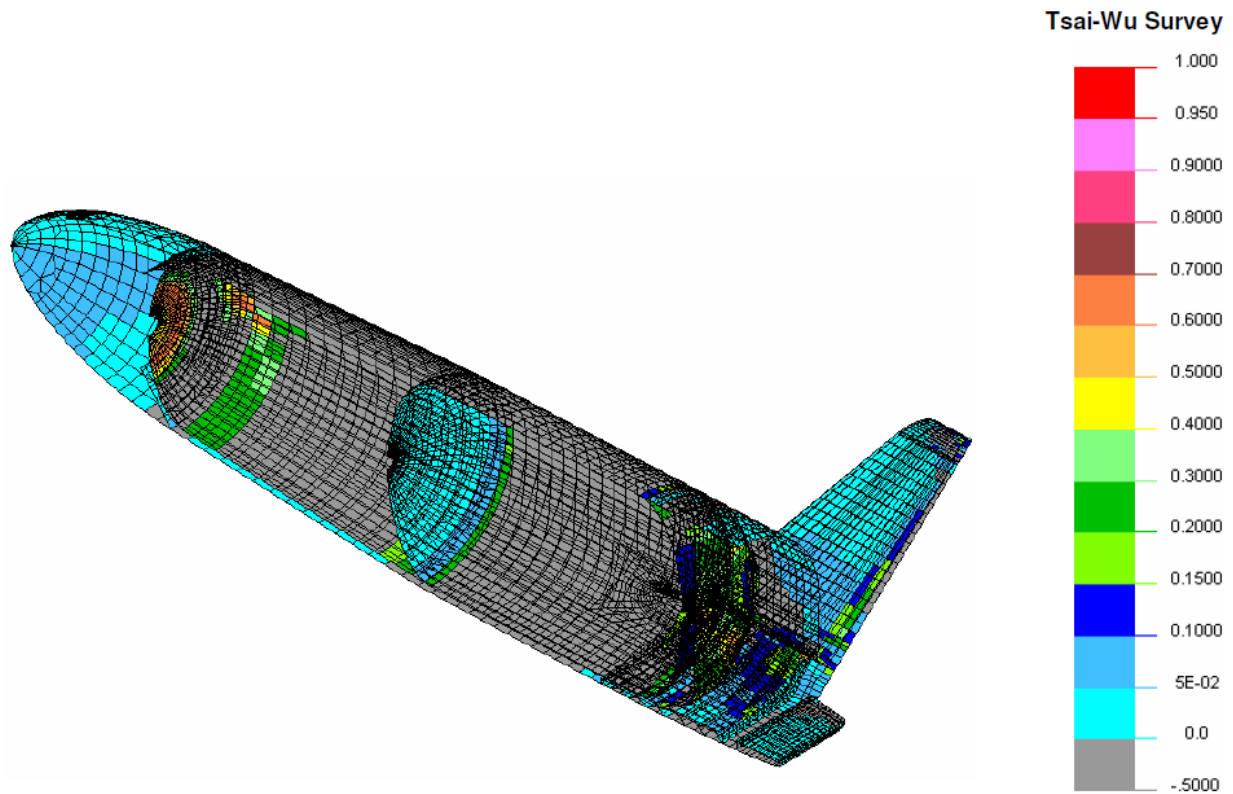


Figure B-76. Tsai-Wu Stress Survey of Vehicle's Composite Structures for the Demonstrator Launch

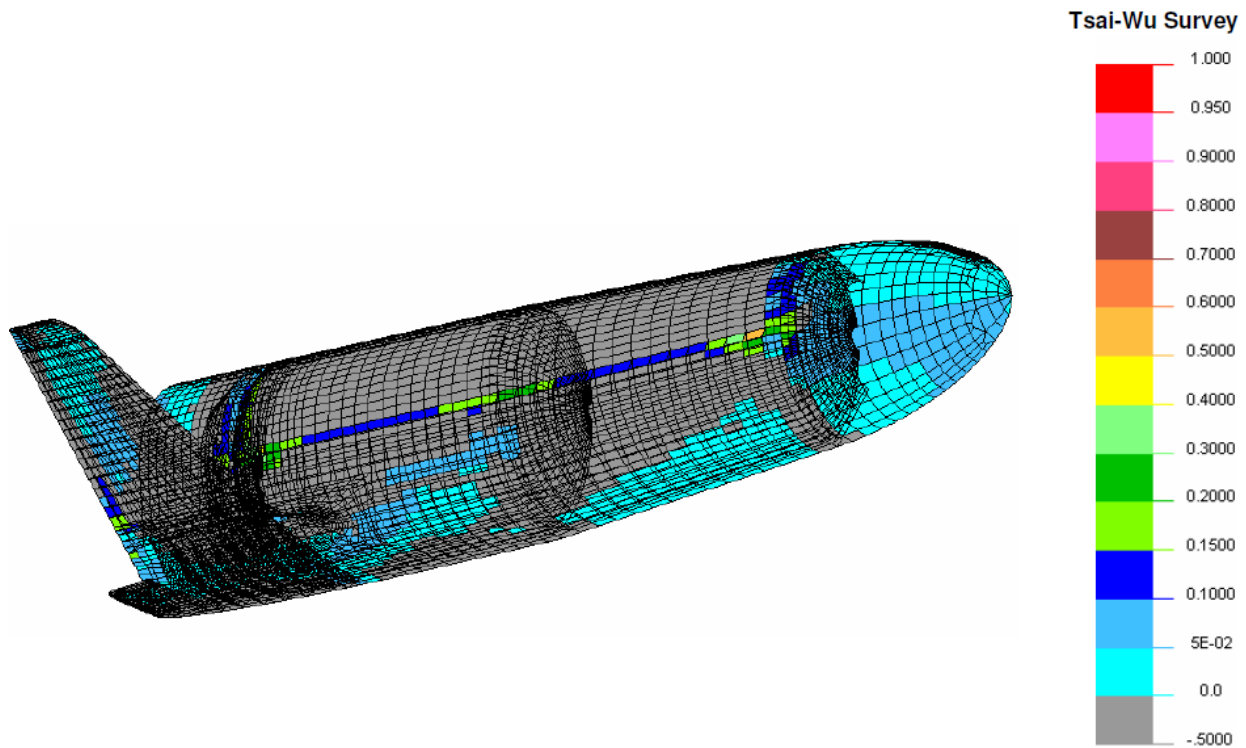


Figure B-77. Tsai-Wu Stress Survey of Vehicle's Composite Structures for the Demonstrator Launch

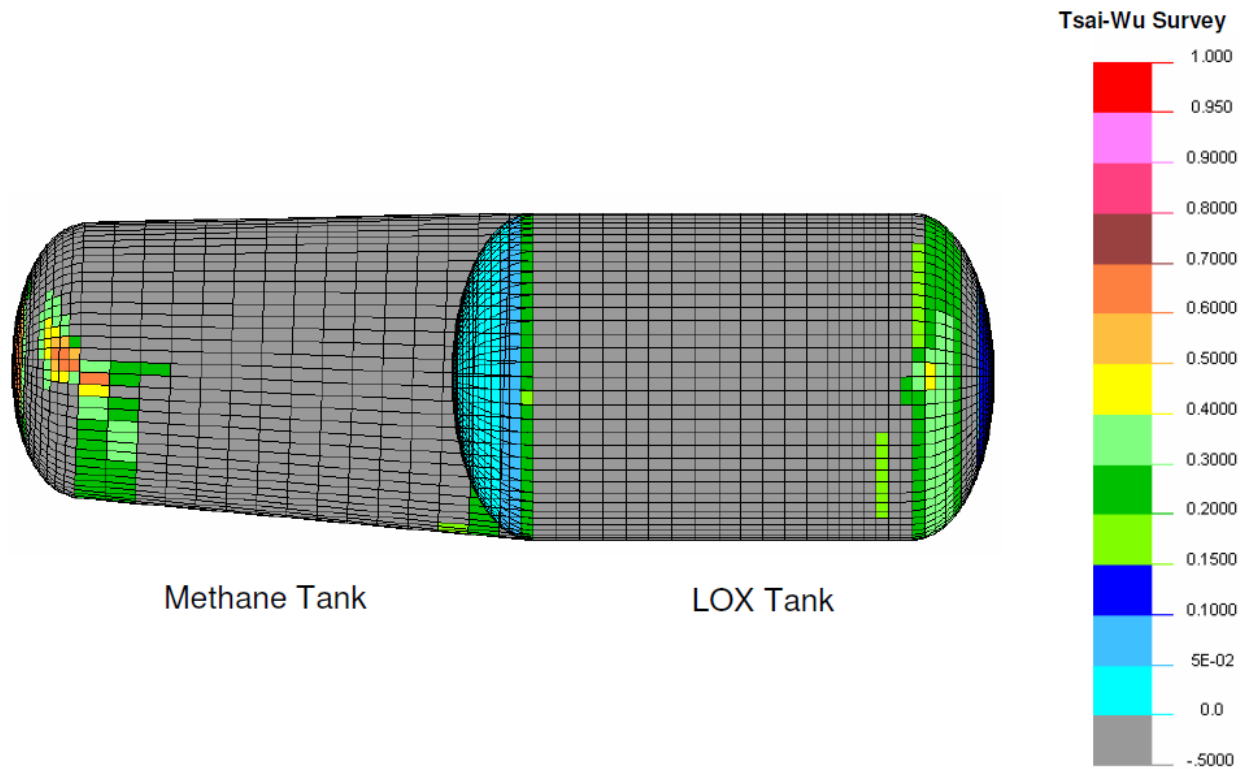


Figure B-78. Tsai-Wu Stress Survey of Vehicle's Composite Structures for the Demonstrator Launch

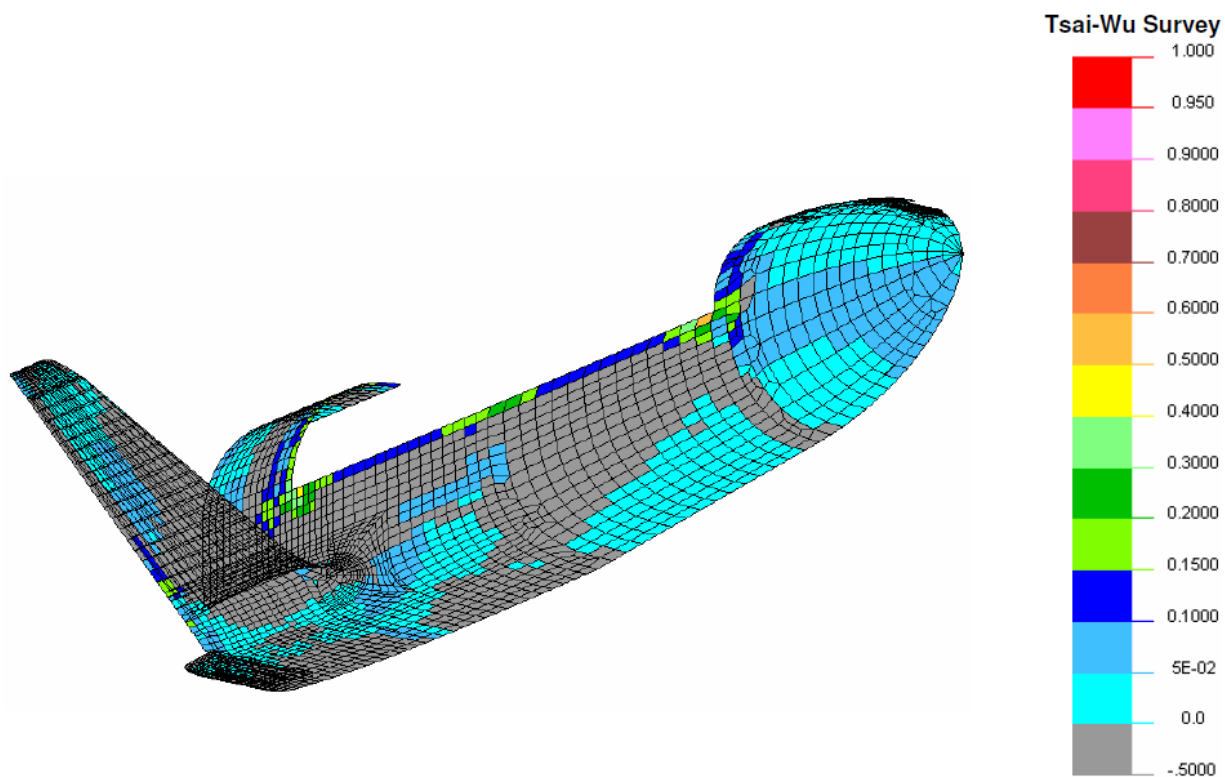


Figure B-79. Tsai-Wu Stress Survey of Vehicle's Composite Structures for the Demonstrator Launch

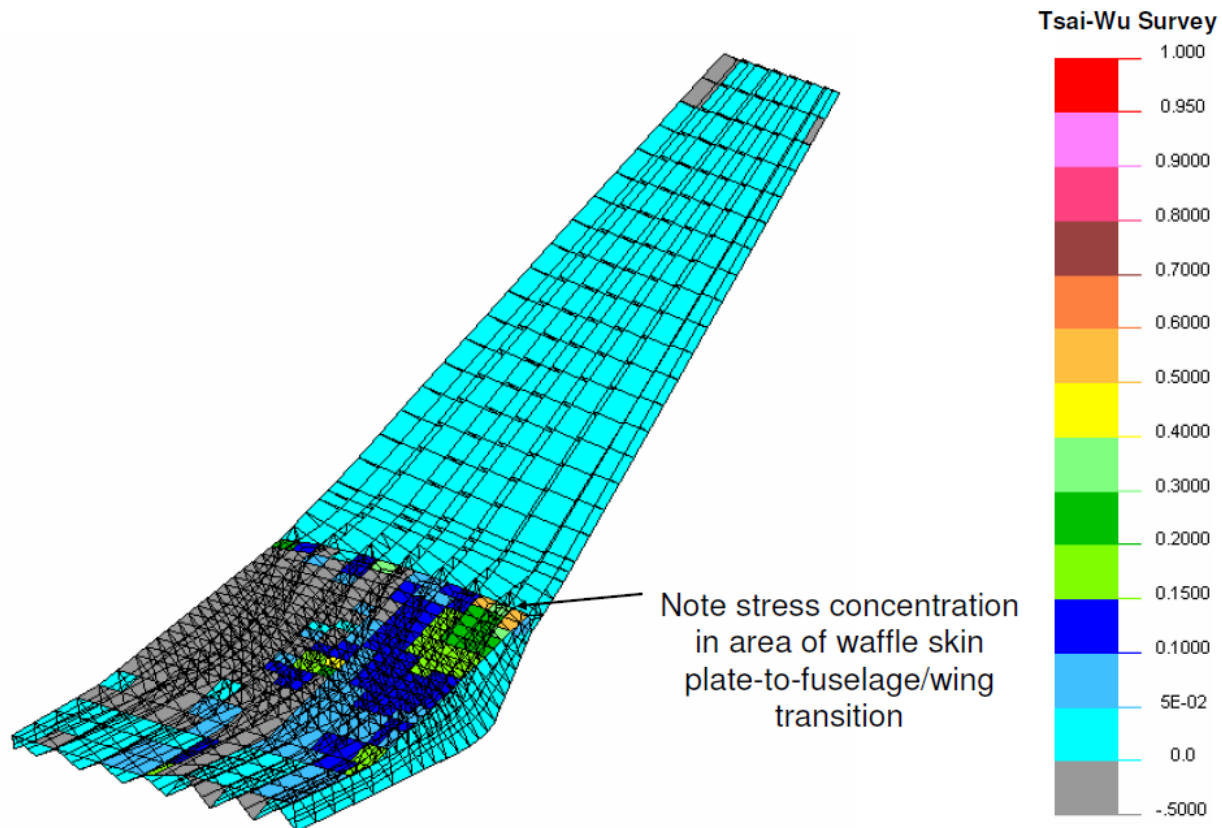


Figure B-80. Tsai-Wu Stress Survey of Vehicle's Composite Structures for the Demonstrator Launch

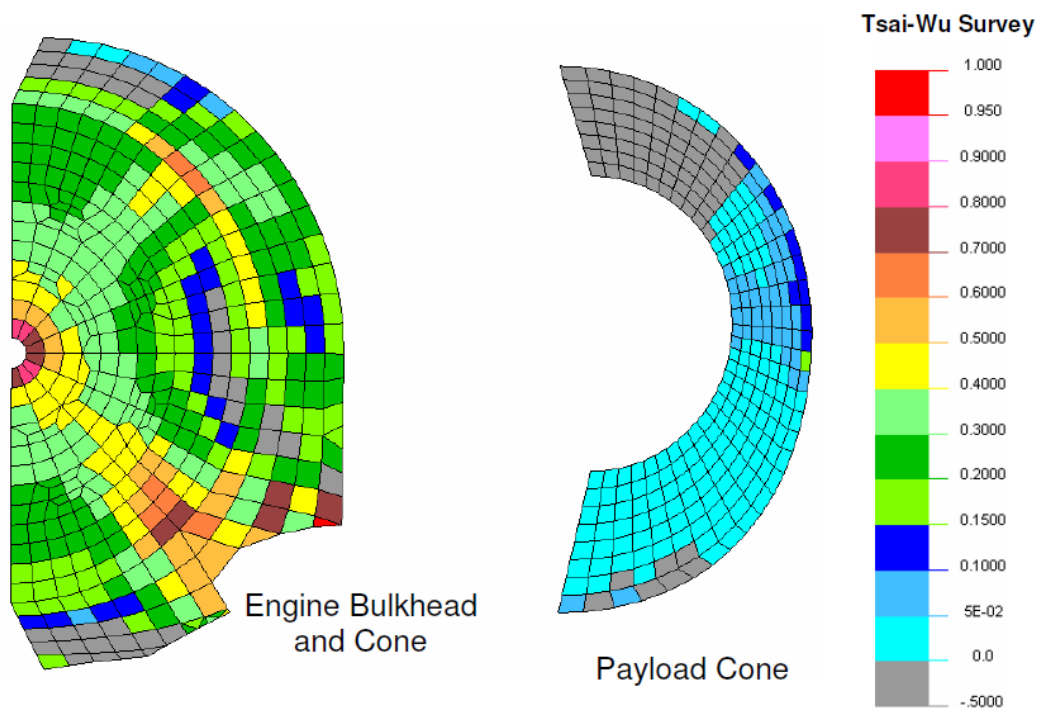


Figure B-81. Tsai-Wu Stress Survey of Vehicle's Composite Structures for the Demonstrator Launch

B5. TPS TRADE STUDY AND ANALYSIS

A very brief study of TPS attachment methods was done, primarily as a means of weight estimation for attachment. TPS design is tasked to UDRI, who has done substantial trades of thermal performance. However, at this time, information about TPS structural properties and performance is not available.

Thus, this analysis considers attachment structures only. Structural integrity of the TPS itself must be addressed at a later date, including bending under pressure load, vibration, and external damage, as well as the obvious temperature resistance.

The vehicle structure upon which TPS will be attached is generally a sandwich core composite. Such a structure cannot carry large transverse or "flatwise" tension, due to relatively low strength of the lightweight core materials. For our selected core material, surface areal tension must be limited to about 500 psi or less, and we cannot count on the thin skin to spread the load. The primary loading that is important for TPS attachment is tension due to negative aero pressures over the large surface area of TPS. Attachment area must be sufficient to meet the core load limit, or possibly a lower adhesive bond limit tension, assuming full vacuum net load conditions on the external surface. For our analysis purposes, the TPS is assumed formed in 2 ft square panels (576 in^2 , vacuum force of 8,467 lbf per panel).

One must assume that the attachment will see temperatures of the cool side of the TPS, which for our choice of resin, would be 350 °F or less (but for more exotic designs might be higher).

The first option for mounting TPS is direct bonding. A typical selection of adhesive is DC93-104 fiber reinforced high temperature RTV, with a tensile strength of about 130 psi at 350 °F. Complete bond coverage is not required to meet the bond strength limit, which is lower than core strength in this case. A bond area of 65 in^2 is sufficient, which can be obtained by a 4 by 4 bond dot pattern of 2.27-inch diameter per dot, for each panel. For a reasonable bond thickness of 0.010 inch, the attachment weight is 0.0344 lbf per panel, or per 4 ft^2 TPS coverage.

Direct bonding advantages are 1) simplicity, 2) low weight, 3) lower skin tension governed by adhesive, and 4) bond can serve as a secondary insulator. Disadvantages are 1) larger thermal transfer surface, 2) relative CTE effects more pronounced due to direct joint, and 3) TPS replacement procedure problematic (labor intensive), unless new methods can be developed (possibly robotic routing, for example). The use of RTV may make replacement an easier task as well.

The second option for mounting TPS is a newly developed mechanical attach with magnetic release, see Figure B-82. Pedestals would be made of metal, with a good choice being Ti 6Al-4V for very high strength/weight. The pedestals could be bonded with something stronger than RTV, as long as it can handle the temperatures, and it is assumed that the core, not bond strength, governs. A bond area of 16.9 in^2 is sufficient, which can be obtained by 4 pedestals per panel, or a single four-pin pedestal at all the mating corners of TPS, with this base area. The base is assumed 0.030 inch thick, which would be needed to spread load adequately. For a reasonable bond thickness of 0.010 inch, the attachment weight is 0.100 lbf per panel, or per 4 ft^2 TPS coverage. This does not include the weight of the TPS internal support frame and corner attach

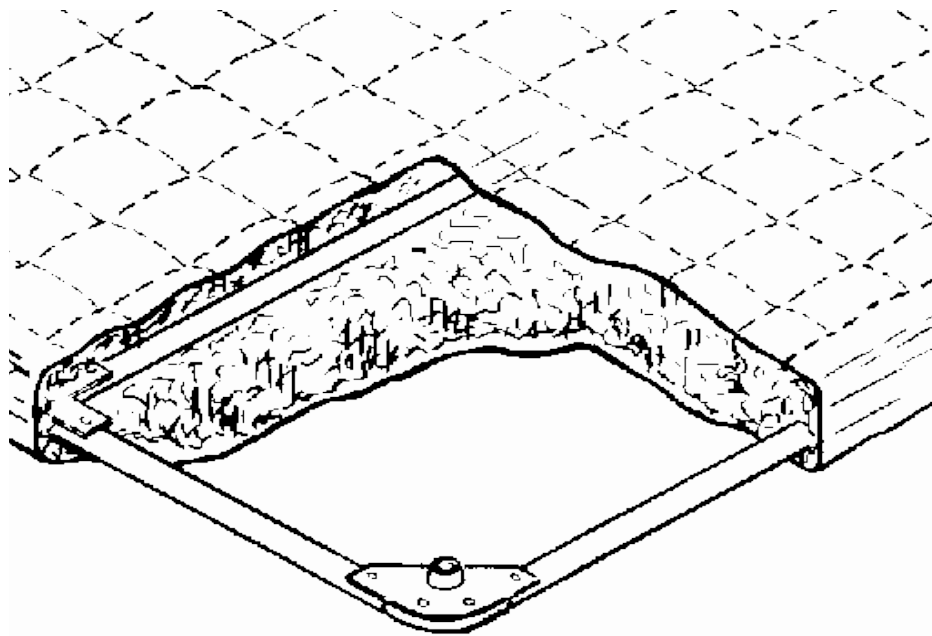
hardware (but the pedestal pin is included).

Clearly, the mechanical attach method has a significant disadvantage in areal weight, and the local skin tension is higher, but tolerable. The big perceived advantage of this approach is ease of replacement, but it has not yet been proven in flight to our knowledge. Another advantage is a less intimate thermal transfer and structural load path, which may allow for lower temperatures at the fuselage skin and less CTE concerns.

It may be possible to further optimize this attach system for minimum weight. The weight of the pedestal base is a large portion, which is necessitated by the need to distribute the pin load into the bond area. It may be possible to reduce weight using a composite pedestal of some kind, or a different geometry to more efficiently spread the force. It would also be desirable to eliminate the TPS internal support frame or make it very light. There is also a tradeoff in TPS panel size and attach weight for this design, whereas the direct bond method does not change in areal weight for panel size change. Optimization is therefore possible.

Further optimization may also be possible at a higher level. For example, if the fuselage sandwich is locally reinforced, then less attachment structure is needed. But these trades must be carefully considered, as manufacturing complexity and cost will be a concern.

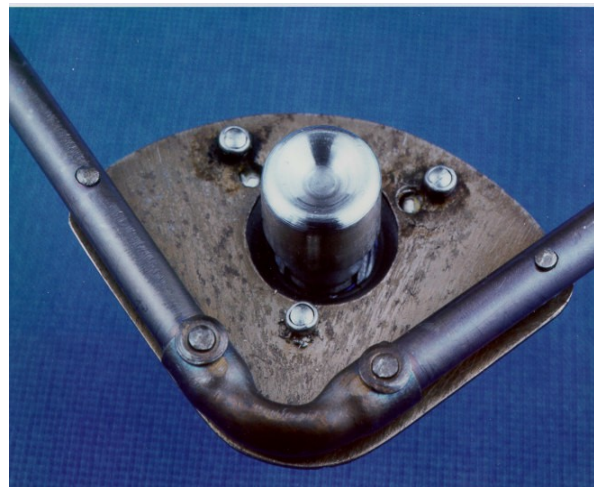
Both attach methods would benefit from test-based design, in which the ability of composite skin to spread load is accounted for. But this must be well proven to rely upon for flight.



(a)



(b)



(c)

Figure B-82. Mechanical TPS Attach Concept

(a) TPS with internal support frame, b) mount pedestal, and c) pedestal magnetic release attach at corners.

B6. SUMMARY AND CONCLUSIONS

A preliminary structural design and analysis was conducted on the primary structures of the HOT EAGLE launch vehicle, using a new integral tank construction and load paths refined since Micro-X. Eight vehicle and two propellant tank load cases were analyzed to verify structural margins. Load cases encompassed various timeline loads from ground handling to flight to landing. After design iteration, all analysis showed positive margins for the structures.

The analysis illuminated critical loads and areas of design that can be further optimized in development. Bimose attachment to a launch vehicle, and launch, is very severe, and requires substantial additional structural reinforcement (approximately 200 lbm). Landing loads also require substantial local reinforcement (120 lbm).

Composite material lay-ups, material call-outs, propellant tank material and wall thicknesses are defined. The design produced a vehicle with a primary structural weight of 1,473 lbm.

The structural design contained within this report uses materials that have significant flight heritage. The processes required to fabricate these structures are well defined and proven industry standards. The integral propellant tanks are of a unique design to take full advantage of the composite materials used to construct them. Additional features of the tanks are the single pressure vessel design with internal bulkhead and external structural shell with internal insulation. Although this design has never been demonstrated, the materials used and the processes to fabricate it are well defined with significant heritage. The design is considered low risk compared to other linerless composite tank possibilities, and the design provides substantial vehicle design advantages over linerless tanks.

B7. REFERENCES

1. Raymer, D., "HOT EAGLE: High Operations Temp Energetic Access to Globe and Launch Experiment, Basic Concept Plans", July 13, 2005
2. Raymer, D., "X-VTOL Spacecraft Conceptual Design Study", April 03.
3. Raymer, D., "Rocket Micro-X Demonstrator Design Study – Overview 08-20-04 Excerpts", Aug 04.
4. Crockett, D. and Davis R., "Micro-X Preliminary Structural Analysis Final Report", Convergence Engineering Corp., April 21, 2005 .

APPENDIX BA: Tsai-Wu Failure Criteria

Following is a brief explanation of how the Tsai-Wu failure criteria was used in this analysis report.

Tsai-Wu is one of a number of failure criteria used in the composite industry. It has some popularity due to its attempt to define failure in a biaxial stress state. Note that failure criteria such as maximum strain and stress are based only on a uniaxial stress state. Essentially Tsai-Wu defines a failure surface in 2D space by the following polynomial expression

$$F = F1*SXX + F2*SYX + F11*SXX**2 + F22*SYX**2 + F33*SXY**2 + F12*SXX*SYX$$

$$\text{With: } F1 = 1/FXT - 1/FXC$$

$$F2 = 1/FYT - 1/FYC$$

$$F11 = 1/(FXT*FXC)$$

$$F22 = 1/(FYT*FYC)$$

$$F33 = 1/FS**2$$

and where F indicates strength, T indicates tensile, C indicates compressive, S indicates shear (as in FS) or applied stress (as in SXX).

The value of F (Tsai-Wu value) can be formulated into the following quadratic equation to determine a strength ratio R of stress state to failure state.

$$(F11*SXX**2 + F22*SYX**2 + F33*SXY**2 + F12*SXX*SYX) R**2 + (F1*SXX + F2*SYX) R - 1 = 0$$

Figure BA-1 illustrates the Tsai-Wu failure surface in 2D space. Included is a comparison to several other failure criteria. The other criteria are not discussed due to the scope of this effort. The author suggests referencing the numerous papers and other publications available on these criteria.

Generally the Tsai-Wu failure criteria is a good predictor of first ply failure, if first ply failure strengths are used in the calculation. However, given its polynomial expression, it cannot define what the actual failure mechanism is (i.e., fiber failure, matrix failure, etc.). To determine this would require looking at the specific stress/strain state for each ply and use a maximum stress/strain or other criteria such as Hashin-Rotem that can identify specific failures.

EMRC's post processor, Display IV, outputs a Tsai-Wu survey plot for each composite element in the model. It does this by calculating a Tsai-Wu value (F) for each ply in the element and then plotting the highest value. A value of $F > 1.0$ indicates a ply failure within that element. To determine which ply failed and the type of failure requires additional post processing of the model. The intent of this preliminary design effort was to adjust the ply schedule of each structure to the point that the Tsai-Wu plots showed positive margins. That is $F < 1.0$ with 1.5x applied loads for margin.

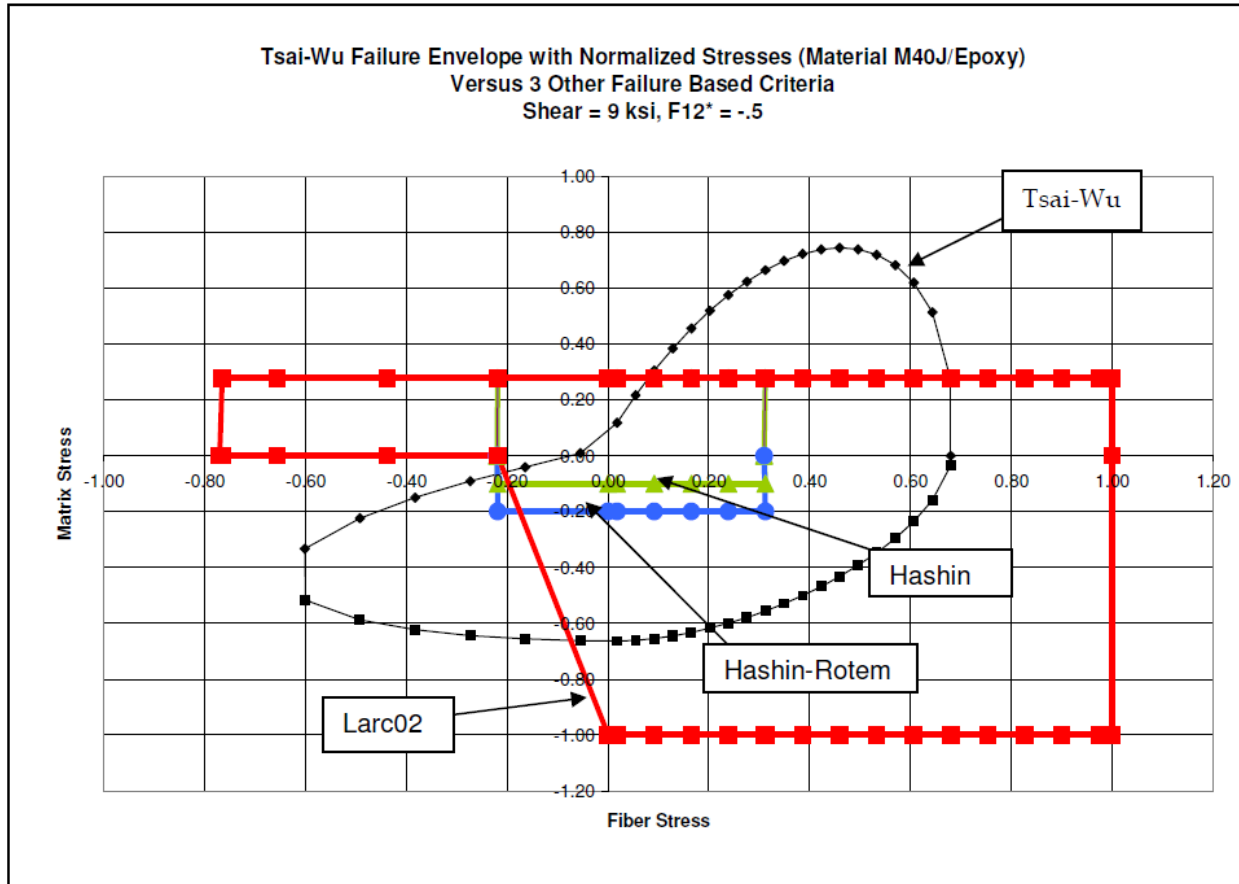


Figure BA-1. Tsai-Wu Failure Envelope Compared with Three Other Failure Criteria (X axis is normalized fiber stress, positive=tension, negative=compression. Y axis is matrix or cross-ply stress. Axis values are normalized to stress/strength. 2D stress plane shown is a slice from the shear third axis at 9 ksi.)

APPENDIX BB: Loads Document

Following is an earlier working summary of vehicle loads. Slight modifications and addition of the demo unit powered flight case were made. Final loads are summarized in Table B-6.

Table BB-1. Vehicle Load Cases

Load Case	Axial g Load	Lateral G Load	Propellant Tanks	Aero load	Engine Thrust	Comments
Vehicle Horizontal Lift	No	2x2.0g down	No propellant, no pressure, no temperature	No	No	Lift g's increased by 2.0 for additional ground handling margins Fwd spreader bar and side lugs, aft center lug Realistic refined lug region model compared to before.
Vehicle Vertical Lift	2x2.0g down	No	No propellant, no pressure, no temperature	No	No	Lift g's increased by 2.0 for additional ground handling margins Fwd spreader bar and side lugs, aft center lug relieved Realistic refined lug region model compared to before.
Launch g's Not analyzed because other loading conditions exceed these.	1.5*3.0g down	No	Full Propellant Mass, 1.5*40 psi and -292 °F temp ox and fuel tank (could get down to 30 psia if this drives design). Outer tank surface temp target 40F.	No	No	Vehicle oriented vertically, back attached to launch vehicle (similar to Bimese attachment) Intended to simulate launch max g's, with possible launch shock factors, before substantial q develops. Realistic refined attach region model compared to before. Envelopes pre-launch g's only. Inertia relief method if possible, otherwise countering g and angular accel. Loads

Load Case	Axial g Load	Lateral G Load	Propellant Tanks	Aero load	Engine Thrust	Comments
Launch max q or alpha-q with g's	1.5*8.0g down	1.5*3.0g	Full Propellant Mass, 1.5*40 psi and -292°F temp ox and fuel tank (could get down to 30 psia if this drives design). Outer tank surface temp target 40F. Assume HOT EAGLE is an upper stage or payload. Won't separate from vehicle or fire until exo. Thus for launch it would have full tanks and be	Yes	No	Vehicle still attached to launch vehicle, at time of launch max q (qmax=1200 psf, Mach 2). Aero load case here mostly axial drag (nose pressure), different than flight case. Realistic refined attach region model compared to before. Assume no aero shroud.
Staging separation Not analyzed because loading conditions exceed these.	No	1.5*2.5g	Full Propellant Mass, 1.5*40 psi and -292°F temp ox and fuel tank (could get down to 30 psia if this drives design). Outer tank surface temp target 40F.	Yes	No	NA
Flight (coast or glideback) maneuvering and alpha-q, or separation	1.5*3.0g Assume limited by throttling back on engine if necessary.	1.5*3.0g	20% Full Propellant Mass, 1.5*40 psi and - 292°F temp ox and fuel tank (could get down to 30 psia if this drives design). Outer tank surface temp target 40°F.	Yes	8200 lbf per engine	Aero loads derived from CFD data if it exists (curve fits interpolated to vehicle model), or manual estimation (qmax=1200 psf, Mach 8), fine tuned to require only small incidental g loads for force balance aside from maneuvering g's. Inertia relief method if possible, otherwise countering g and angular accel. loads. Neglect yaw loading.
Re-entry max alpha-q	1.5*3.0g	4g based on aero reaction Lifting body.	20% Full Propellant Mass, 1.5*40 psi and - 292°F temp ox and fuel tank (could get down to 30 psia if this drives design). Outer tank surface temp target 40°F.	Yes	No	Aero loads derived from CFD data (curve fits interpolated to vehicle model) (qmax= approx 190 psf, Mach 25, to match 4 g's net lateral deceleration), fine tuned to require only small incidental g loads for force balance aside from trajectory g's (given at left).

Load Case	Axial g Load	Lateral G Load	Propellant Tanks	Aero load	Engine Thrust	Comments
Chute Deployment (Pitchover)	1.5*1.0g	g loading according to inertia relief, as well as rotational accel.	20% Full Propellant Mass, 1.5*40 psi and - 292°F temp ox and fuel tank (could get down to 30 psia if this drives design). Outer tank surface temp target 40°F.	No	No	3x vehicle weight concentrated at chute attach to payload cone or other internal structure. Loads also simulating chute opening bearing by chute rope on external shell. Assume post-pitchover engine thrust and decel is not critical case compared to others. Inertia relief method if possible, otherwise countering g and angular accel. loads.
Vertical Landing	1.5*2g before landing, and at landing approach velocity of 10 ft/sec	No	20% Full Propellant Mass, 1.5*40 psi and - 292°F temp ox and fuel tank (could get down to 30 psia if this drives design). Outer tank surface temp target 40°F.	No	1.5*1.05 g *landing weight from one engine	5950 lbf, 204 kip-in moment on each leg (subject to revision for vehicle landing mass, leg design details). Realistic leg and damper attach modeling to airframe.

BB.1 Other important notes:

1. Payload mass to be used = 2000 (HOT EAGLE RUS 5000 lbs, scaled by GLOW to Micro-X size)
2. Some of load cases above may be eliminated by “worst case” analysis or enveloping. However, such analysis must consider that different cases may design different parts of the system. For example, re- entry will likely design belly fairing and wings, but chute or launch g’s may design payload cone. Desire to eliminate as many cases as possible due to budget limitations.
3. Analysis done at full Micro-X size. Mass scaling to smaller size needs to be worked out.
4. Local analysis to be avoided, will burn up too much time. Full system only preferred. System model include flaps, for example, and loads will be applied correctly to flap. Then full analysis includes flap detail results.
5. Major objective is to use reasonable load lug/attach/interface models for proper load transmission to airframe, so that load spreading into main structure and integral tank is reasonably simulated. Maybe stresses not perfect (using conservative external loads for this inaccuracy), but load paths good.

APPENDIX C:
HOT EAGLE Subsystems

14 November 2005

Universal Space Lines LLC 1501 Quail Street, Suite 100 Newport Beach, CA 92660

TABLE OF CONTENTS

Section	Page
C1. Introduction.....	162
C2. Top Level Requirements.....	163
C2.1 Environments.....	163
C2.1.1 Radiation	163
C2.1.2 Vibration.....	163
C2.1.3 Shock.....	164
C2.1.4 Acceleration	165
C2.1.5 Temperature	165
C2.2 Control System Implementation.....	165
C2.2.1 Control system latency	165
C2.2.2 Redundancy	165
C2.3 Program Requirements	165
C2.3.1 Development and acceptance test requirements.....	165
C2.3.2 Programmatic requirements	166
C3. System Requirements / Implementations.....	167
C3.1 Air Data Sensor (ADS).....	167
C3.2 Vertical Position Accuracy Requirements.....	167
C3.3 Navigation / Vehicle State Sensing	169
C3.3.1 Navigation Baseline Configuration.....	169
C3.4 Aero Surface Actuator Loading.....	171
C3.4.1 Body Flaps.....	171
C3.4.2 Elevon.....	171
C3.4.3 Rudder	172
C3.4.4 Candidate Actuators	172
C3.4.5 Actuation Options (Aerosurface and TVC)	174
C3.5 Vehicle Management System	177
C3.5.1 Vehicle interfaces.....	177
C3.5.2 Memory and throughput.....	180
C3.5.3 Obsolescence.....	180
C3.5.4 VMS Baseline Configuration.....	180
C3.6 Instrumentation and Communications.....	181
C3.7 Flight Safety Systems	182
C3.8 Power.....	183
C3.9 Reaction Control System.....	184
C4. Systems Weight Estimate	186
C4.1 Battery Sizing	186
C4.2 Weight Estimates.....	189
C4.2.1 Electronics.....	189
C4.2.2 Power and Wiring.....	189
C4.2.3 Actuation – Electrical.....	192
C4.2.4 Actuation – Hydraulic	192
C4.2.5 Actuation System Selection	194
C4.2.6 Landing Gear – Horizontal Landing	194
C4.2.7 RCS	196

C4.2.8	Miscellaneous.....	199
C4.3	System Weight Comparisons	202

LIST OF FIGURES

Figure	Page
Figure C-1 – LEO Radiation Environment	163
Figure C-2 – Launch Vehicle Vibration Environments - Qualification	164
Figure C-3 – Left Wing Elevon with Actuator Rod	172
Figure C-4 – Actuation Comparison	174
Figure C-5 – Hydraulic Actuator	175
Figure C-6 – Baseline Avionics Configuration	181
Figure C-7 – Traditional Flight Termination System	182
Figure C-8 – Autonomous Flight Safety System	183
Figure C-9 – Pneumatic TVC Implementation	187
Figure C-10 – RCS System Configuration	196
Figure C-11 – Quad Valve Configuration	197
Figure C-12 – ATCS Block Diagram	199

LIST OF TABLES

Figure	Page
Table C-1 – Astech DG18 GPS Real Time Position Accuracy	168
Table C-2 – Navigation Sensor Physical Attributes	170
Table C-3 – Navigation Sensor Environmental Attributes	170
Table C-4 – Actuator Hinge Moment & Force Requirements	172
Table C-5 – EMA Attributes	173
Table C-6 – Hydraulic Actuators	173
Table C-7. VMS Interfaces	178
Table C-8 – Battery Sizing, Baseline Mission, Power Control	186
Table C-9 – Battery Sizing, Baseline Mission, Pneumatic TVC	186
Table C-10 – HOT EAGLE Power Analysis	188
Table C-11 – Avionics / Electronics Weight Estimate	190
Table C-12 – Power and Wiring Weight Estimate	191
Table C-13 – Electrical Actuation Weight	193
Table C-14 – Hydraulic Actuation Weight Estimate	193
Table C-15 – Landing Gear Actuation Weight Estimate – Horizontal Landing	195
Table C-16 – RCS Weight Estimate	198
Table C-17 – Miscellaneous Systems Weight Estimates	201
Table C-18 – CERV Mass Summary	202
Table C-19 – X-33 Mass Summary	203

C1. Introduction

This document presents the results of a preliminary design study of HOT EAGLE avionics, electrical, and subsystems based on the previously completed Micro-X design study. The preliminary design will be based on the vehicle and mission definition used by USL to support the previously completed Micro-X dynamic simulation task. The HOT EAGLE preliminary design study was conducted by identifying subsystem requirements and candidate implementations in order to characterize attributes and compare implementations.

This work was performed under subcontract to Conceptual Research Corporation in support of its "HOT EAGLE" design study of a reusable upper stage for an HLV/ARES-class reusable lower stage. The CRC study also includes a manned Global Transport system based on the HOT EAGLE vehicle concept to perform certain high-value objectives in high-response operational scenarios, and includes the design definition of a subscale technology demonstrator sized appropriately to allow flight on an existing first-stage booster. The CRC study effort was funded by USAF-AFRL/VA and structured as a subcontract from the University of Dayton Research Institute.

C2. Top Level Requirements

C2.1 Environments

These requirements apply to all of the systems. As an example of the effect of environment, one can look to the cost of a 400W C-band transponder produced by Herley-Vega for aerospace applications - \$8K, ruggedized for launch vehicle vibration/shock - \$26K, and hardened for radiation - \$98K (1999 pricing data).

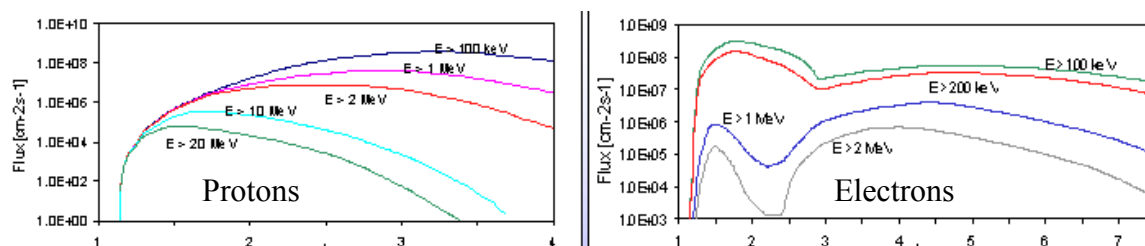


Figure C-1 – LEO Radiation Environment

C2.1.1 Radiation

The avionics will be required to perform in a LEO environment at all inclinations. Figure C-1 illustrates the environment particle density as a function of earth radii (L, ~3,440 nmi). Particle density can increase by orders of magnitude during solar flare events. While the LEO environment is less severe than higher orbits, radiation effects cannot be ignored. Both single event effects (i.e., upsets, latch-up, burn out, etc.) and total dose must be considered. The total dose expected is defined by the environment and exposure time with exposure time being defined by flight time, flight frequency, and the required avionics design life.

Radiation effects are typically mitigated through component selection with known radiation performance (not necessarily hard but known performance), external mitigation techniques (e.g., error detection and correction on memory devices), and fault tolerance (assuming that each element is sufficiently tolerant that the probability of multiple, like events occurring is small). The continuing trend toward smaller feature sizes and lower power electronics will likely result in increased susceptibility.

C2.1.2 Vibration

The launch vibration environment results from the internally generated sources (e.g., engines) and the reflected launch energy being transmitted through the vehicle structure. Figure C-2 shows the vibration qualification environments (limit level + 6dB) of several launch vehicles (obtained from equipment qualification data). The data is assumed to represent the engine section environment of the vehicles based on known equipment locations and the magnitude of the environment. The SIGI (Honeywell INS/GPS) environment shown is typical of military electronics qualification.

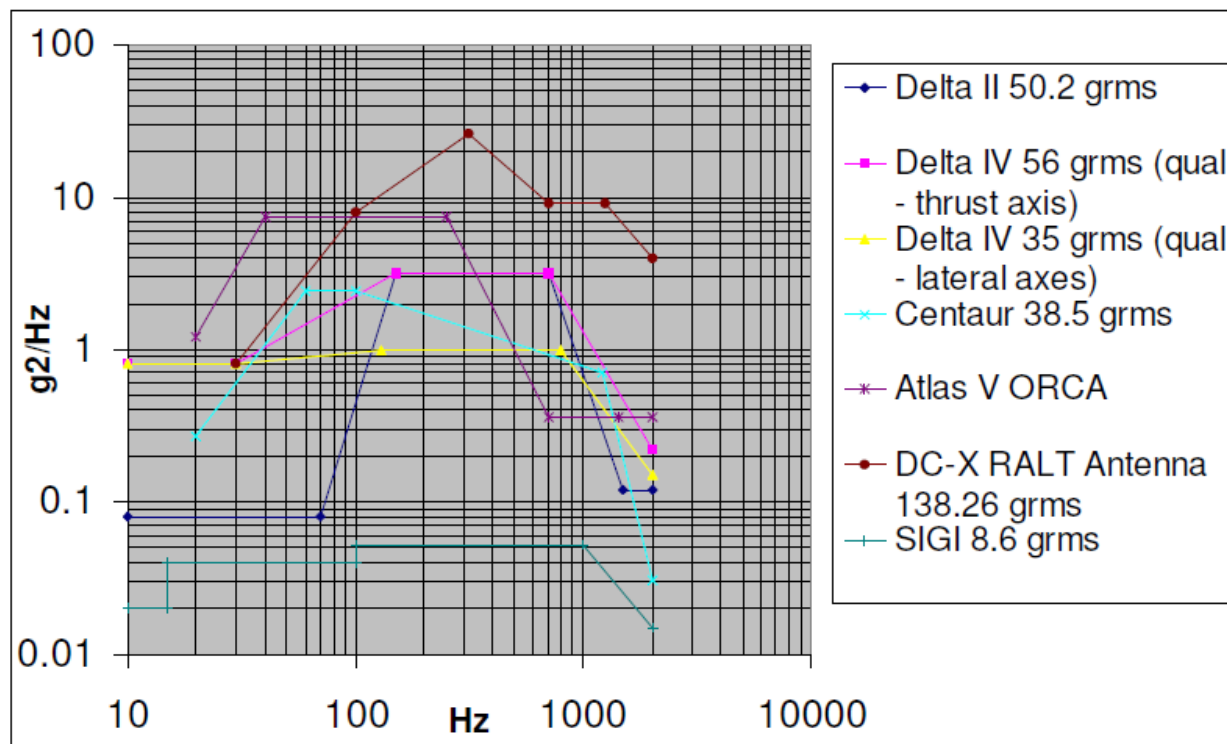


Figure C-2 – Launch Vehicle Vibration Environments - Qualification

The actual HOT EAGLE environment will be dependent on characterization of HOT EAGLE energy sources (engines), reflected energy, and structural configuration. It is assumed that the environment for a HOT EAGLE acting as a second stage would be less than that of a ground launched HOT EAGLE due to the absence of the reflected energy.

Usage of existing design components imposes limitations as the components will have been designed and tested to an existing vibration environment (that may be lower than required for the HOT EAGLE vehicle). Alternatives to address this issue include redesign & re-qualification, vibration isolation, and mass damping. Redesign & re-qualification may not be possible or cost/schedule prohibitive. Vibration isolation adds complexity, weight, and only shifts the frequency of the energy. Mass damping consists of collocating equipment to increase local mass, reducing the local environment.

The design process attempted to identify existing equipment with a “typical” launch vehicle environment in mind.

C2.1.3 Shock

Shock is generated as a result of separation events. It is assumed that the HOT EAGLE operating as a second stage would experience shock events. As with vibration, the “local” environment is a function of proximity to the source and structure between the source and equipment location (transmission path).

The design process will attempted to identify existing equipment with a “typical” launch vehicle environment in mind.

C2.1.4 Acceleration

Acceleration effects are typically “bracketed” by vibration testing, so this typically isn’t an issue. Vehicle dynamics (velocity, acceleration, and jerk) do affect GPS receiver selection.

C2.1.5 Temperature

Equipment is qualified to operate in a specific temperature environment. For example, avionics temperature capability is dictated by the equipment design and the parts (military, industrial, or commercial) used in the design. Equipment must be suitable for the anticipated vehicle environments. The primary means of heat transfer for the avionics is conduction.

The HOT EAGLE will require an active thermal control system for the avionics for both orbital operations and post flight due to internal heating from the reentry heat soak (this is the case of the Shuttle and was the case on both the MDA X-33 design and Lockheed Martin X-33 design). The X-33 design included a ground heat exchanger and cart to provide a preflight and post flight cooling capability.

C2.2 Control System Implementation

These requirements affect all the systems that comprise the vehicle control system (i.e., sensors, processing, and effectors).

C2.2.1 Control system latency

Control system latency requirements influence the vehicle management system processing rate as well as the control system interfaces (i.e., navigation/attitude sensor and control effectors). As seen with previously discussed requirements, usage of existing equipment imposes constraints in that element’s (e.g., navigator) contribution to control loop latency is already set.

We will assume typical latency requirements until the requisite vehicle data exists to generate control system latency and sensor bandwidth requirements.

C2.2.2 Redundancy

The HOT EAGLE demonstrator will be single string. However, the global transport version would likely need to include a redundant control system since it carries humans (using FAR Part 25.1309, JSSG-2008, MIL-F-9490, or NPR 8705.2 as guidance). The global transport variant would also need to include a user interface on board as it is unlikely that one would place humans on a vehicle without providing status and an abort mechanism.

C2.3 Program Requirements

These requirements affect all systems.

C2.3.1 Development and acceptance test requirements

It is assumed that HOT EAGLE components will be required to be qualified and acceptance tested in accordance with typical specifications (i.e., MIL-STD-1540, EWR 127-1 (replaced by AFSPCMAN 91-710 as of 1 July 2004), RCC 319-99, etc.). Dedicated hardware is typically included for qualification testing (assuming that the hardware is not already qualified to a like, or more stringent environments). For the HOT EAGLE demonstration program we will use a “protoqual” approach, such that the test units could be used as spares. All units will be acceptance tested.

Test records will be required to obtain flight approval from a certifying agency (either a test range or the FAA).

C2.3.2 Programmatic requirements

This category includes things like cost and schedule reporting, data items preparation and submittal, parts programs, quality programs, and similar efforts. It is assumed that minimal program “overhead” will be imposed. Obviously a means to track cost and schedule performance will be required and data will be required for certification and system maintenance and support. “Supplier format” data and existing practices (i.e. design, configuration control, and quality) will be utilized.

C3. System Requirements / Implementations

The following paragraphs examine HOT EAGLE actuator and sensor subsystems, using current vehicle sizing and expected flight requirements (or best guess thereof) to help define the requirements and to assist in selecting the subsystems for the demonstrator vehicle.

C3.1 Air Data Sensor (ADS)

An air data sensor is required if accurate angle of attack, side slip angle, air speed, or dynamic pressure values relative to the local air mass are required. Typically, aircraft require some air data, for example, actuator control gains may be based on pitot tube pressure data; or certain flight regimes have a narrow corridor on angle of attack, so an accurate value is required to maintain stable flight. Autonomous horizontal landing vehicles usually use angle of attack and sideslip angle as feedback for guidance commands during the approach and landing phase. Because of wind, air data sensed values (as opposed to inertial calculated values) are likely necessary. ADS are problematic, though, for reentry vehicles because of where they need to be (near or at the nose) and the environment they encounter. Recent “study” vehicles have looked at flush systems to overcome some of these problems. The Shuttle’s air data probe is deployed after the high heating regime of flight, requiring complex installation and calibration. The horizontal landing variant of the HOT EAGLE vehicle will most likely require an air data system (with associated complexities). For a vertically landing system, inertial sensor generated dynamic pressure and angle of attack estimation would be satisfactory for any guidance and control requirements, so pressure measurements would not be required.

For the horizontal landing system, significant effort will be required to design and develop an air data system. Wind tunnel testing is also required to characterize the system. For a vertical landing system, some future effort will be needed to confirm the current estimate that an air data system is not required.

The Shuttle Entry Air Data System (SEADS) effort examined the physical integration, heating, TPS erosion & life, thermal, aero-thermal, dynamic, and vibration environment effects of a flush air data system integrated in the RCC nose cap of the Shuttle (NASA Contractor Report CR-166044). The original design requirement of 2520°F on the nose cap was later increased to 2660°F based on a trajectory change.

Flush air data system physical integration with TPS has also been performed at Langley with the Aeroassist Flight Experiment (NASA Contractor Report 4312). This effort examined vibro-acoustic, aero-thermal, and structural testing of pressure port designs and evaluated compatibility with LI-900, FRCI-12, and LI-2200 insulation tiles at 2300°F, 2800°F, and 2900°F respectively.

The X-33 integrated a 6 plug (2 ports per plug) flush air data system into the vehicle RCC nose cap and chin panel.

C3.2 Vertical Position Accuracy Requirements

Air vehicles performing autonomous landing require accurate altitude position data. For horizontally landing vehicles, the final flare is a function of altitude and needs to be performed with a tight tolerance on altitude to not stall before wheels touch. For vertically landing vehicles, the final sub phases of guidance depend on accurate altitude measurements. The “target” altitude

for achieving the final constant vertical velocity descent to gear touch is the 3 sigma vertical position error. If this vertical position error is 10 feet and final descent velocity is 4 feet per sec, 3 sigma high would require a 20 feet (5 sec) final descent (and the commensurate propellant). (DC-X used 10 feet as its target altitude.)

Typically, a radar altimeter is necessary for that type of accuracy near the ground. A SIGI (Honeywell integrated GPS/INS) has a specified SEP of 50 meters. It goes without saying this is too much for the limited landing propellant available. Adding a WAAS capability to the GPS reduces error to about 3 meters, but WAAS is only available over the United States. A LAAS capable GPS provides the accuracy (1 meter) but we can't expect to have LAAS everywhere we land (for an operational vehicle). For a demonstrator vehicle, flying at one site, LAAS may be enough, but the implementation cost may be more than adding a radar altimeter. We also may not want to rely solely upon external systems (i.e. GPS and GPS augmentation systems) that are affected by antenna visibility. Short flight times (demonstration system) with a very accurate inertial system (e.g., SIGI) may suffice (.01 nmi/hr results in ~10 ft after 10 min, which is acceptable). Note that the radar altimeter typically (for vertically landing vehicles) is not used in the final 10's of feet for landing (DC-X phased it out at ~40 feet), but it's very accurate input to the onboard altitude estimation calculation (prior to phase out) coupled with a good inertial system provides the accuracy required.

The Thales Navigation (Ashtech) DG16 GPS receiver real time position accuracy is provided in Table C-1. The DG16 receiver provides 12 GPS L1 code and carrier channels, 2 SBAS channels, and 2 300 kHz DGPS beacon channels.

Table C-1 – Ashtech DG16 GPS Real Time Position Accuracy

Mode		CEP (m)	95% (m)
Autonomous		3	5
Differential			
	Local Base Station	0.4	0.9
	Beacon	0.9	1.6
	SBAS	1.8	3.8

The Table C-1 data is based on specific tests conducted in Santa Clara and Moscow.

The HOT EAGLE baseline includes a radar altimeter system comprised of the Honeywell HG8505 radar altimeter and LG81BR01 antennas. This is the system that we used on DC-X and interestingly enough was also selected for usage on the X-33. The antennas were originally developed for the Shuttle.

The HG8505 is approximately 4 inches W by 5.15 inches L (base) by 3.5 inches H and weighs approximately 3 pounds. The antennas are approximately 6.95 inches in diameter by 0.54 inch thick with an approximately 1 inch square by 2 inches high connector doghouse located on the back of the antennas and weigh 1.4 pounds. The antennas are preferably installed on a flat surface on the vehicle base 18 to 50 inches apart (we used a 50-inch spacing on DC-X) away from other features to avoid multipath. Installation on a flat surface is preferred as the antennas have a 30° beamwidth and installation on a canted surface (as on DC-X) will affect off axis

performance. The antennas were originally designed to work with the foamed ceramic TPS tile used on the STS.

C3.3 Navigation / Vehicle State Sensing

Navigation sensor suitability must consider the following factors.

- Sensor bandwidth, accuracy, and performance requirements – derived from flight simulation analysis and orbital insertion accuracy requirements. Usually an iterative approach recognizing capability of available sensors.
- Dynamics (velocity, acceleration, and jerk) – especially important for systems that include GPS.
- Initial alignment methodology, installation accuracy, and effect on performance.
- Are additional rate sensors required to provide vehicle bending stabilization? If so, the number of axes and location of the sensors must be determined. It is assumed that the HOT EAGLE vehicle does not require bending stabilization rate sensors.
- GPS antenna position effect on satellite visibility and therefore navigation performance.
- Does selected implementation impose operational limitations (i.e. a PDOP greater than some value required to launch, preflight simulation required to verify accuracy with respect to GPS satellite constellation configuration, etc.)?

C3.3.1 Navigation Baseline Configuration

Existing launch vehicle inertial navigation systems were not considered due to their cost (between \$1M and \$2M per unit depending on quantity) and other configuration issues. The “typical LV” systems that are available (used on Delta family of vehicles and Atlas V) are radiation hardened and include redundant sensors (hexad and pentad configuration respectively) with dual redundant output of navigation data via data buses.

Other available navigation sensors come in two basic flavors, tactical grade inertial measurement units (IMUs) ($\sim 1^\circ/\text{hr}$ gyros, primarily used in missiles) and navigation grade inertial navigation systems (INSs) ($\sim 0.05^\circ/\text{hr}$ gyros, primarily used in aircraft applications). The IMUs are basically just the sensing elements (gyros and accelerometers) and output the raw data (incremental angles and velocities, body rates and accelerations) via a dedicated serial interface. An external computer must process this data into a navigation solution. The INSs consist of an IMU and the processing capability required to generate the navigation solution. The INSs may also include an integral GPS module to enhance the navigation solution (inertial only, GPS only, and blended solutions are typically available). Table C-2 summarizes the candidate hardware physical attributes.

Table C-2 – Navigation Sensor Physical Attributes

		System Weight (lbs)	Equipment Size (in)
IMU/GPS			
	IMU		
	LN-200	1.65	3.5D x 3.4
	HG-1700	1.6	5D x 2.9
INS/GPS			
	LN-100G	21.6	10 x 7 x 7
	H-764 (SIGI)	18.5	9.8 x 7 x 7
INS			
	LN-100L	20.6	10 x 7 x 7
	H-764 (SIGI)	17.5	9.8 x 7 x 7

Candidate hardware environmental attributes are summarized in Table C-3.

We selected an integrated INS/GPS such as the Honeywell H-764 (SIGI) as the baseline sensor for the HOT EAGLE demonstrator. The SIGI is a navigation grade INS which will improve both insertion and landing accuracy. The SIGI includes the navigation function, provides the ability to alter axis definitions and installation error via the data bus, and includes a gyrocompass alignment function reducing development risk.

Table C-3 – Navigation Sensor Environmental Attributes

		Temp	Vib	Pyrotechnic Shock	Applications
IMU/GPS					
	IMU				
	LN-200	-57 to 71 C	11.9 grms, performance 15grms, survival	400g/100Hz, 1500g/1000Hz	Satellites (LN-200S)
	HG-1700	-54 to 85 C	11.9 grms, performance (x-axis)	not quoted	GMLRS, SpaceShip One
INS/GPS					
	LN-100G	-32 to 71 C	8.1 grms, performance 17.4 grms, endurance	1130g/450Hz	X-33
	H-764 (SIGI)	-54 to 71 C	8.6 grms, performance 17.9 grms, endurance	not quoted	STS, ISS, CRV, K-1
INS					
	LN-100L	-32 to 71 C	8.1 grms, performance 17.4 grms, endurance	1130g/450Hz	Athena, MSLS

GPS and other antennas are available from M/A-Com (and EDO, Herley-Vega, and others). The M/A-Com antennas weigh 0.77 pounds and have approximately a triangular mounting plate with a 6.09-inch base and 5.47-inch height (.25 inch thick). The circular antenna element is 2.82 inches in diameter and 0.95 inch high. The antenna is similar in design to M/A-Com's other launch vehicle antennas and is designed for a temperature range of ± 300 °F with short durations to 500 °F.

Note that usage of GPS isn't necessarily the cure all that is commonly advertised.

GPS position is antenna position. We want to place the GPS antennas such that they are pointing generally up to maximize the number of visible satellites and minimize geometric dilution of precision (GDOP). GDOP is inversely proportional to the volume bounded by the vectors from the user to the satellites and affects the quality of the data provided by the GPS. Optimum GDOP is obtained with one satellite at the user's zenith and three satellites at the horizon, 120° apart. Antenna placement to maximize visible satellites becomes an issue with a vehicle in which the definition of generally up changes. Satellite visibility and therefore quality of GPS data throughout the flight needs to be understood in order to assess the true aiding that GPS would provide. One could get a feel for this by performing sensitivity studies, but one would need to fly the trajectory with a satellite simulator to assess real performance.

GPS is not as accurate in the vertical channel as the horizontal. This is a result of the satellite selection scheme (three on the horizon and one at the user's zenith). Note that all in view (i.e., 12 channel) receivers are improved over the early receivers, such as the receiver we used on DC- X, typically had five to six channels). Also, the GPS constellation errors have been reduced. The Global Positioning System Standard Positioning Service Performance Standard (Oct 2001) commits the U.S. Government to provide user equipment range errors of less than or equal to 6 meters RMS across the entire constellation (Tables C-3 through C-5).

C3.4 Aero Surface Actuator Loading

Based on current estimates of vehicle size (and in particular aero surface actuator size) preliminary actuator moment requirements (without margin) were developed. For this analysis, a simple flat plate estimation was used (with a panel load coefficient of 1.0). In further studies actual aerodynamic analysis of the actuator will be used to update this value. During entry, the entry corridor will be defined to constrain heating and loads. Typically, loads for "this type" of vehicle can be constrained to not exceed 300 psf dynamic pressure, so that value is used in the maximum aero force calculation. For each actuator, an estimate of its surface area was generated and used in the force (and moment) calculation.

$$Force = C_{plate} \cdot S_{ref} \cdot \bar{Q}$$

$$Moment = Force \cdot (X_{CP} - X_{hinge})$$

C3.4.1 Body Flaps

Although body flaps may not be required (elevons may provide the necessary roll and pitch authority, but this will be further analyzed) an estimate of their hinge moments are provided. It is assumed there are two flaps, each 3 feet wide and 3 feet long. This results in a max panel force of 2,700 lb and a max panel hinge moment of 4,050 ft-lb when the CP is located at the center of the panel.

C3.4.2 Elevon

The elevon is triangular shaped, with a rectangular aft portion. The aft rectangle is assumed to be 2 feet wide and 0.5 foot long. The forward section (extending forward from the rectangle) is 3.5 feet long (sloping in from the outboard edge to where the rudder attaches to the wing). See Figure C-3.

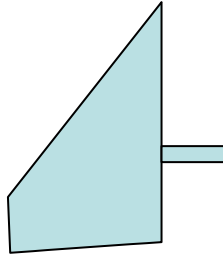


Figure C-3 – Left Wing Elevon with Actuator Rod

This produces an area of 4.5 sq-ft resulting in a maximum panel load of 1,350 lb. Hinge moments are more difficult to estimate for a fully rotating panel. For this analysis, it is assumed that the actuator is attached at a point that bisects the area equally and that the panel load is then applied at a point half way from the actuator pin to the aft end. (This isn't actually correct, but is very conservative and should be good enough for this cursory analysis.) Based on this, the hinge moment (actually the moment required of the actuator pin to rotate the panel) is 810 ft-lb.

C3.4.3 Rudder

The rudder is assumed to be 6 feet tall, extending 2 feet in length aft of the hinge. This results in a maximum panel force of 3,600 lb and a hinge moment of 3,600 ft-lb.

C3.4.4 Candidate Actuators

Table C-4 summarizes the actuator hinge moment requirements and documents actuator force requirements based assuming 2 inch and 3 inch moment arms.

Table C-4 – Actuator Hinge Moment and Force Requirements

	Hinge Moment (ft-lb)	Hinge Moment (in-lb)	Force (lb, 2 in)	Force (lb, 3 in)
Body flap	4050	48600	24300	16200
Elevon	810	9720	4860	3240
Rudder	3600	43200	21600	14400

Candidate actuators are shown in Tables C-5 and C-6.

Table C-5 – EMA Attributes

		Surface / Nozzle Rate (°/sec)	Hinge Moment Req'd (in lbs)	Moment Arm (in)	Stroke (in)	Linear Rate (in/s)	Force (lb)	Freq Response (Hz)	Input Power (hp)	VDC	Peak current @ system voltage	Actuator Weight (lbs)	Controller Weight (lbs)	Redundancy
X-33														
	Elevon (inbd & outbd)	31.5	71,250	3.31 (max), 2.85 (min)	± 1.66	1.74	25,000	4.2	21.5	270	59.3			Dual
	Rudder	30	43,000	3.2 (max), 1.5 (min)	+1.6/-2.8									
1st Stage Launch Vehicle TVC		20			+5.3/-5.5	13.47	20,000	8	28	270	91.5	90	15-20	Simplex
TVC					4.4	3.33	13,200		15.3	120	95.3	33		
2nd Stage Launch Vehicle TVC		10			± 1.54	3.86	1000	4	0.5	28	15.75	8.5	5-15	Simplex
RL-10 control valves (DC-X)		560	150	NA	142°	NA	NA	5		112	5.5	5.5	5.6	Simplex

Table C-6 – Hydraulic Actuators

		Force E/R (lbs)	Actuator Hydraulic Redundancy	Stroke (in)	Weight (lbs)	Comments
F/A-18 A-D						
	Horizontal stabilizer	29950 / 27540	Dual	7.06 - 7.18	82.5	Includes manual input
	Trailing edge flap	17750 / 13000	Dual		43	
	Aileron	13000 / 12100	Simplex		17	
	Rudder	15500 / 13350	Simplex		22	
F-15						
	Stabilator (F-15 A-D)	42500 / 39030	Dual	7.91	64	
	Stabilator (F-15 E)	42500 / 38700	Dual	7.93	81	
	Aileron	23400 / 19000	Simplex	1.468	25	
	Rudder	22000	Simplex		25	
	Diffuser ramp	19900	Simplex	10.17	17	
DC-X						
	Aero surface	6060	Simplex	± 3.3	25	Reworked Thor actuator (41.2" L)
	TVC	1932	Simplex	± 3.235	30	Reworked Thor actuator (31.5" L)

C3.4.5 Actuation Options (Aerosurface and TVC)

Three types of actuators are shown in Figure C-4. Hydraulic actuation is currently used in the F/A-18, B777, and F-22 control surfaces. The F-35 (JSF) and A380 are using EHA control surface actuation (the A380 is also using hydraulic actuators). Usage of EHAs eliminates the central hydraulic system and associated distribution plumbing, reducing weight and leak potential. Several EMA demonstration programs have been conducted, demonstrating high power EMA implementations (primarily TVC and control surface actuation). EMA usage has primarily been limited to lower power requirement usages (e.g. valve actuation). Note that the X-33 used EMAs for control surface actuation (25K lb design force, 1.74 in/sec rate). EMAs eliminate hydraulics entirely and the associated servicing and thermal concerns at the expense of increased electrical power requirements). For a given size actuator, an EMA will require the most electrical power and a hydraulic actuator the least. In many cases, EMAs will be powered by higher voltage (120 VDC or 270 VDC) to reduce current requirements and hence component size (analogous to increasing pressure in a hydraulic system).

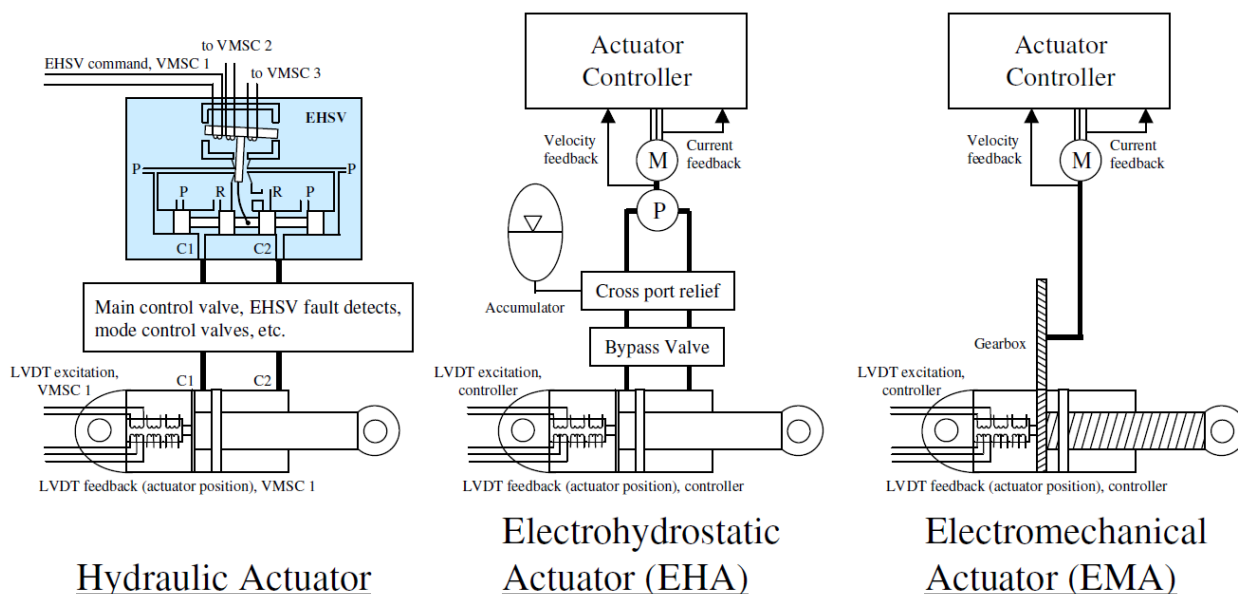


Figure C-4 – Actuation Comparison

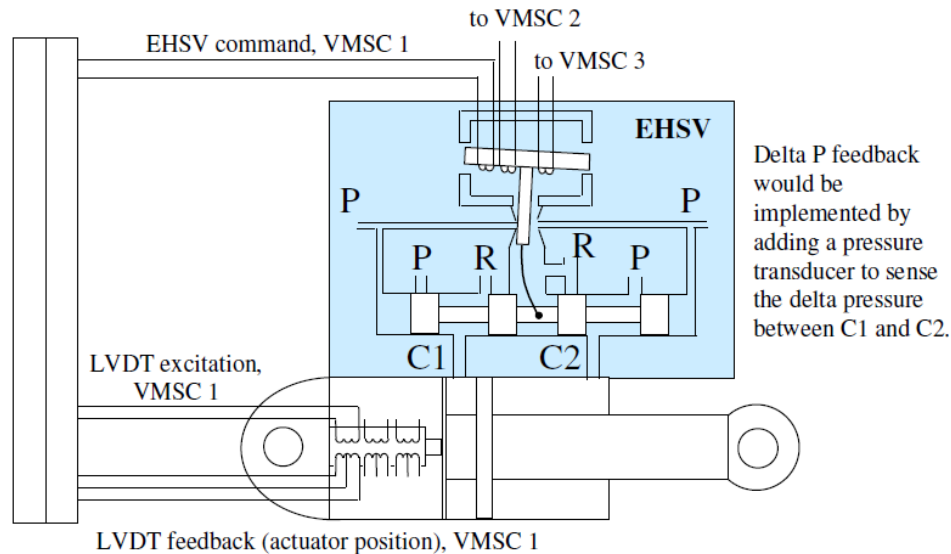


Figure C-5 – Hydraulic Actuator

C3.4.5.1 Hydraulic Actuator Implementation

Figure C-5 depicts a simple hydraulic actuator to illustrate the typical primary interfaces. More complex actuators may have additional interfaces (e.g., dual EHSVs, EHSV fail detects, a main control valve (with LVDT position), solenoid shut off valves, mechanical input).

The actuator depicted is hydraulically simplex (critical reusable vehicle flight control actuators are typically hydraulically dual) and uses an electrohydraulic servovalve (EHSV) to control the position (extend and retract) of the main ram as shown. The EHSV spool valve shuttles in response to EHSV command current to connect pressure to C2 and return to C1 (retract) or pressure to C1 and return to C2 (extend). The EHSV may be substituted with a direct drive valve (DDV, either linear or rotary) that directly moves the spool valve (electrical current requirements are higher, but these valves are not prone to plugging as EHSVs are).

A linear variable differential transformer (LVDT) is used to provide main ram position feedback. Electrical interfaces to the EHSV and LVDT are typically redundant to provide fault tolerance and interface with the loop closure electronics located in the vehicle management system computers (VMSCs) (called flight control computers in the F/A-18, actuator control electronics in the B777, and vehicle management system racks in the F-22). Note that the transition from redundant to simplex occurs at a device where the probability of a single point failure affecting all channels is minimized. Each of the redundant EHSV and LVDT electrical inputs is connected to one of the redundant VMSC channels. Main control valve position (for more complex actuators) or main ram differential pressure may also provide actuator control loop rate feedback (not depicted on the actuator diagram). The LVDTs may include center taps for fault monitoring. If center taps are not included (for cost or other reasons), cross channel monitoring is used for fault detection.

A hydraulically dual actuator duplicates the actuator hydraulic control elements (e.g., EHSV) with additional ports (e.g., C3 and C4) that control the main ram (either in a series or tandem configuration).

C3.4.5.2 Electrohydrostatic Actuator Implementation

EHAs use a reversible, DC motor driven pump to direct pressure to either the C1 or C2 port of the main ram to extend or retract the actuator. Hydraulic fluid storage is integral to the actuator and components are manifolded to minimize leak potential.

Actuator loop closure and motor commutation electronics are typically housed in an enclosure separate from the VMSCs (due to EMI concerns associated with motor commutation, proprietary design issues, and / or differing redundancy levels).

The typical dual implementation is to duplicate the control elements (e.g., actuator control electronics, motor, pump, reservoir, etc.) with additional ports (e.g., C3 and C4) that control the main RAM.

C3.4.5.3 EMA Implementation

EMAs eliminate all hydraulics and use a DC motor to drive a ball screw actuator via a gearbox.

Actuator loop closure and motor commutation electronics are typically housed in an enclosure separate from the VMSCs (due to EMI concerns associated with motor commutation, proprietary design issues, and / or differing redundancy levels).

The typical dual implementation is to duplicate the control elements (e.g., actuator control electronics, motor) such that either channel can drive the ball screw actuator.

C3.4.5.4 Actuator Considerations

The move to the more electric aircraft seeks to eliminate the central hydraulic system and plumbing by replacing hydraulic actuators with EMAs and/or electrohydrostatic actuators (EHAs). There are several motivations. Elimination of the redundant distribution systems will reduce maintenance requirements through the removal of equipment and lines typically spread throughout the vehicle and minimized leak potential. Survivability will be enhanced by reducing the vulnerable area of the vehicle. Weight will also likely be reduced through the elimination of redundant hydraulic distribution to critical actuators. This is especially true for larger aircraft with longer tubing runs and higher horsepower actuators. Area used for systems routing can be reduced. There also is a desire to remove (or at least minimize) a flammable liquid operating at high temperature and pressure.

These benefits don't come for free. An EMA or EHA will be heavier than an equivalent hydraulic actuator and its loop closure electronics will be heavier than loop closure electronics for a hydraulic actuator. This increased actuator weight is partially due to the additional components required (e.g., motors, pumps, gearboxes, etc.). An EHA power system must be sized to provide full power capability for the actuator, whereas a central hydraulic system is sized to worst case overall system needs (i.e., less than the sum of the maximum flow rates of all of the actuators).

Another area to be aware of is failure state. Hydraulic actuators can be designed to fail in a desired state (i.e., damped, stowed, etc.). Since EHAs are essentially hydraulic actuators, this is also generally true for EHAs. EMAs typically fail at the last commanded position and typically have a backdrive force requirement specified, for example enabling a control surface to align

with the aerodynamic force. Some folks have expressed concern with the EMA ball screw failures (e.g. jamming) as opposed to the ram of a hydraulic actuator.

C3.5 Vehicle Management System

The vehicle management system (VMS) provides the core processing required to operate and control the vehicle.

The vehicle management system (VMS) will provide the following functionality.

- Vehicle guidance, navigation, and control
- Attitude control
- Engine control
- TVC control
- Tank pressurization
- Tank gauging
- Data gathering and provision to ground personnel
- Process system commands (received via a command uplink)
- Separation system initiation (for a second stage variant)
- Parachute initiation (vertical landing variant)
- Landing gear initiation
- Payload interface provision (for a second stage variant)
- System health verification (to the extent possible as dictated by interfacing equipment).
- Modular user interface (for global transport variant, not included in demonstrator weight)

C3.5.1 Vehicle interfaces

The VMS configuration is largely determined by the number, type (electrical definition), and locations of the vehicle interfaces. Interface definition is also required to estimate power requirements, wiring weight/cost, and telemetry data rate. The desired data rates are required to estimate processing requirements, data bus utilization (if applicable), and telemetry data rate.

An initial HOT EAGLE VMS subsystems interface list is shown in Table C-7. The list was used as a representative set of interfaces to define VMS requirements.

The VMS interfaces also include vehicle operational interfaces such as hard line telemetry, ground processing/launch control, software load, etc. and data bus and other interfaces to other avionics and communications elements.

Interface provisions also need to be made to accommodate the payload or personnel module. The demonstrator vehicle will only include provision for a payload interface.

Table C-7. VMS Interfaces

		SAMPLE RATE (HZ)	BPS	Pressure	Temperature	Discrete output (O/G)	Discrete input (O/G)	Valve driver	Actuator interface	Frequency	Gauging
VEHICLE PROPULSION											
Oxidizer Propellant System											
	Oxidizer Pump Inlet Pressure	12.5	200	1							
	Oxidizer Pump Inlet Temperature	12.5	200		1						
	Oxidizer Fill and Drain Valve Open Control	12.5	12.5					1			
	Oxidizer Fill and Drain Closed Talkback	12.5	12.5				1				
	Oxidizer Chilledown Valve Open Control	12.5	12.5					1			
	Oxidizer Chilledown Valve Open Talkback	12.5	12.5				1				
	Oxidizer Chilledown Valve Close Talkback	12.5	12.5				1				
	O2 Autogenous Pressurization Supply	12.5	200	1							
	O2 Autogenous Low Flow Pressurization Valve	12.5	12.5					1			
	O2 Autogenous High Flow Pressurization Valve	12.5	12.5					1			
	O2 Tank Re-Pressurization Valve	12.5	12.5					1			
	Oxidizer Vent Valve Open Control	12.5	12.5					1			
	Oxidizer Tank Pressure 1, 2, 3	12.5	600	3							
	Oxidizer Cut-off Propellant Gauging 1, 2, 3	12.5	37.5								3
	Oxidizer Fill Propellant Gauging 1, 2, 3	12.5	37.5								3
Fuel Propellant System											
	Fuel Pump Inlet Pressure	12.5	200	1							
	Fuel Pump Inlet Temperature	12.5	200		1						
	Fuel Fill & Drain Valve Open Control	12.5	12.5					1			
	Fuel Fill & Drain Closed Talkback	12.5	12.5				1				
	Fuel Chilledown Valve Open Control	12.5	12.5					1			
	Fuel Chilledown Valve Open Talkback	12.5	12.5				1				
	Fuel Chilledown Valve Close Talkback	12.5	12.5				1				
	Fuel Low Flow Pressurization Valve	12.5	12.5					1			
	Fuel High Flow Pressurization Valve	12.5	12.5					1			
	Fuel Tank Re-Pressurization Valve	12.5	12.5					1			
	Fuel Vent Valve Open Control	12.5	12.5					1			
	Fuel Tank Pressure 1, 2, 3	12.5	37.5	3							
	Fuel Cut-off Propellant Gauging 1, 2, 3	12.5	37.5								3
	Fuel Fill Propellant Gauging 1, 2, 3	12.5	37.5								3
Pressurization System											
	Helium Storage Pressure	12.5	200	1							
	Helium Storage Temperature	12.5	200		1						
	Helium Regulator 1 Downstream Pressure	12.5	200	1							
	Helium Regulator 2 Downstream Pressure	12.5	200	1							
	Helium Regulator Downstream Temperature	12.5	200		1						
	Engine Fuel System Purge Valve	12.5	12.5					1			
	Engine Oxidizer System Purge Valve	12.5	12.5					1			
GN2 Purge System											
	Vehicle Cavity Temperatures	12.5	600		3						

Table C-7. VMS Interfaces (cont.)

		SAMPLE RATE (HZ)	BPS	Pressure	Temperature	Discrete output (O/G)	Discrete input (O/G)	Valve driver	Actuator interface	Frequency	Gauging
RCS											
	Storage Pressure	12.5	200	1							
	Storage Temperature	12.5	200		1						
	Nitrogen regulator 1 Downstream Pressure	12.5	200	1							
	Nitrogen regulator 2 Downstream Pressure	12.5	200	1							
	Nitrogen regulator 1 Downstream Temperature	12.5	200		1						
	Nitrogen regulator 2 Downstream Temperature	12.5	200		1						
	Cluster Inlet temperature	12.5	800		4						
	Thruster Valve	50	800					16			
MAIN ENGINE INSTRUMENTATION											
	<i>Main Engine Turbomachinery</i>										
	Oxidizer Pump Inlet Pressure	12.5	800	4							
	Oxidizer Pump Discharge Pressure	12.5	800	4							
	Oxidizer Turbine Inlet Pressure	12.5	800	4							
	Fuel Pump Inlet Pressure	12.5	800	4							
	Fuel Pump Discharge Pressure	12.5	800	4							
	Fuel Turbine Inlet Pressure	12.5	800	4							
	Oxidizer Turbine Inlet Temperature	12.5	800		4						
	Fuel Turbine Inlet Temperature	12.5	800		4						
	Oxidizer Rotor Speed Sensor	50	3200							4	
	Fuel Rotor Speed Sensor	50	3200							4	
	<i>Main Engine Injector</i>										
	Oxidizer Injector Inlet Pressure	50	3200	4							
	Fuel Injector Inlet Pressure	50	3200	4							
	Oxidizer Injector Inlet Temperature	12.5	800		4						
	Fuel Injector Inlet Temperature	12.5	800		4						
	<i>Main Engine Thrust Chamber</i>										
	Chamber Temperature 1	12.5	800		4						
	Chamber Temperature 2	12.5	800		4						
	TCA Fuel Jacket Inlet Pressure	12.5	800	4							
	TCA Fuel Jacket Inlet Temperature	12.5	800		4						
	TCA Fuel Jacket Outlet Temperature	12.5	800		4						
	Chamber Pressure 1, 2	50	6400	8							
	<i>Main Engine Valves</i>										
	Main Oxidizer Valve Controller	50	3200						4		
	Main Fuel Valve Controller	50	3200						4		
	Oxidizer Supply Valve Open Control	12.5	50					4			
	Fuel Supply Valve Open Control	12.5	50					4			
	Thrust Chamber Augmented Spark Igniter	12.5	50					4			
	Oxidizer Purge Valve Open Control	12.5	50					4			
	Fuel Purge Valve Open Control	12.5	50					4			
	Oxidizer Valve Open Talkback	12.5	50				4				
	Oxidizer Valve Closed Talkback	12.5	50				4				
	Fuel Valve Open Talkback	12.5	50				4				
	Fuel Valve Closed Talkback	12.5	50				4				

Table C-7. VMS Interfaces (concl.)

			SAMPLE RATE (HZ)	BPS	Pressure	Temperature	Discrete output (O/G)	Discrete input (O/G)	Valve driver	Actuator interface	Frequency	Gauging
ACTUATION												
	Control Surfaces											
		Body flap - port	50	800						1		
		Body flap - starboard	50	800						1		
		All moving elevon - port	50	800						1		
		All moving elevon - starboard	50	800						1		
		Rudder - port	50	800						1		
		Rudder - starboard	50	800						1		
LANDING GEAR												
		Gear down command	12.5	50					4			
		Gear up and locked indication	12.5	50			4					
		Gear down and locked indication	12.5	50			4					
PARACHUTE DEPLOYMENT												
		Drouge Release	12.5	12.5					1			
		Drouge Deploy	12.5	12.5					1			
		Main Deploy	12.5	12.5					1			
TOTALS				49475	59	46	8	22	57	14	8	12

C3.5.2 Memory and throughput

Memory and throughput requirements for a reusable vehicle exceed those of a expendable launch vehicle as reusable vehicles are generally more complex (i.e., additional systems), must accommodate re-entry and landing, and typically include functionality to assist in maintenance and turn around activities. Still, requirements are within the capability of currently available systems.

C3.5.3 Obsolescence

Obsolescence is a big issue for the VMS and avionics in general. The rate at which the VMS will become obsolete will largely depend on the configuration selected (i.e., based on commercial product versus military product and parts selected). The VMS design must ultimately include addressing the obsolescence issue to present a complete life cycle picture. Consideration must also be given to the usage of operating systems and software methodologies that abstract the software from the peculiar hardware to minimize the effort associated with rehosting the software.

C3.5.4 VMS Baseline Configuration

The baseline VMS / avionics configuration is shown in Figure C-6.

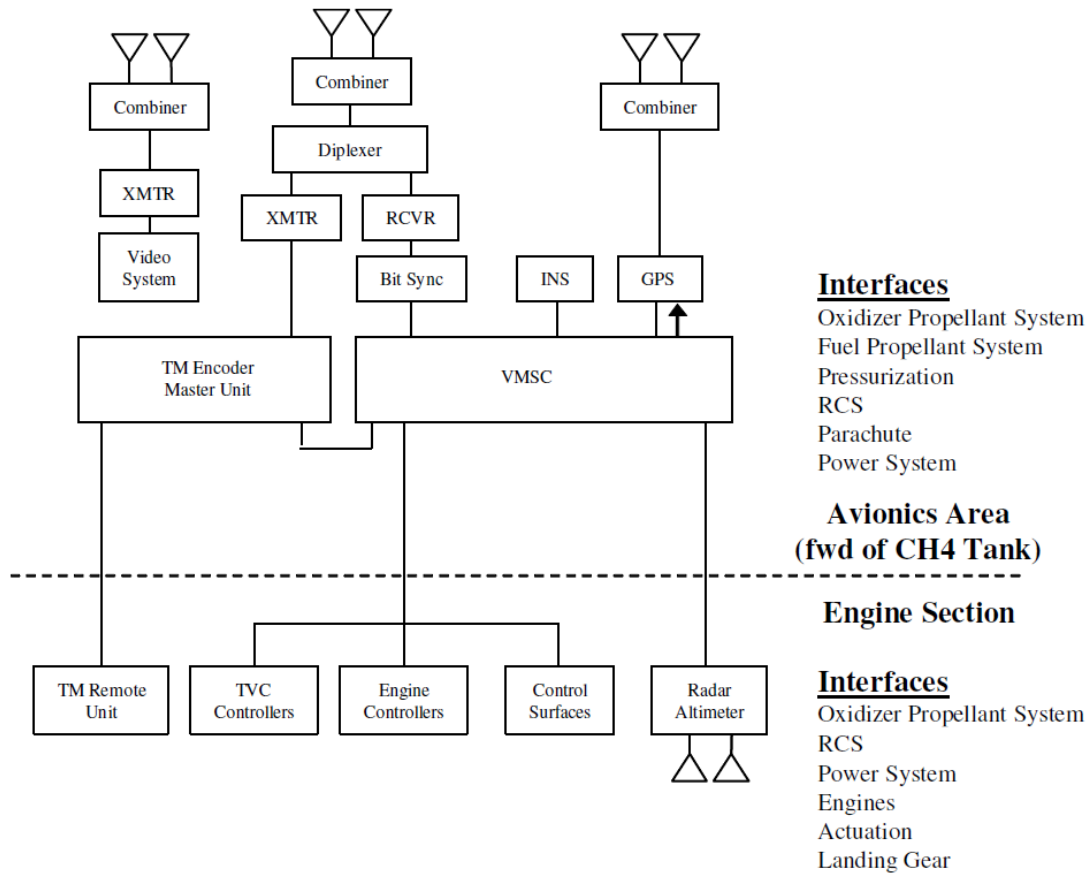


Figure C-6 – Baseline Avionics Configuration

The system consists of a VMS computer (VMSC) located in the avionics area interfaced to distributed control elements located in the engine section via a data bus. The VMSC interfaces with the systems located in the avionics area and the distributed controllers interface with systems located in the engine section as noted on the diagram. Additional distributed controllers may make sense to reduce wiring weight.

C3.6 Instrumentation and Communications

An instrumentation system (telemetry remote unit(s) and master unit) is included to acquire and process vehicle data. Vehicle instrumentation and data is required to support vehicle operations, maintenance activities, and the substantiation of design analyses. Operational data is required to service, control, and monitor the vehicle. Maintenance data is required to status vehicle integrity for flight preparation and vehicle turn around tasking. Additional flight test instrumentation is typically included to substantiate design analyses and associated assumptions. Flight test instrumentation may be accommodated with the addition of modules and remote units to the existing system or the addition of a completely separate system. The baseline configuration does not include accommodation for additional flight test instrumentation. It is assumed that weight allocation for flight test instrumentation would be taken from payload capability.

Command and telemetry interfaces with ground personnel are included to provide the capability to monitor flight events and command abort modes. A minimum of two antennas (i.e., top and

bottom) will be required to maintain connectivity. Note that the bottom antenna must accommodate the re-entry heating environment.

We've also included the provision for a video system. L3 Telemetry West offers a video compression system (VCS 700) that can select from 4 or more video cameras and provide a single video feed to the ground (3.1 inches W by 3.5 inches L by 3.5 inches H, < 2 lb). A separate transmission path is provided due to minimize the data rate of each link.

C3.7 Flight Safety Systems

Regulatory and certifying agencies require flight safety systems (in accordance with AFSPCMAN 91-710, RCC319-99, RCC 324-01, or similar documents) to track vehicle flight and terminate flight in the event of anomalous flight.

Two independent and adequate sources of tracking data are required. This is typically the vehicle navigation solution data transmitted to the ground via telemetry and a second source. The second source has typically been radar transponder, but recently independent GSP receiver data transmitted on an independent telemetry link have been used.

The traditional flight termination system consists of two UHF antennas interfaced to two receivers using a hybrid such that each receiver can see both antennas. The receivers initiate flight termination based on commands received from ground personnel. Termination is a basic two-step procedure, the arm command terminates thrust and the destruct command initiates vehicle destruction. Each receiver is powered by an independent power source as shown in Figure C-7.

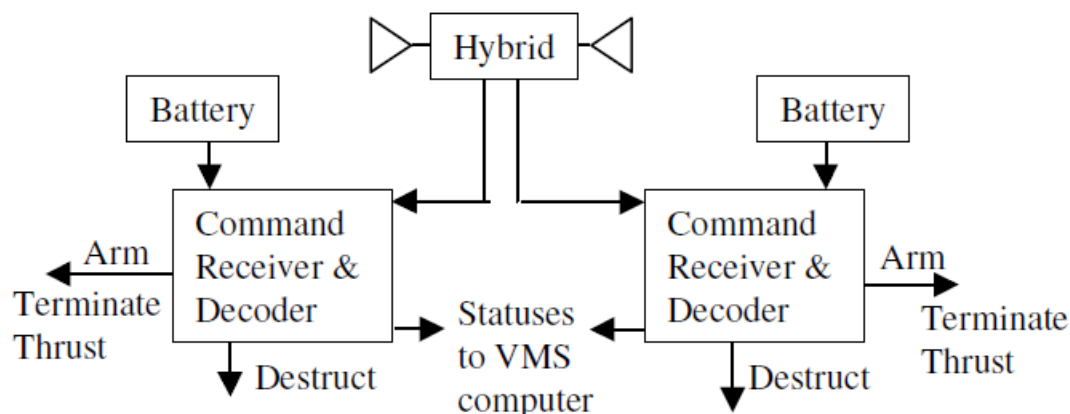


Figure C-7 – Traditional Flight Termination System

An emerging approach is to implement an autonomous flight safety system (AFSS) eliminating the required ground linkage and launch infrastructure. An example implementation is shown in Figure C-8.

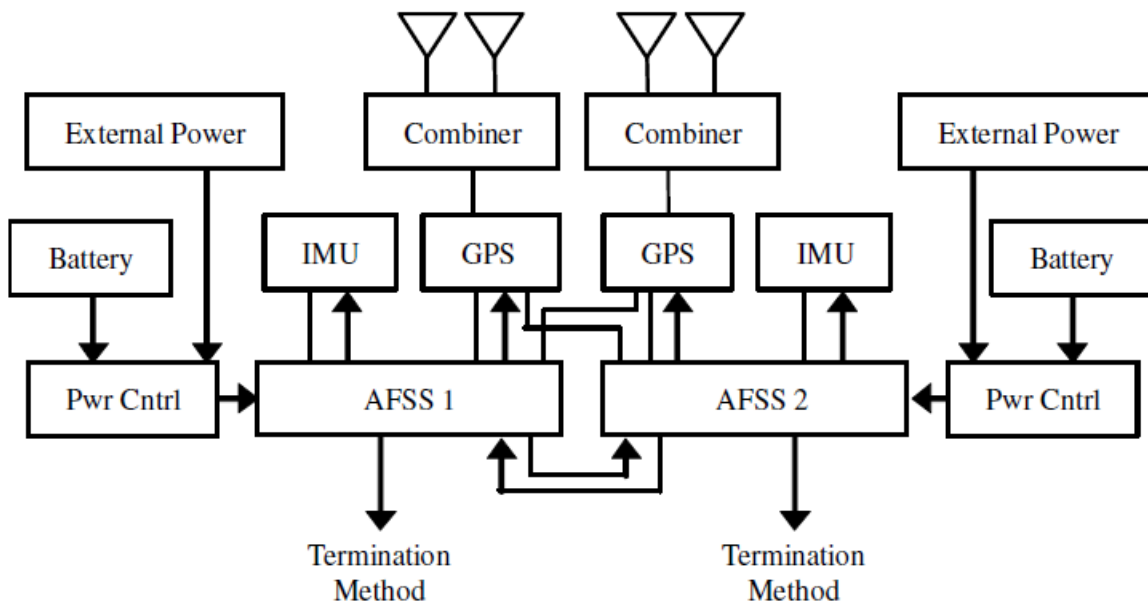


Figure C-8 – Autonomous Flight Safety System

We may choose to implement an AFSS on the HOT EAGLE demonstrator vehicle to demonstrate the capability. At least three flights are required to demonstrate the AFSS implementation. As such, the demonstrator vehicle will be required to carry the traditional flight safety systems until the AFSS has been demonstrated.

The traditional FTS weight is included in the HOT EAGLE systems weight summary. The AFSS system weight isn't included as it's roughly equivalent to the FTS weight, which would be removed for an operational vehicle. For flight test, the added weight for carrying both systems would need to come out of the payload capability. We may also not want to pursue an AFSS for the demonstrator, so including the weight would unnecessarily penalize the vehicle.

C3.8 Power

Total amp-hour and maximum current requirements are needed to specify the power source. These requirements are determined using an operational timeline (equipment sequencing and powered durations (duty cycles)) and equipment power requirements. Margin is added as required (based on data maturity and desired timeline margin).

Usage of EMAs would drive the usage of a two voltage level power system, high voltage for actuation (likely 270 VDC) and low voltage for the other systems (28 VDC). Higher voltage is used to reduce current requirements and hence wire and component size. Even many lower force systems use voltages greater than 28 VDC to minimize current requirements and hence weight.

The HOT EAGLE vehicle will use lithium-ion batteries. Lithium-ion batteries have very high specific energy and energy density and a very low self-discharge rate (~5% capacity loss after 3 months). Lithium-ion batteries are being used by the F-35, being retrofit into the B-2 (Lithion, Inc.), and have been used in space (AEA Technology).

C3.9 Reaction Control System

An initial HOT EAGLE RCS sizing (shown below) indicated that RCS placed in the nose would be more efficient than an aft location.

Moment arm (thruster location):

Assumptions using data from MicroX vehicle layout

Thrusters near nose provide ~16-foot lever arm to C.G. along body X axis (pitch and yaw) They provide about 2-foot lever arm along Y axis (roll)

Thrusters near base provide ~10-foot lever arm to C.G. along body X axis (pitch and yaw) They provide about 3-foot lever arm along Y axis (roll)

=> Nose is better location, but packaging may be problematic.

Assume two clusters of three thrusters each, one cluster on each side.

Weight during entry is approximately 12,500 lb

Moments of inertia (roughly estimated):

Baseline vehicle: $I_{yy} = I_{zz} = 32,000 \text{ slug-ft}^2$; $I_{xx} = 4,400 \text{ slug-ft}^2$ Troop carrier: $I_{yy} = I_{zz} = 50,000 \text{ slug-ft}^2$; $I_{xx} = 5,200 \text{ slug-ft}^2$

For analysis, assume $I_{yy} = I_{zz} = 40,000 \text{ slug-ft}^2$; $I_{xx} = 5,000 \text{ slug-ft}^2$

Assume RCS is only used exo-atmospheric (no aero disturbance). Since vehicle is aerodynamically stable, there is no need for it in atmosphere. These assumptions were used for this initial RCS sizing. In actuality, the vehicle is not aerodynamically stable and we will use RCS in the upper atmosphere.

Thruster sizing:

For design purposes, assume we want vehicle to achieve max attitude rate of 5 deg/sec in 10 sec: $0.5 \text{ deg/sec/sec} = .00873 \text{ rad/sec/sec}$.

For MOIs assumed, this requires: 350 ft-lb in pitch and 45 ft-lb in roll. For a nose RCS: Requires 22 and 23 lbf respectively (pitch and roll).

Assuming 2 “on” thrusters, this puts RCS thrust at 10 – 12 lbf each. (pitch and roll, yaw uses 1 thruster)

For aft RCS: Requires 35 and 15 lbf, respectively. Use 35 lbf at driver, so each thruster needs to be 15 to 20 lbf.

=> Again, nose is better (similar moments for common thrusters)

Want attitude rate to be within a +/- 0.1 deg/sec band.

Use half this band to set minimum pulse: 0.1 deg/sec (with 0.5 deg/sec/sec from above)

Results in 0.2 sec minimum pulse width. (i.e., thrust has to be able to turn off (no thrust) within 0.2 sec of start.)

Fuel usage:

Large Maneuver:

Since 10 sec required to reach max attitude rate (and another 10 sec to stop), each “large maneuver” requires 20 sec of thruster ON time.

Assume one Large maneuver per orbit (very conservative) and a 10 orbit flight. (Or

alternatively, assume 10 of the vehicle's orbits will require a large maneuver.) Results in 200 sec of ON time.

Small Maneuver (station keep):

Since +/- 0.1 deg/sec band on attitude rate, assume half (0.05 deg/sec) is average attitude rate.

Assuming a +/- 1 deg attitude error band, it takes 40 sec to "cross" the band.

With a 0.2 sec min ON time, there is a .2 sec burn every 40 sec (limit cycling), or .3 sec/min = 27 sec ON time per orbit.

With 10 orbits, results in 270 sec ON time.

Total ON time per flight: 470 sec.

For Cold gas, assume 30 sec Isp: Nose RCS: $22/30 \times 470 = 345$ lb gas

Aft RCS: $35/30 \cdot 470 = 550$ lb gas

Bi-prop, assume 300 sec Isp: Nose: 35 lbs propellant

Aft: 55 lbs propellant

For comparison: X-15 had 100 lb roll thrusters and 150 lb pitch/yaw thrusters, but had MOI of 30,000 and 200,000 sl-ft², respectively (5 times that of MicroX). Scaling X-15 by 1/5 results in 20 lb and 30 lb thrusters for roll and pitch, comparable to my results above.

The RCS baseline includes 8 thrusters located in the nose of the vehicle. The assumed configuration is 2 up, 2 down, 2 right, and 2 left. The downward pointing thrusters would likely need to point at an approximately 45 degree angle off vertical to avoid penetrating the TPS on the bottom of the vehicle (similar to the Shuttle nose RCS and X-33 RCS installations).

C4. Systems Weight Estimate

C4.1 Battery Sizing

Figure C-9 provides an estimate of HOT EAGLE power requirements. The Figure C-9 analysis was performed for a VTVL configuration and the mission timeline defined in the HOT EAGLE Interim Report 2, dated 30 August 2005. The VTVL configuration was chosen as power requirements are assumed to be slightly greater for a powered landing. The HOT EAGLE avionics and subsystems are per Section C-3 herein using EMAs for aerosurface and TVC actuation to scope the associated power requirements. Loads are identified with duty cycles estimated per flight phase to generate a current profile and overall power (amp-hour) requirement. The analysis assumes that nonessential loads are turned off during the orbital coast to reduce power requirements. A healthy margin (50%) was added to the power requirement due to the uncertainty in the load, duty cycle, and equipment estimates.

The power requirements were then used to size the 28 VDC and 270 VDC batteries. Table C-8 shows the resulting battery weights using AEA Technology 180 Wh/kg lithium ion cells (AEA 18650LV cells). 20% was added to the cell weights to account for enclosures based on existing battery characteristics.

Table C-8 – Battery Sizing, Baseline Mission, Power Control

			Amp Hours	Watt Hours	Weight (180 Wh/kg)	Weight, cells (lb)	Weight
28 VDC Battery Sizing			342.16	9580.4	53.2	117.1	140.5
270 VDC Battery Sizing			53.69	14495.2	80.5	177.2	212.6

The impact of using pneumatic TVC actuation was also examined. This configuration would essentially replace the EMA electric motors with an air motor. The impact to the actuation power is shown in Table C-9.

Table C-9 – Battery Sizing, Baseline Mission, Pneumatic TVC

			Amp Hours	Watt Hours	Weight (180 Wh/kg)	Weight, cells (lb)	Weight
28 VDC Battery Sizing			342.16	9580.4	53.2	117.1	140.5
270 VDC Battery Sizing			36.05	9734.2	54.1	119.0	142.8

Pneumatic actuation wouldn't change the actuator weight much as the electric motor would be replaced by an air motor as shown in Figure C-9. The potential weight savings is in the 270 VDC battery sizing (approximately 70 pounds (212.6 – 142.8)). Much if not all of this savings would be offset by the required pneumatic system plumbing and components. In addition to the components shown in Figure C-9, we'd want to include a DC powered air motor to exercise the TVC actuators during preflight checkout or maintenance activities without requiring the engines to be operational. Although the pneumatic implementation would be insensitive to duty cycle as the electrical implementation is (i.e., the 270 VDC battery sizing is based on an assumed duty cycle with a 50% margin).

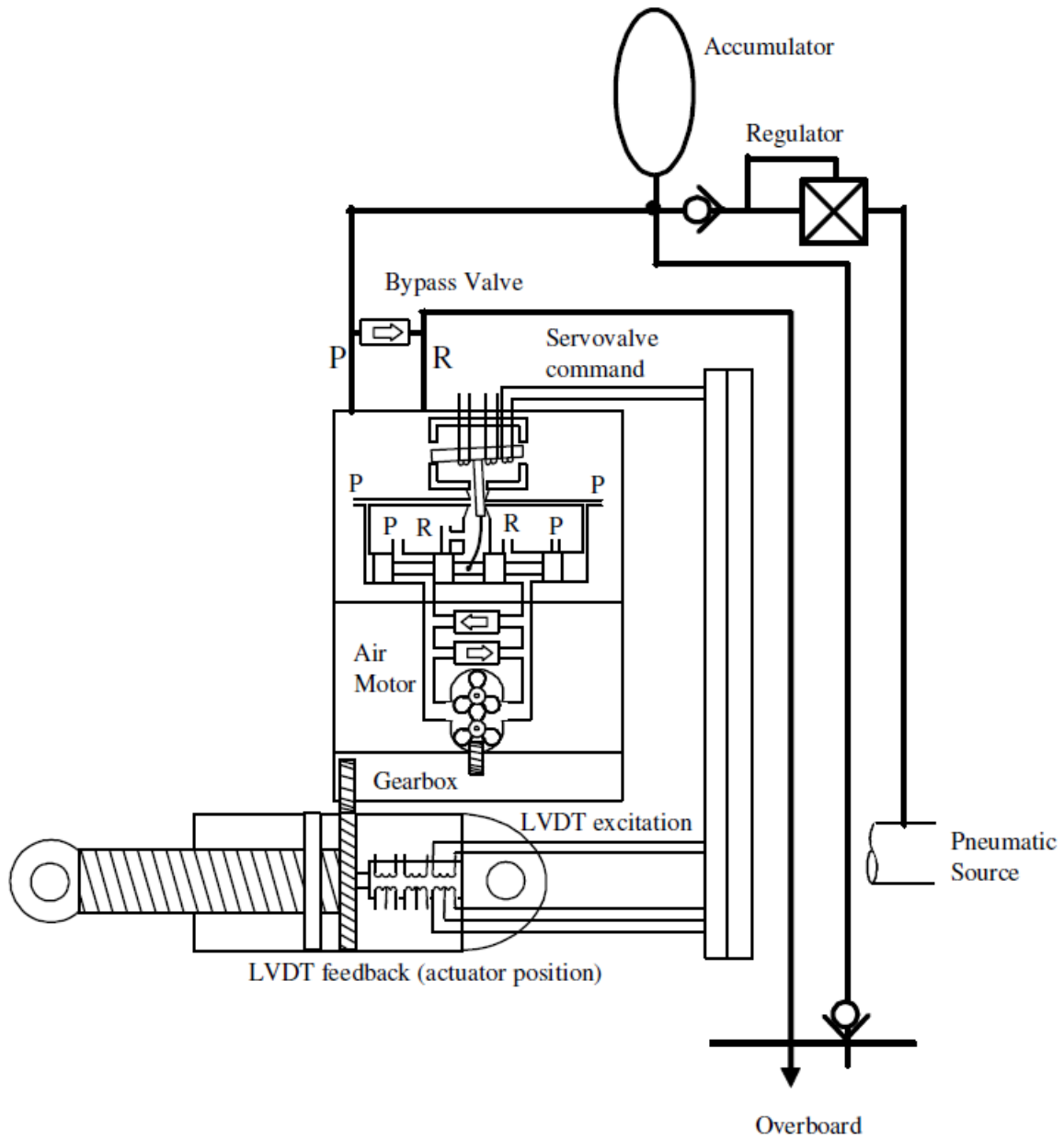


Figure C-9 – Pneumatic TVC Implementation

Table C-10 – HOT EAGLE Power Analysis

				Prelaunch		1st Stage Burn		Separation		2nd Stage Burn		Coast		2nd Stage		Payload Deploy		Coast		Deorbit		Entry - Exo		Entry - Atm		Rotation		Landing			
				-1080	sec	0	sec	229	sec	1	sec	240	sec	440	sec	3140	sec	3170	sec	3175	sec	40975	sec	41095	sec	41795	sec	43965	sec	43695	sec
				1080	sec			229	sec	1	sec	240	sec	2700	sec	30	sec	5	sec	37800	sec	120	sec	700	sec	2070	sec	25	sec	37	sec
Item		Qty	Amps	Basis		%	A	%	A	%	A	%	A	%	A	%	A	%	A	%	A	%	A	%	A	%	A	%	A		
38 VDC																															
Avionics Area (Wtd of CH4 tank)																															
VMS																															
	VMSC	1	2	Falcon (no RIU)	100	2.00	100	2.00	100	2.00	100	2.00	100	2.00	100	2.00	100	2.00	100	2.00	100	2.00	100	2.00	100	2.00	100	2.00	100	2.00	
	IMU	1	0.70	LN-200	100	0.70	100	0.70	100	0.70	100	0.70	100	0.70	100	0.70	100	0.70	100	0.70	100	0.70	100	0.70	100	0.70	100	0.70	100	0.70	
	GPS Receiver	1	0.06	DG14	100	0.06	100	0.06	100	0.06	100	0.06	100	0.06	100	0.06	100	0.06	100	0.06	100	0.06	100	0.06	100	0.06	100	0.06	100	0.06	
	GPS Combiner	1	0	NA																											
	GPS Antenna	2	0	Included in DG14																											
	Command Bit Sync	1	1.07	L3 TW ABS 400	100	1.07	100	1.07	100	1.07	100	1.07	100	1.07	100	1.07	100	1.07	100	1.07	100	1.07	100	1.07	100	1.07	100	1.07	100	1.07	
	Command Receiver	1	1.00	L3 TW TRX	100	1.00	100	1.00	100	1.00	100	1.00	100	1.00	100	1.00	100	1.00	100	1.00	100	1.00	100	1.00	100	1.00	100	1.00	100	1.00	
	Remote Air Data Modules	6	0.21	Goodrich 2014M	100	1.29	100	1.29	100	1.29	100	1.29	0	0.00	100	1.29	0	0.00	0	0.00	0	0.00	0	0.00	100	1.29	100	1.29	100	1.29	
Data System																															
	TM Encoder Master Unit	1	2.14	L3 TW	100	2.14	100	2.14	100	2.14	100	2.14	100	2.14	100	2.14	100	2.14	100	2.14	100	2.14	100	2.14	100	2.14	100	2.14	100	2.14	
	TM Transmitter	1	3.21	ST-810S	100	3.21	100	3.21	100	3.21	100	3.21	10	0.32	100	3.21	100	3.21	10	0.32	100	3.21	100	3.21	100	3.21	100	3.21	100	3.21	
	Diplexer	1	0	NA																											
	Combiner	1	0	NA																											
	Antenna	2	0	NA																											
Video System																															
	Camera	2	0.09	Sony XC555	100	0.18	100	0.18	100	0.18	100	0.18	0	0.00	100	0.18	0	0.00	0	0.00	0	0.00	0	0.00	100	0.18	100	0.18	100	0.18	
	Video Encoder	1	1.07	L3 TW VCU700	100	1.07	100	1.07	100	1.07	100	1.07	0	0.00	100	1.07	0	0.00	0	0.00	0	0.00	0	0.00	100	1.07	100	1.07	100	1.07	
	Transmitter	1	3.21	ST-810S	100	3.21	100	3.21	100	3.21	100	3.21	0	0.00	100	3.21	0	0.00	0	0.00	0	0.00	0	0.00	100	3.21	100	3.21	100	3.21	
	Combiner	1	0	NA																											
	Antenna	2	0	NA																											
Power System																															
	Power Distribution Unit	1	1.50	SWAG	100	1.50	100	1.50	100	1.50	100	1.50	100	1.50	100	1.50	100	1.50	100	1.50	100	1.50	100	1.50	100	1.50	100	1.50	100	1.50	
Oxidizer Propellant System																															
	Valve Drivers	6	1.00		50	3.00	50	3.00	50	3.00	50	3.00	20	1.20	50	3.00	20	1.20	20	1.20	20	1.20	20	1.20	20	1.20	50	3.00	50	3.00	
	Propellant Gaging Signal Conditioner	1	0.50	SWAG - LMS	100	0.50	100	0.50	100	0.50	100	0.50	100	0.50	100	0.50	100	0.50	100	0.50	100	0.50	100	0.50	100	0.50	100	0.50	100	0.50	
Pressurization System																															
	Valve Drivers	2	1.00		50	1.00	50	1.00	50	1.00	50	1.00	20	0.40	50	1.00	20	0.40	20	0.40	20	0.40	20	0.40	20	0.40	50	1.00	50	1.00	
RCS																															
	RCS Thrusters	8	1.00		5	0.40	0	0.00	0	0.00	20	1.60	5	0.40	20	1.60	5	0.40	5	0.40	20	1.60	20	1.60	5	0.40	0	0.00	0	0.00	
Engine Section																															
VMS																															
	Remote Interface Unit	1	1.50		100	1.50	100	1.50	100	1.50	100	1.50	100	1.50	100	1.50	100	1.50	100	1.50	100	1.50	100	1.50	100	1.50	100	1.50	100	1.50	
	Radar Altimeter	1	0.57	HG8505	100	0.57	0	0.00	0	0.00	0	0.00	0	0.00	0	0.00	0	0.00	0	0.00	0	0.00	0	0.00	0	0.00	100	0.57	100	0.57	
	Radar Altimeter Antenna	2	0.00	NA																											
	Control Surface Loop Closure Electronics	6	1.00	SWAG	100	6.00	0	0.00	0	0.00	0	0.00	0	0.00	0	0.00	0	0.00	0	0.00	0	0.00	50	3.00	100	6.00	100	6.00	100	6.00	
	Engine Controllers	5	2.60	Single Ch DEREK	100	13.00	0	0.00	0	0.00	100	13.00	0	0.00	100	13.00	0	0.00	0	0.00	0	0.00	0	0.00	0	0.00	0	0.00	100	13.00	
	TVC Loop Closure Electronics	5	1.50	SWAG	100	7.50	0	0.00	0	0.00	100	7.50	0	0.00	100	7.50	0	0.00	0	0.00	0	0.00	0	0.00	0	0.00	0	0.00	100	7.50	
Data System																															
	TM Remote Unit	1	1.70	L3 TW	100	1.70	100	1.70	100	1.70	100	1.70	100	1.70	100	1.70	100	1.70	100	1.70	100	1.70	100	1.70	100	1.70	100	1.70	100	1.70	
Power System																															
	Power Distribution Unit	1	1.50		100	1.50	100	1.50	100	1.50	100	1.50	100	1.50	100	1.50	100	1.50	100	1.50	100	1.50	100	1.50	100	1.50	100	1.50	100	1.50	
Fuel Propellant System																															
	Valve Drivers	6	1.00		50	3.00	50	3.00	50	3.00	50	3.00	20	1.20	50	3.00	20	1.20	20	1.20	20	1.20	20	1.20	20	1.20	50	3.00	50	3.00	
	Propellant Gaging Signal Conditioner	1	0.50	SWAG - LMS	100	0.50	100	0.50	100	0.50	100	0.50	100	0.50	100	0.50	100	0.50	100	0.50	100	0.50	100	0.50	100	0.50	100	0.50	100	0.50	
Parachute Deployment																															
	Deployment Commands - Valve Drivers	3	1.00		0	0.00	0	0.00	0	0.00	0	0.00	0	0.00	0	0.00	0	0.00	0	0.00	0	0.00	0	0.00	0	0.00	100	3.00	100	3.00	
Landing Gear																															
	Valve Drivers	4	1.00		0	0.00	0	0.00	0	0.00	0	0.00	0	0.00	0	0.00	0	0.00	0	0.00	0	0.00	0	0.00	0	0.00	0	0.00	100	4.00	
TOTALS																															
	A				57.60			30.13		30.13		52.23		17.69		52.23		20.58		17.69		21.78		29.24		32.33		39.70		64.20	
	Ah				17.28			2.00		0.01		2.90		13.27		0.44		0.03		185.77		0.73		5.69		18.59		0.28		0.66	
270 VDC																															
VMS																															
	Elevon Actuator	2	92	Hot Eagle Act Req	5	9.2	0	0	0	0	0	0	0	0	0	0.00	0	0	0	0.00	0	0	5	9.2	20	36.8	20	36.8	20	36.8	
	Rudder Actuator	2	23	Elevon / 4	5	2.3	0	0	0	0	0	0	0	0	0	0.00	0	0	0	0.00	0	0	5	2.3	20	9.2	20	9.2	20	9.2	
	Body Flap Actuator	2	92	Hot Eagle Act Req	5	9.2	0	0	0	0	0	0	0	0	0	0.00	0	0	0	0.00	0	0	5	9.2	20	36.8	20	36.8	20	36.8	
	TVC Actuator	10	92	Elevon	5	46	0	0	0	0	20	184	0	0	20	184.00	0	0	0	0.00	0	0	0	0	0	0	0	20	184		
TOTALS																															
	A				66.70			0.00		0.00		184.00		0.00		184.00		0.00		0.00		0.00		20.70		82.80		82.80		266.80	
	Ah				20.01			0.00		0.00		10.22		0.00		1.53		0.00		0.00		0.00		4.03		47.61		0.58		2.74	
0.5																															

C4.2 Weight Estimates

The following paragraphs provide HOT EAGLE system weight estimates. The weights are estimated for the HOT EAGLE demonstrator vehicle configuration and mission definition. Margin is added to the estimated weight based on the fidelity of the estimate (3% for existing items, 5% for existing items with some uncertainty, and 15% for estimates with larger uncertainty). The margin could also be applied toward system installation weight. The operational vehicle would require systems redundancy for the crewed vehicle.

C4.2.1 Electronics

The electronics were split between the area forward of the CH₄ tank and the engine section (aft of the LOX tank) as shown in Table C-11. The electronics in the engine section are placed there to be close to the various interfaces to minimize wiring weight. This split configuration complicates the active thermal control system (ATCS) requirements in that cooling is required in both areas. An ATCS is required due to the extended time on orbit and post flight heat soak from the thermal protection system.

The electronics systems included in Table C-11 are in accordance with the descriptions in Section C-3 herein.

We discussed the addition of a star tracker, but have decided to not include an additional attitude sensor at this time, pending future analysis. For reference, a Ball CT-602 star tracker weighs 11.9 pounds, without the shade. The larger impact is likely the installation, protective doors, and door actuation mechanisms.

The design includes data transmission of data to the ground only. A 10% duty cycle is included in the power analysis to provide transmission of data to the ground during the orbital coast period (1.5 hours of transmit time for the 10.5-hour orbital coast period). Alternately, one could transmit data to TDRSS. The CMC Cincinnati 30W TDRSS transmitter weighs 14.5 pounds and draws ~6.86A of power (greater than twice that of the transmitter included in the power analysis). WFF is developing a 30W TDRSS transmitter weighing ~1 pound at a significantly reduced cost as compared to the CMC Cincinnati unit.

C4.2.2 Power and Wiring

The power and wiring weight estimate is shown in Table C-12. The 28 VDC battery sizing is based on the HOT EAGLE power estimate using the AEA 18650LV cells and selectively powering the 28 VDC loads as required during the various mission phases as described in paragraph C4.1 herein.

The power distribution units house solid state power controllers (SSPCs). The SSPCs provide a relay and circuit breaker function to enable load control and protect system wiring.

The wire weight is based on the DC-X wire weight as it's a similarly sized and complexity vehicle. The HOT EAGLE estimate includes the entire DC-X avionics area wire weight plus 60% of the DC-X cable weights. Placement of HOT EAGLE electronics in the engine section should result in reduced cable lengths for the bulk of the interfaces, hence the 60% factor applied.

Table C-11 – Avionics / Electronics Weight Estimate

Item	Qty	Weight (lbs)	Margin (%)	Weight Total (lbs)	Basis	Comments
Avionics Area (fwd of CH4 tank)						
VMS						
VMSC	1	15.00	15	17.25	Space Micro	Control system redundancy required for crewed vehicles
IMU	1	18.50	3	19.06	SIGI	
GPS Receiver	1	1.19	3	1.22	DG14 (Sensor)	
GPS Combiner	1	0.20	15	0.23		
GPS Antenna	2	0.77	3	1.59	M/A-Com	
Command Bit Sync	1	1.56	3	1.61	L3 TW ABS 400	
Command Receiver	1	1.50	3	1.55	L3 TW TRX	
Remote Air Data Modules	6	2.00	3	12.36	Goodrich 2014M	
Data System						
TM Encoder Master Unit	1	6.80	3	7.00	L3 TW	
TM Transmitter	1	0.63	3	0.64	CTS 910	Assume transmission to ground only
Diplexer	1	0.50	15	0.58		
Combiner	1	0.20	15	0.23		
Antenna	2	1.00	3	2.06	M/A-Com	
Video System						
Camera	2	0.63	5	1.32	Sony XC555 & mounting	
Video Encoder	1	1.81	3	1.87	L3 TW VCU700	
Transmitter	1	0.63	3	0.64	CTS 910	Assume transmission to ground only
Combiner	1	0.20	15	0.23		
Antenna	2	1.00	3	2.06	M/A-Com	
Oxidizer Propellant System						
Propellant Gaging Signal Conditioner	1	0.94	3	0.97	Liquid Measurements Sys	
Flight termination						
Battery	2	6.60	3	13.60	Space Vector 2.2Ah (NiCd)	
CRD	2	6	3	12.36	CE CRD 120/205	
Coupler	1	0.20	15	0.23		
UHF band antennas	2	1.30	3	2.68	M/A-Com	
Range tracking						
C band transponder	1	2.69	3	2.77	Herley MD400C	
Splitter	1	0.20	15	0.23		
C band antenna	2	1.00	3	2.06	M/A-Com	
Total				106.38		
Engine Section						
VMS						
Remote Interface Unit	1	4.00	15	4.60	Space Micro	
Radar Altimeter	1	3.00	3	3.09	HG8505	Could be located in avionics area for HL configuration
Radar Altimeter Antenna	2	1.90	3	3.91	LG81BR01	
Control Surface Loop Closure Electronics	6	15.00	15	103.50	Hot Eagle Act Req	Weight reduced for hydraulic actuation
Engine Controllers	4	14.00	15	64.40	Single Ch DEREK	4 engines - HL variant
TVC Loop Closure Electronics	4	22.00	15	101.20	Hot Eagle Act Req	4 engines - HL variant, Weight reduced for hydraulic actuation
Data System						
TM Remote Unit	1	5.30	3	5.46	L3 TW	
Fuel Propellant System						
Propellant Gaging Signal Conditioner	1	0.94	3	0.97	Liquid Measurements Sys	
Total				287.13		

Table C-12 – Power and Wiring Weight Estimate

Item						Qty	Weight (lbs)	Margin (%)	Weight Total (lbs)	Basis	Comments
				Avionics Area (fwd of CH4 tank)							
				<i>Power System</i>							
				28 VDC Battery		1	140.50	15	161.58	Hot Eagle Power - VTVL, pwr control	
				Power Distribution Unit - 28		1	20.00	15	23.00		
				Engine Section							
				<i>Power System</i>							
				Power Distribution Unit - 28		1	20.00	15	23.00		
				Total (w/o battery)					46.00		
				Wiring		1	381.20	15	438.38	DC-X avionics area plus 60% cables	DC-X weight reduced based on routing distance
											Accounts for power and signal wiring
									691.96		

C4.2.3 Actuation – Electrical

The electrical actuation estimate is shown in Table C-13. The 270 VDC battery sizing is based on the HOT EAGLE power estimate using the AEA 18650LV cells and selectively powering the 28 VDC loads as required during the various mission phases as described in paragraph C4.1 herein.

The power distribution units house solid state power controllers (SSPCs). The SSPCs provide a relay and circuit breaker function to enable load control and protect system wiring.

The actuator weights are based on HOT EAGLE aero surface actuation requirements as documented in paragraph C3.4.4 herein. Note that the body flaps may not be required.

In order to compare the electrical actuation system weight with the hydraulic actuation system weight, one must add the landing gear hydraulic power source weight (as documented in Table C-15 (Gear Hydraulic Power Source (EMA configuration) entry). An accumulator and nitrogen bottle is provided as a source of hydraulic power for each gear. This brings the total electrical actuation weight to 1157.59 pounds.

C4.2.4 Actuation – Hydraulic

The Micro-X APU was used as the power source for the hydraulic pump. The Micro-X APU tanks and air weight were increased by a factor of 2.6 as the current mission profile requires ~39 minutes of run time versus the Micro-X 15 minutes. As noted on the spread sheet, there are a couple of items from the Micro- X report that may not be part of the APU system weight.

The hydraulic system component weight breakdown is a mixture of existing equipment (in some cases justified with a second estimate) and items from the Micro-X report as noted in the “Comments” column. A DC powered pump was added such that system checkout could be conducted without running the APU.

The F-16 horizontal stabilizer actuator weight from the Micro-X report was used for the aero surface weights. The F-16 horizontal stabilizer actuator weight seems light for what is most likely a dual hydraulic system actuator with a 20,000 lbf capability. Table C-6 provides attributes of other hydraulic actuators. The DC-X TVC actuator weights from Table C-6 were used for the engine TVC actuators.

Table C-13 – Electrical Actuation Weight

Item	Qty	Weight (lbs)	Margin (%)	Weight Total (lbs)	Basis	Comments
Engine Section						
Power System						
270 VDC Battery	1	212.60	15	244.49		
Power Distribution Unit - 270	1	20.00	15	23.00		
Actuators						
Elevon Actuator	2	33.00	15	75.90	Hot Eagle Act Req	
Rudder Actuator	2	90.00	15	207.00	Hot Eagle Act Req	
Body Flap Actuator	2	90.00	15	207.00	Hot Eagle Act Req	Body flaps may not be required
TVC Actuator	8	33.00	15	303.60	Elevon	4 engines - HL variant
Total				1060.99		

Table C-14 – Hydraulic Actuation Weight Estimate

Item	Qty	Weight (lbs)	Margin (%)	Weight Total (lbs)	Basis	Comments
Engine Section						
Power System						
APU (modified F-16 EPU)	1	70.00	5	73.50	Micro-X Final Report	
APU Tanks & Air	2.6	162.00	15	484.38	Micro-X Final Report	3X as final report weight provided 15 minutes - current mission requires 39.4 min
APU Installation	1	50.00	15	57.50	Micro-X Final Report	
APU Oil HX	1	40.00	15	46.00		Assume HX part of ATCS
Air Bottle	1	15.00	15	17.25	Micro-X Final Report	Not sure what this is, seems redundant to APU tanks & air
Misc Equipment	1	100.00	15	115.00	Micro-X Final Report	Not sure if this belongs as part of APU system weight
Hydraulic System						
Pump	1	8.90	3	9.17	Vickers PV3-075 (22.73 gpm)	
Reservoir	1	30.00	15	34.50	Aircraft bootstrap reservoir (600 cu in)	DC-X used 3 Thor accumulators as reservoirs (45 lbs, 576 cu in total)
Accumulator	2	15.00	15	34.50	2 Thor accumulators (DC-X)	Aircraft brake accumulator 27.55 lb, 200 cu in
DC Pump	1	22.00	15	25.30	X-36 pump	Used for ground checkout, DC-X also used DC pumps, but I don't have weights
Filters, lines, press ducers, & misc	1	50.00	15	57.50	Micro-X Final Report	Think that this is probably low
Hydraulic fluid weight	1	50.00	16	58.00	Micro-X Final Report	50 lbs, ~ 7 gallons, ~1650 cu in
Actuators						
Elevon Actuator	2	18.00	15	41.40	Micro-X Final Report	
Rudder Actuator	2	18.00	15	41.40	Micro-X Final Report	
Body Flap Actuator	2	18.00	15	41.40	Micro-X Final Report	Body flaps may not be required
TVC Actuator	10	30.00	15	345.00	DC-X TVC actuators	
Total				1481.80		

C4.2.5 Actuation System Selection

The electrical actuation system weight is used in the vehicle weight as the weight is lower than that of the hydraulic implementation. Other discriminators were also examined.

The Shuttle APU system was examined to identify potential complications as a result of the extended HOT EAGLE orbital time. A water spray boiler is used to cool the Shuttle APU oil and the hydraulic system hydraulic fluid. The water spray boiler has heaters to prevent freezing of the cooling water storage and delivery lines. The APU oil system is pressurized with nitrogen to enable APU start in zero g (one APU is started prior to entry) and heaters are used to control the oil temperature on orbit. The hydraulic system includes two electrically powered pumps to circulate fluid to keep the system warm and to keep the accumulator pressurized on orbit. Heaters are also used in areas of the hydraulic system where fluid circulation is ineffective. A water system is included to cool the APU injector in the event that an APU restart is required prior to the normal 180 minute cool down time. Heaters are used on the injector cooling and APU fuel supply and delivery system to control on orbit temperatures. The hydraulic actuation weights in Reference 2 do not include accommodations for these type of environmental issues.

It is not believed that electromechanical actuators (EMAs) have similar environmental concerns (or at least not to the same extent). EMAs typically have operating temperature ranges of -55 °C to 125 °C or higher temperatures and lithium-ion batteries have an operating range of -40 °C to 65 °C.

The potential issue with usage of batteries to power EMAs is that limited power is provided and therefore adequate margin must be included. The HOT EAGLE battery sizing calculations include 50% margin.

We did not examine the impact of using liquid injection TVC (LITVC) or probe TVC (PTVC). Both of these implementations would affect the engine nozzle design and the LITVC system would affect the propellant system design. The advantage of these type systems is that the TVC actuators are replaced with a number of simple, less expensive, and likely lighter 28 VDC solenoid valves.

We also did not examine the usage of EHAs due to their limited availability.

C4.2.6 Landing Gear – Horizontal Landing

The landing gear control components shown in Table C-15 are based on systems identified for the A-12 aircraft. Actuation weights were reduced by a factor of 2 based on assumed reduced gear & door weights. Control elements weight (e.g., control valves) could have been reduced due to reduced flow demand, but since the factor of 2 on actuation elements was a SWAG, we chose to not alter the control component weights.

Table C-15 – Landing Gear Actuation Weight Estimate – Horizontal Landing

			Item	Qty	Weight (lbs)	Margin (%)	Weight Total (lbs)	Basis	Comments
			Avionics Area (fwd of CH4 tank)						
			Electronics						
			Landing Gear Control Unit	1	7.75	5	8.14		
			Brake / Anti-Skid Controller	1	7.75	5	8.14	A-12	
			Landing Gear Installation						
			Nose Landing Gear	1	TBD				
			NLG Control						
			Control valve	1	6.50	3	6.70	A-12	
			Extend / retract actuator	1	6.00	3	6.18	A-12 weight / 2, reduced gear weight	
			Down & locked actuator	1	4.50	3	4.64	A-12	
			Door actuators	2	2.80	3	5.77	A-12 weight / 2, reduced door weight	
			Door latch actuator	1	4.38	3	4.51	A-12 weight / 2, reduced door weight	
			Swivel joint	1	2.50	3	2.58	A-12	
			Sequencing / shuttle valves	3	0.50	3	1.55	A-12	
			Switching valve	1	4.00	3	4.12	A-12	
			Tubing	1	4.00	3	4.12		40 ft of 3/8 in tubing is 3.84 pounds
			Nose Wheel Steering						
			Selecter valve	1	1.85	3	1.91	A-12	
			NWS power unit	1	18.50	3	19.06	A-12 weight / 2, reduced gear weight	
			Swivel joint	1	2.50	3	2.58	A-12	
			Engine Section						
			Landing Gear Installation						
			Main Landing Gear	2	TBD				
			MLG Control						
			Control valve	1	4.50	3	4.64	A-12	
			Extend / retract actuator	2	7.50	3	15.45	A-12 weight / 2, reduced door weight	
			Door / gear uplatch actuator	2	4.70	3	9.68	A-12 weight / 2, reduced door weight	
			Door uplock	2	4.38	3	9.01	A-12 weight / 2, reduced door weight	
			Shuttle valves	5	0.50	3	2.58	A-12	
			Tubing	1	4.00	3	4.12		40 ft of 3/8 in tubing is 3.84 pounds
			Brake / Anti-skid Control						
			Control valve	1	9.75	3	10.04	A-12	
			Swivels	2	2.50	3	5.15	A-12	
			Brake accumulator	1	27.55	3	28.38	A-12	
			Accumulator charging valve	1	2.50	3	2.58	A-12	
			Shuttle valves	2	2.50	3	5.15	A-12	
			Pressure transducers	5	0.50	3	2.58	A-12	
			Brake accumulator dump valve	1	4.00	3	4.12	A-12	
			Tubing	1	2.00	3	2.06		
							185.48		
			Gear Hydraulic Power Source (EMA configuration)						Required per gear (3 total systems)
			Accumulator	1	40.00	15	46.00	SWAG	
			Nitrogen cylinder	1	30.00	15	34.50	SWAG	to expand the size of the accumulator
			Hydraulic fluid	1	14.00	15	16.10		~ 2 gallons
							96.60		
			Total				282.08		

Tubing weights were based on 3/8-inch tubing as 3/8-inch tubing is believed to be a compromise between too small and too large.

The weight of the gear itself was not determined. The X-33 used modified F-15 gear that's about 1,500 pounds as shown in Attachment 2. The F-15 gear is much beefier than required for the approximately 20,000 pound HOT EAGLE. We'll need to identify a suitable existing gear as we cannot likely afford a gear development program. It may make sense just to allocate 4% of takeoff gross weight for gear (or use a similar parametric estimating method).

We also examined the hydraulic power system weight required for the electrical control surface and TVC actuation configuration. With this configuration, accumulators are included to lower each gear, similar to the approach used on the X-33. This implementation was examined to compare the electrical and hydraulic actuation implementations.

For reference, the DC-X landing gear system (control valve, 4 gear, and sensors) weighed 1,240 pounds. The DC-X gear was actuated pneumatically using pressurization system gas, but was required to be stowed manually. The X-36 gear weighed 79.3 pound total (1,245 pound takeoff gross weight).

C4.2.7 RCS

The RCS weights shown in Table C-16 are based on a launch vehicle system implementation and the Figure C-10 block diagram which reflects the system implementation discussed in paragraph C3.9 herein.

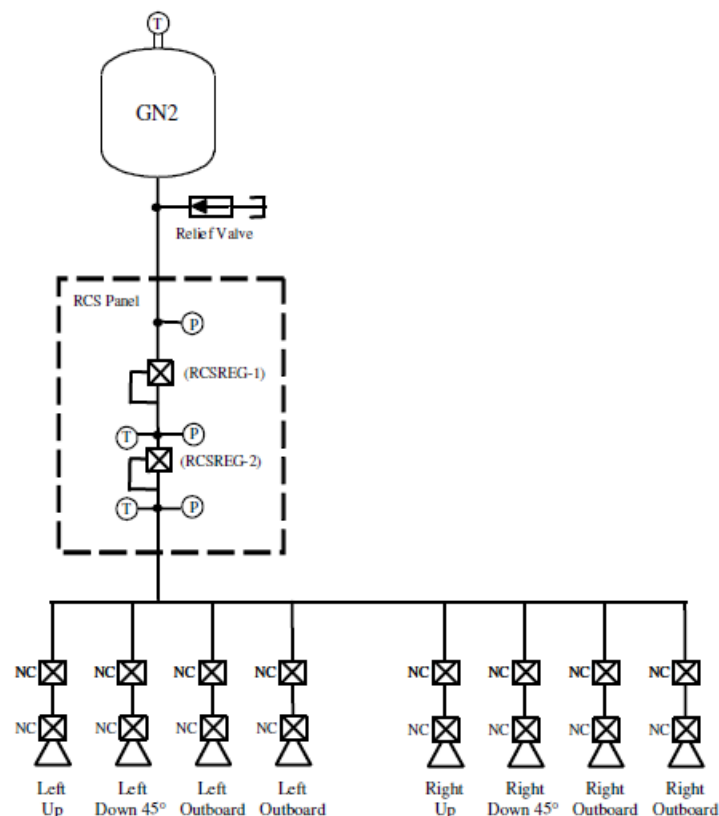


Figure C-10 – RCS System Configuration

Isolation valves are included to enable a stuck on thruster to be turned off. We didn't go so far as to use quad valve arrangements used in some systems as shown in Figure C-11. In the case of a stuck on valve, the series valve can be used to shut off flow and in the case of a non-functional solenoid valve, the parallel path can be used.

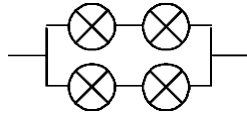


Figure C-11 – Quad Valve Configuration

The GN2 bottle was included to make the system independent of other systems or implementations. The Micro-X report suggests that APU hot gas could be used for RCS propellant, but it strikes me that the APU is not operational during exo-atmospheric portions of the mission. The GN2 bottle may be undersized since it was based on a launch vehicle application with a shorter orbital duration.

Table C-16 – RCS Weight Estimate

Item				Qty	Weight (lbs)	Margin (%)	Weight Total (lbs)	Basis	Comments
Avionics Area (fwd of CH4 tank)									
Reaction Control System									
			GN2 Bottle	1	44.00	15	50.60		
			Isolation valve	8	1.25	15	11.50		
			Thruster / solenoid	8	1.40	15	12.88		
			RCS Panel	1	8.00	15	9.20		
			Regulator	2	3.00	15	6.90		
			Pressure transducer	3	0.50	15	1.73		
			Temperature transducer	3	0.75	15	2.59		
			Relief valve / quick disconnect	1	1.50	15	1.73		
			Fittings	1	8.00	15	9.20		
			Tubing	1	11.00	15	12.65		
							118.97		

C4.2.8 Miscellaneous

The air data lines are included in the miscellaneous systems weight estimate (Table C-17). The remote air data modules are included in the avionics / electronics estimate. The system is assumed to be a flush air data system in a cruciform arrangement with dual ports placed at six locations. There will be some weight associated with integrating the air data ports into the nose of the vehicle that should be included as part of the structural weight.

The HOT EAGLE will need an active thermal control system to control the temperature of the avionics and potentially other systems during the extended exo-atmospheric operational time and during the post flight thermal protection system heat soak. A sample ATCS implementation is shown in Figure C-12.

Redundant pumps (active / standby) flow coolant through ground and flight heat exchangers to control the temperature of the electronics mounted on cold plates. Pressure and temperature sensors are included to provide system control and fault detection.

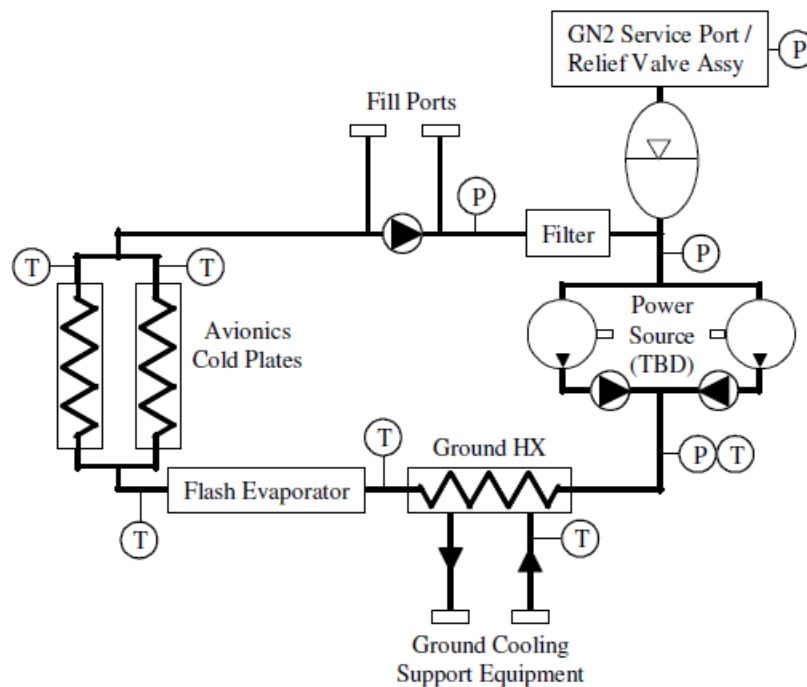


Figure C-12 – ATCS Block Diagram

Pump power source - Electrical power will be used to facilitate ground operations and provide more independence in terms of system location. The circulation pump load is currently not included in the HOT EAGLE power estimate. These types of not quantified loads are why we are carrying a 50% margin in the power system sizing.

Flight heat sink – A flash evaporator is included to provide an in flight heat sink. The water for the flash evaporator is included in the weight estimate, but power requirements for keeping the water from freezing is not currently included in the HOT EAGLE power estimate.

System configuration – Having the avionics (and other heat sources and sinks) locations split between the area forward of the CH₄ tank and aft of the LOX tank necessitates the routing of coolant (likely ethylene glycol / water) between the two areas. Further analysis will be required to trade collocation against ATCS complexity.

Grounding – Probably more detail than we need to get into at this point, but placing electronics on cold plates necessitates ensuring that a suitable ground path is provided (since the cold plates are isolated from structure). A suitable ground path may be provided through the fasteners or necessitate the addition of grounding straps.

We assume that the internal temperature rise due to TPS heat soak would necessitate post flight cooling (since this is the case on the STS and was common to both X-33 designs). The purpose of the ground heat exchanger is to provide a heat sink for the post landing and other ground environments requiring cooling (e.g., hot day operations). The ground connections will likely not be made until landing plus several minutes, so the system must be designed to maintain acceptable temperatures during this time period.

The ATCS weight is based on the weight of the X-33 system (407 pounds) and a NASA crew exigency return vehicle (CERV) study (580 pounds). The HOT EAGLE weight was reduced based on the need for less avionics cooling than the redundant X-33 avionics or the redundant CERV with crew station systems.

If crew are added to the HOT EAGLE vehicle, we'll need to add pressurization, atmosphere revitalization, supply and wastewater, and personnel provisions. We'd also need to add controls and displays and, as discussed in paragraph C2.2.2 herein, systems redundancy would be required for a crewed vehicle.

Table C-17 – Miscellaneous Systems Weight Estimates

[illegible]

C4.3 System Weight Comparisons

Table C-18 and C-19 provide mass summaries for the NASA CERV (NASA / CR-2000-210548) and the X-33 representing two system dry weight extremes and are provided for reference.

Table C-18 – CERV Mass Summary

	<u>Weight,lb</u>
1.0 Wing group	289
2.0 Tail group	0
3.0 Body group	4,480
4.0 TPS	980
5.0 Landing and auxiliary systems	390
6.0 Main propulsion	0
7.0 Propulsion systems (OMS & RCS)	329
8.0 Pressurization, pneumatics & purge	137
9.0 Prime power	1,530
10.0 Electrical conversion and distribution	266
11.0 Surface controls	92
13.0 Avionics	651
14.0 Environmental control	939
15.0 Personnel provisions	546
16.0 Margin	1,063
	<hr/>
Inert weight	11,692
17.0 Personnel (clothes, etc.)	1,925
18.0 Payload accommodation	0
19.0 Payload returned	0
20.0 Residual and reserve fluids	180
	<hr/>
Landed weight	13,797
22.0 RCS propellant	124
23.0 OMS propellant	620
24.0 O ₂ ,N ₂ , H ₂ O, He, and NH ₃	449
	<hr/>
On-orbit weight	14,990

Table C-19 – X-33 Mass Summary

X-33 Weight Statement

	WEIGHT (lb)	
TAIL / AEROSURFACES		5,520
Canted Fins (2)	3,231	
Vertical Fins (2)	1,469	
Body Flaps (2)	820	
VEHICLE BODY		26,880
TPS Support Structure	4,137	
Landing Gear Support Structure	1,853	
Intertank Structure	647	
Thrust Structure	2,894	
Hold-down and Release Structure	821	
Cryo LH2 Tanks (2)	8,811	
Cryo LO2 Tank	6,076	
Secondary Structure	1,641	
THERMAL PROTECTION SYSTEM		11,033
Body	7,982	
Canted Fins	1,547	
Body Flaps	671	
Cryo Insulation	832	
LANDING SYSTEM		2,115
Nose Landing Gear	290	
Main Landing Gear	1,227	
Hydraulics and Controls	598	
MAIN PROPELLANT SYSTEM		3,665
Accessories Systems	1,204	
LH2 Main Feed, Fill and Drain, Vent	732	
LO2 Main Feed, Fill and Drain, Vent	1,604	
Integrated Helium System	125	
MAIN ASCENT ENGINES (2)		15,036
Basic Engine	14,948	
Cowl Seal	88	
REACTION CONTROL SYSTEM		1,477
Thrusters (8)	285	
Oxygen Storage Tanks (2)	300	
Methane Storage Tanks (3)	525	
System Mounting Structure	82	
Instrumentation	5	
Vehicle Propellant Lines	152	
System Integration	128	
ELECTRICAL POWER GENERATION		1,999
Battery Power Subsystem	1,283	
Power Control	716	
ELECTRICAL DISTRIBUTION		493
Circuitry	398	
Installation	95	

Table C-19 – X-33 Mass Summary (concl.)

	WEIGHT (lb)	
SURFACE CONTROLS		1,981
Surface Control Actuators (8)	638	
PLADs (2)	190	
Controllers (8) and Installation	414	
Electrical Cabling and Installation	738	
AVIONICS		1,465
GPS / INS	72	
Radar Altimeter	24	
Air Data System	38	
Telemetry and Communications	16	
Vehicle Management System	349	
Vehicle Health Management	310	
Range Safety	34	
JPL Avionics Experiment	35	
Avionics Cabling and Installation	586	
ENVIRONMENTAL CONTROLS		947
Leak Detection	117	
Purge and Vent	423	
Active Thermal Control	407	
FLIGHT TEST INSTRUMENTATION		805
DRY MASS		73,415
BALLAST		2,463
BALLASTED DRY MASS		75,878
RESIDUAL FLUIDS		575
Residual Fluids - RCS	235	
Residual Fluids - Ascent	340	
RESERVE FLUIDS		276
Reserve Propellant - RCS	32	
Reserve Propellant - Ascent	244	
UNUSABLE ASCENT PROPELLANT		1,547
Tanks	937	
Feed Lines	291	
Engines	319	
RCS PROPELLANT		492
Methane	234	
Oxygen	258	
MECO MASS		78,767
ASCENT PROPELLANT - USABLE		206,667
Liquid Hydrogen	30,570	
Liquid Oxygen	176,097	
GROSS LIFT-OFF WEIGHT		285,434
START-UP PROPELLANT		4,022
TOTAL GROSS WEIGHT		289,456